Semiclassical treatment of transport and spin relaxation in spin-orbit coupled systems

Im Fachbereich Physik der
Freien Universität Berlin
eingereichte

Dissertation

von

Matthias Clemens Lüffe

aus Warendorf

Berlin, im Januar 2012

1. Gutachterin: Prof. Dr. Tamara Nunner
2. Gutachter: PD Dr. Daniel Sebastiani

Tag der Einreichung: 16. Januar 2012
Tag der Disputation: 10. Februar 2012

Meinen Eltern gewidmet.

Gyroscope

This admirable gadget, when it is
    Wound on a string and spun with steady force,
Maintains its balance on most any smooth
    Surface, pleasantly humming as it goes.
It is whirled not on a constant course, but still
    Stands in unshivering integrity
For quite some time, meaning nothing perhaps
    But being something agreeable to watch,
A silver nearly silence gleaning a still-
    ness out of speed, composing unity
From spin, so that its hollow spaces seem
    Solids of light, until it wobbles and
Begins to whine, and then with an odd lunge
    Eccentric and reckless, it skids away
And drops dead into its own skeleton.

Howard Nemerov
(1920-1991)

Contents

1. Introduction

The poem by Howard Nemerov prefixed to this thesis describes what is familiar to everyone who, as a child, has played with a humming top. The elementary yet charming physics of such a classical gyroscope balancing on a "smooth surface" is based on the (of course imperfect) conservation of its angular momentum. In the realms of quantum mechanics, this phenomenon finds its approximate counterpart—although not a strict analog—in the *spin*, discovered and formalized as an *intrinsic* angular momentum of the electron in seminal works by Pauli [1925], Uhlenbeck and Goudsmit [1925], and Dirac [1928a;b]. Being actually much more than only some "admirable gadget" of quantum theorists, the electron spin influences many properties of the matter that surrounds us every day: through the spin-statistics theorem [Fierz, 1939; Pauli, 1940] and Pauli's exclusion principle [Pauli, 1925] it provides the very basis for large-scale stability of many-electron systems and determines in part the structure of the periodic table of elements.

Recently, the electron spin has indeed become a favorite toy of many condensed matter physicists, and even a whole new research field, dubbed *spintronics*, has emerged [Wolf *et al.*, 2001; Awschalom *et al.*, 2002; Žutić *et al.*, 2004; Awschalom and Flatté, 2007]. From an—admittedly somewhat constricted—spintronics perspective, one could argue that Nemerov's poem is a description of what in a sober scientific language would be called a *spin relaxation* process. In this picture, the "quite some time, meaning nothing perhaps" until the gyroscope "drops dead into its own skeleton" represents the *spin's lifetime* (proving that physicists' jargon is not that prosaic after all). A central challenge of spintronics is precisely that this relaxation time during which one can control a localized or itinerant spin means actually a lot: it can decide about the feasibility of efficient spin-based (quantum) information storage and processing in the future.

Another, even younger area of research that offers bright prospects for technological applications and at the same time provides a test bed for fundamental physics hitherto unaccessible in the laboratory is *graphene* [Geim and Novoselov, 2007]. Concerning the dichotomy of application-oriented versus fundamental scientific interest, it is certainly justifiable to say that, while in spintronics the practical aspect prevails, in the graphene research both kinds of motivation are rather equilibrated—on a very high level. Materials scientists attempt to exploit the unique mechanical properties and the huge thermal and electrical conductivities of the two-dimensional carbon allotrope, and theorists are thrilled by the possibility to investigate numerous effects connected with the relativistic nature of the electrons in graphene, which behave like *massless, chiral Dirac fermions*.

As postmodern as the introductory poem by Nemerov are, in a sense, the methods employed in todays condensed matter theory. Concepts and techniques have been borrowed from different branches and eras of physics and developed further (*e.g.*, quantum field theoretical tools such as the Feynman diagrams from quantum electrodynamics). For instance, the *semiclassical* description of nonequilibrium phenomena, which we will make abundant

use of in this thesis, combines the Boltzmann equation dating back to the 19th century with several quantum mechanical features (notably spin and Fermi statistics) from the "classical modern" period of physics in the 20th century. The general goal is to describe concrete observable phenonema rather than to find grand unified theories, which allows for a (most of the time) tolerant coexistence of alternative (or sometimes complementary) formal approaches. Nevertheless, the plurality of approaches raises the question for their equivalence in certain contexts.

The present thesis is concerned with problems belonging to two seemingly distinct global topics—spintronics and graphene. However, as will become clear in the remainder of this introductory chapter, these two fields have more in common than the fact that both have been in the spotlight of condensed matter physics over the past years, with two very recent Nobel Prizes in Physics[1] being an expression and, obviously, a reinforcement of this focus.

1.1. Spintronics

The 2007 Nobel Prize in Physics was awarded to Peter Grünberg and Albert Fert for their independent discovery of the *Giant magnetoresistance* [Grünberg *et al.*, 1986; Baibich *et al.*, 1988; Binasch *et al.*, 1989]. This effect is observed in layered metallic structures composed of alternating ferromagnetic and nonmagnetic films. The presence of a magnetic field causes a significant decrease in the electrical resistance of these compounds. Apart from having a tremendous technological impact through the use of the Giant magnetoresistance and of the related *Tunnel magnetoresistance* [Jullière, 1975] in read heads for commercial data storage devices, the experimental achievements of Grünberg and Fert are generally considered the "birth of spintronics".

Yet, the present activities in this research field are based on pioneering work that dates back much earlier (see D'yakonov [2008]): at a time when spin as a concept was still unknown, Wood and Ellett [1924] observed that polarization-resolved fluorescence measurements on mercury vapor were influenced by the magnetic field of the earth. This effect was thoroughly investigated and given a physical interpretation by Hanle [1924], with whose name it is connected to date. The subject was taken up again by Brossel and Kastler [1949] in their studies of optical pumping in atoms, which included three basic steps that later became programmatic for spintronics: optical excitation of a nonequilibrium distribution of angular momentum, its subsequent manipulation with magnetic fields and, finally, detection of the resulting distribution via the polarization of its luminescence. Lampel [1968] developed analogous techniques for the *optical orientation of the carrier spins in semiconductors* (see also Meier and Zakharchenya [1984]). In the sequel, a lot of experimental and theoretical effort was devoted to these kinds of problems. An important result by D'yakonov and Perel' [1971] was their prediction of spin currents that flow transversely to charge currents in semiconductors with spin-orbit coupling. This phenomenon was later named *spin Hall effect* [Hirsch, 1999]. The recent experimental observation [Kato *et al.*, 2004; Wunderlich *et al.*, 2005; Sih *et al.*, 2005] of the resulting spin accumulation

[1] Speaking of highly rated awards, it is fair to mention that the little piece of "spin relaxation literature" that we chose as an epigraph for this thesis has played its part in earning Howard Nemerov the Pulitzer Prize for poetry in 1978.

at the sample boundaries of electron as well as hole systems has prompted a vivid theoretical debate about the underlying mechanisms (see, *e.g.*, Sinova *et al.* [2004]; Engel *et al.* [2007]). Unlike the Giant magnetoresistance, which can be understood within a two-channel picture ("spin-up" and "spin-down" with respect to some quantization axis), the theoretical description of the spin Hall effect (and of other phenomena relevant to spintronics such as the current-induced spin torque [Ralph and Stiles, 2008]), requires a *coherent* treatment of the spin.

In a broad sense, spintronics deals with spin-related effects in solids, including equilibrium phenomena (with respect to the spin degree of freedom) such as the aforementioned Giant magnetoresistance. D'yakonov [2004] narrows the subject as follows:

> "What most people apparently mean by spintronics is the fabrication of some useful devices using a) creation of a non-equilibrium spin density in a semiconductor, b) manipulation of the spins by external fields, and c) detection of the resulting spin state."

This sketches the program of what has since become established as *semiconductor spintronics* [Fabian *et al.*, 2007; D'yakonov, 2008].

Research in this field is largely fueled by the technological interest to improve on the performance of conventional semiconductor microelectronics. To date the chip industry has kept up with the pace described by "Moore's law" [Moore, 1965], an empirical observation saying that the number of transistors on an integrated circuit doubles approximately in every 18 to 24 months. Recently, the Intel Corporation announced a new three-dimensional "Tri-Gate" structure with a 22 nm scale, as opposed to 32 nm in the present transistor generation [Cartwright, 2011]. However, even with such ingenious exploits within conventional technology as the extension of the transistor architecture to the third dimension, further improvements in terms of, *e.g.*, reduction of power consumption will become increasingly difficult to achieve in the future. Here, semiconductor spintronics offers new vistas through a radical change in paradigm: the idea is to largely stick to the highly developed semiconductor structures of existing microelectronics (including the elaborate lithographical fabrication techniques), but to exploit the conduction electrons' spin degree of freedom in addition to their charge for information storage (as already done in MRAMs and hard drives) *and processing*. Possible advantages lie in a better integration of the two functionalities—processing and storage of information—as well as in increased operation speeds and higher energy efficiency. The latter expectation is based on the fact that, being time reversal symmetric by definition, spin currents can, in principle, flow *dissipationless* [Murakami *et al.*, 2003]. This is a particularly important point, since Joule heating is a key limiting factor for further miniaturization.

1.1.1. Spin-orbit interactions and spin relaxation

A great asset of using semiconductor structures as spintronics devices is that therein spin polarization can be generated and coherently manipulated without ferromagnetism or external magnetic fields [Awschalom and Samarth, 2009] via *spin-orbit coupling*.

In atomic physics, spin-orbit interactions reveal themselves as corrections in the spectra, which can be modeled by including in the Hamiltonian describing electrons with mass m

and momentum $\boldsymbol{p}$ the *Thomas term*

$$H_{\text{Thomas}} = \frac{e\,\hbar}{4m^2c^2}\,\boldsymbol{\sigma}\cdot(\boldsymbol{\nabla}V\times\boldsymbol{p})\,. \tag{1.1}$$

It is derived as a relativistic correction to the Pauli equation. Here, V is the atomic potential and $\boldsymbol{\sigma}$ denotes the vector of Pauli matrices.[2] In general, the spin-orbit coupling is small due to its relativistic origin (the huge energy gap between electrons and positrons $2mc^2$ appears in the denominator).

In semiconductor structures, however, the effects of spin-orbit interaction can be magnified considerably, depending on band structure parameters and confining potentials. In the absence of magnetic fields (*i.e.*, if time-reversal symmetry is granted) and if, in addition, the potential in which the electrons move is space-inversion symmetric, the electronic states for given wave vector $\boldsymbol{k}$ are two-fold degenerate, $\epsilon_\uparrow(\boldsymbol{k}) = \epsilon_\downarrow(\boldsymbol{k})$. This spin-degeneracy can be lifted if the space inversion asymmetry is broken either by the crystal structure (*bulk inversion asymmetry*, *e.g.*, in materials of the zinc-blende type [Dresselhaus, 1955]) or as a consequence of the *structure inversion asymmetry* due to a confining potential as frequently encountered in semiconductor heterostructures [Bychkov and Rashba, 1984].[3]

Using $\boldsymbol{k}\cdot\boldsymbol{p}$ theory [Moss, 1980] and the envelope function approximation one can describe the physics of structures that are based on direct semiconductors within the 8×8 *Kane Model* [Winkler, 2003]. The band structure is depicted in Figure 1.1: besides the spin-degenerate s-type conduction band this model takes into account the light and heavy hole bands and the spin-orbit split-off band (all of them p-type and also spin degenerate). We recall that the famous two-band Pauli equation is obtained in the nonrelativistic limit of the Lorentz invariant four-band Dirac equation (electrons coupled to positrons). The spin-orbit interaction Hamiltonian (1.1) is a leading-order relativistic correction. Analogously, using quasi-degenerate perturbation theory (*Löwdin partitioning*[4]), one derives from the coupled equations for the eight bands of the Kane model an effective 2×2 Hamiltonian for the conduction band electrons [Winkler, 2003]. The result is an energy eigenvalue equation for the envelope function spinor of the conduction band electrons that resembles the Pauli equation with relativistic corrections. As constituents of the Hamiltonian one finds, in addition to the kinetic energy (with an effective mass expressed in terms of the band structure parameters), a Zeeman term (with an effective g-factor), a Darwin term and, in particular, as the analog of the Thomas term (1.1), the effective spin-orbit coupling

$$H_{\text{soi}} = \frac{P^2}{3}\left[\frac{1}{E_0^2}+\frac{1}{(E_0+\Delta_0^2)}\right]\boldsymbol{\sigma}\cdot(\boldsymbol{\nabla}V\times\boldsymbol{k})\,. \tag{1.2}$$

Here, E_0 and Δ_0 are the fundamental band gap and the spin-orbit split-off energy, respectively (see Figure 1.1), and P parametrizes the strength of the coupling between

[2] The Pauli matrices read

$$\sigma_x \equiv \begin{pmatrix}0 & 1\\ 1 & 0\end{pmatrix},\quad \sigma_y \equiv \begin{pmatrix}0 & -i\\ i & 0\end{pmatrix}\quad\text{and}\quad \sigma_z \equiv \begin{pmatrix}1 & 0\\ 0 & -1\end{pmatrix}.$$

[3] Further contributions, which are not considered in this thesis, can arise from strain or from the lack of microscopic symmetry of the atoms at the interface.

[4] In the context of the derivation of the Pauli equation with relativistic corrections, this technique is also known as *Foldy-Wouthuysen transformation.*

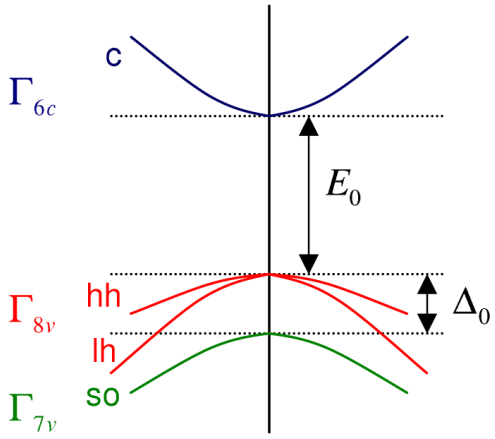

Figure 1.1.: Band structure of the 8×8 Kane model: conduction band (c), heavy hole band (hh), light hole band (lh) and spin-orbit split-off band (so) All bands are two-fold spin-degenerate. Indicated are further the fundamental band gap E_0 and the spin-orbit splitting Δ_0. *This figure is adopted from Fabian et al. [2007].*

conduction and valence band.

In Eq. (1.2) V can, for instance, represent the Coulomb potential of charged impurities. As a result of this *extrinsic spin-orbit coupling* the spin of an electron that scatters from impurities precesses during the collision processes. Thus, impurity scattering contributes to the decay of spin polarization—a mechanism called *Elliot-Yafet spin relaxation* [Elliott, 1954; Yafet, 1963].

Next we consider the *Rashba spin-orbit interaction* [Bychkov and Rashba, 1984] arising from structure inversion asymmetry, *e.g.*, in a two-dimensional electron gas (2DEG) realized inside a GaAs/AlGaAs heterostructure with an imbalance of doping on both sides of the quantum well. Then the relevant potential gradient in Eq. (1.2) is the average electric field in z-direction that is due to this asymmetric confining potential. By integrating out the (out-of-plane) motion in z-direction one obtains a Zeeman-like term, but with an effective magnetic field $\boldsymbol{b}_R(\boldsymbol{k})$ that depends on the in-plane wave vector $\boldsymbol{k} \equiv (k_x, k_y)$. Its magnitude increases linearly with the one of the momentum argument k. The directional dependence is shown in Figure 1.2 b). It is characterized by a winding number $N = 1$. For a momentum-dependent in-plane field $\boldsymbol{b}(\boldsymbol{k})$, N is defined by the relation

$$\hat{b}_x + i\hat{b}_y \quad = \quad e^{i\theta_0 + iN\theta}\,. \tag{1.3}$$

Here, θ is the polar angle of $\boldsymbol{k}$ and θ_0 is a constant phase ($\theta_0 = \pi$ for $\boldsymbol{b} = \boldsymbol{b}_R$).

In order to also account for effects of bulk inversion asymmetry of the crystal lattice one has to resort to the *extended Kane model* [Winkler, 2003], which includes another six energetically higher p-type conduction bands. This yields the *Dresselhaus spin-orbit coupling* field [Dresselhaus, 1955] $\boldsymbol{b}_D(\boldsymbol{k})$, which is a priori *cubic* in k. However, taking again the mean value of the momentum component in the growth direction of the quantum well,

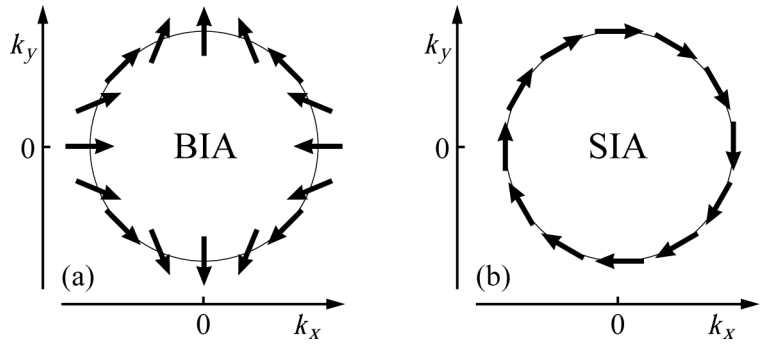

Figure 1.2.: Sketch of the two kinds of linear-in-momentum spin-orbit fields in semiconductor devices with bulk inversion asymmetry (BIA) or structure inversion asymmetry (SIA): a) the linear Dresselhaus field $\boldsymbol{b}_D(\boldsymbol{k})$ has a negative winding sense (winding number -1); b) the Rashba field $\boldsymbol{b}_R(\boldsymbol{k})$ has a positive winding sense (winding number +1). *This figure is taken from Winkler [2006].*

$k_z^2 \to \langle k_z^2 \rangle$, one can split off a linear contribution with winding number $N = -1$, see Figure 1.2 a). Since $\langle k_z^2 \rangle \approx (\pi/d)^2$ where d is the quantum well width, the linear Dresselhaus spin-orbit coupling is dominant over the cubic contributions for thin quantum wells, where $d \ll k_F^{-1}$ (with k_F denoting the Fermi momentum). Nevertheless, cubic Dresselhaus interactions can become important, in particular in the special situation considered in Chapters 3 and 4 of this thesis where the effects of the two linear contributions cancel each other (see also Section 1.1.2 below).

Both kinds of intrinsic spin-orbit interaction discussed above cause *D'yakonov-Perel' spin relaxation* [D'yakonov and Perel', 1972], which, unlike the extrinsic Elliot-Yafet relaxation, occurs *between* the scattering events: the spin precesses about the spin-orbit field $\boldsymbol{b}(\boldsymbol{k})$, which changes with every momentum scattering event, see Figure 1.3. If the precession frequency is of the order of (or larger than) the scattering rate the spin is completely randomized already after a few scattering processes. In the opposite limit of weak spin-orbit coupling or strong scattering, the precession angle between two collisions is small. Then the spin is subject to a diffusion process where the scattering actually *stabilizes* the spin: the more scattering, the larger the spin lifetime.[5] The D'yakonov-Perel' mechanism is typically the dominant source of spin relaxation in semiconductor quantum wells.

1.1.2. Towards maximizing spin lifetimes and coherence lengths

A paradigmatic (yet in its pure form so far not realized) device of semiconductor spintronics that relies on the manipulation of the spin via intrinsic spin-orbit fields is the *spin field-effect transistor* proposed by Datta and Das [1990]. The idea is to inject a spin current[6] from a spin-polarized source lead (*e.g.*, a semi-metal or ferromagnetic semicon-

[5] This phenomenon is often referred to as "motional narrowing" in analogy with the reduction of line widths in NMR spectroscopy due to disorder in local magnetic fields.

[6] For a survey on spin-injection, see Fabian *et al.* [2007].

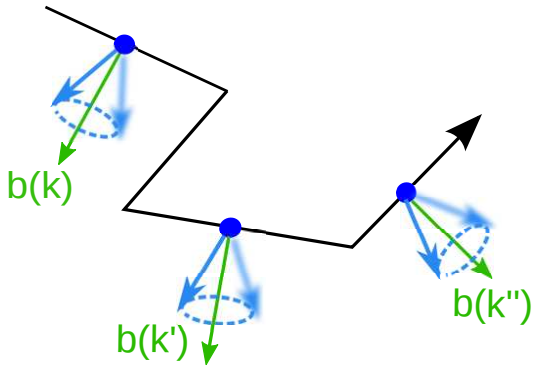

Figure 1.3.: Schematic D'yakonov-Perel' spin relaxation: The black line is the trajectory of an electron; the blue arrows mark the electron spin, which precesses about the momentary spin-orbit field $\boldsymbol{b}(\boldsymbol{k})$ (green). The frequent change of the precession axis results in a random walk behavior with the scattering effectively *stabilizing* the spin.

ductor) into a two-dimensional semiconductor structure with Rashba spin-orbit coupling that is tunable via an electrostatic gate. Depending on the magnitude of the spin-orbit interaction, which determines the precession period, the itinerant spin will, at the moment when it arrives at the other end of the sample, more or less match the polarization of the drain lead, thus making it easy or hard to flow off (see Figure 1.4). As a result, the permeability of the device for spin currents can be controlled all-electrically. Obviously, this principle requires that the spins remain coherent during their passage through the device. Therefore, the original proposal was for a *ballistic* situation, where spin dephasing due to, *e.g.*, D'yakonov-Perel' relaxation, does not play a role. In order to lift this strict and experimentally demanding requirement Schliemann *et al.* [2003] came up with the idea to use a sample where linear Dresselhaus spin-orbit interaction in addition to the Rashba coupling is present. Then, under certain conditions, which include in particular that both kinds of linear spin-orbit coupling have to be of equal magnitude, the D'yakonov-Perel' spin relaxation mechanism is effectively suppressed. Conceptually this allows the construction of a Datta-Das-type spin field effect transistor even in the presence of (spin-independent) scattering.

A closer investigation of the Hamiltonian describing such a spin-orbit tuned semiconductor system with equal Rasbha and Dresselhaus spin-orbit coupling lead to the discovery of an exact SU(2) symmetry and the prediction of the *persistent spin helix* by Bernevig *et al.* [2006]. The actual realization of such a long-lived spin density wave was achieved recently by means of optical orientation of electron spins in an n-type GaAs/AlGaAs quantum well [Koralek *et al.*, 2009]. This experiment confirms the prediction of the persistent spin helix, but it also raises new questions, *e.g.*, for an explanation of the observed temperature dependence of the spin helix lifetime. In Chapter 3 of this thesis we are able to present results on that topic, which are based on the solution of a semiclassical spin diffusion equation (*cf.* Burkov *et al.* [2004]; Mishchenko *et al.* [2004]; Stanescu and Galitski [2007]; Weng *et al.*

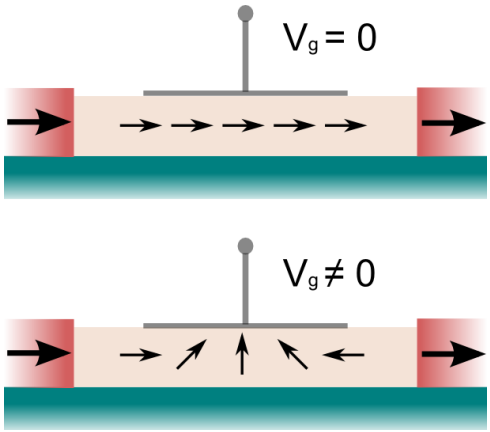

Figure 1.4.: Sketch of the Datta-Das spin transistor: the Rashba spin-orbit interaction (acting as an effective magnetic field perpendicular to the plane) is tunable via the gate voltage. For zero Rashba field (upper panel) the spin polarization injected from the left source lead passes through unchanged; for finite Rashba field (lower panel) the itinerant spins precess, and the spin conductance varies depending on the strength of the spin-orbit coupling. In the situation depicted in the lower panel no spin current flows because in the drain (right lead) there are no states available for electron with a spin that points to the right.

[2008]). In particular, we show that electron-electron interactions (which have no effect in the perfectly SU(2) symmetric situation, see also Section 1.1.3) come into play when the special symmetry underlying the persistent spin helix is broken by cubic Dresselhaus interactions, explaining the temperature-dependent lifetime [Lüffe *et al.*, 2011].

The physics of the persistent spin helix appears also in other contexts, such as the ac driven spin helix proposed by Duckheim *et al.* [2009] and the *Spin Hall Effect Transistor* experiment by Wunderlich *et al.* [2010], which realizes an analog of the persistent spin helix in single-particle transport.

1.1.3. Effects of Coulomb interaction

The Coulomb interaction, being *per se* SU(2) invariant, does not directly couple to the electron spin. However, it is well known that electron-electron interactions can affect spin transport and spin diffusion by relaxing spin currents via the *spin Coulomb drag* [D'Amico and Vignale, 2000; 2001; 2002; Flensberg *et al.*, 2001; D'Amico and Vignale, 2003]. Let us imagine a situation where the center of mass of a population of spin-up electrons has a finite velocity relative to the one of spin-down electrons, *i.e.*, a spin current flows. In that case, as depicted in Figure 1.1.3 for a single scattering event, electron-electron collisions exchange momentum between the two populations and tend to equalize the center-of-mass motion of spin-up electrons and spin-down electrons. As a result, the spin current decays

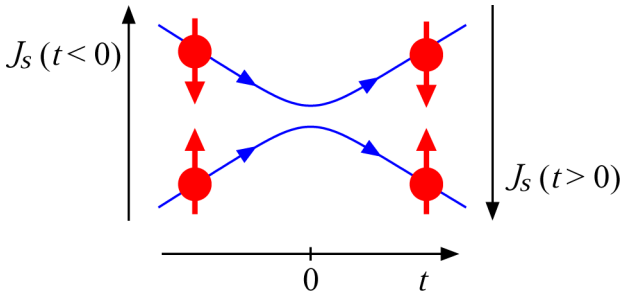

Figure 1.5.: Schematic representation of the non-conservation of spin currents in a Coulomb scattering process: before the scattering event both electron spins contribute to the up-spin current. After the collision the total momentum is unchanged, but the sign of the spin current has flipped. *This figure is taken from Winkler [2006].*

due to Coulomb interaction.[7] D'Amico and Vignale [2000] showed that this mechanism inhibits spin diffusion. The predicted temperature-dependent reduction of the diffusion constant was readily observed by Weber *et al.* [2005].

Since Coulomb interactions provide a mechanism of momentum scattering, they tend to increase spin lifetimes in situations where the D'yakonov-Perel' spin relaxation is operative [Wu and Ning, 2000; Weng and Wu, 2003; Glazov and Ivchenko, 2003]. In clean samples at not too low temperatures, electron-electron scattering can even dominate the D'yakonov Perel' dynamics. For a review on spin Coulomb drag effects in semiconductor spintronics, see D'Amico and Ulrich [2010]. In Chapter 3 of the present thesis we incorporate electron-electron scattering in the spin diffusion equations that describe the persistent spin helix, thus generalizing the Boltzmann equation based derivation of the spin Coulomb drag by Flensberg *et al.* [2001] to a *spin coherent* treatment.

Besides two-particle scattering, there is a second way in which Coulomb interaction influence the spin dynamics in semiconductors: as is well known from the spin diffusion in spin-polarized liquid ^{3}He [Leggett and Rice, 1968; Leggett, 1970], in a three-dimensional Fermi liquid the individual spins precess about the molecular field (as obtained within a Hartree-Fock mean field approach) caused by a local average spin polarization. The exchange field thus exerts a torque on spin currents, which influences the drift-diffusion dynamics of the spin density (rendering it *nonlinear*, in particular). Takahashi *et al.* [1999] showed that this anomalous spin diffusion occurs also in a degenerate two-dimensional electron gas at low temperatures. In measurements by Stich *et al.* [2007], a nonlinear behavior of the spin relaxation was observed, which can be attributed to the Hartree-Fock precession [Weng and Wu, 2003].

In Chapter 4 of this thesis we study the consequences of the Hartree-Fock interaction on the dynamics of the persistent spin helix. The nonlinear precession term that enters the spin diffusion equation brings about changes in the lifetime of the persistent spin helix

[7] In analogy with hydrodynamics one can understand the spin Coulomb drag as corresponding to the laminar friction between two neighboring layers of a liquid that have a relative velocity.

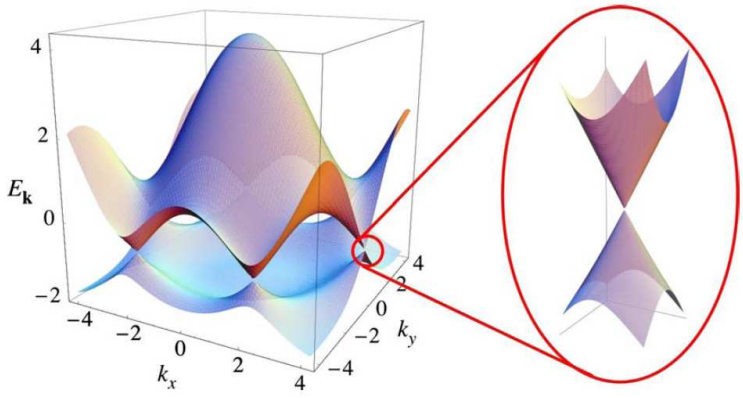

Figure 1.6.: The energy bands for electrons and holes in graphene as derived from a tight-binding Hamiltonian [Wallace, 1947] touch at the Dirac points. In their vicinity the dispersion is linear, with a slope given by the group velocity, which is approximately 300 times smaller than the velocity of light. *This figure is taken from Castro Neto et al. [2009].*

and affects its shape. We estimate quantitatively that a realization of the regime where these effects are observable should be within reach of current experimental techniques.

1.2. Graphene

The 2010 Nobel Prize in Physics was awarded to Andre Geim and Konstantin Novoselov in recognition of their experimental achievement to isolate the two-dimensional allotrope of carbon known as *graphene* [Novoselov *et al.*, 2004]. In the sequel of this first ever realization of a two-dimensional crystal, graphene has attracted extensive attention for its promising material properties (high mechanical stability and stiffness, extraordinary thermal and electrical mobility) and for a variety of theoretically intriguing phenomena such as the Klein tunneling (for an overview see Calogeracos and Dombay [1999]), a stunning minimal conductivity at seemingly zero carrier density, an anomalous integer quantum Hall effect at room temperature [Schakel, 1991; Novoselov *et al.*, 2005] and, most recently, a giant spin Hall effect [Abananin *et al.*, 2011]. The experimental and applied aspects have been reviewed by Geim and Novoselov [2007]. In particular, a lot of work has been devoted to the study of the electrical conductivity of graphene. For a review on the electronic peculiarities of graphene, see Castro Neto *et al.* [2009] and Das Sarma *et al.* [2011].

For neutral monolayer graphene the low-lying electronic excitations are, within a tight-binding model, well described as massless, chiral Dirac fermions in two dimensions [Wallace, 1947; Semenoff, 1984; Castro Neto *et al.*, 2009]. The characteristic Dirac cones in the dispersion express pseudospin-orbit coupling, where the pseudospin derives from a sublattice index (the honeycomb lattice being *bipartite*). The conical electron and hole bands touch at the two inequivalent *Dirac points* K and K' in the Brillouin zone, see Fig-

ure 1.6. In the low energy theory this introduces a valley index in addition to the indices for peudospin and real spin. Neglecting the real spin index (or keeping it implicit) and introducing the four-spinor (u_A, u_B, u'_A, u'_B), where the lower indices (A,B) represent the sublattice and the prime (no prime) indicates the Dirac cone K' (K), one can write the effective Hamiltonian as

$$H \;=\; \hbar\, v_F\, \Pi_z \otimes \boldsymbol{\sigma}\cdot\boldsymbol{k}\,. \tag{1.4}$$

Here, Π_z and $\sigma_{x,y}$ are Pauli matrices in the space of Dirac points and sublattices, respectively, and $v_F \approx 1/300\,c$ is the constant group velocity. If the scattering between the two Dirac cones is negligible it is enough to consider a single Dirac cone, which corresponds indeed to the physics of massless Dirac particles. A comparison of the Hamiltonian $H = \hbar\, v_F\, \boldsymbol{\sigma}\cdot\boldsymbol{k}$ for the cone K and the dispersion $\epsilon_{\boldsymbol{k}} = \pm\hbar\, v_F\, k$ shows that the spinor (u_A, u_B) is also an eigenvector of the *chirality* operator $\boldsymbol{\sigma}\cdot\boldsymbol{k}/|k|$, with eigenvalues ± 1.

We mention that also the surface states of *three-dimensional topological insulators* such as $Bi_{1-x}Sb_x$, Bi_2Te_3, Sb_2Te_3 and Bi_2Se_3, which have recently attracted a lot of attention, are governed by Dirac cone physics (with only one cone to start with) [Fu *et al.*, 2007; Moore and Balents, 2007; Roy, 2009; Hsieh *et al.*, 2008; Zhang *et al.*, 2009; Xia *et al.*, 2009], see also Hasan and Kane [2010].

Like in conventional semiconductors, one can change the chemical potential of a graphene sheet via doping or external electrostatic gates. This makes it possible to study transport of electrons as well as holes. Furthermore, the tuning of the Fermi wave number k_F with respect to the mean free path ℓ given by, *e.g.*, impurity scattering, allows to access two qualitatively different transport regimes: the (almost) undoped case with $\ell\, k_F \ll 1$ corresponds to the *Dirac regime*, where quantum coherences are most important, producing the bigger part of the striking phenomenology that graphene is famous for. At higher doping one enters the *Boltzmann regime* where $\ell\, k_F \gg 1$. Here, an approximate treatment with a semiclassical kinetic equations becomes meaningful, and the leading-order results for, *e.g.*, the electrical conductivity are rather intuitive. However, effects of electron-hole coherence (*i.e.*, pseudospin-orbit coupling) can find their expression in next-to-leading order corrections in the transport quantities. This is discussed in detail in Chapter 5 of this thesis, where we calculate the first-order quantum correction to the Drude conductivity of graphene (*cf.* Auslender and Katsnelson [2007]; Trushin and Schliemann [2007]; Culcer and Winkler [2007b]; Liu *et al.* [2008]). We find that the result is sensitive to the choice of formalism that one uses to derive collision terms and we observe that the discrepancies can be removed to some extent by using an unconventional ansatz distribution function. We further find that for the problem at hand it is important to include principal value parts, which are often neglected, in the calculation (see also Auslender and Katsnelson [2007]).

1.3. Generic Hamiltonian

A common feature of the different systems considered in this thesis is the prominent role of (pseudo)spin-orbit coupling. One should, however, keep in mind that the microscopic origins of, on the one hand, the spin-orbit coupling in GaAs/AlGaAs quantum wells and, on

the other hand, the pseudospin-orbit coupling in monolayer graphene are of a fundamentally different nature: the former case is a reminiscence of genuinely relativistic physics (in the sense of a Lorentz invariant formulation of quantum mechanics), whereas the latter is a consequence of the bipartite honeycomb lattice whose band structure happens to exhibit Dirac cones.[8]

On a practical level, when it comes to setting up a semiclassical but (pseudo)spin-coherent description of either the spin relaxation in semiconductor quantum wells or the electrical conductivity of graphene, one is confronted with a nonequilibrium problem where the undisturbed[9] Hamiltonian has the generic form

$$H_0 \;=\; \epsilon_0(k) + \boldsymbol{\sigma}\cdot\boldsymbol{b}(\boldsymbol{k})\,. \tag{1.5}$$

Here, $\epsilon_0(k) = \frac{\hbar^2 k^2}{2m}$ for semiconductors (m being the effective mass) as opposed $\epsilon_0(k) = 0$ in the case of graphene. The general isotropic (pseudo)spin-orbit coupling

$$\boldsymbol{b} \;=\; b(k)\,\hat{\boldsymbol{b}}(\theta) \tag{1.6}$$

is characterized by the winding number N as defined in Eq. (1.3). This includes, in particular, Rashba and linear Dresselhaus spin-orbit coupling with $b(k) \propto k$ and $N = \pm 1$ as well as cubic Dresselhaus spin-orbit interaction with $b(k) \propto k^3$ and $N = \pm 3$. (The total spin-orbit coupling in quantum wells with a bulk inversion asymmetric material is then the sum of the three contributions.) For electrons close to the Dirac point K in monolayer graphene the pseudospin-orbit coupling (1.6) is given by $b = \hbar\, v_{\mathrm{F}}\, k$ (with the constant $v_F \approx 1/300\, c$) and $\hat{\boldsymbol{b}} = \hat{\boldsymbol{k}}$, *i.e.*, $N = 1$. For the Dirac cone K', one has again $b = v_{\mathrm{F}}\, k$, but now $\hat{\boldsymbol{b}} = (\cos\theta, -\sin\theta)$, *i.e.*, $N = -1$. Note that also the Hamiltonian commonmly studied in the context of bilayer graphene (with $b = \hbar^2 k^2/2m$ and $N = 2$) as well as similar Hamiltonians for multilayer graphene [McCann and Fal'ko, 2006; Guinea *et al.*, 2006; Koshino and Ando, 2007; Min and MacDonald, 2008] belong to the class of Hamiltonians given in Eq. (1.5).

An important difference between semiconductors and monolayer graphene lies in the fact that the quasiparticles in the latter are *massless* Dirac fermions. As a consequence, one has $\epsilon_0(k) = 0$, and all kinetic energy is in the pseudospin-orbit coupling. This makes an expansion as in the semiconductor case, where spin-orbit coupling terms are small corrections to a large leading-order term determined by $\epsilon_0(k)$, impossible (see Chapter 5).

1.4. Outline of this thesis

In Chapter 2 we recall some useful tools and concepts of nonequilibrium theory. This lays the basis for the derivation of semiclassical kinetic equations in the context of concrete realizations of the generic spin-orbit coupled Hamiltonian (1.5) in the subsequent chapters. Using such a semiclassical approach we investigate in Chapter 3 the lifetime

[8] Spin-orbit interaction of genuine relativistic origin is of course also present in graphene, but due to its smallness it can be safely neglected in our considerations of transport in the Boltzmann regime.

[9] As a perturbation in the nonequilibrium problem we will add electron-impurity interactions or electron-electron interactions. In the case of graphene we will further include an electromagnetic potential, since we will be interested in the electrical conductivity.

of the persistent helix in the presence of symmetry breaking mechanisms and Coulomb scattering. Chapter 4 is devoted to the study of effects of the Coulomb exchange interaction on the persistent spin helix state. We focus on the influence on the lifetime as well as on qualitative changes in the shape of the spin density wave. Finally, in Chapter 5, we apply the methods introduced in Chapter 2 as a comparative study to the problem of pseudospin-orbit coupling corrections in the electrical conductivity of graphene in the Boltzmann regime. The concluding Chapter 6 summarizes the results and gives an outlook on potential future avenues of research related to the content of this thesis.

2. Methods of quantum kinetic theory

The rich phenomenology of nonequilibrium systems reflects the diversity of the physical objects involved and of their mutual microscopic interactions. In general, details of this kind elude a macroscopic thermodynamic description. In order to capture these at least to some extent one often resorts to a description based on the *kinetic theory*. This approach deals to some level of precision, *i.e.*, down to certain length- and timescales, with the *microscopic processes* in nonequilibrium systems.

Historically the first and arguably the simplest playground for the kinetic theory is the classical ideal gas. This theoretical model was scrutinized by Clausius, Maxwell, Boltzmann and others in the second half of the 19th century. The underlying assumption is that point-like particles move along classical trajectories and occasionally undergo instantaneous collisions with other particles. This picture allows for a description with the famous classical *Boltzmann equation* [Boltzmann, 1872] for the one-particle distribution function in phase space.

By complementing the Boltzmann equation *ad hoc* with some basic quantum mechanical features (such as the Fermi statistics for degenerate electrons) a *semiclassical Boltzmann equation* can be obtained on heuristic grounds. This will be concretized in the first section of the present chapter. In the remaining sections we will give a basic introduction to several established approaches of nonequilibrium quantum theory, which will serve as the basis for a systematic derivation of spin coherent semiclassical kinetic equations in later chapters: the *Nonequilibrium statistical operator formalism* (NSO) as presented in Section 2.2 is the starting point for our derivation of kinetic equations and, in a second step, coupled diffusion equations for the three components of the spin density in Chapter 3. Here, the collision integral for two-particle scattering will play a particularly important in explaining experimental observations on the persistent spin helix. Also in Chapter 5 we will use the Nonequilibrium statistical operator—this time with a focus on the collision terms for electron-impurity scattering in graphene, where we keep corrections from electron-hole (*i.e.* pseudospin) coherences. For comparison we will also apply the *Green's function approach* (see Section 2.3) to this problem in Chapter 5.

2.1. The semiclassical Boltzmann equation

We follow Smith and Jensen [1989] in presenting the fundamentals of the Boltzmann equation. Let us first consider an ensemble of *classical* particles that is described by the single-particle distribution function in phase space $f(\boldsymbol{r}, \boldsymbol{p}, t)$. This function fulfills the equation

$$\frac{\partial f}{\partial t} + \frac{\partial}{\partial x_\nu}\left(v_\nu f\right) \quad = \quad \left.\frac{\partial f}{\partial t}\right|_{\text{coll}} \tag{2.1}$$

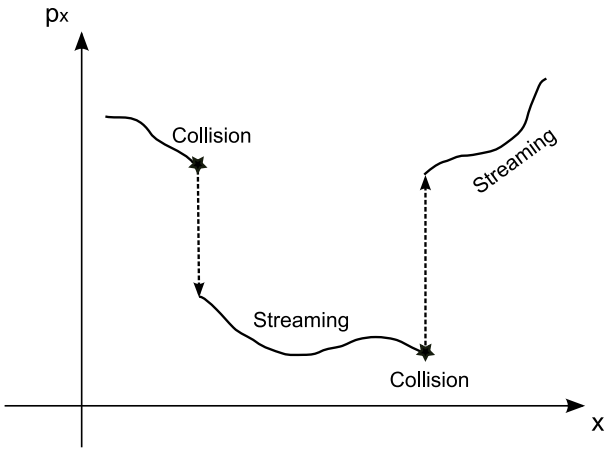

Figure 2.1.: Schematic phase space trajectory of a particle that is part of an ensemble described by the Boltzmann equation: The smooth drift (or streaming) due to moderate potential gradients is interrupted by collisions that change the momentum abruptly.

with $\partial/\partial x_\nu \equiv (\partial/\partial \boldsymbol{r}, \partial/\partial \boldsymbol{p})$ and the six-dimensional generalized velocity $\boldsymbol{v} \equiv (\dot{\boldsymbol{r}}, \dot{\boldsymbol{p}})$. The left-hand side of this equation expresses that the number of particles in a differential phase space volume changes depending on the (phase space) currents of particles flowing in or out, which can be written as a six-dimensional divergence of the phase space density analogously to the continuity equation in hydrodynamics. On the right-hand side, we have a source term due to instantaneous momentum scattering. If we follow the phase space trajectory of a single particle, the left-hand side represents its drift under the action of smooth gradients, whereas the *collision term* on the right-hand side takes into account abrupt changes of its momentum due to scattering, see Figure 2.1. Exploiting the Hamilton equations, $\dot{\boldsymbol{r}} = \partial H/\partial p$ and $\dot{\boldsymbol{p}} = -\partial H/\partial r$, we see that the second term in the divergence $v_\nu\, \partial f/\partial x_\nu + f\, \partial v_\nu/\partial x_\nu$ vanishes, and thus Eq. (2.1) takes the form

$$\frac{\partial f}{\partial t} + \dot{\boldsymbol{r}} \cdot \frac{\partial f}{\partial \boldsymbol{r}} + \dot{\boldsymbol{p}} \cdot \frac{\partial f}{\partial \boldsymbol{p}} \quad = \quad \left.\frac{\partial f}{\partial t}\right|_{\text{coll}} . \tag{2.2}$$

We want to keep the freedom to describe charged particles under the action of a magnetic field $\boldsymbol{B} = \boldsymbol{\nabla} \times \boldsymbol{A}$ with the vector potential $\boldsymbol{A}$. Therefore, it is preferable to write the distribution function and the Boltzmann equation (2.2) in terms of the *kinetic momentum*

$$\boldsymbol{k}(\boldsymbol{r}, \boldsymbol{p}, t) \quad = \quad \boldsymbol{p} - e\boldsymbol{A}(\boldsymbol{r}, t) \tag{2.3}$$

rather than the canonical momentum $\boldsymbol{p}$. The distribution function is unchanged, since the relation

$$f_{\boldsymbol{k}}(\boldsymbol{r}, t)\, \mathrm{d}\boldsymbol{r}\, \mathrm{d}\boldsymbol{k} \quad = \quad f(\boldsymbol{r}, \boldsymbol{p}, t)\, \mathrm{d}\boldsymbol{r}\, \mathrm{d}\boldsymbol{p} \tag{2.4}$$

holds, and from Eq. (2.3) one has $\mathrm{d}\boldsymbol{k} = \mathrm{d}\boldsymbol{p}$. Thus, Eq. (2.2) can be rewritten with $\boldsymbol{p}$ replaced by $\boldsymbol{k}$ and with the last term on the left-hand side containing the force $\boldsymbol{F} = \dot{\boldsymbol{k}}$.

Let us next introduce some quantum mechanics by giving the phase space distribution function a discrete spin index $\sigma = \uparrow, \downarrow$ (having Fermions in mind). Then the Boltzmann equation for $f_{\boldsymbol{k}\,\sigma}(\boldsymbol{r}, t)$ reads

$$\frac{\partial f_{\boldsymbol{k}\,\sigma}}{\partial t} + \boldsymbol{v} \cdot \frac{\partial f_{\boldsymbol{k}\,\sigma}}{\partial \boldsymbol{r}} + \boldsymbol{F} \cdot \frac{\partial f_{\boldsymbol{k}\,\sigma}}{\partial \boldsymbol{k}} \;=\; \left.\frac{\partial f_{\boldsymbol{k}\,\sigma}}{\partial t}\right|_{\text{coll}} . \tag{2.5}$$

One might immediately object that in quantum mechanics, due to Heisenberg's uncertainty principle, the concept of a phase space distribution fails. However, if one considers *Wigner's quasi-probability distribution* (see *e.g.* Rammer [1998])

$$f_{\boldsymbol{k}\,\sigma}(\boldsymbol{r}, t) \;=\; \int \mathrm{d}\boldsymbol{x}\, e^{i\boldsymbol{k}\cdot\boldsymbol{x}} \langle \psi^\dagger_\sigma(\boldsymbol{r} - \boldsymbol{x}/2, t)\, \psi_\sigma(\boldsymbol{r} + \boldsymbol{x}/2, t) \rangle \,, \tag{2.6}$$

where $\psi^\dagger_\sigma(\boldsymbol{r}, t)$ ($\psi_\sigma(\boldsymbol{r}, t)$) is a field operator that creates (annihilates) an electron with spin projection[1] σ at time t and position $\boldsymbol{r}$, one can deal with it quite analogously to the classical phase space distribution function. This includes, in particular, the applicability of a semiclassical Boltzmann equation of the form (2.5). An important condition for this to work is that the mean free path ℓ of the Fermions is much larger than the Fermi wavelength, *i.e.*, $k_F \ell \gg 1$, where k_F is the Fermi momentum.[2] In addition, the Boltzmann equation in the form (2.5) is only valid if the potentials yielding the force term vary only little on the scale of the Fermi wavelength.

The right-hand side of the semiclassical Boltzmann equation contains the collision integrals for, *e.g.*, electron-impurity scattering and electron-electron scattering,

$$\left.\frac{\partial f_{\boldsymbol{k}\,\sigma}}{\partial t}\right|_{\text{coll}} \;=\; \mathcal{J}^{\text{imp}}_{\boldsymbol{k}\,\sigma} + \mathcal{J}^{\text{e-e}}_{\boldsymbol{k}\,\sigma} . \tag{2.7}$$

The rate of change in $f_{\boldsymbol{k}\,\sigma}$ due to elastic, spin conserving scattering off non-magnetic impurities is given by

$$\mathcal{J}^{\text{imp}}_{\boldsymbol{k}\,\sigma} \;=\; \sum_{\boldsymbol{k'}} W_{\boldsymbol{k}\boldsymbol{k'}}\, \delta(\epsilon_{\boldsymbol{k}\,\sigma} - \epsilon_{\boldsymbol{k'}\,\sigma})\, [f_{\boldsymbol{k'}\,\sigma} - f_{\boldsymbol{k}\,\sigma}] \,. \tag{2.8}$$

The interpretation of this equation is rather intuitive: the density $f_{\boldsymbol{k}\,\sigma}$ gains from scattering processes with probability (per unit time) $W_{\boldsymbol{k}\boldsymbol{k'}}\, \delta(\epsilon_{\boldsymbol{k}\,\sigma} - \epsilon_{\boldsymbol{k'}\,\sigma})$ that change momentum $\boldsymbol{k'}$ into $\boldsymbol{k}$ to the extent that particles with momentum $\boldsymbol{k'}$ are available (hence the term $\propto f_{\boldsymbol{k'}\,\sigma}$). Conversely, it is decreased by processes changing $\boldsymbol{k}$ into $\boldsymbol{k'}$ (term $\propto f_{\boldsymbol{k}\,\sigma}$), for which we assumed the same probability, $W_{\boldsymbol{k'}\boldsymbol{k}} = W_{\boldsymbol{k}\boldsymbol{k'}}$. Quantum mechanics enters also here if the transition probability for the process $|\boldsymbol{k}\,\sigma\rangle \to |\boldsymbol{k'}\,\sigma\rangle$ and *vice versa* is calculated with *Fermi's golden rule* (see *e.g.* Sakurai [1994]).

The relaxation of the distribution function $f_{\boldsymbol{k}\,\sigma}$ due to electron-electron collisions is taken into account via the additional collision integral

$$\begin{aligned} \mathcal{J}^{\text{e-e}}_{\boldsymbol{k}\,\sigma} \;=\; & 2\pi \sum_{\boldsymbol{k'}\boldsymbol{q}\,\sigma'} W^{\text{e-e}}_{\sigma\sigma'}(q, |\boldsymbol{k'} - \boldsymbol{k} - \boldsymbol{q}|)\, \delta(\epsilon_{\boldsymbol{k}\,\sigma} + \epsilon_{\boldsymbol{k'}\,\sigma'} - \epsilon_{\boldsymbol{k}+\boldsymbol{q}\,\sigma} - \epsilon_{\boldsymbol{k'}-\boldsymbol{q}\,\sigma'}) \\ & \times \left[(1 - f_{\boldsymbol{k}\,\sigma})\,(1 - f_{\boldsymbol{k'}\,\sigma'})\, f_{\boldsymbol{k}+\boldsymbol{q}\,\sigma}\, f_{\boldsymbol{k'}-\boldsymbol{q}\,\sigma'} - (1 - f_{\boldsymbol{k}+\boldsymbol{q}\,\sigma}) \left(1 - f_{\boldsymbol{k'}-\boldsymbol{q}\,\sigma'}\right) f_{\boldsymbol{k}\,\sigma}\, f_{\boldsymbol{k'}\,\sigma'} \right] \end{aligned} \tag{2.9}$$

[1] With respect to some fixed quantization axis.

[2] Strictly speaking this so-called *Landau criterion* is in low dimensions $d < 3$ not sufficient to justify a Boltzmann-equation treatment. However, in this work this point is of no importance, since we are not interested in effects of, *e.g.*, weak localization. For details, see *e.g.* Rammer [1998].

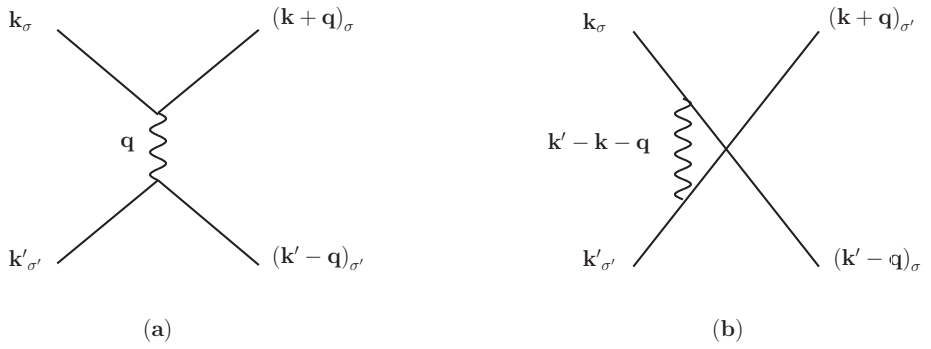

Figure 2.2.: Momentum conserving scattering of two electrons characterized by the states $|\boldsymbol{k}\,\sigma\rangle$ and $|\boldsymbol{k'}\,\sigma'\rangle$. The wiggled line represents the Coulomb interaction. If $\sigma' = \sigma$, the final states of the processes (a) and (b) are indistinguishable, and therefore their transition amplitudes need to be summed up coherently, yielding the rate (2.10).

with a transition rate due to two-particle scattering

$$W^{\mathrm{e-e}}_{\sigma\sigma'}(q, |\boldsymbol{k'}-\boldsymbol{k}-\boldsymbol{q}|) \;=\; V(q)^2 - \delta_{\sigma\sigma'}\, V(q)\, V(|\boldsymbol{k'}-\boldsymbol{k}-\boldsymbol{q}|)\,, \tag{2.10}$$

where $V(q)$ denotes the matrix element of the Coulomb potential in momentum space. The transition amplitudes for indistinguishable scattering processes (see Figure 2.1) are summed up *coherently*, *i.e., before* taking the absolute square of the matrix element in Fermi's golden rule. This explains the form of the transition rate (2.10), which has additional exchange contribution for scattering events between electrons with the same spin projection $\sigma = \sigma'$.

The structure of the distribution function factors in two-body collision integral (2.9) reflects the fact that, according to Pauli's exclusion principle, only a single electron can occupy each state. Thus, for the scattering process depicted in Figure 2.1 (a) to occur, it is not enough that both initial states $|\boldsymbol{k}\,\sigma\rangle$ and $|\boldsymbol{k'}\,\sigma'\rangle$ are occupied, but it is also required that the final states $|\boldsymbol{k}+\boldsymbol{q}\,\sigma\rangle$ and $|\boldsymbol{k'}-\boldsymbol{q}\,\sigma'\rangle$ are unoccupied. This translates into the characteristic Pauli blocking factors, *e.g.* $(1 - f_{\boldsymbol{k}+\boldsymbol{q}\,\sigma})$.[3] In equilibrium the electron-electron collision integral must be zero. In fact, this is one way to derive the famous Fermi-Dirac distribution, which has precisely the property that it makes the integrand of Eq. (2.9) vanish.

Note that the semiclassical Boltzmann equation (2.9) is *not* spin coherent, *i.e.,* it does not describe the evolution of all three spin (density) components, but only of the spin projections on a pre-defined quantization axis. Therefore, it is not possible to capture phenomena that are related to, *e.g.*, spin precession about a magnetic (or spin-orbit) field. Below we will see how spin coherent semiclassical kinetic equations can be derived from the *Liouville-von Neumann equation* for the density matrix (see Chapter 5.5.1) or using other nonequilibrium formalisms as introduced in Sections 2.2 and 2.3 of the present Chapter.

[3] In general, also the electron-impurity collision integral contains Pauli blocking factors. However, for $W_{\boldsymbol{k'k}} = W_{\boldsymbol{kk'}}$ they drop out, yielding the simple structure of Eq. (2.8).

2.2. Zubarev's Nonequilibrium statistical operator method

The Nonequilibrium statistical operator (NSO) approach as presented in detail in the book by Zubarev *et al.* [1996] is a fully-fledged, second-quantized formalism describing the irreversible evolution of nonequilibrium (quantum) systems. In the context of topics that the present thesis is concerned with, it was recently used by Auslender and Katsnelson [2007] for the derivation of a pseudospin coherent collision integral for graphene. We have chosen to present the NSO formalism in a rather detailed manner here, because it appears to be less standard than, *e.g.*, the Kadanoff-Baym or Keldysh methods (see Section 2.3). In outlining the NSO approach to the derivation of quantum kinetic equations for systems with weak interactions we closely follow Zubarev *et al.* [1996].

2.2.1. Reduced description of nonequillibrium problems

The theoretical description of nonequilibrium processes in quantum systems poses a seemingly paradoxical challenge: on the one hand, one wants to take into account the microscopic evolution according to the Liouville-von Neumann equation of motion for the density matrix, which is time *reversible*; on the other hand, one has to fulfill, as a basic principle of thermodynamics, the macroscopic demand to maximize the information entropy, which necessarily introduces time *irreversibility*. One way out of this dilemma consists in a *reduced description* relying on restricted information about the system. For instance, one can work with a coarse-grained density matrix that is averaged over small volumes in momentum space or over small time intervals.

In the NSO formalism the reduced description is based on the assumption that the state of the system is fully characterized by a set of macroscopic observables $\langle P_m \rangle^t$, which are time-dependent mean values of the *relevant operators* P_m,

$$\langle P_m \rangle^t \;=\; \mathrm{Tr}\,[\hat{\rho}(t)\, P_m]\,. \tag{2.11}$$

Here, $\hat{\rho}$ is the usual quantum mechanical statistical operator and m is a general index, which is possibly composite (*e.g.*, for momentum and spin). The relevant operators are chosen according to the timescale on which the description is meant to be accurate. To illustrate this point it is instructive to recall the hierarchy of different relaxation times in the *classical* dilute gas. In this model, each particle moves along smooth classical trajectories until, after an average free time τ_f, it enters the small interaction radius of another particle. The interaction occurs quickly during the collision time τ_c. The third timescale, τ_r, characterizes the relaxation into a local equilibrium within a volume that is macroscipically small but still large enough to contain many particles. Finally, τ_{eq} is the time it takes the system to reach its global equilibrium state. Clearly, we have the relations (see Fig. 2.2.1)

$$\tau_c \ll \tau_f \ll \tau_r \ll \tau_{\mathrm{eq}}\,. \tag{2.12}$$

If one wishes to capture the dynamics down to time intervals $\Delta t \lesssim \tau_c$, there is no chance for a reduced description, and thus one has to solve the full many body problem. For time intervals $\tau_c \ll \Delta t \ll \tau_r$ a *kinetic* description in terms of the single-particle distribution

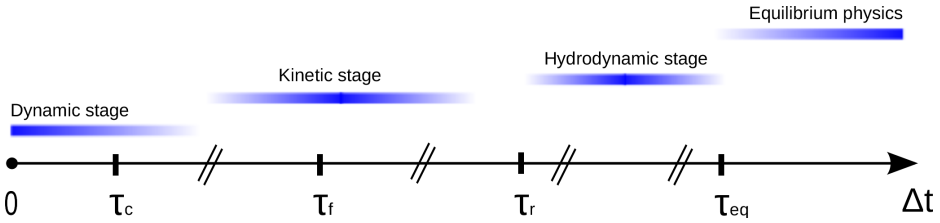

Figure 2.3.: Hierarchy of timescales in the classical dilute gas, *cf.* Eq. (2.12). Note that not all of these timescales are necessarily meaningful in all systems: *e.g.*, in a very dilute gas one has $\tau_f \lesssim \tau_{\rm eq}$, rendering the hydrodynamic stage obsolete.

function $f(\boldsymbol{r},\boldsymbol{p},t)$ as the relevant operator is meaningful. The next level is the *hydrodynamic* one. It applies in the regime $\tau_r \ll \Delta t \ll \tau_{\rm eq}$, where a local equilibrium is already established and the local densities of particle number, momentum, and energy play the role of relevant observables. The state of global equilibrium that is established for times $\Delta t \gtrsim \tau_{\rm eq}$ is completely characterized by the particle number density and temperature.

In the following we will be interested in the kinetic regime of a *quantum* gas of weakly interacting fermionic or bosonic quasiparticles. The relevant operator is

$$P_{ll'} \;=\; c_l^\dagger c_{l'}, \tag{2.13}$$

where $c_l^\dagger$ (c_l) are creation (annihilation) operators for single particle states $|l\rangle$. In this reduced description the relevant observables are the mean values of single-particle operators A, which are obtained from the single-particle density matrix

$$f_{ll'}(t) \;=\; \langle P_{l'l}\rangle^t \;=\; \mathrm{Tr}\,[\hat\rho(t)\, c_{l'}^\dagger c_l] \tag{2.14}$$

as

$$\langle A\rangle^t \;=\; \mathrm{Tr}_l[A\, f(t)] \;=\; \sum_{l\,l'} A_{ll'}\, f_{l'l}(t)\,. \tag{2.15}$$

2.2.2. Relevant statistical operator

For given $\langle P_{l'l}\rangle^t$, Eq. (2.14) does not unambiguously fix the statistical operator $\hat\rho(t)$. In equilibrium thermodynamics the valid distribution is the one that maximizes the information entropy. This leads to the famous Gibbsian ensembles. Analogously, for nonequilibrium problems one introduces as an auxiliary quantity the *relevant statistical operator* $\hat\rho_{\rm rel}(t)$, which among all statistical operators $\hat\rho'(t)$ yielding the correct expectation values $\langle P_{l'l}\rangle^t$ guarantees a maximum of entropy $S' = -\mathrm{Tr}\,[\hat\rho'(t)\,\ln\hat\rho'(t))]$. In order to find the absolute extremum of entropy under the constraints $\langle P_{l'l}\rangle^t = \mathrm{Tr}\,[\hat\rho'(t)\,P_{l'l}]$ and $\mathrm{Tr}\,\hat\rho'(t) = 1$, the Lagrange parameters $F_{ll'}(t)$ and $\lambda(t)$ are introduced. With the functional

$$S' \;=\; -\mathrm{Tr}\,[\hat\rho'(t)\,\ln\hat\rho'(t))] - \sum_{ll'} F_{ll'}(t)\,\mathrm{Tr}\,[\hat\rho'(t)\,P_{l'l}] - \lambda(t)\,\mathrm{Tr}\,\hat\rho'(t) \tag{2.16}$$

the extremal distribution is then determined from the vanishing of its first variation, $\delta S' = 0$. This procedure yields

$$\hat{\rho}_{\mathrm{rel}}(t) \;=\; \exp\left(-1-\lambda(t)-\sum_{ll'} F_{ll'}(t)\,P_{l'l}\right). \tag{2.17}$$

The normalization condition for $\hat{\rho}_{\mathrm{rel}}(t)$ fixes $\lambda(t)$, which then relates to the distribution function

$$Z(t) \;=\; \mathrm{Tr}\left[\exp\left(-\sum_{ll'} F_{ll'}(t)\,P_{l'l}\right)\right] \tag{2.18}$$

according to

$$1+\lambda(t) \;=\; \ln\, Z(t)\,. \tag{2.19}$$

The Lagrange multipliers $F_{ll'}(t)$ are determined by the self-consistency relation (cf. Eq. (2.14))

$$f_{ll'}(t) \;=\; \langle c_{l'}^{\dagger} c_l\rangle_{\mathrm{rel}}^{t}, \tag{2.20}$$

where the lower index is to say that the average must be taken with respect to $\hat{\rho}_{\mathrm{rel}}(t)$.

Averages of the form $\langle C_1\, C_2 \ldots C_s\rangle_{\mathrm{rel}}$, where C_j stands for either a creation operator $c_j^{\dagger}$ or an annihilation operator c_j, allow for *Wick decomposition*. For a proof we refer to Zubarev *et al.* [1996]. Here, we only state the important and advantageous practical implications. To this end, the *pairing* of two operators is introduced as $\overbrace{C_i\, C_j} \equiv \langle C_i\, C_j\rangle_{\mathrm{rel}}$. When permuting the operators and then pairing the first with the second, the third with the fourth and so on, we obtain a *complete system of pairings* $\overbrace{C_{i_1}\, C_{i_2}} \ldots \overbrace{C_{i_{s-1}}\, C_{i_s}}$. The content of *Wick's theorem* is that the average $\langle C_1\, C_2 \ldots C_s\rangle_{\mathrm{rel}}$ is the sum of all complete systems of pairings, each of which, in the case of fermions, obtains the sign $(-1)^{\mathcal{P}}$ with $\mathcal{P}$ indicating the parity of the permutation. Since the relevant statistical operator connects only states with the same number of particles, only pairings of the form

$$\langle c_{l'}^{\dagger} c_l\rangle_{\mathrm{rel}} \;=\; f_{ll'}\,, \tag{2.21}$$

$$\langle c_{l'} c_l^{\dagger}\rangle_{\mathrm{rel}} \;=\; \delta_{ll'} \mp f_{ll'} \tag{2.22}$$

contribute to the sum ("$-$" stands for fermions and "$+$" for bosons in Eq. (2.22)). For example, one has

$$\begin{aligned}\langle c_1\, c_2^{\dagger}\, c_3^{\dagger}\, c_4\rangle_{\mathrm{rel}} \;&=\; \langle c_1\, c_2^{\dagger}\rangle_{\mathrm{rel}}\,\langle c_3^{\dagger}\, c_4\rangle_{\mathrm{rel}} \mp \langle c_1\, c_3^{\dagger}\rangle_{\mathrm{rel}}\,\langle c_2^{\dagger}\, c_4\rangle_{\mathrm{rel}} \\ &=\; (\delta_{12}\mp f_{12})\, f_{43} \mp (\delta_{13}\mp f_{13})\, f_{42}\,. \end{aligned} \tag{2.23}$$

2.2.3. Liouville-von Neumann equation with broken time-reversal symmetry

It is important to note that the relevant distribution (2.17) is not yet the solution to a given quantum kinetic problem, since it is determined only implicitly by the macroscopic

observables $\langle P_{l'l}\rangle^t$ that determine the Lagrange parameters $F_{ll'}(t)$. In general, it does not satisfy the microscopic Liouville-von Neumann equation ($\hbar \equiv 1$)

$$\partial_t \hat{\rho}(t) + i\, L\, \hat{\rho}(t) \quad = \quad 0\,, \tag{2.24}$$

with the Liouville operator

$$L\, \hat{\rho} \quad = \quad [H_{\rm tot}, \hat{\rho}]\,, \tag{2.25}$$

where $H_{\rm tot}$ is the full Hamiltonian in second quantization. Nevertheless, with the help of the relevant statistical operator one can construct a solution of a *time irreversible* Liouville-von Neumann equation to be derived in the following, which fulfills both the microscopic and macroscopic demands.

Let us start from Eq. (2.24) and assume that at an initial point in time t_i in the past the system was described by the relevant distribution,

$$\hat{\rho}(t_i) \quad = \quad \hat{\rho}_{\rm rel}(t_i). \tag{2.26}$$

Thus, initially the statistical operator satisfies Eq. (2.14) as well as the Liouville-von Neumann equation (2.24). However, this is not the case for later times, because $\hat{\rho}(t)$ evolves according to Eq. (2.24), whereas the temporal evolution of $\hat{\rho}_{\rm rel}(t)$ is determined by the one of the observables via the self-consistency relation (2.20). Let us for notational simplicity first consider a time-independent Hamiltonian. (The generalization to problems with an explicit time dependence will become clear below when the time-ordering operator is introduced.) We then have, from Eq. (2.24) with (2.26),

$$\hat{\rho}(t) \quad = \quad e^{-i(t-t_i)\, L} \hat{\rho}_{\rm rel}(t_i). \tag{2.27}$$

In order to reflect that a macroscopic system loses the detailed memory of its initial state after some microscopic time and assuming that all times between a certain t_0 in the remote past and t are equally probable as the starting point for the evolution according to Eq. (2.27), we take its average over t_i,

$$\hat{\rho}(t) \quad = \quad \frac{1}{t-t_0} \int_{t_0}^{t} {\rm d}t_i\, e^{-i(t-t_i)L} \hat{\rho}_{\rm rel}(t_i). \tag{2.28}$$

The interval $t - t_0$ over which the average is performed has to be large enough to allow for all relevant physical correlations to build up (eventually let $t_0 \to -\infty$). Taking the time derivative we see that the averaged distribution (2.28) satisfies a modified Liouville-von Neumann equation with a source term,

$$\partial_t \hat{\rho}(t) + i\, L\, \hat{\rho}(t) \quad = \quad -\frac{\hat{\rho}(t) - \hat{\rho}_{\rm rel}(t)}{t-t_0}. \tag{2.29}$$

In Eq. (2.28) we take the limit $t - t_0 \equiv \tilde{t} \to \infty$ by introducing $t_1 \equiv t_i - t$ and using

$$\lim_{\tilde{t}\to\infty} \frac{1}{\tilde{t}} \int_{-\tilde{t}}^{0} {\rm d}t\, f(t) \quad = \quad \lim_{\eta\to 0^+} \eta \int_{-\infty}^{0} {\rm d}t\, f(t)\, e^{\eta\, t} \tag{2.30}$$

to obtain

$$\hat{\rho}(t) \;=\; \lim_{\eta\to 0^+}\eta\int_{-\infty}^{0}\mathrm{d}t_1\, e^{i\,t_1\,L}\hat{\rho}_{\mathrm{rel}}(t_1+t). \tag{2.31}$$

Before the limit process is performed, the statistical operator (2.31) obeys the Liouville-von Neumann equation with an infinitesimal source term ($\eta \to 0^+$),

$$(\partial_t + i\,L)\,\hat{\rho}(t) \;=\; -\eta\,[\hat{\rho}(t)-\hat{\rho}_{\mathrm{rel}}(t)]\,. \tag{2.32}$$

The source term introduces time irreversibility by picking the retarded solution when the average of an observable A is calculated from a statistical operator $\hat{\rho}(t)$ satisfying (2.32) according to

$$\langle A\rangle^t \;=\; \lim_{\eta\to 0^+}\lim_{\substack{N/V\,=\,\mathrm{const.}\\ V\to\infty}}\mathrm{Tr}\,[\hat{\rho}(t)\,A]. \tag{2.33}$$

It is important to take the thermodynamic limit first, see Zubarev *et al.* [1996].

2.2.4. Perturbation theory for weak interactions

Consider the total Hamiltonian

$$H_{\mathrm{tot}} \;=\; H_t^0 + V\,, \tag{2.34}$$

which contains, in addition to the part H_t^0 (where we now allow for an explicit time dependence) describing non-interacting (quasi-)particles, a weak interaction V. It is assumed that the former has the property

$$\frac{1}{i\hbar}\,[c_{l'}^\dagger c_l, H_t^0] \;=\; \sum_{m\,m'} i\,\Omega_{ll'mm'}(t)\,c_{m'}^\dagger c_m\,. \tag{2.35}$$

(In this section we display $\hbar$ explicitly.) In particular, when writing the second-quantized single-particle Hamiltionian as

$$H_t^0 \;=\; \sum_{l\,l'} h^0(l',l;t)\,c_{l'}^\dagger c_l \tag{2.36}$$

in terms of the matrix element $h^0(l',l;t)$ of the first-quantized Hamiltonian, one has

$$\Omega_{ll'mm'}(t) \;=\; \frac{1}{\hbar}\left[\delta_{lm}\,h^0(m',l';t) - \delta_{l'm'}\,h^0(l,m;t)\right]. \tag{2.37}$$

If it were not for the interaction V, one could, by virtue of relation (2.35), obtain a closed system of equations for the single-particle density matrix (2.14) simply by multiplying the Liouville-von Neumann equation (2.32) by $c_{l'}^\dagger c_l$ and taking the trace. In the presence of interactions this is in general not possible because the commutator with V does not necessarily take the form (2.35). However, as will be shown in the following, it is possible to approximately construct the nonequilibrium statistical operator to a given order in the

interaction, which then allows to derive a closed set of equations, *i.e.*, a kinetic equation describing the nonequilibrium problem at hand.

For the Hamiltonian (2.34) the retarded Liouville-von Neumann equation (2.32) becomes

$$(\partial_t + \eta)\,\hat{\rho}(t) + \frac{1}{i\hbar}\left[\hat{\rho}(t), H_t^0\right] \;=\; \eta\,\hat{\rho}_{\rm rel}(t) - \frac{1}{i\hbar}\left[\hat{\rho}(t), V\right], \tag{2.38}$$

which is (as can be easily verified by insertion) equivalent to the integral equation

$$\begin{aligned}\hat{\rho}(t) \;&=\; \eta\int_{-\infty}^{t} \mathrm{d}t'\, e^{-\eta\,(t-t')}\,\mathcal{U}_0(t,t')\,\hat{\rho}_{\rm rel}(t')\,\mathcal{U}_0^\dagger(t,t') \\ &\quad - \int_{-\infty}^{t} \mathrm{d}t'\, e^{-\eta\,(t-t')}\,\mathcal{U}_0(t,t')\,\frac{1}{i\hbar}\left[\hat{\rho}(t'), V\right]\mathcal{U}_0^\dagger(t,t')\end{aligned} \tag{2.39}$$

with the time-ordered evolution operator

$$\mathcal{U}_0(t,t') \;=\; \hat{T}\, e^{-\frac{i}{\hbar}\int_{t'}^{t}\mathrm{d}\tau\, H_\tau^0}. \tag{2.40}$$

Here, the time-ordering operator $\hat{T}$ positions the factors of an arbitrary product of operators according to their time arguments (the one with the earliest time argument goes to the very right and so on). Partial integration of the first term on the right-hand side of Eq. (2.39) yields

$$\begin{aligned}&\hat{\rho}(t) \;=\; \hat{\rho}_{\rm rel}(t) \\ &-\int_{-\infty}^{t} \mathrm{d}t'\, e^{-\eta\,(t-t')}\,\mathcal{U}_0(t,t')\left\{\partial_{t'}\hat{\rho}_{\rm rel}(t') + \frac{1}{i\hbar}\left[\hat{\rho}_{\rm rel}(t'), H_{t'}^0\right] + \frac{1}{i\hbar}\left[\hat{\rho}(t'), V\right]\right\}\mathcal{U}_0^\dagger(t,t').\end{aligned} \tag{2.41}$$

Let us next multiply Eq. (2.38) by $c_{l'}^\dagger c_l$ and take the trace. This gives

$$\partial_t\, f_{ll'}(t) - i\sum_{m\,m'}\Omega_{ll'mm'}(t)\,f_{mm'}(t) \;=\; \mathcal{J}_{ll'}(t) \tag{2.42}$$

with on the right-hand side what will become the collision term,

$$\mathcal{J}_{ll'}(t) \;=\; -\frac{1}{i\hbar}\mathrm{Tr}\left\{[V, c_{l'}^\dagger c_l]\,\hat{\rho}(t)\right\}. \tag{2.43}$$

In order to write a perturbation expansion in the interaction V starting vom Eq. (2.42) with Eq. (2.41), we need to relate the time derivative $\partial_{t'}\hat{\rho}_{\rm rel}(t')$ in Eq. (2.41) to V. Using Eq. (2.42) we can write

$$\partial_t\,\hat{\rho}_{\rm rel}(t) \;=\; \sum_{l\,l'}\frac{\delta\hat{\rho}_{\rm rel}(t)}{\delta f_{ll'}(t)}\left\{i\sum_{m\,m'}\Omega_{ll'mm'}(t)\,f_{mm'}(t) + \mathcal{J}_{ll'}(t)\right\}. \tag{2.44}$$

It can be shown[4] that

$$-\,i\sum_{l\,l'}\sum_{m\,m'}\frac{\delta\hat{\rho}_{\rm rel}(t)}{\delta f_{ll'}(t)}\,\Omega_{ll'mm'}(t)\,f_{mm'}(t) \;=\; \frac{1}{i\hbar}\left[\hat{\rho}_{\rm rel}(t), H_t^0\right] \tag{2.45}$$

[4]Apply to the $\hat{\rho}_{\rm rel}(t)$ on the left-hand side and the right-hand side of Eq. (2.45), respectively, the relation $\partial_\alpha e^{A(\alpha)} = \int_0^1 \mathrm{d}x\, e^{xA}\partial_\alpha A\, e^{(1-x)A} = \int_0^1 \mathrm{d}x\, e^{(1-x)A}\partial_\alpha A\, e^{xA}$ and the Kubo identity $[B, e^A] = \int_0^1 \mathrm{d}x\, e^{xA}\,[B,A]\,e^{-xA}\,e^A$. Here, A, B are operators and α is a general parameter. Further make use of Eqs. (2.17) and (2.35).

Thus, Eq. (2.44) takes the form

$$\partial_t\,\hat{\rho}_{\rm rel}(t)+\frac{1}{i\hbar}\left[\hat{\rho}_{\rm rel}(t),H_t^0\right] \;=\; \sum_{l\,l'}\frac{\delta\hat{\rho}_{\rm rel}(t)}{\delta f_{ll'}(t)}\,\mathcal{J}_{ll'}(t), \tag{2.46}$$

and upon insertion in Eq. (2.41) the nonequilibrium statistical operator is given as

$$\begin{aligned}\hat{\rho}(t) \;&=\; \hat{\rho}_{\rm rel}(t)\\ &-\int_{-\infty}^{t}\mathrm{d}t'\,e^{-\eta\,(t-t')}\,\mathcal{U}_0(t,t')\left\{\sum_{l\,l'}\frac{\delta\hat{\rho}_{\rm rel}(t')}{\delta f_{ll'}(t')}\,\mathcal{J}_{ll'}(t')+\frac{1}{i\hbar}\,[\hat{\rho}(t'),V]\right\}\mathcal{U}_0^\dagger(t,t').\end{aligned} \tag{2.47}$$

With this, Eqs. (2.42)-(2.43) provide an *exact* kinetic equation for the density matrix,

$$\begin{aligned}\partial_t\,f_{ll'}(t)-i\sum_{m\,m'}\Omega_{ll'mm'}(t)\,f_{mm'}(t) \;&=\; \frac{1}{i\hbar}\langle[c_{l'}^\dagger c_l,V]\rangle_{\rm rel}^t-\frac{1}{i\hbar}\int_{-\infty}^{t}\mathrm{d}t'\,e^{-\eta\,(t-t')}\,\times\\ \times\mathrm{Tr}\left\{\mathcal{U}_0^\dagger(t,t')\,[c_{l'}^\dagger c_l,V]\,\mathcal{U}_0(t,t')\left(\sum_{m\,m'}\frac{\delta\hat{\rho}_{\rm rel}(t')}{\delta f_{mm'}(t')}\,\mathcal{J}_{mm'}(t')+\frac{1}{i\hbar}\,[\hat{\rho}(t'),V]\right)\right\}.\end{aligned} \tag{2.48}$$

Next we apply the *Born approximation* in order to write a tractable kinetic equation accurate to second order in the interaction. To this end, assuming that the nonequilibrium problem is analytic in the interaction strength, we write the statistical operator and the collision integral as a series in V,

$$\hat{\rho}(t) \;=\; \hat{\rho}_{\rm rel}(t)+\sum_{k=1}^{\infty}\hat{\rho}^{(k)}(t),\qquad \mathcal{J}_{mm'}(t) \;=\; \sum_{k=1}^{\infty}\mathcal{J}_{mm'}^{(k)}(t), \tag{2.49}$$

where terms marked with a superscript (k) are proportional to V^k. By inserting (2.49) in (2.48), neglecting terms of third or higher order in the interaction and exploiting the cyclic invariance of the trace, one obtains

$$\begin{aligned}\partial_t\,f_{ll'}(t)-i\sum_{m\,m'}\Omega_{ll'mm'}(t)\,f_{mm'}(t) \;&=\; \frac{1}{i\hbar}\langle[c_{l'}^\dagger c_l,V]\rangle_{\rm rel}^t-\frac{1}{\hbar^2}\int_{-\infty}^{t}\mathrm{d}t'\,e^{-\eta\,(t-t')}\,\times\\ \times\mathrm{Tr}\left\{\hat{\rho}_{\rm rel}(t')\left(\Big[V,[(c_{l'}^\dagger c_l)(t,t'),V(t,t')]\Big]+i\hbar\sum_{m\,m'}\frac{\delta\mathcal{J}_{ll'}^{(1)}(t,t')}{\delta f_{mm'}(t')}\,c_{m'}^\dagger c_m\right)\right\},\end{aligned} \tag{2.50}$$

where the double time dependence of the operators is according to the Heisenberg picture,

$$A(t,t') \;=\; \mathcal{U}_0^\dagger(t,t')\,A\,\mathcal{U}_0(t,t'), \tag{2.51}$$

and the first order (mean field) term is

$$\mathcal{J}_{ll'}^{(1)}(t) \;=\; \frac{1}{i\hbar}\langle[c_{l'}^\dagger c_l,V]\rangle_{\rm rel}^t. \tag{2.52}$$

Notice that the averages in Eqs. (2.52) and (2.50) are taken with respect to the *relevant* statistical distribution, which allows for Wick decomposition. However, there is still one

practical obstacle to overcome: the time dependence of the relevant statistical operator on the integration variable t' means that memory effects are contained. The *Markov approximation* allows us to get rid of those. In the present context it actually amounts to a consistent implementation of the Born approximation, since the time dependence of the statistical operator $\hat{\rho}_{\mathrm{rel}}(t')$ in Eq. (2.50) is only needed to first order in the interaction, *i.e.*, without the right-hand side of Eq. (2.46). Thus, the full evolution is replaced by the free evolution,

$$\hat{\rho}_{\mathrm{rel}}(t') \;=\; \mathcal{U}_0^\dagger(t,t')\,\hat{\rho}_{\mathrm{rel}}(t)\,\mathcal{U}_0(t,t') + \mathcal{O}(V)\,, \tag{2.53}$$

leading to[5]

$$\partial_t\, f_{ll'}(t) - i\sum_{m\,m'} \Omega_{ll'mm'}(t)\, f_{mm'}(t) \;=\; \mathcal{J}^{(1)}_{ll'}(t) + \mathcal{J}^{(2)}_{ll'}(t) + \mathcal{O}(V^3) \tag{2.54}$$

with Eq. (2.37) $\mathcal{J}^{(1)}_{ll'}(t)$ as defined in Eq. (2.52) and the *second-order collision term in Markovian form*,

$$\mathcal{J}^{(2)}_{ll'}(t) = -\frac{1}{\hbar^2}\int_{-\infty}^{t} \mathrm{d}t'\, e^{\eta(t'-t)} \left\langle \Big[V(t'-t),[V,c^\dagger_{l'}c_l]\Big] + i\hbar \sum_{m\,m'} \frac{\delta \mathcal{J}^{(1)}_{ll'}(t)}{\delta f_{mm'}(t)}\, c^\dagger_{m'}c_m \right\rangle^{t}_{\mathrm{rel}}\,. \tag{2.55}$$

2.2.5. Gradient expansion and semiclassical approximation

As yet, Eq. (2.54) does not quite resemble the Boltzmann equation (2.5). In particular, the force term and the velocity term do not appear explicitely. These drift terms arise ultimately from the second term on the left-hand side of Eq. (2.54) upon Wigner transformation and *first-order gradient expansion*. This will be explained in the remainder of the present subsection.

We introduced the Wigner transformed density matrix already in Eq. (2.6). Note, however, that the general form of Eq. (2.54) with its abstract and possibly composed indices gives us the freedom to keep the matrix structure in spin space while treating the spatial coordinates semiclassically, *i.e.,* going over to slowly varying center-of-mass coordinates and integrating out the fast oscillating relative coordinates. In the following we will therefore work with the semiclassical density matrix

$$f_{\boldsymbol{k}\,\sigma\sigma'}(\boldsymbol{r},t) \;=\; \int \mathrm{d}\boldsymbol{x}\, e^{i\boldsymbol{k}\cdot\boldsymbol{x}} \langle \psi^\dagger_{\sigma'}(\boldsymbol{r}-\boldsymbol{x}/2,t)\,\psi_\sigma(\boldsymbol{r}+\boldsymbol{x}/2,t)\rangle \tag{2.56}$$

instead of the spin-diagonal version Eq. (2.6). We can easily rewrite Eq. (2.54) for field operators in real space, $\psi_\sigma(\boldsymbol{r})$ ($\psi^\dagger_\sigma(\boldsymbol{r})$) instead of the creation (annihilation) operator c_l ($c^\dagger_l$), *i.e.,* understand the composed index l as space coordinate and spin. In order to obtain an equation for $\partial_t f_{\boldsymbol{k}\,\sigma\sigma'}(\boldsymbol{r},t)$ we apply the Wigner transformation to Eq. (2.54).

[5] Use that, with Eq. (2.53), $\mathcal{J}^{(1)}_{ll'}(t,t') \approx \mathcal{J}^{(1)}_{ll'}(t)$ and $\sum_{m\,m'} \frac{\delta \mathcal{J}^{(1)}_{ll'}(t)}{\delta f_{mm'}(t')} c^\dagger_{m'}c_m \approx \sum_{m\,m'} \frac{\delta \mathcal{J}^{(1)}_{ll'}(t)}{\delta f_{mm'}(t')} (c^\dagger_{m'}c_m)(t,t')$, see Zubarev *et al.* [1996].

The second term on the left-hand side is a convolution product in real space of single-particle Hamiltonian and density matrix. Upon Wigner transformation the convolution of two operators X and Y is translated according to[6]

$$[X\,Y]\,(\boldsymbol{r},t;\boldsymbol{k},\omega) \longrightarrow X(\boldsymbol{r},t;\boldsymbol{k},\omega)\,e^{\frac{i}{2}\mathcal{D}}\,Y(\boldsymbol{r},t;\boldsymbol{k},\omega)\,, \tag{2.57}$$

where the matrix product in spin remains, but the convolution of time and real space variables is replaced by a *Moyal product* with a Poisson-bracket-like gradient $\mathcal{D}$.

The *semiclassical approximation* consists in taking the gradient expansion of this exponential operator only to first order. The underlying assumption is that external perturbations, such as electromagnetic potentials, change negligibly on length and time scales of the de Broglie wavelength λ_{B} and the time $\tau_{\mathrm{B}} \equiv \lambda_{\mathrm{B}}/v_{\mathrm{F}}$. In a *gauge invariant* formulation applicable to situations where the electromagnetic fields are weak and vary "slowly" (see *e.g.* Zubarev *et al.* [1996]), one introduces the kinetic momentum $\boldsymbol{k}(\boldsymbol{p},\boldsymbol{r},t) = \boldsymbol{p} - e\,\boldsymbol{A}(\boldsymbol{r},t)$ (*cf.* Eq. (2.3)) and the renormalized frequency $\tilde{\omega}(\omega,\boldsymbol{r},t) = \omega - e\,\phi(\boldsymbol{r},t)$ and lets $\{\boldsymbol{r},\boldsymbol{k},t,\tilde{\omega}\}$ become the new set of independent variables (*i.e.*, $\partial_{r_i}\boldsymbol{k} = 0$). This changes the gradient into

$$\mathcal{D} \;=\; \overleftarrow{\partial}_{r_i}\overrightarrow{\partial}_{k_i} - \overleftarrow{\partial}_{k_i}\overrightarrow{\partial}_{r_i} + \overleftarrow{\partial}_{\tilde{\omega}}\overrightarrow{\partial}_{t} - \overleftarrow{\partial}_{t}\overrightarrow{\partial}_{\tilde{\omega}} + E_i(\overleftarrow{\partial}_{\tilde{\omega}}\overrightarrow{\partial}_{k_i} - \overleftarrow{\partial}_{k_i}\overrightarrow{\partial}_{\tilde{\omega}}) + \epsilon_{ijl}B_i\overleftarrow{\partial}_{k_j}\overrightarrow{\partial}_{k_l} \tag{2.58}$$

with the notation $X\overleftarrow{\partial}Y := (\partial X)Y$ and $X\overrightarrow{\partial}Y := X(\partial Y)$.

Operating this gradient on the single-particle Hamiltonian and the density matrix in the second term of Eq. (2.54) yields the familiar velocity term (*cf.* Eq. (2.2)), a driving term containing the electric field E and, in the presence of a magnetic field $\boldsymbol{B}$, the Lorentz force and the spin precession term. For the generic Hamiltonian (1.5) one further obtains a term for the spin precession about the spin-orbit field (see already Eq. (3.16)), which will play an important role in the following chapters.

2.3. Green's function approaches

Green's functions are a widely used tool for the description of equilibrium as well as nonequilibrium physics. In this section we briefly summarize the key elements of the *Kadanoff-Baym approach* to nonequilibrium phenomena, which is for the kind of problems addressed in the remainder of this thesis (in particular Chapter 5) equivalent to the *Keldysh formalism*.[7] Since the involved concepts (*e.g.* the *self-energy*) and basic equations are more established than the Nonequilibrium statistical operator method presented in Section 2.2 and extensive literature on the subject is available, we refrain from presenting explicit derivations. For details of this kind consult, *e.g.*, Haug and Jauho [2008] on the Kadanoff-Baym formalism and Rammer [2007] on the Keldysh method.

[6] Here we consider the general case where also the time variable is Wigner transformed.

[7] In general, Kadanoff-Baym is more powerful than Keldysh because it can deal with interaction terms in the equilibrium Hamiltonian and incorporates effects of initial correlations, thus making the study of transient phenomena possible6.

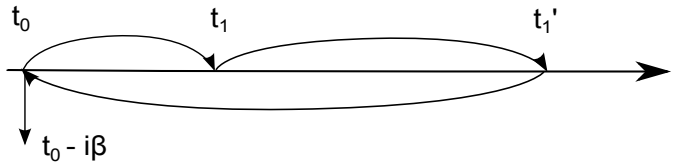

Figure 2.4.: Contour C. The integration starts from t_0 and then goes slightly above the real axis (C_1) towards $\max(t_1, t_{1'})$, then it goes back to t_0 slightly below the real axis (C_2) and finally to $t_0 - i\,\beta$, where $\beta \equiv k_B T$. In the depicted situation, t_1 is located on C_1.

The central quantity is the *contour ordered Green's function*

$$G(1,1') \;=\; -i\langle \hat{T}_C\,[\psi(1)\psi^\dagger(1')]\rangle\,, \tag{2.59}$$

where we abbreviated the arguments of the field operators, *e.g.*, $(1) \equiv (\boldsymbol{r_1}, t_1)$. The contour ordering operator $\hat{T}_C$ arranges the operators according to the position of their time arguments on the Kadanoff-Baym contour depicted in Figure 2.3. The time dependence of the field operators is according to the Heisenberg picture.

Depending on the position of the time arguments, the contour ordered Green's function can be one of the four

$$G(1,1') \;=\; \begin{cases} G_c(1,1') & t_1, t_{1'} \in C_1 \\ G^{>}(1,1') & t_1 \in C_2,\, t_{1'} \in C_1 \\ G^{<}(1,1') & t_1 \in C_1,\, t_{1'} \in C_2 \\ G_{\tilde{c}}(1,1') & t_1, t_{1'} \in C_2 \end{cases}\,, \tag{2.60}$$

where $G_c(1,1')$ ($G_{\tilde{c}}(1,1')$) is called the *(anti)causal* Green's function and $G^{>}(1,1')$ ($G^{<}(1,1')$) the *greater (lesser)* Green's function. Furthermore, it is useful to introduce the *retarded* and *advanced* Green's functions

$$G^r(1,1') \;=\; \theta(t_1 - t_{1'})\left[G^{>}(1,1') - G^{<}(1,1')\right], \tag{2.61}$$

$$G^a(1,1') \;=\; \theta(t_{1'} - t_1)\left[G^{<}(1,1') - G^{>}(1,1')\right]. \tag{2.62}$$

The ultimate goal is to derive tractable kinetic equations based on the equation of motion for the nonequilibrium Green's function. Using a transformation that involves S-Matrices defined along the contour C and along a simpler contour without an excursion into along the imaginary axis at the end, one can bring the contour ordered Green's function to a form that has a perturbation expansion based on Wick's theorem (see Section 2.2.2). For details we refer to Haug and Jauho [2008].

Introducing a *self-energy* Σ to resum effects of the interaction one can writing the *Dyson equation* for the contour-ordered Green's function (see *e.g.* Rammer [2007]). An analytical continuation from the complex arguments to real times is most conveniently achieved by using *Langreth's rules* [Haug and Jauho, 2008]. This yields the *generalized Kadanoff-Baym equation* [Kadanoff and Baym, 1962; Langreth and Wilkins, 1972] in its integral form,

$$G^{<} \;=\; G^{\mathrm{R}}\,\Sigma^{<}\,G^{\mathrm{A}} + (1 + G^{\mathrm{R}}\,\Sigma^{\mathrm{R}})\,G^{0<}\,(1 + \Sigma^{\mathrm{A}} G^{\mathrm{A}})\,, \tag{2.63}$$

where all products are to be interpreted as convolution products in real space/time and in spin variables. The retarded and advanced components are determined by the Dyson equations $((G^0)^{-1} - \Sigma^{\mathrm{R}})G^{\mathrm{R}} = 1$ and $((G^0)^{-1} - \Sigma^{\mathrm{A}})G^{\mathrm{A}} = 1$.

In Chapter 5.5.3 we will see with the concrete example of electron-impurity interactions how this equation is further transformed into the differential form of the Kadanoff-Baym equation and ultimately into a kinetic equation with drift terms and a collision integral. We will further discuss the issue of an appropriate ansatz for the solution of such equations.

3. Relaxation of the persistent spin helix – the role of electron-electron scattering

In this chapter we study the dynamics of an unusually (*a priori* infinitely) long-lived helical wave of spin polarization that can exist in semiconductor quantum wells where the Rashba and linear Dresselhaus spin-orbit interactions are precisely of equal magnitude. The relaxation of this *persistent spin helix* [Bernevig *et al.*, 2006] displays, according to recent measurements by Koralek *et al.* [2009], an intriguing temperature dependence with, notably, a so far unexplained maximum. In order to address the temperature-dependent lifetime of this peculiar excitation we derive and solve a semiclassical spin diffusion equation, taking into account spin-dependent impurity scattering, cubic Dresselhaus spin-orbit interactions and, in particular, electron-electron interactions in addition to the basic ingredients (*i.e.*, Rashba and linear Dresselhaus spin-orbit coupling and spin-independent impurity scattering). By comparison with data of Koralek *et al.* we establish that in the experimentally relevant regime the lifetime of the persistent spin helix is mainly determined by the interplay of cubic Dresselhaus spin-orbit coupling and electron-electron scattering. We propose that a spatially damped spin profile can have even larger lifetimes than the genuine persistent spin helix state. Most of the results presented here have been published in Lüffe *et al.* [2011].

3.1. Motivation and experiment

Semiconductor devices with important spin-orbit interactions have attracted extensive attention over the past years (for a survey, see Awschalom *et al.* [2002]; Žutić *et al.* [2004]; Awschalom and Flatté [2007]). The coupling between the orbital motion of the charge carriers and their spin allows for an electric generation and manipulation of spin polarization in the absence of ferromagnetism or external magnetic fields. This opens up the perspective of adding the spin degree of freedom to the existing semiconductor logic in information technology while circumventing the challenge to artificially integrate local magnetic fields in devices [Awschalom and Samarth, 2009]. On the other hand, spin-orbit interactions inevitably contribute to spin dephasing and spin relaxation. In general, this is an unwelcome effect, since, from the point of view of technological applications, it is obviously desirable to maximize the spin lifetimes and spin coherence lengths.

A promising candidate setting where spin-orbit coupling could be exploited for spin manipulation, but at the same time the unwanted spin-orbit coupling induced spin relaxation is absent (or minimal) is a two-dimensional electron systems with Rashba and linear Dresselhaus spin-orbit interactions of equal magnitude. Schliemann *et al.* [2003] were the first to notice that the case of equal Rashba and Dresselhaus spin-orbit coupling is special and they used this insight to propose a *nonballistic* version of the famous Datta-Das

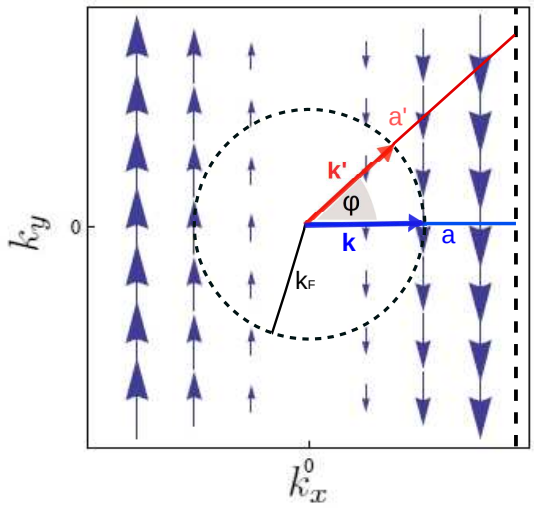

Figure 3.1.: Blue arrows mark the spin-orbit field $\boldsymbol{b}(\boldsymbol{k}) = -2\,\alpha\,v_F\,k_x\,\hat{\boldsymbol{y}}$ in momentum space for Rashba and linear Dresselhaus spin-orbit interactions of equal strength α. The dashed circle is the Fermi circle. Two electron spins that are initially oriented in z-direction and travel with the Fermi velocity v_F along paths a and a' (in real space), respectively, precess about $\hat{\boldsymbol{y}}$ by the *same* angle $\omega = 2\,b\,t = 2\,b'\,t' = -4\,\alpha\,k_F\,a$. The larger traveling time $t' = t/\cos\phi$ is exactly made up for by the smaller precession frequency $b' = b\cos\phi$. For $a = 2\pi/q_0$, with the "magic" wave number $q_0 = 4\,k_F\,\alpha$, both spins perform a full precession by $\omega = 2\pi$. Thus, within a helical spin density profile of wave vector $q_0\,\hat{\boldsymbol{x}}$, it does not matter how exactly the individual spins of the ensemble diffuse and precess back and forth due to spin-independent scattering—they will always match the orientation of this profile, thus rendering it *persistent*.

spin field effect transistor [Datta and Das, 1990]. Later, Bernevig *et al.* [2006] uncovered a novel SU(2) symmetry in the corresponding Hamiltonian. This symmetry implies the perfect conservation of a helical spin density wave with a "magic" wave vector whose magnitude depends on the spin-orbit coupling strength. They named this peculiar excitation the *persistent spin helix* (PSH). Its characteristic shape is depicted in the lower panel of Figure 3.3.

As put forward by Bernevig *et al.* [2006] and shown explicitly by Chen and Chang [2008], an alternative way of deriving the persistent spin helix is to see the spin-orbit interaction as a non-Abelian SU(2) gauge potential [Jin *et al.*, 2006] and to apply a gauge transformation (acting as a local spin rotation) that, under the PSH conditions, maps the Hamiltonian on the one of the free electron gas. The transformed PSH profile, which is simply a uniform spin polarization, is then obviously conserved. In this context, see also Yang *et al.* [2008], Tokatly and Sherman [2010] and Geißler [2010].

On a less abstract level the PSH can also be understood as arising from the combination of spin diffusion and spin precession: as depicted in Figure 3.1, the momentum-dependent

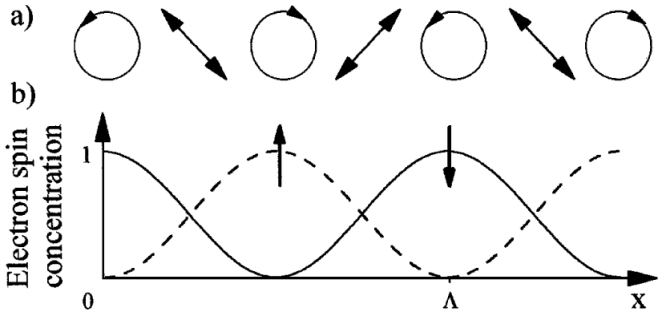

Figure 3.2.: Schematic creation of a spin grating in a GaAs quantum well: a pair of coherent near-bandgap laser beams with perpendicular linear polarizations are brought to interfere at the semiconductor surface, producing a pattern of photon helicity as shown in panel a). Since, via the optical orientation effect (see Meier and Zakharchenya [1984]), the photon helicity couples directly to the spin of the excited carriers, a sinusoidal profile of out-of-plane spin polarization is created [panel b)], which in turn translates into a grating of different diffraction indices for photons of different helicity, allowing for the time-resolved detection of the spin grating with polarized probe pulses. *This figure is adopted from Cameron et al. [1996].*

spin-orbit field is aligned in the y-direction with its magnitude increasing linearly with the projection of the momentum argument on the x-axis. If an itinerant spin-up electron from within the PSH starts, for instance, at the crest of z-spin polarization and travels with the Fermi velocity along the PSH wave vector (here the x-direction), its spin precesses precisely by a full angle 2π during the time it takes to cover the distance of one PSH wavelength, *i.e.*, to reach the neighboring crest. If the electron propagates off direction, the spin will still match the phase of the surrounding spin density (the initial PSH profile) everywhere because the larger traveling time to the neighboring crest is exactly compensated by the smaller precession frequency.

A remarkable progress on the experimental side was the recent realization of the persistent spin helix in a GaAs/AlGaAs quantum well by Koralek *et al.* [2009]. They applied the technique of *transient spin grating* (TSG) spectroscopy [Cameron *et al.*, 1996] in order to optically excite a sinusoidal pattern of out-of-plane spin polarization with the "magic" PSH wave vector (see Figure 3.2 and upper panel of Figure 3.3). Due to the presence of symmetry breaking effects in a real quantum well no state of infinite lifetime was observed, but instead two exponentially decaying modes (see Figure 3.4a), which Koralek *et al.* labeled the spin-orbit *reduced* and *enhanced* mode—the latter being the actual PSH (see lower panel of Figure 3.3). Although the lifetime of the observed PSH mode is not infinite it is still of the order of 100 ps, exceeding typical transient spin grating lifetimes by two orders of magnitude. Interestingly, as can be seen in Figure 3.5, the observed temperature dependence of the PSH lifetime displays a maximum close to 100 K.

In order to enhance the stability of the PSH it is necessary to figure out what the

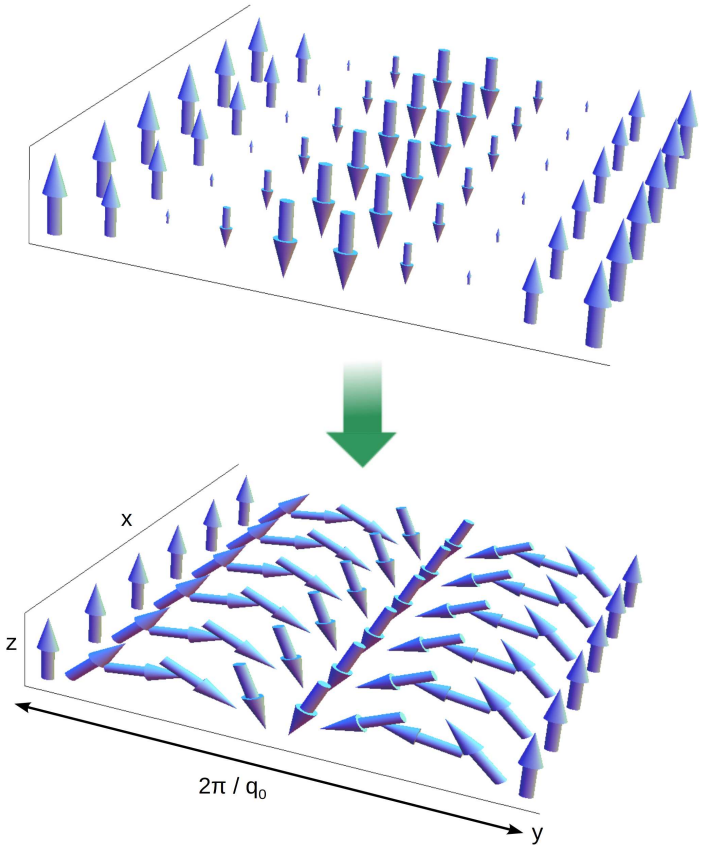

Figure 3.3.: Schematic representation of the transient spin grating experiment by Koralek *et al.*: initially, a sinusoidal profile of z-spin density with the "magic" wave number q_0 is excited in the GaAs quantum well (upper panel) using the optical orientation effect. This initial condition is a superposition of two helical modes with opposite winding sense. The backward winding mode decays quickly on the timescale τ_R, leaving only the forward winding *persistent spin helix* mode (lower panel) with the much longer lifetime τ_E.

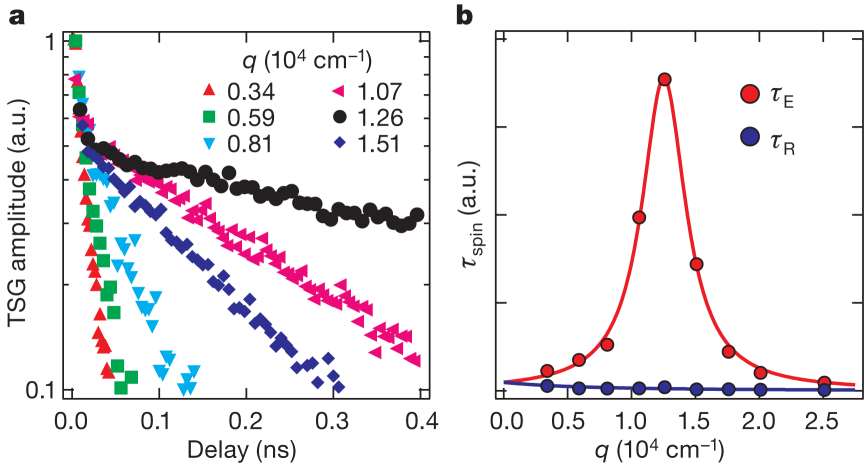

Figure 3.4.: **a**. Temporal evolution of the z-spin density for different wave numbers q as monitored by analyzing the intensities of transmitted and reflected polarized probe pulses (for details of the detection scheme see Weber [2005]). The decay follows a double-exponential function, from which the lifetimes of the spin-orbit *enhanced* and *reduced* modes, τ_E and τ_R, are deduced. **b**. When approaching the "magic" wave number q_0, τ_E increases by nearly two orders of magnitude. *This figure is taken from Koralek et al. [2009].*

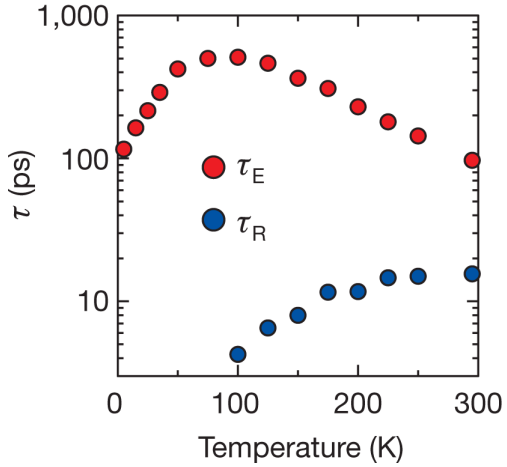

Figure 3.5.: Temperature-dependent lifetimes of each helix mode for the wave number q_0 (as determined by maximizing τ_E at fixed temperature $T = 75$ K). *This figure is taken from Koralek et al. [2009].*

dominant relaxation mechanisms are. The temperature dependence of the PSH lifetime suggests the involvement of electron-electron interactions [Koralek *et al.*, 2009], which are known to relax spin currents via the *spin Coulomb drag* effect [D'Amico and Vignale, 2000; Flensberg *et al.*, 2001; D'Amico and Vignale, 2003; Weber *et al.*, 2005]. However, since electron-electron interactions *per se* respect the SU(2) symmetry of the PSH state, they cannot be the sole reason for a finite lifetime, but other symmetry breaking mechanisms must be present as well.

It is the purpose of the present chapter to develop a theoretical understanding of the PSH lifetime and of possible ways to improve upon this lifetime. In particular, we consider the effect of Coulomb scattering in the diffusive D'yakonov-Perel' regime. Regarding symmetry breaking mechanisms, our model (Section 3.2) takes into account the effect of extrinsic spin-orbit coupling (see *e.g.* Raimondi and Schwab [2009]), which results from the interaction of the conduction electron spins with the impurities, as well as cubic Dresselhaus spin-orbit interaction, which is known to be present in the experimental quantum well to a non-negligible amount [Koralek *et al.*, 2009]. In Section 3.3, we show in which ways these effects enter the spin diffusion equation (*cf.* Burkov *et al.* [2004]; Mishchenko *et al.* [2004]; Stanescu and Galitski [2007]; Weng *et al.* [2008]) that describes the dynamics of the spin density. In Section 3.4 we discuss the resulting PSH lifetime. The symmetry-breaking mechanisms of our model are at first considered separately and under the simplifying assumption that the renormalization of the linear Dresselhaus spin-orbit coupling due to cubic one is negligible. We propose a spatially damped initial spin profile in order to enhance the TSG lifetime in presence of symmetry breaking mechanisms. For the experimental parameters of Koralek *et al.* [2009] it turns out that electron-electron interactions in combination with cubic Dresselhaus spin-orbit interactions are the key ingredients to qualitatively explain the temperature dependence of the PSH lifetime (Section 3.5). We also find reasonable quantitative agreement in the (temperature) range of validity of our theory. A summary and outlook on possible extensions of the theory are given in the concluding Section 3.6.

3.2. Model

As discussed in the introductory Chapter 1.1.1, in the standard envelope-function description (see *e.g.* Winkler [2003]), the spin-orbit interaction of conduction band electrons in a semiconductor quantum well takes the form of a momentum-dependent, in-plane effective magnetic field. The two dominant contributions to this field are linear in the in-plane momentum: The Rashba field [Bychkov and Rashba, 1984], which has winding number 1 in momentum space (*cf.* Eq. (1.3)), is caused by structure inversion asymmetry and can be tuned by changing the doping imbalance on both sides of the quantum well. The linear Dresselhaus contribution [Dresselhaus, 1955], in contrast, has winding number -1. Its physical origin is the bulk inversion asymmetry of the zinc-blende type quantum well material. It is proportional to the kinetic energy of the electron's out-of-plane motion and therefore decreases quadratically with increasing well width. In addition, a small cubic Dresselhaus spin-orbit interaction is present as well.

We write the Hamiltonian for conduction band electrons in the (001) grown quantum

well as

$$H \;=\; H_0 + H_{\rm imp} + H_{\text{e-e}}. \tag{3.1}$$

The first term represents a two-dimensional electron gas (2DEG) with a quadratic dispersion and intrinsic spin-orbit interaction,

$$H_0 \;=\; \sum_{s,s';\boldsymbol{k}} \psi^\dagger_{\boldsymbol{k}s'}\, \mathcal{H}_{0s's}\, \psi_{\boldsymbol{k}s}\,, \tag{3.2}$$

where the 2×2 matrix in spin space

$$\mathcal{H}_0 \;=\; \epsilon_k + \boldsymbol{b}(\boldsymbol{k}) \cdot \boldsymbol{\sigma} \tag{3.3}$$

exhibits the form of our generic single-particle Hamiltonian (1.5). The symbols $\psi^\dagger_{\boldsymbol{k}s}$ ($\psi_{\boldsymbol{k}s}$) are creation (annihilation) operators for electrons with momentum $\boldsymbol{k}$ and spin projection s. Within the envelope function approximation [Winkler, 2003] one finds $\epsilon_k = \frac{\hbar^2 k^2}{2\,m}$ where m is the effective mass. The vector of Pauli matrices is denoted by $\boldsymbol{\sigma}$. The in-plane spin-orbit field

$$\boldsymbol{b}(\boldsymbol{k}) \;=\; \boldsymbol{b}_R(\boldsymbol{k}) + \boldsymbol{b}_D(\boldsymbol{k}) \tag{3.4}$$

contains Rashba as well as linear and cubic Dresselhaus spin-orbit interactions of the form (henceforth we set $\hbar \equiv 1$)

$$\boldsymbol{b}_R(\boldsymbol{k}) \;=\; \alpha\, v_F \begin{pmatrix} k_y \\ -k_x \end{pmatrix}, \tag{3.5}$$

$$\begin{aligned} \boldsymbol{b}_D(\boldsymbol{k}) \;=\;& v_F \cos 2\phi \left[\beta' \begin{pmatrix} -k_x \\ k_y \end{pmatrix} - \gamma\, \frac{k^3}{4} \begin{pmatrix} \cos 3\theta \\ \sin 3\theta \end{pmatrix}\right] \\ &+ v_F \sin 2\phi \left[\beta' \begin{pmatrix} k_y \\ k_x \end{pmatrix} + \gamma \frac{k^3}{4} \begin{pmatrix} \sin 3\theta \\ -\cos 3\theta \end{pmatrix}\right] \end{aligned} \tag{3.6}$$

(see *e.g.* Weng *et al.* [2008]). Here, v_F is the Fermi velocity, the angle θ gives the direction of $\boldsymbol{k}$ with respect to the x axis and ϕ denotes the angle between the latter and the (100) crystal axis. The strength of the Rashba spin-orbit field is controlled by α and the coefficient for linear Dresselhaus coupling β' contains a momentum-dependent renormalization due to the presence of cubic Dresselhaus coupling,

$$\beta' \;=\; \beta - \gamma\, k^2/4\,, \tag{3.7}$$

where the "bare" linear Dresselhaus coefficient β is related to the one for cubic Dresselhaus γ via $\beta = \gamma \langle k_z^2 \rangle = \gamma\, (\pi/d)^2$ (d being the quantum well width). We assume in the following that the spin-orbit interaction is small compared to the Fermi energy E_F, *i.e.*, $b_F/E_F \ll 1$, where $b_F \equiv b(k_F)$ with k_F denoting the Fermi momentum.

Furthermore, we have included in Eq. (3.1) electron-impurity interactions,

$$H_{\rm imp} \;=\; \frac{1}{V} \sum_{s,s';\boldsymbol{k},\boldsymbol{k'}} \psi^\dagger_{\boldsymbol{k'}s'} U_{\boldsymbol{k'}\boldsymbol{k}s's}\, \psi_{\boldsymbol{k}s} \tag{3.8}$$

(henceforth we set the volume $V \equiv 1$). The impurity potential is a matrix in spin space,

$$\hat{U}_{\boldsymbol{k}\boldsymbol{k'}} \;=\; V^{\mathrm{imp}}_{\boldsymbol{k}\boldsymbol{k'}}\left(\{\boldsymbol{R}_i\}\right)\left(1+\sigma_z\, i\,\lambda_0^2/4\,\left[\boldsymbol{k}\times\boldsymbol{k'}\right]_z\right), \tag{3.9}$$

where the spin-dependent part arises from extrinsic spin-orbit interaction of the conduction electrons with the impurity potential, *cf.* Raimondi and Schwab [2009]. In real space the matrix operator for electron-impurity interactions reads

$$\hat{U}(\boldsymbol{x}) \;=\; V^{\mathrm{imp}}(\boldsymbol{x}) + i\,\lambda_0^2/4\left[\boldsymbol{\sigma}\times\boldsymbol{\nabla}V^{\mathrm{imp}}(\boldsymbol{x})\right]\cdot\boldsymbol{\nabla} \tag{3.10}$$

with $V^{\mathrm{imp}}(\boldsymbol{x}) = \sum_i v(\boldsymbol{x}-\boldsymbol{R}_i)$, where $v(\boldsymbol{x})$ denotes the potential of each single impurity, and $\{\boldsymbol{R}_i\}$ are the impurity positions (eventually to be averaged over). The material parameter $\lambda_0 = 4.6\times10^{-10}\,\mathrm{m}$, obtained from band structure calculations for GaAs (*cf.* Eq. (1.2)), characterizes the spin-orbit coupling for conduction band electron spins in the presence of electric fields. It is also hidden in the Rashba spin-orbit coupling constant, where the electric field is not caused by impurity potentials but by the confining quantum well potential. Eq. (3.9) with $V^{\mathrm{imp}}_{\boldsymbol{k}\boldsymbol{k'}}\left(\{\boldsymbol{R}_j\}\right) = \sum_j v(\boldsymbol{k'}-\boldsymbol{k})\, e^{-i(\boldsymbol{k'}-\boldsymbol{k})\cdot\boldsymbol{R}_j}$ is then obtained by Fourier transformation.

Finally, the Hamiltonian (3.1) contains electron-electron interactions

$$H_{\text{e-e}} \;=\; \frac{1}{2}\sum_{\substack{\boldsymbol{k_1}\ldots\boldsymbol{k_4}\\ s_1,s_2}} V_{\boldsymbol{k_3},\boldsymbol{k_4},\boldsymbol{k_1},\boldsymbol{k_2}}\,\psi^\dagger_{\boldsymbol{k_4}s_2}\psi^\dagger_{\boldsymbol{k_3}s_1}\psi_{\boldsymbol{k_1}s_1}\psi_{\boldsymbol{k_2}s_2} \tag{3.11}$$

with the Thomas-Fermi screened Coulomb potential (see *e.g.* Akkermans and Montambaux [2007])

$$V_{\boldsymbol{k_3},\boldsymbol{k_4},\boldsymbol{k_1},\boldsymbol{k_2}} \;=\; \delta_{\boldsymbol{k_1}+\boldsymbol{k_2}-\boldsymbol{k_3}-\boldsymbol{k_4},0}\,\frac{v(|\boldsymbol{k_3}-\boldsymbol{k_1}|)}{\epsilon(|\boldsymbol{k_3}-\boldsymbol{k_1}|)}\,, \tag{3.12}$$

where $v(q) = \frac{\hbar^2 2\pi}{m\,q\,a^*}$ is the Fourier-transformed Coulomb potential in 2d and $\epsilon(q) \approx 1+\frac{2}{q\,a^*}$ denotes the polarizability. Here, $a^* = \frac{\hbar^2 4\pi\,\epsilon_0\,\epsilon_r}{m\,e^2}$ is the effective Bohr radius. For the GaAs dielectric constant we will take the typical value $\epsilon_r = 12.9$ [Blakemore, 1987] in numerical evaluations.

3.3. Derivation of the spin diffusion equation

In this section, starting with the semiclassical kinetic equation (3.16) for the spin density, we derive the general spin diffusion equation (3.48). This derivation is based on the expansion of the momentum space spin density in terms of winding numbers (Eqs. (3.22)-(3.25)) and uses the separation of time scales in the D'yakonov-Perel' regime [D'yakonov and Perel', 1972]. More precisely, by momentum integration of the kinetic equation, we derive continuity equations (3.31)-(3.33) for the isotropic spin components and the generalized Ohm's laws, Eqs. (3.38) and (3.45), for the anisotropic spin components. Plugging the steady state solutions for the anisotropic spin components into the isotropic equations we arrive at the general spin diffusion equation (3.48). It is valid for general initial and

boundary conditions and takes into account all SU(2) breaking elements of our model as presented in the previous section. Eq. (3.48) is the basis of our investigation of the PSH lifetime in the following Sections 3.4 and 3.5, where the choice of a definite initial condition similar to the experiment by Koralek *et al.* [2009] reduces the problem to the 2×2 diffusion equations (3.59) and (3.74), respectively.

3.3.1. Semiclassical kinetic equation

Our goal is to describe the dynamics of the spin density in real space. Using the Nonequilibrium statistical operator method[1] (see Chapter 2 and Zubarev *et al.* [1996]) we derive kinetic equations for the charge and spin components of the Wigner transformed density matrix

$$\hat{\rho}_{\boldsymbol{k}}(\boldsymbol{x},t) \;=\; n_{\boldsymbol{k}}(\boldsymbol{x},t) + \boldsymbol{s}_{\boldsymbol{k}}(\boldsymbol{x},t)\cdot\boldsymbol{\sigma}, \tag{3.13}$$

where (*cf.* Eq. (2.56))

$$\rho_{\boldsymbol{k};ss'}(\boldsymbol{x},t) \;=\; \int \mathrm{d}\boldsymbol{r}\, e^{i\boldsymbol{k}\cdot\boldsymbol{r}} \langle \psi^\dagger_{s'}(\boldsymbol{x}-\boldsymbol{r}/2,t)\,\psi_s(\boldsymbol{x}+\boldsymbol{r}/2,t)\rangle\,. \tag{3.14}$$

If we restrict our calculation to the zeroth order in b/E_F and furthermore neglect terms that are nonlinear in the spin density $\boldsymbol{s}_{\boldsymbol{k}}(\boldsymbol{x},t)$,[2] the equations for charge and spin read

$$\partial_t\, n_{\boldsymbol{k}} + \boldsymbol{v}\cdot\partial_{\boldsymbol{x}}\, n_{\boldsymbol{k}} \;=\; \mathcal{J}^{\text{imp}}_{\boldsymbol{k}} + \mathcal{J}^{\text{e-e}}_{\boldsymbol{k}}, \tag{3.15}$$

$$2\,\boldsymbol{s}_{\boldsymbol{k}}\times\boldsymbol{b}(\boldsymbol{k}) + \partial_t\,\boldsymbol{s}_{\boldsymbol{k}} + \boldsymbol{v}\cdot\partial_{\boldsymbol{x}}\,\boldsymbol{s}_{\boldsymbol{k}} \;=\; \boldsymbol{\mathcal{J}}^{\text{imp}}_{\boldsymbol{k}} + \boldsymbol{\mathcal{J}}^{\text{e-e}}_{\boldsymbol{k}} \tag{3.16}$$

with $v_i = k_i/m$, where the index $i = x, y$ labels the in-plane spatial directions. Note that the spin and charge equations decouple in this approximation because the gradient terms containing $\partial_{k_i}\boldsymbol{b}(\boldsymbol{k})$, which would connect them, are of higher order in b/E_F. Moreover, in the diffusive limit $b_F\tau \ll 1$ (where τ is the momentum relaxation time), they would yield terms of higher order in the small parameter $b_F\tau$, see Burkov *et al.* [2004] and Stanescu and Galitski [2007]. On the right-hand side of Eqs. (3.15)-(3.16), we have the collision integrals for impurity scattering,

$$\mathcal{J}^{\text{imp}}_{\boldsymbol{k}} = -\sum_{\boldsymbol{k}'} W_{\boldsymbol{k}\boldsymbol{k}'}\,\delta(\Delta\epsilon)\,\Delta n\left\{1+\frac{\lambda_0^4}{16}\left[(\boldsymbol{k}\times\boldsymbol{k}')_z\right]^2\right\}, \tag{3.17}$$

$$\boldsymbol{\mathcal{J}}^{\text{imp}}_{\boldsymbol{k}} = -\sum_{\boldsymbol{k}'} W_{\boldsymbol{k}\boldsymbol{k}'}\,\delta(\Delta\epsilon)\left\{\Delta\boldsymbol{s}+\frac{\lambda_0^2}{2}\left[\boldsymbol{k}\times\boldsymbol{k}'\right]_z\begin{pmatrix}-s'_y\\ s'_x\\ 0\end{pmatrix}+\frac{\lambda_0^4}{16}\left[\boldsymbol{k}\times\boldsymbol{k}'\right]_z^2\begin{pmatrix}s_x+s'_x\\ s_y+s'_y\\ s_z-s'_z\end{pmatrix}\right\}, \tag{3.18}$$

[1] Alternative derivations with the Keldysh formalism or standard density matrix approaches yield, to the desired zeroth order in b_F/E_F, the same equations. Note, however, that to general orders in b_F/E_F, important differences between the formalisms may arise, see Chapter 5 and Kailasvuori and Lüffe [2010].

[2] In principle, an additional Hartree-Fock precession term (of second order in $\boldsymbol{s}_{\boldsymbol{k}}$ and first order in the electron-electron interaction V) in Eq. (3.16) could become important (see Chapter 4), as well as quadratic in $\boldsymbol{s}_{\boldsymbol{k}}$ terms in the electron-electron collision integrals (3.19)-(3.20). However, for small polarization these effects can be neglected. The clean (double-)exponential decay of the transient spin grating as documented in Fig. 1a in Koralek *et al.* [2009] is a strong hint that in this particular experiment nonlinear effects are irrelevant.

with the transition rate $W_{\boldsymbol{k}\boldsymbol{k}'} = 2\,\pi\,n_i\,|v\,(\boldsymbol{k}' - \boldsymbol{k})\,|^2$, where n_i is the impurity concentration, $\Delta\epsilon \equiv \epsilon_k - \epsilon_{k'}$, $\Delta n \equiv n_k - n_{k'}$ and $\Delta\boldsymbol{s} \equiv \boldsymbol{s}_k - \boldsymbol{s}_{k'}$, as well as electron-electron scattering,

$$\begin{aligned}\mathcal{J}^{\text{e-e}}_{\boldsymbol{k_1}} = \; & 2\,\pi \sum_{2,3,4} \left(2|V_{1234}|^2 - V_{1234}V_{1243}\right)\delta(\Delta\tilde{\epsilon}) \qquad (3.19)\\ & \left[(1-n_1)(1-n_2)\,n_3\,n_4 - (1 \leftrightarrow 3,\; 2 \leftrightarrow 4)\right],\\ \boldsymbol{\mathcal{J}}^{\text{e-e}}_{\boldsymbol{k_1}} = \; & 2\,\pi \sum_{2,3,4} \delta(\Delta\tilde{\epsilon})\;\{(1-n_1)(1-n_2)\,n_3\,n_4 \qquad (3.20)\\ & \left[2|V_{1234}|^2\left(\frac{\boldsymbol{s}_3}{n_3} - \frac{\boldsymbol{s}_1}{1-n_1}\right) - V_{1234}V_{1243}\left(\frac{\boldsymbol{s}_3}{n_3} + \frac{\boldsymbol{s}_4}{n_4} - \frac{\boldsymbol{s}_1}{1-n_1} - \frac{\boldsymbol{s}_2}{1-n_2}\right)\right]\\ & - (1 \leftrightarrow 3,\; 2 \leftrightarrow 4)\;\}\,.\end{aligned}$$

Here, we abbreviated $j \equiv \boldsymbol{k_j}$ (where $j = 1, 2, 3, 4$ labels initial and final states of the two collision partners) and $\Delta\tilde{\epsilon} \equiv \epsilon_{\boldsymbol{k_1}} + \epsilon_{\boldsymbol{k_2}} - \epsilon_{\boldsymbol{k_3}} - \epsilon_{\boldsymbol{k_4}}$.

In our approximation the charge kinetic equation (3.15) decouples from the spin kinetic equation (3.16) and is independently solved by the Fermi-Dirac distribution $n_{\boldsymbol{k}}(\boldsymbol{x}, t) = f(\epsilon_k) = \left[1 + e^{(\epsilon_k - E_F)/k_B T}\right]^{-1}$, where k_B is the Boltzmann constant and T the temperature. Since we are not interested in charge transport or local charge excitations, we assume that the charge distribution is given by this spatially uniform solution. In the next subsection we use the spin kinetic equation (3.16) to derive a drift-diffusion equation for the spin density in real space [Burkov *et al.*, 2004; Mishchenko *et al.*, 2004; Stanescu and Galitski, 2007; Weng *et al.*, 2008].

3.3.2. Spin diffusion equation in the D'yakonov-Perel' regime

In the following, we consider the *D'yakonov-Perel' regime* of strong scattering or weak spin-orbit interaction [D'yakonov and Perel', 1972], *i.e.*,

$$b_F\tau \;\ll\; 1\,. \qquad (3.21)$$

During the average time interval τ between collisions that alter the momentum of an electron—and thereby the effective spin-orbit field $\boldsymbol{b}(\boldsymbol{k})$—its spin precesses about this field by the small angle $b_F\tau$, see Figure 1.3. This results in a random walk behavior of the spin (in the context of the PSH, see Yang and Orenstein [2010]). The spin polarization is actually *stabilized* by the momentum scattering: the stronger the scattering, the slower the D'yakonov-Perel' spin relaxation.

In the spirit of the original derivation by D'yakonov and Perel' [1972] we exploit the separation of the timescales that govern the evolution of *isotropic* (in momentum space) and *anisotropic* parts of the spin distribution function. Since we deal with a spatially inhomogeneous spin density we make the additional assumption that the timescale connected with the gradient term in Eq. (3.16) is large as compared to the transport time, *i.e.* $v_F\,q\,\tau \ll 1$, where q is a typical wave vector of the Fourier transformed spin density. Thus, when speaking of "orders in $b_F\tau$" in the following, we actually have in mind "orders in $\max\{b_F\tau,\, v_F\,q\,\tau\}$".

In order to solve the spin kinetic equation (3.16) we split off an isotropic component $\boldsymbol{S}(\boldsymbol{x},t)$ from the spin density $\boldsymbol{s_k}$ and expand the remaining anisotropic component in winding numbers and powers of momentum k,

$$\boldsymbol{s_k}(\boldsymbol{x},t) \;=\; -\frac{2\,\pi}{m}\,f'(\epsilon_k)\,\boldsymbol{S} + \boldsymbol{s}_{\boldsymbol{k},1}(\boldsymbol{x},t) + \tilde{\boldsymbol{s}}_{\boldsymbol{k},1}(\boldsymbol{x},t) + \boldsymbol{s}_{\boldsymbol{k},3}(\boldsymbol{x},t) \tag{3.22}$$

with

$$\boldsymbol{s}_{\boldsymbol{k},1}(\boldsymbol{x},t) \;=\; f'(\epsilon_k)\,\frac{k}{m}\sum_{n=\pm1}\boldsymbol{\delta k_n}(\boldsymbol{x},t)\,e^{i\,n\,\theta}, \tag{3.23}$$

$$\tilde{\boldsymbol{s}}_{\boldsymbol{k},1}(\boldsymbol{x},t) \;=\; f'(\epsilon_k)\,\frac{k^3}{k_F^2\,m}\sum_{n=\pm1}\boldsymbol{\delta \tilde{k}_n}(\boldsymbol{x},t)\,e^{i\,n\,\theta}, \tag{3.24}$$

$$\boldsymbol{s}_{\boldsymbol{k},3}(\boldsymbol{x},t) \;=\; f'(\epsilon_k)\,\frac{k^3}{k_F^2\,m}\sum_{n=\pm3}\boldsymbol{\delta k_n}(\boldsymbol{x},t)\,e^{i\,n\,\theta}. \tag{3.25}$$

The anisotropic components of the distribution function arise due to the gradient term in the Boltzmann equation and due to precession about the spin-orbit field. Since the spin-orbit fields (3.5), (3.6) contain terms with winding numbers ±1 and ±3, only these winding numbers need to be considered for the anisotropic part of the spin density to lowest order in $b_F\tau$. This point will become clear in the course of the derivation of diffusion equations (see discussion below (3.38)). The same applies for the powers of k: we need to include in our ansatz only those powers that are contained in the driving terms resulting from the Hamiltonian (3.3). We therefore consider a k-term and a k^3-term in the ansatz for the winding-number-±1 terms of the spin density (3.23) and (3.24), because the winding-number-±1 driving terms of the kinetic equation (3.16) are the gradient term, the linear Rashba and Dresselhaus spin-orbit fields as well as the renormalization of the linear Dresselhaus term due to cubic Dresselhaus spin-orbit interaction. The winding-number-±3 component of the spin density (3.25), on the other hand, contains only a k^3-term, since only the cubic Dresselhaus spin-orbit field contributes to windin number ±3 in the kinetic equation (3.16).

In the following we consider point-like impurities, *i.e.*, *isotropic* scattering with a rate

$$\tau^{-1} \;=\; m\,n_i\,v(0)^2\,. \tag{3.26}$$

Furthermore, we assume low temperature $T \ll T_F \equiv E_F/k_B$ and perform a Sommerfeld expansion up to order $(T/T_F)^2$ in all momentum integrations of distribution functions: from the standard Sommerfeld technique in the theory of the Fermi gas it is well known that the approximation

$$\int_0^\infty \mathrm{d}\epsilon\,g(\epsilon)\,f(\epsilon) \;=\; \int_0^{E_F}\mathrm{d}\epsilon\,g(\epsilon) + \frac{\pi^2}{6}\,(k_BT)^2\,g'(E_F) + \mathcal{O}(T^4/T_F^4) \tag{3.27}$$

holds, where $f(\epsilon)$ is the Fermi distribution and $g(\epsilon)$ is a function of the energy that varies slowly for $\epsilon \approx E_F$. In the derivation of the spin diffusion equation we have to deal with

powers of momentum k^2, k^3, k^4, k^6, k^8. Since the dispersion is quadratic, and the 2d DOS is constant, the problem reduces to ($n = 1, \frac{3}{2}, 2, 3, 4$)

$$\begin{aligned}\int_0^\infty \mathrm{d}\epsilon\, \epsilon^n\, f'(\epsilon) &= -\int_0^\infty \mathrm{d}\epsilon\, n\, \epsilon^{n-1}\, f(\epsilon) \\ &= -(E_F)^n \left[1 + n\ (n-1)\, \frac{\pi^2}{6} \left(\frac{k_B\, T}{E_F}\right)^2\right] + \mathcal{O}(T^4/T_F^4)\,. \end{aligned} \tag{3.28}$$

Thus, the powers k^3, k^4, k^6 and k^8 are not simply replaced by $-k_F^3, \cdots - k_F^8$ upon momentum integration, but acquire corrections according to the prescription

$$\int_0^\infty \mathrm{d}\epsilon_k\, f'(\epsilon_k)\, k^n \;=\; -k_F^n\, z_n(T) \tag{3.29}$$

with $z_2(T) = 1$ and the Sommerfeld functions

$$\begin{aligned} z_3(T) &= 1 + \tfrac{\pi^2}{8}\, \tfrac{T^2}{T_F^2} + \mathcal{O}\left(\tfrac{T^4}{T_F^4}\right), & z_4(T) &= 1 + \tfrac{\pi^2}{3}\, \tfrac{T^2}{T_F^2}\,, \\ z_6(T) &= 1 + \pi^2\, \tfrac{T^2}{T_F^2}\,, & z_8(T) &= 1 + 2\,\pi^2\, \tfrac{T^2}{T_F^2} + \mathcal{O}\left(\tfrac{T^4}{T_F^4}\right). \end{aligned} \tag{3.30}$$

With the goal of obtaining diffusion equations for the real space spin density we start by momentum integration of the kinetic equation, $\frac{1}{(2\pi)^2}\int \mathrm{d}\boldsymbol{k}$ [Eq. (3.16)], using the ansatz (3.22). This yields the *isotropic* equation for the isotropic component of the spin density,

$$\begin{aligned} \partial_t\, S_x &= \frac{k_F^2}{2\,\pi}\left\{\frac{1}{2m}\left(\partial_x \delta\hat{k}_{c,x} + \partial_y \delta\hat{k}_{s,x}\right) + \alpha v_F \delta\hat{k}_{c,z} - \beta v_F\Big(\sin 2\phi\, \delta\bar{k}_{c,z} + \cos 2\phi\, \delta\bar{k}_{s,z}\Big)\right\} \\ &\quad - z_4\, \gamma_{\mathrm{ey}}\, S_x\,, \end{aligned} \tag{3.31}$$

$$\begin{aligned} \partial_t\, S_y &= \frac{k_F^2}{2\,\pi}\left\{\frac{1}{2m}\left(\partial_x \delta\hat{k}_{c,y} + \partial_y \delta\hat{k}_{s,y}\right) + \alpha v_F \delta\hat{k}_{s,z} + \beta v_F\left(\sin 2\phi\, \delta\bar{\bar{k}}_{s,z} - \cos 2\phi\, \delta\bar{\bar{k}}_{c,z}\right)\right\} \\ &\quad - z_4\, \gamma_{\mathrm{ey}}\, S_y\,, \end{aligned} \tag{3.32}$$

$$\begin{aligned} \partial_t\, S_z &= \frac{k_F^2}{2\,\pi}\left\{\frac{1}{2m}\left(\partial_x \delta\hat{k}_{c,z} + \partial_y \delta\hat{k}_{s,z}\right) - \alpha v_F(\delta\hat{k}_{c,x} + \delta\hat{k}_{s,y})\right. \\ &\qquad \left. + \beta v_F\left[\sin 2\phi\left(\delta\bar{k}_{c,x} - \delta\bar{\bar{k}}_{s,y}\right) + \cos 2\phi\left(\delta\bar{\bar{k}}_{c,y} + \delta\bar{k}_{s,x}\right)\right]\right\}, \end{aligned} \tag{3.33}$$

with

$$\begin{aligned} \boldsymbol{\delta\hat{k}}_{c(s)} &= \boldsymbol{\delta k}_{c(s)} + z_4 \boldsymbol{\delta\tilde{k}}_{c(s)}\,, \\ \boldsymbol{\delta\bar{k}}_{c(s)} &= \boldsymbol{\delta\hat{k}}_{c(s)} - \zeta(z_4 \boldsymbol{\delta k}_{c(s)} + z_6 \boldsymbol{\delta\tilde{k}}_{c(s)} + z_6 \boldsymbol{\delta k}_{c3(s3)})\,, \\ \boldsymbol{\delta\bar{\bar{k}}}_{c(s)} &= \boldsymbol{\delta\hat{k}}_{c(s)} - \zeta(z_4 \boldsymbol{\delta k}_{c(s)} + z_6 \delta\tilde{\boldsymbol{k}}_{c(s)} - z_6 \boldsymbol{\delta k}_{c3(s3)})\,. \end{aligned} \tag{3.34}$$

Here,

$$\zeta \;=\; \frac{\gamma\, k_F^2}{4\,\beta} \tag{3.35}$$

represents the ratio of cubic and linear Dresselhaus coupling strengths and we have introduced

$$\begin{aligned} \boldsymbol{\delta k}_{c(c3)} &= 2\,\mathrm{Re}\;\boldsymbol{\delta k}_{1(3)}, \qquad \boldsymbol{\delta \tilde{k}}_{c} &= 2\,\mathrm{Re}\;\boldsymbol{\delta \tilde{k}}_{1}, \\ \boldsymbol{\delta k}_{s(s3)} &= -2\,\mathrm{Im}\;\boldsymbol{\delta k}_{1(3)}, \qquad \boldsymbol{\delta \tilde{k}}_{s} &= -2\,\mathrm{Im}\;\boldsymbol{\delta \tilde{k}}_{1}. \end{aligned} \tag{3.36}$$

Eqs.(3.31)-(3.33) can be seen as continuity equations for the spin density where the anisotropic components $\boldsymbol{\delta k}_{c(s)}$, $\boldsymbol{\delta k}_{c(s)3}$ and $\boldsymbol{\delta \tilde{k}}_{c(s)}$ play the role of (generalized) spin currents. The impurity collision integral (3.18) contains a spin-dependent part due to extrinsic spin-orbit interaction, which acts as a sink for in-plane spin-polarization with the Elliot-Yafet relaxation rate [Raimondi and Schwab, 2009]

$$\gamma_{\mathrm{ey}} = \left(\frac{\lambda_0\, k_F}{2}\right)^4 \frac{1}{\tau}\,. \tag{3.37}$$

This relaxation mechanism can be understood as the net effect of the electron spins precessing by a small angle about the extrinsic spin-orbit field *during* the collision with an impurity. Since this field is perpendicular to the electronic motion, *i.e.*, it points in z-direction, the z component of the isotropic spin density is unaffected by the Elliot-Yafet mechanism.

The anisotropic components $\boldsymbol{\delta k}_{c(s)}$, $\boldsymbol{\delta \tilde{k}}_{c(s)}$ and $\boldsymbol{\delta k}_{c3(s3)}$ can in turn be expressed in terms of the isotropic spin density S_i by integrating the kinetic equation (3.16) multiplied with the velocity over momentum, where, this time, we omit the time derivative. The justification is that, in order to capture the slow precession-diffusion dynamics of the real space spin density, it is sufficient to interpret the time derivative as a coarse-grained one, *i.e.* $\partial_t \boldsymbol{S} \to \Delta \boldsymbol{S}/\Delta t$ with $\Delta t \approx b_F^{-1} \gg \tau$. Then the fast relaxation of the anisotropic components into the steady state at the beginning of each Δt contributes to the average over this time interval only with terms of higher order in $b_F\tau$. For an explicit demonstration we refer to Appendix A. Another way of seeing this is in analogy with the Born-Oppenheimer approximation: similarly to the fast moving electrons in a molecule, which almost instantaneously find their equilibrium positions with respect to the slowly vibrating nuclei, the anisotropic parts of the spin distribution quickly adjust to the momentary isotropic spin density. The backaction of the anisotropic parts on the isotropic spin density is then well described using their steady state solution.

By integrating $\frac{1}{(2\pi)^2}\int \mathrm{d}\boldsymbol{k}\, v_{x(y)}$ [Eq. (3.16)], equating terms of the same order in k and

solving for the coefficients, we obtain the following anisotropic equations:

$$
\begin{aligned}
\delta k_{c,x} &= 4\pi\left[\alpha v_F(1+z_4\gamma_{\rm sw}\tau_1)-\beta v_F\sin 2\phi(1-z_4\gamma_{\rm sw}\tau_1)\right]\tau_1 S_z \\
&\quad +\frac{2\pi}{m}\tau_1\left(\partial_x S_x+z_4\gamma_{\rm sw}\tau_1\partial_y S_y\right), \\
\delta k_{c,y} &= -4\,\pi\beta v_F\tau_1\cos 2\phi\;(1-z_4\gamma_{\rm sw}\tau_1)\;S_z+\frac{2\,\pi}{m}\tau_1\left(\partial_x\,S_y-z_4\gamma_{\rm sw}\tau_1\partial_y\,S_x\right), \\
\delta k_{c,z} &= 4\,\pi\left(-\alpha v_F+\beta v_F\sin 2\phi\right)\tau_1 S_x+4\,\pi\beta v_F\,\tau_1\cos 2\phi\,S_y+\frac{2\,\pi}{m}\tau_1\partial_x\,S_z\,, \\
\delta k_{s,x} &= -4\,\pi\beta v_F\tau_1\cos 2\phi\;(1-z_4\gamma_{\rm sw}\tau_1)\;S_z+\frac{2\,\pi}{m}\tau_1\left(\partial_y\,S_x-z_4\gamma_{\rm sw}\tau_1\partial_x\,S_y\right), \\
\delta k_{s,y} &= 4\pi\left[\alpha v_F(1+z_4\gamma_{\rm sw}\tau_1)+\beta v_F\sin 2\phi(1-z_4\gamma_{\rm sw}\tau_1)\right]\tau_1 S_z \\
&\quad +\frac{2\,\pi}{m}\tau_1\left(\partial_y\,S_y+z_4\gamma_{\rm sw}\tau_1\partial_x\,S_x\right), \\
\delta k_{s,z} &= 4\,\pi\beta v_F\,\tau_1\cos 2\phi\,S_x-4\,\pi\left[\alpha v_F+\beta v_F\sin 2\phi\right]\tau_1 S_y+\frac{2\,\pi}{m}\tau_1\partial_y\,S_z\,, \\
\delta\tilde{k}_{c,x} &= -\delta\tilde{k}_{s,y}=\;4\,\pi\beta v_F\zeta\sin 2\phi\tilde{\tau}_1(1-\frac{z_6}{z_4}\gamma_{\rm sw}\tilde{\tau}_1)S_z\,, \\
\delta\tilde{k}_{c,y} &= \delta\tilde{k}_{s,x}=\;4\,\pi\beta v_F\zeta\cos 2\phi\tilde{\tau}_1(1-\frac{z_6}{z_4}\gamma_{\rm sw}\tilde{\tau}_1)S_z\,, \\
\delta\tilde{k}_{c,z} &= -4\,\pi\,\beta v_F\zeta\tilde{\tau}_1(\sin 2\phi\,S_x+\cos 2\phi\,S_y)\,, \\
\delta\tilde{k}_{s,z} &= -4\,\pi\,\beta v_F\zeta\tilde{\tau}_1(\cos 2\phi\,S_x-\sin 2\phi\,S_y)\,.
\end{aligned}
\tag{3.38}
$$

The spin densities S_i act as sinks and sources in the equations for the anisotropic coefficients $\delta k_{\pm1,\pm3,i}, \delta\tilde{k}_{\pm1,i}$. Since the spin densities $S_i(t=0)$ are determined by the initial conditions, they are of zeroth order in $b_F\tau$, whereas the anisotropic coefficients $\delta k_{\pm1,\pm3,i}, \delta\tilde{k}_{\pm1,i}$ are already of first order in $b_F\tau$. If we had included parts with higher winding numbers $\pm2, \pm4, \pm5, \ldots$ in our ansatz, these would have been generated only indirectly via the $\delta k_{\pm1,\pm3,i}, \delta\tilde{k}_{\pm1,i}$ (all of which are already of first order in $b_F\tau$) and would therefore be of even higher order in $b_F\tau$.

In the Eqs. (3.38) we have defined the rate of "swapping of the spin currents" [Lifshits and D'yakonov, 2009] as

$$
\gamma_{\rm sw} \;=\; \left(\frac{\lambda_0\,k_F}{2}\right)^2\frac{1}{\tau}\,, \tag{3.39}
$$

which is due to extrinsic spin-orbit interaction like the Elliot-Yafet rate $\gamma_{\rm ey}$ (Eq. (3.37)), but of lower order in λ_0. It leads to a "swapping of spin currents" because a finite $\gamma_{\rm sw}$ generates, *e.g.*, a S_y spin current in response to a gradient of the S_x spin density in x direction. Eqs. (3.38) are valid to linear order in $\tau\,\gamma_{\rm sw}\ll 1$.

Since the anisotropic components $\boldsymbol{\delta k}_{\pm1}$ and $\boldsymbol{\delta\tilde{k}}_{\pm1}$ are related to (generalized) spin currents, the anisotropic equations (3.38) express generalized Ohm's laws. In accordance with *Matthiessen's rule* (see *e.g.* Smith and Jensen [1989]), the effective relaxation times for the anisotropic parts of the spin distribution function are obtained as the inverse sum of the collision integrals for normal impurity scattering, spin-dependent impurity scattering

and electron-electron scattering,

$$\tau_1 \;=\; \left(\frac{1}{\tau} + \gamma_{\rm ey}\, z_6 + \frac{1}{\tau_{\text{e-e},1}}\right)^{-1}, \tag{3.40}$$

$$\tilde{\tau}_1 \;=\; \left(\frac{1}{\tau} + \gamma_{\rm ey}\, \frac{z_8}{z_4} + \frac{1}{z_4\,\tilde{\tau}_{\text{e-e},1}}\right)^{-1}. \tag{3.41}$$

Here, the rates $\tau_{\text{e-e},1}^{-1}$, $\tilde{\tau}_{\text{e-e},1}^{-1}$ account for the decay of the respective component ($\boldsymbol{s}_{\boldsymbol{k},1}$ or $\tilde{\boldsymbol{s}}_{\boldsymbol{k},1}$) of the spin distribution due to two-particle Coulomb scattering. The rate at which winding-number-±1 and linear-in-k components of the spin distribution relax due to electron-electron interaction is

$$\tau_{\text{e-e},1}^{-1} \;=\; \Gamma(n=1,p=1,l=1)\,, \tag{3.42}$$

where

$$\begin{aligned}\Gamma(n,p,l) \;=\; -\frac{1}{k_B\,T\,k_F^{p+l} m\,(2\pi)^4}\iiint \mathrm{d}\boldsymbol{k_1}\,\mathrm{d}\boldsymbol{k_2}\,\mathrm{d}\boldsymbol{k_3}\,\delta(\Delta\tilde{\epsilon}) \\ k_1^l\,[1-f(\epsilon_{k_3})]\,[1-f(\epsilon_{\boldsymbol{k_1}+\boldsymbol{k_2}-\boldsymbol{k_3}})]\,f(\epsilon_{k_1})f(\epsilon_{k_2}) \\ \big\{2|V(|\boldsymbol{k_1}-\boldsymbol{k_3}|)|^2\,[\cos(n[\theta_3-\theta_1])\,k_3^p - k_1^p] \\ +V(|\boldsymbol{k_1}-\boldsymbol{k_3}|)V(|\boldsymbol{k_2}-\boldsymbol{k_3}|) \\ [k_1^p + \cos(n[\theta_2-\theta_1])k_2^p - \cos(n[\theta_3-\theta_1])k_3^p \\ -\cos(n[\theta_{1+2-3}-\theta_1])\,|\boldsymbol{k_1}+\boldsymbol{k_2}-\boldsymbol{k_3}|^p]\big\}\,.\end{aligned} \tag{3.43}$$

The rate (3.42) is related to the spin Coulomb drag conductivity [D'Amico and Vignale, 2000; Flensberg *et al.*, 2001; D'Amico and Vignale, 2003] via the Drude formula. The analogous expression for the winding-number-±1 but cubic-in-k components is

$$\tilde{\tau}_{\text{e-e},1}^{-1} \;=\; \Gamma(n=1,p=3,l=1) \tag{3.44}$$

with $\Gamma(n,p,l)$ from Eq. (3.43).

In order to find the anisotropic equations for $\boldsymbol{\delta k}_{\pm3}$ we follow a similar procedure as before and integrate $\frac{1}{(2\pi)^2}\int \mathrm{d}\boldsymbol{k}\, e^{\pm i3\theta}$ [Eq. (3.16)]. This results in

$$\begin{aligned}\boldsymbol{\delta k}_{c3} &= \gamma\, v_F\, k_F^2\, \pi\, \tau_3 \begin{pmatrix} \sin 2\phi\, S_z \\ -\cos 2\phi\, S_z \\ \cos 2\phi\, S_y - \sin 2\phi\, S_x \end{pmatrix}, \\ \boldsymbol{\delta k}_{s3} &= \gamma\, v_F\, k_F^2\, \pi\, \tau_3 \begin{pmatrix} \cos 2\phi\, S_z \\ \sin 2\phi\, S_z \\ -\sin 2\phi\, S_y - \cos 2\phi\, S_x \end{pmatrix}\end{aligned} \tag{3.45}$$

with

$$\tau_3 = \left(\frac{1}{\tau} + \gamma_{\rm ey}\,\frac{z_8}{z_3} + \frac{1}{z_3\,\tau_{\text{e-e},3}}\right)^{-1}. \tag{3.46}$$

The electron-electron scattering rate that enters the effective relaxation time (3.46) for the winding-number-± 3 parts of the spin distribution is given by Eq. (3.43) as

$$\tau_{\text{e-e},3}^{-1} \;=\; \Gamma(n=3, p=3, l=0)\,. \tag{3.47}$$

Finally we insert the steady-state solutions for the anisotropic coefficients, Eqs. (3.38) and (3.45), into the isotropic equations (3.31)-(3.33) and thus obtain a closed set of coupled diffusion equations for the three vector components of the spin density,

$$\begin{aligned}
\partial_t S_x &= \left(D\,\boldsymbol{\nabla}^2 - \Gamma_x - \gamma_{\text{cD}}\, z_6 - \gamma_{\text{ey}}\, z_4\right) S_x + L\, S_y + \left(K_{xz}\,\partial_x - M\,\partial_y\right)\, S_z\,, \\
\partial_t S_y &= \left(D\,\boldsymbol{\nabla}^2 - \Gamma_y - \gamma_{\text{cD}}\, z_6 - \gamma_{\text{ey}}\, z_4\right) S_y + L\, S_x + \left(K_{yz}\,\partial_y - M\,\partial_x\right)\, S_z\,, \\
\partial_t S_z &= \left(D\,\boldsymbol{\nabla}^2 - \Gamma_x - \Gamma_y - 2\,\gamma_{\text{cD}}\, z_6 - \Gamma_{\text{sw}}\right)\, S_z - \left(K_{zx}\,\partial_x - M_z\,\partial_y\right)\, S_x \\
&\quad - \left(K_{zy}\,\partial_y - M_z\,\partial_x\right)\, S_y\,.
\end{aligned} \tag{3.48}$$

On its diagonal, the diffusion operator that corresponds to Eqs. (3.48) (when writing them in matrix form) contains the genuine diffusion terms with $\boldsymbol{\nabla}^2 = \partial_x^2 + \partial_y^2$ and the Elliot-Yafet relaxation rate γ_{ey} due to extrinsic spin-orbit interaction. Also on the diagonal, we have the D'yakonov'-Perel' relaxation rates $\Gamma_{x(y)}$ and γ_{cD} which reflect the randomization of the spin orientation due to precession (between the collisions) about the winding-number-± 1 and winding-number-± 3 spin-orbit fields, respectively. The S_x component suffers relaxation as a consequence of precession about the y component of the spin-orbit field only, and *vice versa*. In contrast, the S_z component is relaxed by the precession about the full spin-orbit field. Thus the relaxation rate of S_z due to precession is the sum of the ones for S_x and S_y, plus a correction Γ_{sw} for processes that involve the swapping of the spin currents due to extrinsic spin-orbit interaction. Due to precession there are also off-diagonal rates L, which couple the in-plane spin components, as well as several off-diagonal mixed diffusion-precession rates, which are accompanied by partial derivatives.

In terms of the parameters of our model and previously defined quantities the coefficients in the spin diffusion equation (3.48) are given by:

$$\gamma_{\text{cD}} = \frac{1}{8}\, v_F^2\, \gamma^2\, k_F^6\, \tau_3\,, \tag{3.49}$$

$$\begin{aligned}
\Gamma_{x(y)} = \frac{1}{4}\, q_0^2 \Bigg(& D \mp \frac{\beta}{\alpha}\left[2\,D - \zeta\, z_4\,(D + \tilde{D})\right] \sin 2\phi \\
& + \frac{\beta^2}{\alpha^2}\left[D - \zeta\, z_4\,(D + \tilde{D}) + \zeta^2 z_6\, \tilde{D}\right]\Bigg)\,,
\end{aligned} \tag{3.50}$$

$$\Gamma_{\text{sw}} = \frac{1}{2}\, q_0^2\, \gamma_{\text{sw}} \left[D\,\tau_1\, z_4 - \frac{\beta^2}{\alpha^2}\left(D\,\tau_1\, z_4 - \zeta\,\tilde{D}\,\tilde{\tau}_1\, z_6 - \zeta\, D\,\tau_1\, z_4^2 + \zeta^2\,\tilde{D}\,\tilde{\tau}_1\,\frac{z_6^2}{z_4}\right)\right], \tag{3.51}$$

$$K_{xz(yz)} = q_0 \left(D \mp \frac{\beta}{\alpha} \left[D - \frac{1}{2} \zeta \, z_4 \, (D + \tilde{D}) \right] \sin 2\phi \right) \tag{3.52}$$
$$+ \frac{1}{2} \gamma_{\mathrm{sw}} \, q_0 \left(\tau_1 \, D \, z_4 \pm \frac{\beta}{\alpha} \left[\tau_1 \, D \, z_4 - \zeta \, \tilde{\tau}_1 \, \tilde{D} \, z_6 \right] \sin 2\phi \right),$$
$$K_{zx(zy)} = q_0 \left(D \mp \frac{\beta}{\alpha} \left[D - \frac{1}{2} \zeta \, z_4 \, (D + \tilde{D}) \right] \sin 2\phi \right) \tag{3.53}$$
$$+ \frac{1}{2} \gamma_{\mathrm{sw}} \, \tau_1 \, q_0 \, D \, z_4 \left[1 \pm \frac{\beta}{\alpha} \, (1 - \zeta \, z_4) \sin 2\phi \right],$$
$$M = \cos 2\phi \, q_0 \, \frac{\beta}{\alpha} \left[D - \frac{1}{2} \zeta \, z_4 \, (D + \tilde{D}) \right] \tag{3.54}$$
$$- \frac{1}{2} \gamma_{\mathrm{sw}} \, q_0 \, \cos 2\phi \, \frac{\beta}{\alpha} \left[\tau_1 \, D \, z_4 - \zeta \, \tilde{\tau}_1 \, \tilde{D} \, z_6 \right],$$
$$M_z = \cos 2\phi \, q_0 \, \frac{\beta}{\alpha} \left[D - \frac{1}{2} \zeta \, z_4 \, (D + \tilde{D}) \right] \tag{3.55}$$
$$- \frac{1}{2} \gamma_{\mathrm{sw}} \, \tau_1 \, q_0 \, D \, z_4 \, \cos 2\phi \, \frac{\beta}{\alpha} \, (1 - \zeta \, z_4),$$
$$L(\phi) = \cos 2\phi \, \frac{1}{2} \, q_0^2 \, \frac{\beta}{\alpha} \left[D - \frac{1}{2} \zeta \, z_4 \, (D + \tilde{D}) \right] \tag{3.56}$$

with the PSH wave vector

$$q_0 = 4 \, v_F \, m \, \alpha \tag{3.57}$$

and the effective diffusion constants

$$D = \frac{1}{2} \, v_F^2 \, \tau_1, \quad \tilde{D} = \frac{1}{2} \, v_F^2 \, \tilde{\tau}_1. \tag{3.58}$$

At $T = 0$, we have $z_n = 1$, and the electron-electron scattering is suppressed due to the lack of phase space for final states, such that $\tilde{D} = D$. Then, the spin diffusion equation (3.48) agrees (except for the sign of L) with the one presented in Weng *et al.* [2008] if we leave extrinsic spin-orbit interactions aside. If we further omit cubic Dresselhaus spin-orbit interaction in our diffusion equation, it also concurs with the one of Bernevig *et al.* [2006] provided that the spin-charge coupling is negligible.

3.4. Persistent spin helix in the presence of symmetry breaking mechanisms

In this section, we use the spin diffusion equation (3.48) to calculate the lifetime of the persistent spin helix. We consider extrinsic spin-orbit interaction, cubic Dresselhaus spin-orbit interaction, and simple spin-flip scattering as possible symmetry breaking mechanisms. In order to allow for simple analytical solutions we discuss each of the candidate mechanisms separately. In the case of cubic Dresselhaus spin-orbit interaction we neglect at first the renormalization of the linear Dresselhaus spin-orbit interaction (see Eq. (3.7)). This is formally achieved by setting $\zeta = 0$ in Eqs. (3.50)-(3.56) while keeping the γ_{cD}

Table 3.1.: Specification of the rate X and the integer N in Eq. (3.59)

	Simple spin flips	Extr. spin-orbit int.	Cubic Dress.
X	$1/\tau_{\mathrm{sf}}$	γ_{ey}	$\gamma_{\mathrm{cD}}\, z_6$
N	1	0	2

term in Eq. (3.48). However, we will include the renormalization of the linear Dresselhaus spin-orbit interaction when we discuss a possible stationary solution in the present section and also when we compare to the experimental results in a GaAs/AlGaAs quantum well [Koralek *et al.*, 2009] in Section 3.5.

We choose our coordinate system such that the x axis points in the (110)-crystal direction, corresponding to $\phi = \frac{\pi}{4}$ in Eqs. (3.50)-(3.56). Then, considering an initial spin polarization that is uniform in x-direction, due to $L(\frac{\pi}{4}) = M(\frac{\pi}{4}) = 0$ the S_x component decouples from the S_y and S_z components and we can set $S_x = 0$. Since $\alpha = \beta$, Eq. (3.48) reduces for the remaining S_y and S_z components to

$$\partial_t \boldsymbol{S} \;=\; \begin{pmatrix} D\,\partial_y^2 - q_0^2\,D - X & 2\,q_0\,D\,\partial_y \\ -2\,q_0\,D\,\partial_y & D\,\partial_y^2 - q_0^2\,D - N\,X \end{pmatrix} \boldsymbol{S}, \tag{3.59}$$

where the relaxation rates due to the respective symmetry-breaking mechanism are represented by X and an integer N according to Table 3.1.

For the SU(2) symmetric situation ($X = 0$) there exists a steady state solution with the wave vector q_0. This is the persistent spin helix state. More precisely, for an initial spin polarization of the form

$$\boldsymbol{S}(\boldsymbol{x}, t=0) \;=\; S_0 \begin{pmatrix} 0 \\ 0 \\ \cos q_0 y \end{pmatrix}, \tag{3.60}$$

similar to the experimental set-up of Koralek *et al.*, one finds that the time-dependent solution to Eq. (3.59) is

$$\boldsymbol{S}^{X=0}(y,t) \;=\; \frac{S_0}{2} \begin{pmatrix} [e^{-4\,q_0^2\,D\,t} - 1]\,\sin q_0 y \\ [e^{-4\,q_0^2\,D\,t} + 1]\,\cos q_0 y \end{pmatrix}. \tag{3.61}$$

In the stationary limit $t \to \infty$ this reduces to the persistent spin helix state. The solution (3.61) can, for instance, be constructed by applying the Laplace transformation in order to eliminate the time variable. Then the spatial part reduces to an eigenvalue problem. After solving the eigenvalue problem Eq. (3.61) is obtained by an inverse Laplace transformation.

In the presence of symmetry breaking mechanisms, *i.e.*, for $X \neq 0$, one can still find a steady state solution of the form

$$\begin{aligned} S_y(y) \;&=\; -\frac{S_0}{2}\, e^{-y/l_X}\, C_1\, \sin q_X y\,, \\ S_z(y) \;&=\; \frac{S_0}{2}\, e^{-y/l_X}\, (C_2\, \sin q_X y + \cos q_X y)\,. \end{aligned} \tag{3.62}$$

This solution is a spatially damped persistent spin helix state with the coefficients

$$
\begin{aligned}
l_X^{-1} &= \frac{q_0}{2}\sqrt{2\,\Xi+(N+1)\,\xi-2}\,, \\
q_X &= \frac{q_0}{2}\sqrt{2\,\Xi-(N+1)\,\xi+2}\,, \\
C_1 &= \frac{4\sqrt{2\,\Xi-(1+N)\,\xi+2}\,\Big[4+(3\,N+1)\,\xi-N\,(N-1)\,\xi^2-(4+(N-1)\,\xi)\,\Xi\Big]}{\xi^2\,(-8(N^2-1)+(N-1)^3\xi)}\,, \\
C_2 &= \frac{8-(N-1)^2\xi^2-4\,(2\,\Xi-(N+1)\,\xi)}{(N-1)\,\xi\,\sqrt{8\,(N+1)\xi-(N-1)^2\xi^2}}\,,
\end{aligned}
\tag{3.63}
$$

where $\xi \equiv X/(q_0^2\,D)$ and $\Xi \equiv \sqrt{(1+\xi)(1+N\,\xi)}$. For $\xi \to 0$ the $t \to \infty$ asymptotics of Eq. (3.61), *i.e.*, the truly persistent spin helix state in the absence of SU(2) breaking mechanisms, is readily recovered. The spatially damped persistent spin helix state (3.62) can in principle be excited with the initial spin polarization profile

$$
\boldsymbol{S}(\boldsymbol{x}, t=0) \;=\; S_0\, e^{-y/l_X} \begin{pmatrix} 0 \\ 0 \\ \cos q_X y \end{pmatrix}. \tag{3.64}
$$

Although the spatially damped persistent spin helix is clearly a valid steady state solution when the symmetry breaking is caused by simple spin flips or extrinsic spin orbit interaction, it is not obvious that this applies also to the case of cubic Dresselhaus spin orbit interaction, since we have neglected the renormalization of the linear Dresselhaus spin orbit interaction ($\zeta \neq 0$), which might lead to a finite lifetime of the spatially damped state. Nevertheless, even when the renormalization of the linear Dresselhaus spin orbit interaction is taken into account one can still find a steady state solution of the form (3.62) when the ratio of the linear Rashba and Dresselhaus spin orbit interactions is given by

$$
\frac{\beta}{\alpha} \;=\; \frac{D}{D-\frac{1}{2}\,\zeta\,z_4\,(D+\tilde{D})}. \tag{3.65}
$$

It should generally be possible to fulfill this relation for realistic experimental parameters upon appropriate tuning of the spin-orbit interaction or the temperature. According to Eqs. (3.52)-(3.53), we then have $K_{yz}(\frac{\pi}{4}) = K_{zy}(\frac{\pi}{4}) = 2\,q_0\,D$, as in Eq. (3.59). Furthermore,

$$
\begin{aligned}
\Gamma_y(\pi/4) &= q_0^2\,D\,[1+F(T)]\,, \\
\Gamma_z(\pi/4) &= q_0^2\,D\,[1+2\,F(T)]\,,
\end{aligned}
\tag{3.66}
$$

with

$$
F(T) \;=\; \frac{1}{4}\Big(\frac{D^2-\zeta z_4\,D\,(D+\tilde{D})+\zeta^2 z_6\,D\,\tilde{D}}{D^2-\zeta z_4 D(D+\tilde{D})+\frac{1}{4}\zeta^2 z_4^2 (D+\tilde{D})^2}-1\Big). \tag{3.67}
$$

Thus, the spin diffusion equation can still be cast into the form of Eq. (3.59) when the symmetry breaking rate X is redefined as $\tilde{X} = X + q_0^2 D\,F(T)$. For this symmetry breaking

rate $\tilde{X}$ and spin orbit couplings satisfying (3.65) the spatially damped spin profile of the form (3.62)-(3.63) is, again, infinitely long-lived.

This stationary state should in principle be realizable in the GaAs/AlGaAs quantum well of Koralek *et al.*, because there the ratio of β/α almost fulfills relation (3.65) at a temperature of $T = 100$ K. For the parameters of the GaAs/AlGaAs quantum well used by Koralek *et al.* the steady state solution is characterized by a wavevector $q_{\tilde{X}} \approx q_0$ and a damping length of hardly more than one PSH wavelength, $l_{\tilde{X}} \approx 1.06\,\frac{2\pi}{q_0}$. Although a spin grating with such a strong spatial damping might be difficult to realize in practice, it should be noted that the required damping length is $\propto \zeta^{-1}$, so that one can expect much longer damping lengths for thinner quantum wells, where the importance of cubic Dresselhaus spin-orbit coupling (as compared to the linear one) is reduced.

We now want to consider the conventional PSH solution. If we stick to an initial spin polarization with the form of a plane wave (3.60) similar to the experimental set-up, the time-dependent solution of Eq. (3.59) is characterized by a double-exponential decay,

$$S_y(y,t) \;=\; \frac{S_0}{2}\,\sin q_0 y\,\frac{4\,q_0^2\,D\left(e^{-\frac{t}{\tau_R}}-e^{-\frac{t}{\tau_E}}\right)}{\sqrt{(4\,q_0^2\,D)^2+(N-1)^2\,X^2}}\,, \tag{3.68}$$

$$S_z(y,t) \;=\; \frac{S_0}{2}\,\cos q_0 y\left[e^{-\frac{t}{\tau_R}}+e^{-\frac{t}{\tau_E}}+\frac{(N-1)\,X\left(e^{-\frac{t}{\tau_R}}-e^{-\frac{t}{\tau_E}}\right)}{\sqrt{(4\,q_0^2\,D)^2+(N-1)^2\,X^2}}\right] \tag{3.69}$$

with the spin-orbit-*enhanced* and *-reduced* lifetimes

$$\tau_{E(R)}^{-1} \;=\; 2\,q_0^2\,D+\frac{1}{2}\,(N+1)\,X \mp \frac{1}{2}\sqrt{(4\,q_0^2\,D)^2+(N-1)^2\,X^2}\,. \tag{3.70}$$

In the absence of any symmetry-breaking relaxation mechanism, *i.e.*, for $X = 0$, the proper persistent spin helix state ($\tau_E = \infty$) is recovered. Expanding Eq. (3.70) for small $X/(4\,q_0^2\,D) \ll 1$ we obtain

$$\tau_E \;\approx\; \frac{2}{(N+1)}\,X^{-1}+\left(\frac{N-1}{N+1}\right)^2\frac{1}{4\,q_0^2\,D}\,, \tag{3.71}$$

$$\tau_R \;\approx\; \frac{1}{4\,q_0^2\,D}-\frac{(N+1)\,X}{2\,(4\,q_0^2\,D)^2}\,. \tag{3.72}$$

The reduced lifetime τ_R is not very sensitive to details of the (weak) symmetry-breaking mechanism. Correspondingly, the temperature dependence of the reduced lifetime τ_R is almost independent of the precise mechanism (and is essentially determined by the electron-electron relaxation rate $\tau_{\text{e-e},1}^{-1}$ contained in D via τ_1, see Eq. (3.40)). The temperature dependence of the enhanced lifetime τ_E, by contrast, depends crucially on the symmetry breaking mechanism under consideration and thus offers a way to discriminate between the different mechanisms. For small symmetry breaking terms the enhanced lifetime τ_E is proportional to the inverse of the respective scattering rate X^{-1}. Therefore also the temperature dependence of τ_E is determined by the one of the scattering rate. For simple spin-flip scattering $X = \tau_{\text{sf}}^{-1}$ we expect a temperature-independent lifetime τ_E due

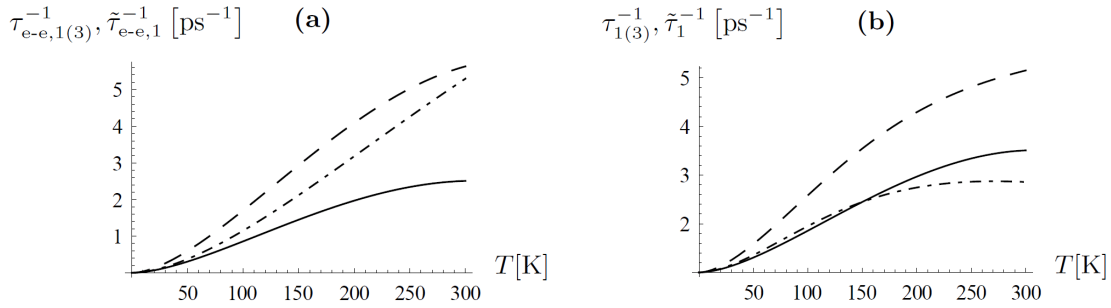

Figure 3.6.: (a) Temperature-dependent relaxation rates due to electron-electron interactions: $\tau^{-1}_{\text{e-e},1}$ (solid curve), $\tilde{\tau}^{-1}_{\text{e-e},1}$ (dot-dashed curve) and $\tau^{-1}_{\text{e-e},3}$ (dashed curve) as computed numerically from Eq. (3.42) using the experimental parameters of Koralek *et al.* [2009]. For comparison: the inverse transport time at $T = 100$K is $\tau^{-1} = 1\ \text{ps}^{-1}$. (b) The resulting effective relaxation rates: τ_1^{-1} (solid), τ_3^{-1} (dashed) and $\tilde{\tau}_1^{-1}$ (dot-dashed), *cf.* Eqs. (3.40)-(3.41) and (3.46).

to a constant τ_{sf}. For extrinsic spin-orbit interactions with $X = \gamma_{\text{ey}}$, the only temperature dependence to leading order in $X/(4\,q_0^2\,D)$ comes from the Sommerfeld corrections. Thus τ_E decreases quadratically with temperature. For cubic Dresselhaus spin-orbit interaction one finds

$$\tau_E \;\approx\; \frac{2}{3}\,\gamma_{\text{cD}}^{-1} z_6^{-1} \tag{3.73}$$

and therefore τ_E is proportional to τ_3^{-1} (see Eq. (3.49)). Since τ_3 decreases with temperature as a consequence of the enhanced electron-electron scattering $\tau^{-1}_{\text{e-e},3}$ (see Eq. (3.46)) the lifetime τ_E increases initially with temperature due to the motional narrowing effect in the D'yakonov-Perel' regime. The presence of the Sommerfeld function z_6, on the other hand, leads to a decrease of τ_E with increasing temperature. Thus for cubic Dresselhaus spin-orbit interaction we find that the temperature dependence is governed by a competition between increasing and decreasing contributions. We will compare this theoretical interpretation with experimental results for the persistent spin helix in GaAs/AlGaAs quantum wells [Koralek *et al.*, 2009] in the next section.

3.5. Persistent spin helix in GaAs/AlGaAs quantum wells

In order to address the lifetime of the PSH observed experimentally in GaAs/AlGaAs quantum wells we consider cubic Dresselhaus spin-orbit coupling alongside with extrinsic spin-orbit interaction as possible symmetry breaking mechanisms in our model. We further include the renormalization of the linear Dresselhaus coupling constant due to cubic Dresselhaus spin-orbit interaction ($\zeta \neq 0$ in Eqs. (3.50)-(3.56)). Analogously to the previous section we can set $S_x = 0$. Then the spin diffusion equation (3.48) reduces for the

remaining components S_y and S_z to

$$\partial_t \boldsymbol{S} \;=\; \begin{pmatrix} D\,\partial_y^2 - Y & K_{yz}(\frac{\pi}{4})\,\partial_y \\ -K_{zy}(\frac{\pi}{4})\,\partial_y & D\,\partial_y^2 - Z \end{pmatrix} \boldsymbol{S} \tag{3.74}$$

with

$$\begin{aligned} Y &= \Gamma_y(\pi/4) + \gamma_{\mathrm{cD}}\, z_6 + \gamma_{\mathrm{ey}}\, z_4\,, \\ Z &= \Gamma_x(\pi/4) + \Gamma_y(\pi/4) + 2\,\gamma_{\mathrm{cD}}\, z_6 + \Gamma_{\mathrm{sw}}\,. \end{aligned} \tag{3.75}$$

For an initial spin polarization of the form $\boldsymbol{S}(\boldsymbol{x}, t = 0) = S_0\,(0,\, 0,\, \cos q_0 y)$ the time-dependent solution is a double-exponential function,

$$S_y(y,t) \;=\; \frac{S_0}{2}\,\sin q_0 y\,\frac{2\,K_{yz}\,q_0\,(e^{-\frac{t}{\tau_R}} - e^{-\frac{t}{\tau_E}})}{\sqrt{4\,K_{yz}(\frac{\pi}{4})\,K_{zy}(\frac{\pi}{4})\,q_0^2 + (Z-Y)^2}}\,, \tag{3.76}$$

$$S_z(y,t) \;=\; \frac{S_0}{2}\,\cos q_0 y\left[e^{-\frac{t}{\tau_R}} + e^{-\frac{t}{\tau_E}} + \frac{(Z-Y)\left(e^{-\frac{t}{\tau_R}} - e^{-\frac{t}{\tau_E}}\right)}{\sqrt{4\,K_{yz}(\frac{\pi}{4})\,K_{zy}(\frac{\pi}{4})\,q_0^2 + (Z-Y)^2}}\right], \tag{3.77}$$

where the spin-orbit-enhanced relaxation rate τ_E^{-1} and a spin-orbit-reduced relaxation rate τ_R^{-1} are now given as

$$\tau_{E(R)}^{-1} \;=\; \frac{1}{2}\,(Y+Z) + q_0^2\,D \mp \frac{1}{2}\,\sqrt{(Y-Z)^2 + 4\,q_0^2\,K_{yz}(\pi/4)\,K_{zy}(\pi/4)}\,. \tag{3.78}$$

It may be instructive to expand the relaxation rate of the enhanced mode up to linear order in the small rate γ_{cD} (assuming that $\gamma_{\mathrm{cD}}/q_0^2\,D \ll 1$ is the smallest parameter of the problem) and to subsequently expand the zeroth order terms of this expansion up to the quadratic order in deviations from $\beta/\alpha = 1$ and $\zeta = 0$. This procedure yields

$$\tau_E^{-1} \;\approx\; \frac{3}{2}\,\gamma_{\mathrm{cD}}\, z_6 + \frac{3}{8}\,q_0^2\,D\left[z_3\,\zeta^2 + \left(\frac{\beta}{\alpha} - 1\right)^2 - z_2\left(1 + \frac{\tilde{D}}{D}\right)\zeta\left(\frac{\beta}{\alpha} - 1\right)\right]. \tag{3.79}$$

The zero temperature limit $\tau_E^{-1} \overset{T=0}{\to} \frac{3}{2}\,\gamma_{\mathrm{cD}}(T=0) + \frac{3}{8}\,D\,q_0^2\left(\zeta - \frac{\beta}{\alpha} + 1\right)^2$ is minimal (and equal to the zero-temperature limit of the simplified result (3.73) in the previous section, where we have neglected the renormalization of linear due to cubic Dresselhaus coupling) for $\beta/\alpha = 1 + \zeta$, *i.e.*, $\alpha = \beta'$ instead of $\alpha = \beta$ (*cf.* Stanescu and Galitski [2007]).

In order to quantitatively compare our theory with the experimental findings of Koralek *et al.* we need to calculate the coefficients that occur in Eq. (3.78)—in particular the temperature-dependent rates for electron-electron scattering. Fig. 3.6 (a) shows numerical results for $\tau_{\mathrm{e\text{-}e},1}^{-1}$, $\tilde{\tau}_{\mathrm{e\text{-}e},1}^{-1}$ and $\tau_{\mathrm{e\text{-}e},3}^{-1}$ (for intermediate steps, see Appendix B) for the parameters of Koralek *et al.* For the practical purpose of obtaining continuous curves for the lifetimes we have interpolated the discrete set of points we obtained by Monte Carlo integration of Eqs. (3.42)-(3.47) with a fit to the functional form $A\,T^2 + B\,T^2 \ln T$. This form has been shown to describe the low-temperature behavior of the spin Coulomb drag conductivity in

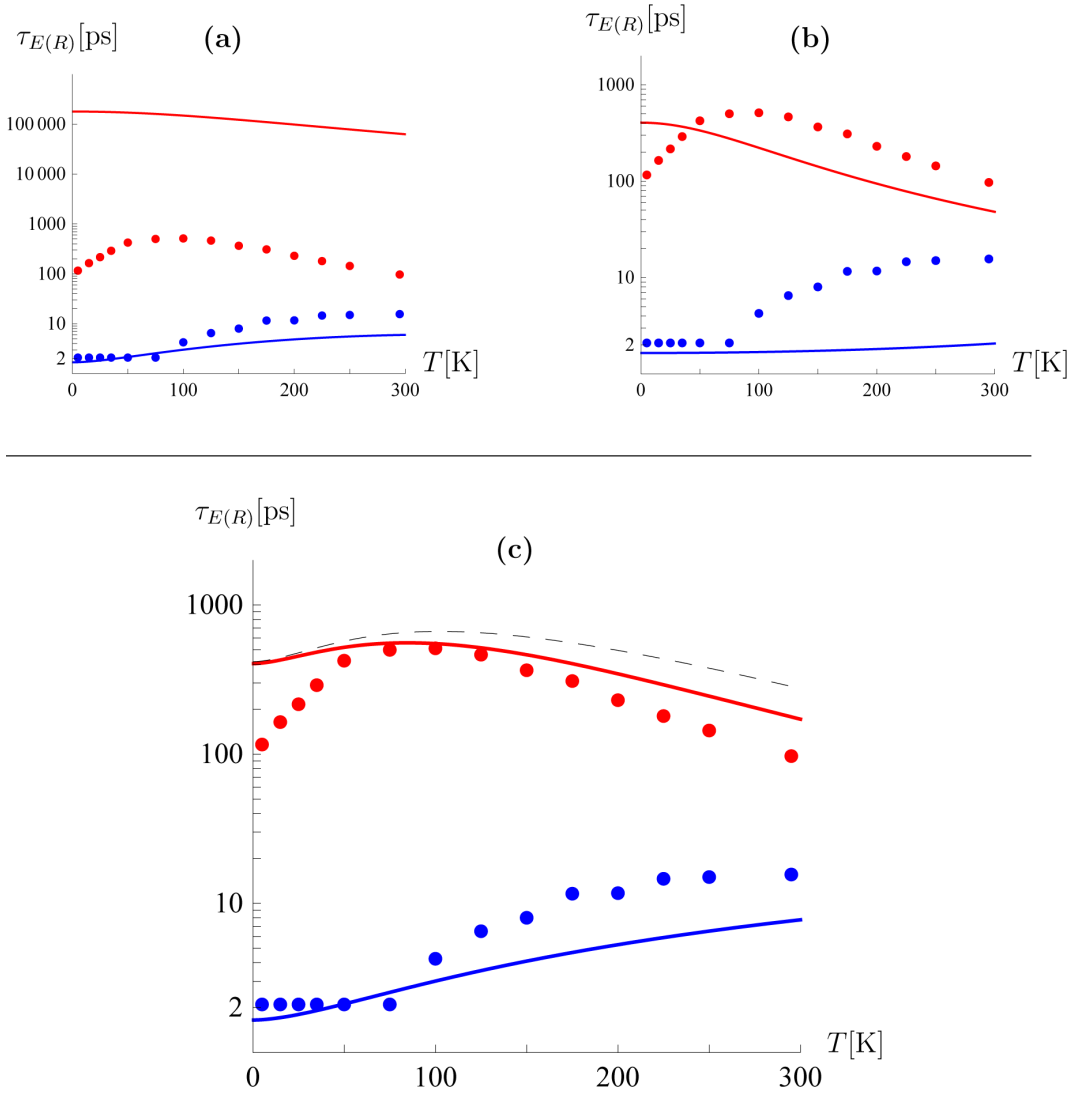

Figure 3.7.: Temperature-dependent lifetimes of the enhanced (red) and reduced (blue) PSH modes. The points are experimental data from Koralek *et al.* [2009]. Solid lines are our theoretical results in different approximations: (a) including only extrinsic spin-orbit interactions (no cubic Dresselhaus spin-orbit interactions and electron-electron interactions); (b) including extrinsic and cubic Dresselhaus spin-orbit interaction, but no electron-electron interaction; (c) including extrinsic and cubic Dresselhaus spin-orbit interactions as well as electron-electron interactions; here, the thin dashed line shows for comparison the simplified result (3.73).

D'Amico and Vignale [2003]. With these electron-electron scattering rates we find for the effective scattering rates in Eqs. (3.40)-(3.41) and (3.46) the values depicted in Fig. 3.6(b).

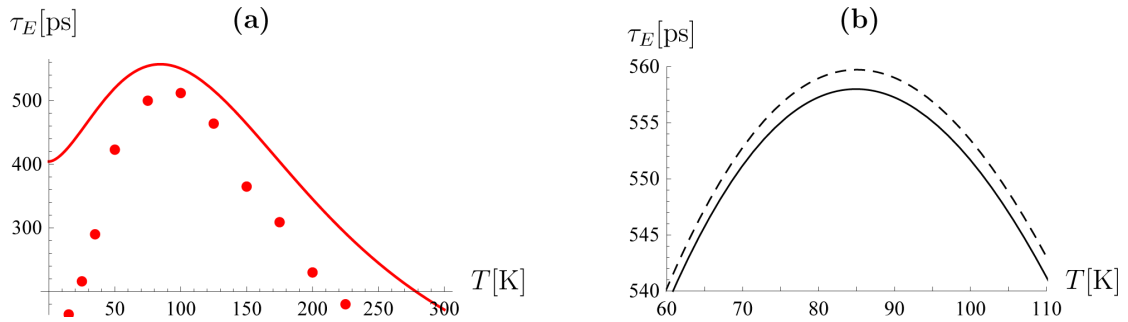

Figure 3.8.: (a) Linear plot of the enhanced lifetime τ_E as measured by Koralek *et al.* [2009] (points) and calculated theoretically (solid line) taking into account linear and cubic Dresselhaus spin-orbit interactions as well as electron-electron scattering. (b) Zoom into the maximum of of the theoretical curve for τ_E. The dashed line is the result *without* extrinsic spin-orbit interaction.

In Fig. 3.7, we show the numerical results for the temperature dependence of the spin-orbit-enhanced and -reduced lifetimes $\tau_{E(R)}$ where we use the experimental parameters of Koralek *et al.*[3] In particular, we take $T_F = 400$ K as the Fermi temperature, $\alpha = 0.0013$ for the Rashba spin-orbit interaction and $\gamma\, v_F = 5.0$ eV Å^3 for the cubic Dresselhaus spin-orbit interaction. We assume $\zeta = 0.2$ for the ratio of cubic-to-linear Dresselhaus spin-orbit coupling and adjust the linear Dresselhaus spin-orbit interaction to $\beta = 1.29\,\alpha$ in order to maximize τ_E for $T = 75$ K—the temperature at which also in the experiment the spin-orbit interaction was tuned to maximize τ_E.

Note that over the whole temperature range depicted in Fig. 3.7 we use for the transport relaxation time the value $\tau = 1$ ps, which is correct for $T = 100$ K.[4] Since the experimental τ exhibits a neat decrease with increasing temperature—roughly by one order of magnitude between 5 and 100 K—due to mechanisms that are not included in our model, we cannot expect our results to accurately match the experimental data for very low and high temperatures. At intermediate temperatures around 100 K, *i.e.*, in the temperature range where our theory should be most applicable, we find good agreement between our theory and the experimental lifetimes, see Fig. 3.7 (c). We observe a maximum in τ_E close to where the experimental data points exhibit one, see also the non-logarithmic plot in Figure 3.8 (a). Also the size of τ_E as well as of τ_R is very close to the experimental values. Since the scattering rates due to extrinsic spin-orbit interaction are very small in the GaAs/AlGaAs quantum well under consideration ($\gamma_{\rm ey}/\gamma_{\rm cD} \approx 10^{-4}$ and $\tau\,\gamma_{\rm sw} \approx 3\times 10^{-3}$), effects of extrinsic spin-orbit interaction turn out to be negligible, see Fig. 3.8 (b). A calculation which includes extrinsic spin-orbit interactions and electron-electron interactions but excludes cubic Dresselhaus spin-orbit interaction (Figure 3.7 (a)) yields enhanced lifetimes that exceed the experimental ones by a factor $\sim 10^2 - 10^3$.

Interestingly, the simple result (3.73) for the enhanced lifetime, where we neglected the

[3] These parameters are in turn partly obtained from fits to the theory of Stanescu and Galitski [2007].
[4] J. D. Koralek, private communication.

renormalization of the linear Dresselhaus spin-orbit interaction due to cubic Dresselhaus spin-orbit interaction, is a fairly good approximation (see dashed curve in Fig. 3.7 (c)). Thus the simple interpretation of the temperature dependence of τ_E can also be extended to the present situation. The formation of the maximum in τ_E at intermediate temperatures around 100 K is caused by the competition between two effects: on the one hand, τ_E increases with temperature due to increasing electron-electron scattering, which leads in the presence of symmetry breaking cubic Dresselhaus interaction to the usual motional-narrowing effect in the D'yakonov-Perel' regime (*cf.* Glazov and Ivchenko [2003]). On the other hand, the magnitude of Sommerfeld corrections increases with temperature reducing the lifetime τ_E in two ways: (i) by increasing the effective cubic Dresselhaus scattering rate $\gamma_{\mathrm{cd}}\, z_6$ and (ii) by increasing the linear renormalization of the Dresselhaus spin-orbit interaction, which leads to a detuning of the Rashba and the effective linear Dresselhaus spin-orbit interactions.

The important effect of electron-electron scattering for the temperature dependence of the lifetimes τ_E and τ_R can also be deduced from Fig. 3.7 (b), where we show the lifetimes excluding the effect of electron-electron interactions. Obviously, the initial increase of the lifetimes with temperature is absent for both τ_E and τ_R in the absence of electron-electron interaction.

Deviations between our theory and the experimentally observed lifetimes are more pronounced for very low temperatures and for high temperatures. We suppose that at high temperatures symmetry breaking mechanisms that are not captured by our model (*e.g.*, effects involving phonons) can become important. Furthermore, since the Fermi temperature in the GaAs/AlGaAs quantum well under consideration is only $T_F = 400$ K we cannot expect our calculation, which is based on a low-order Sommerfeld expansion, to be as accurate in the high temperature range above 200 K. The disagreement at low temperatures, on the other hand, results most likely from the fact that we do not take into account the temperature dependence of the transport lifetime but rather use the experimental 100 K-transport lifetime $\tau(100\ \mathrm{K}) = 1$ ps at all temperatures. In reality, however, the transport lifetime increases with decreasing temperature such that $b_F\tau_1 \gtrsim 1$ for low temperatures, *i.e.*, the system is outside the D'yakonov-Perel' regime and our theory is no longer applicable. In this low temperature regime other approaches, which account for strong spin-orbit interaction, should be used [Bernevig and Hu, 2008; Liu *et al.*, 2011].

3.6. Summary

Using a Boltzmann-type approach we have derived semiclassical spin-diffusion equations for a 2DEG with Rashba and linear Dresselhaus spin-orbit interactions that also take into account the cubic Dresselhaus spin-orbit interaction, extrinsic spin-orbit interaction and electron-electron scattering. Our results for the temperature-dependent lifetime of the persistent spin helix are, within the range of validity of our diffusive low-temperature theory, in qualitative and reasonable quantitative agreement with recent measurements by Koralek *et al.* [2009].

It turns out that the influence of extrinsic spin-orbit interaction is negligible for the parameters of the experiment. The lifetime of the PSH at finite temperatures is mainly

a result of the interplay of cubic Dresselhaus spin-orbit interaction and electron-electron scattering: due to the latter, the relaxation rate of winding-number-± 3 components of the spin distributions function in momentum space grows with increasing temperature. Since, in the D'yakonov-Perel' regime, the *inverse* of this rate enters the effective relaxation rate due to cubic Dresselhaus spin-orbit interaction, electron-electron interactions tend to increase the PSH lifetime with increasing temperature. However, at some point the competition with positive finite-temperature corrections in the expression of the relaxation rate is won by the latter, which explains the formation of a maximum. Another contribution to the reduction of the lifetime are temperature-induced deviations from the symmetry point due to a momentum-dependent renormalization of the linear Dresselhaus coupling constant in the presence of cubic Dresselhaus spin-orbit interaction.

Note that, qualitatively, the mechanism described above would as well work with extrinsic spin-orbit interaction as the only SU(2) violating ingredient in the model. In that case, ordinary spin Coulomb drag would be responsible for the PSH lifetime to increase with temperature, whereas, again, Sommerfeld expansion corrections would tend to decrease the lifetime. Thus, apart from the issue of the PSH lifetime and leaving cubic Dresselhaus spin-orbit interaction and extrinsic spin-orbit interaction aside, we have presented the generalization of the Boltzmann-equation derivation of spin Coulomb drag for the *collinear* case (only spin-up and spin-down) by Flensberg *et al.* [2001] to a *coherent* description, which is necessary to capture a spin precession term. In order to respond to the cubic Dresselhaus spin-orbit interaction in our problem we have extended the calculation to distribution functions which contain winding-number-± 3 components.

We propose a spatially damped sinusoidal spin profile as initial condition for a TSG experiment in order to further enhance the PSH lifetime. In theory, the infinite lifetime can thus be restored in presence of symmetry breaking mechanisms as long as these appear as relaxation rates in the spin diffusion equation.

In order to further refine the theory for general situations where the cubic Dresselhaus spin-orbit interaction might be less dominant, it would be interesting for future work to include disorder in the local Rashba spin-orbit coupling or spin-dependent electron-electron scattering (a variant of the Elliot-Yafet mechanism, but based on two-particle Coulomb scattering). These relaxation mechanisms are currently discussed in the context of spin relaxation in (110) grown GaAs quantum wells [Sherman, 2003; Glazov *et al.*, 2010].

4. Effects of Coulomb exchange interaction on the persistent spin helix

In this chapter we investigate how the persistent spin helix is affected by the mean field (Hartree-Fock) contribution of the electron-electron interactions, which we have neglected all along in Chapter 3. As a consequence of the nonlinear nature of this extended problem, the lifetime of the spin-density wave becomes dependent on the degree of initial spin-polarization. We find that for large initial spin polarizations in the percentage range a considerable increase in the relaxation time is to be expected. Furthermore, we find qualitative changes in the shape of the spin helix with, in particular, the so far inactive third component of the spin polarization vector (*i.e.*, S_x when coordinates are chosen as in Chapter 3) and higher harmonics coming into play.

4.1. Introduction

The persistent spin helix has been introduced in Chapter 3 as a peculiar spin-density wave of infinite lifetime that exists in two-dimensional electron systems with Rashba and linear Dresselhaus spin-orbit interactions of equal magnitude [Bernevig *et al.*, 2006]. We have seen that in real systems the lifetime of the persistent spin helix is no longer infinite due to the presence of additional terms that break the SU(2) symmetry of the Hamiltonian. For the particular experimental realization of a spin helix in a GaAs/AlGaAs quantum well by Koralek *et al.* [2009], cubic Dresselhaus spin-orbit interaction has been proposed as the primary suspect among other candidate symmetry breaking mechanisms that can cause a finite lifetime of the persistent spin helix state [Koralek *et al.*, 2009; Lüffe *et al.*, 2011]. As pointed out by Koralek *et al.*, the observed temperature dependence of the lifetime of the persistent spin helix suggests that also electron-electron interactions strongly affect the relaxation process. Developing this idea to the stage of a quantitative theory, we have found in Chapter 3 that the inclusion of Coulomb scattering, in combination with cubic Dresselhaus spin-orbit interaction as the required symmetry breaking mechanism, can fairly well account for the observed temperature dependent PSH lifetime [Lüffe *et al.*, 2011].

Regarding the influence of Coulomb interactions, in our previous treatment we have only considered electron-electron *collisions*, which are of second order in the electron-electron interaction, but we have neglected the mean field Hartree-Fock term, which arises in first order. This approximation is valid when the initial spin polarization is small and it appears to be appropriate for the description of the experiment by Koralek *et al.* However, it is also possible to realize large initial spin polarizations experimentally [Stich *et al.*, 2007]. The Hartree-Fock term then acts as an effective magnetic field pointing along the local spin polarization, which can enhance the spin lifetime considerably [Weng and Wu, 2003;

Stich *et al.*, 2007]. As put forward by Takahashi *et al.* [1999], the influence of the molecular field produced by an average spin polarization in a degenerate two-dimensional electron gas is analogous to the spin diffusion dynamics in liquid ^{3}He in 3d, where the exchange field of the average spin exerts a torque on spin currents [Leggett and Rice, 1968; Leggett, 1970].

In the present chapter it is our goal to analyze the effect of the Hartree-Fock term on the persistent spin helix in the diffusive D'yakonov Perel' regime. In particular, we want to answer the following questions:

(i) what effect does the Hartree-Fock field have on the lifetime of the persistent spin helix and

(ii) does it qualitatively modify the pattern of the persistent spin helix?

We restrict our calculation to zero temperature in order to avoid formal complications due to, *e.g.*, the renormalization of linear Dresselhaus spin-orbit coupling by the cubic one (*cf.* Chapter 3). This approximation seems acceptable also for quantitative evaluations and predictions, since the temperature dependence of the Hartree-Fock interaction turns out to be weak.

The structure of this chapter is the following: in Section 4.2 we derive the Hartree-Fock contribution to the kinetic equation for the spin density within the Nonequilibrium statistical operator method. In Section 4.3 we obtain the spin diffusion equations valid in the diffusive D'yakonov Perel' regime including the effect of the Hartree-Fock field. Then we analyze in Section 4.4 the effect of the Hartree-Fock interaction on the lifetime (Subsection 4.4.2) and the pattern (Subsection 4.4.3) of the persistent spin helix for small cubic Dresselhaus spin-orbit interactions—a regime that can also be addressed perturbatively. Finally, in Subsection Section 4.4.4, we consider the influence of the Hartree-Fock field in a situation where the cubic Dresselhaus spin-orbit interaction is of similar order of magnitude as the linear Rashba and Dresselhaus spin-orbit interactions. In this parameter regime nonlinear effect turn out to be quite pronounced.

4.2. Derivation of the Hartree-Fock term

In this section, we derive the Hartree-Fock mean field term due to electron-electron interactions. Its consequences for the persistent spin helix will be studied in the following. Our considerations are based on the model Hamiltonian of a GaAs quantum well as presented in Chapter 3.2, which includes Rashba as well as linear and cubic Dresselhaus spin-orbit coupling and, in addition, electron-impurity and electron-electron interactions.

In a first step we go back to the general expressions from Chapter 2.2, which have served us in Chapter 3 as a starting point for the derivation of the kinetic equation for the spin density (3.16) including the collision integrals for electron-impurity scattering and electron-electron scattering. We recall that for a general nonequilibrium problem, where the system Hamiltonian $H = H_0 + V$ contains an exactly solvable single-particle part H_0 and an interaction V, the Nonequilibrium statistical operator formalism (see Chapter 2.2) permits to derive a closed set of equations describing the irreversible temporal evolution of the density matrix $f_{ll'}(t) \equiv \langle \psi^\dagger_{l'} \psi_l \rangle^t = \mathrm{Tr}[\rho(t)\, \psi^\dagger_{l'} \psi_l]$. For our purpose, l is a composed

index for both momentum and spin. The kinetic equation in Born approximation (*i.e.*, up to quadratic order in V) reads (*cf.* Eq. (2.54))

$$\partial_t \langle \psi^\dagger_{l'} \psi_l \rangle^t - i \, \langle [H_0, \psi^\dagger_{l'} \psi_l] \rangle^t \;=\; J^{(1)}_{ll'}(t) + J^{(2)}_{ll'}(t) \,. \tag{4.1}$$

The commutator becomes a simple linear combination of density matrix entries, resulting for the particular Hamiltonian under consideration in the gradient term and the precession term on the left-hand side of Eq. (3.16). On the right-hand side of Eq. (4.1), we have the second-order (in the interaction V) collision term $J^{(2)}_{ll'}(t)$, *cf.* Eq. (2.55), and the first-order mean field term (2.52)

$$J^{(1)}_{ll'}(t) \;=\; \frac{i}{\hbar} \left\langle [V, \psi^\dagger_{l'} \psi_l] \right\rangle^t_{\mathrm{rel}} \,. \tag{4.2}$$

Here, the average is with respect to the relevant statistical operator (see Chapter 2.2.2), thus allowing for a decomposition according to Wick's theorem.

Taking for H_0 the spin-orbit coupled Hamiltonian from Chapter 3.2 with Rashba as well as linear and cubic Dresselhaus spin-orbit interaction and identifying $V = H_{\mathrm{imp}} + H_{\mathrm{e\text{-}e}}$ with the Hamiltonians for the electron-impurity interactions and electron-electron interactions, one obtains, upon Wigner transformation and first-order gradient expansion of the left-hand side, kinetic equations for the charge and spin parts of the density matrix with the corresponding second-order collision integrals (see Chapter 3.3). In the case of electron-impurity interaction the mean field contribution (4.2) vanishes. This is, however, *not* the case for electron-electron interactions.

In Chapter 3 we neglected the mean field term (4.2) because in the particular experiment by Koralek *et al.* [2009] the initial polarization S_0 was supposedly so small that nonlinear effects of the Hartree-Fock precession term were negliglible. The fact that no dependence of the persistent spin helix lifetime on the magnitude of the initial polarization S_0 could be observed[1] fosters this view. However, it would be beneficial to understand the smallness of the term from a calculation with the parameters of this very experiment (and thus possibly find an upper boundary for the polarization that was actually reached). Apart from that, it is interesting to study the consequences of the mean field term for general parameter regimes.

We evaluate the mean field term (4.2) for electron-electron interactions (*cf.* Eq. (3.11))

$$H_{\mathrm{e\text{-}e}} \;=\; \frac{1}{2} \sum_{\substack{\boldsymbol{k_1} \ldots \boldsymbol{k_4} \\ s_1, s_2, s_3, s_4}} V_{\boldsymbol{k_3} s_3, \boldsymbol{k_4} s_4, \boldsymbol{k_1} s_1, \boldsymbol{k_2} s_2} \, \psi^\dagger_{\boldsymbol{k_4} s_4} \psi^\dagger_{\boldsymbol{k_3} s_3} \psi_{\boldsymbol{k_1} s_1} \psi_{\boldsymbol{k_2} s_2} \tag{4.3}$$

with the Thomas-Fermi screened Coulomb potential

$$V_{\boldsymbol{k_3} s_3, \boldsymbol{k_4} s_4, \boldsymbol{k_1} s_1, \boldsymbol{k_2} s_2} \;=\; \delta_{\boldsymbol{k_3} + \boldsymbol{k_4} - \boldsymbol{k_1} - \boldsymbol{k_2}, 0} \, \delta_{s_1, s_3} \, \delta_{s_2, s_4} \, \tilde{v}(|\boldsymbol{k_3} - \boldsymbol{k_1}|) \,, \tag{4.4}$$

where $\tilde{v}(k) = \frac{v(k)}{\epsilon(k)}$ with the Fourier transform of the Coulomb potential in 2d, $v(q) = \frac{\hbar^2 2\pi}{\epsilon_q m \, q \, a^*}$, and the polarizability $\epsilon_q \approx 1 + \frac{2}{q \, a^*}$. We recall from Chapter 3.2 that $a^* = \frac{\hbar^2 4\pi \, \epsilon_0 \, \epsilon_r}{m \, e^2}$ denotes the effective Bohr radius.

[1] J. D. Koralek, private communication.

In the following we will occasionally shorten the expressions by writing, *e.g.*, $\psi_1 \equiv \psi_{\boldsymbol{k}_1 s_1}$. Evaluation of the commutator in (4.2) yields in this notation

$$\begin{aligned} J^{\mathrm{ee}(1)}_{11'} &= \frac{i}{\hbar}\left\langle [H_{\text{e-e}}, \psi^\dagger_{1'}\psi_1]\right\rangle_{\mathrm{rel}} \\ &= \frac{1}{i\,\hbar}\sum_{2'3'23} V_{2'3'23}\left(\delta_{13'}\left\langle \psi^\dagger_{1'}\psi^\dagger_{2'}\,\psi_2\,\psi_3\right\rangle_{\mathrm{rel}} - \delta_{1'3}\left\langle \psi^\dagger_{3'}\psi^\dagger_{2'}\,\psi_2\,\psi_1\right\rangle_{\mathrm{rel}}\right). \end{aligned} \tag{4.5}$$

Upon Wick decomposition of the averages

$$\begin{aligned} \left\langle \psi^\dagger_1\psi^\dagger_2\,\psi_3\,\psi_4\right\rangle_{\mathrm{rel}} &= -\left\langle \psi^\dagger_1\,\psi_3\right\rangle_{\mathrm{rel}}\left\langle \psi^\dagger_2\,\psi_4\right\rangle_{\mathrm{rel}} + \left\langle \psi^\dagger_1\,\psi_4\right\rangle_{\mathrm{rel}}\left\langle \psi^\dagger_2\,\psi_3\right\rangle_{\mathrm{rel}} \\ &= -\delta_{\boldsymbol{k}_1\,\boldsymbol{k}_3}\,\delta_{\boldsymbol{k}_2\,\boldsymbol{k}_4}\,f_{s_1s_3}(\boldsymbol{k}_1)\,f_{s_2s_4}(\boldsymbol{k}_2) + \delta_{\boldsymbol{k}_1\,\boldsymbol{k}_4}\,\delta_{\boldsymbol{k}_2\,\boldsymbol{k}_3}\,f_{s_1s_4}(\boldsymbol{k}_1)\,f_{s_2s_3}(\boldsymbol{k}_2) \end{aligned} \tag{4.6}$$

and by exploiting the Kronecker symbols we obtain a mean field term that is diagonal in momentum but remains a matrix in spin space,

$$J^{\mathrm{ee}(1)}_{ss'}(\boldsymbol{k}) = \frac{1}{i\hbar}\sum_{\boldsymbol{k'}}\tilde{v}(|\boldsymbol{k'}-\boldsymbol{k}|)\left[\big(f(\boldsymbol{k'})\,f(\boldsymbol{k})\big)_{ss'} - \big(f(\boldsymbol{k})\,f(\boldsymbol{k'})\big)_{ss'}\right]. \tag{4.7}$$

By decomposing the spin space matrices according to

$$\hat{f}(\boldsymbol{k}) = n_{\boldsymbol{k}} + \boldsymbol{\sigma}\cdot\boldsymbol{s}_{\boldsymbol{k}}\,, \qquad \hat{J}^{\mathrm{ee}(1)}_{\boldsymbol{k}} = J^{\mathrm{ee}(1)}_{\boldsymbol{k}} + \boldsymbol{\sigma}\cdot\boldsymbol{J}^{\mathrm{ee}(1)}_{\boldsymbol{k}}\,, \tag{4.8}$$

one finds that the mean field term does not affect the charge density $n_{\boldsymbol{k}}$ (since $J^{\mathrm{ee}(1)}_{\boldsymbol{k}} = 0$), but has an influence on the spin density $\boldsymbol{s}_{\boldsymbol{k}}$, with the additional term

$$\boldsymbol{J}^{\mathrm{ee}(1)}_{\boldsymbol{k}} = -\frac{2}{\hbar}\,s_{\boldsymbol{k}}\times\int\frac{\mathrm{d}\boldsymbol{q}}{(2\pi)^2}\,\tilde{v}(q)\,s_{\boldsymbol{k}+\boldsymbol{q}} \tag{4.9}$$

entering on the right-hand side of the kinetic equation for the spin density (*cf.* Eq. (3.16))

$$\partial_t\,\boldsymbol{s}_{\boldsymbol{k}} + 2\,\boldsymbol{s}_{\boldsymbol{k}}\times\boldsymbol{b}(\boldsymbol{k}) + \boldsymbol{v}\cdot\partial_{\boldsymbol{x}}\boldsymbol{s}_{\boldsymbol{k}} = \boldsymbol{J}^{\mathrm{imp}}_{\boldsymbol{k}} + \boldsymbol{J}^{\mathrm{ee}(1)}_{\boldsymbol{k}}\,. \tag{4.10}$$

4.3. Spin diffusion equation with Hartree-Fock precession

The goal of the present section is to derive from the kinetic equation (4.10) a spin diffusion equation (*cf.* Chapter 3.3.2) that enables us to discuss the effect of the Hartree-Fock interaction on the persistent spin helix. In the presence of cubic Dresselhaus spin-orbit interaction this state is characterized by the vector components

$$S_x = 0\,, \qquad S_y = -S_0\,e^{-\frac{t}{\tau_E}}\sin q_0 y\,, \qquad S_z = S_0\,e^{-\frac{t}{\tau_E}}\left(\sqrt{1+\frac{\gamma^2_{\mathrm{cD}}}{\Gamma^2}} - \frac{\gamma_{\mathrm{cD}}}{\Gamma}\right)\cos q_0 y\,. \tag{4.11}$$

These are obtained from our result for the transient spin grating experiment, Eqs. (3.68)-(3.69), in the limit of large times (use that $\tau_R \ll \tau_E$). We recall that the PSH lifetime τ_E is given as (*cf.* Eq. (3.70))

$$\frac{1}{\tau_E} = \frac{1}{2}\left(\Gamma + 3\,\gamma_{\mathrm{cD}} - \sqrt{\Gamma^2+\gamma^2_{\mathrm{cD}}}\right), \tag{4.12}$$

where $\Gamma = 4q_0^2 D$ with the PSH wave vector $q_0 = 4mv_F\alpha$ and the ordinary diffusion constant $D = \frac{1}{2}v_F^2\tau_1$. The relaxation rate $\gamma_{\mathrm{cD}} = \frac{1}{8}v_F^2\gamma^2 k_F^6\tau_3$ results from cubic Dresselhaus scattering, *cf.* Eq. (3.49). Here, $\tau_{1(3)}$ is the effective relaxation time for the winding-number-$\pm1(\pm3)$ parts of the phase-space spin distribution function. Although in our model (with spin-independent, *isotropic* scattering from point-like impurities and no electron-electron scattering, since $T = 0$) we have $\tau_1 = \tau_3 = \tau$, this is not true in general, *cf.* Eqs. (3.40) and (3.46). Therefore we use the more general $\tau_{1(3)}$ in all expressions in order to make an extension to including, *e.g.*, second-order electron-electron interaction at finite temperatures straightforward.

We follow the approach used already in Chapter 3.3.2 to set up a diffusion equation for the spin density $\boldsymbol{s}_{\boldsymbol{k}}$, which is valid in the diffusive D'yakonov-Perel' regime, *i.e.*, in the case $b_F\tau \ll 1$, where the spin polarization is stabilized due to strong scattering. In order to solve Eq. (4.10) for the real-space spin density $\boldsymbol{S}(\boldsymbol{x},t)$ we expand the spin density into k-space winding numbers (*cf.* Eq. (3.22)),

$$\boldsymbol{s}_{\boldsymbol{k}}(\boldsymbol{x},t) \;=\; \boldsymbol{s}_{\boldsymbol{k},0}(\boldsymbol{x},t) + \boldsymbol{s}_{\boldsymbol{k},1}(\boldsymbol{x},t) + \boldsymbol{s}_{\boldsymbol{k},3}(\boldsymbol{x},t)\,. \tag{4.13}$$

We include in this ansatz distribution the isotropic component

$$\boldsymbol{s}_{\boldsymbol{k},0}(\boldsymbol{x},t) \;=\; -\frac{2\pi\hbar^2}{m}\,f'(\epsilon_k)\,\boldsymbol{S}(\boldsymbol{x},t) \tag{4.14}$$

and anisotropic components with winding numbers ±1 and ±3 of the form ($n = 1, 3$)

$$\boldsymbol{s}_{\boldsymbol{k},n}(\boldsymbol{x},t) \;=\; f'(\epsilon_k)\,\frac{k^n}{k_F^{n-1}m}\sum_{l=\pm n}\boldsymbol{\delta k_l}(\boldsymbol{x},t)\,e^{i\,l\,\theta}\,. \tag{4.15}$$

As discussed in Chapter 3.3.2, all contributions with other winding numbers would be of higher order in $b_F\tau$ and therefore they can be safely neglected in the diffusive regime considered in the following. Note, however, that in Eq. (4.13) we do not include a term like the $\tilde{\boldsymbol{s}}_{\boldsymbol{k},1}$ from Eq. (3.22), *i.e.*, we do not consider the effects of cubic Dresselhaus spin-orbit coupling renormalizing the linear one (which is consistent with a strict zero temperature calculation).

Inserting the ansatz distribution (4.13) into the Hartree-Fock interaction term (4.9) and anticipating that we will, as in Chapter 3.3.2, consider the kinetic equations for different winding numbers ($l = 0, \pm1, \pm3$) by integrating $\frac{1}{(2\pi)^2}\int \mathrm{d}\boldsymbol{k}\,e^{il\theta}$ [Eq. (4.10)], we find that the Hartree-Fock term can be written in the compact form

$$\boldsymbol{J}_{\boldsymbol{k}}^{\mathrm{ee}(1)} \;=\; \boldsymbol{S}\times\left[\chi_1(k)\,\boldsymbol{s}_{\boldsymbol{k},1} + \chi_3(k)\,\boldsymbol{s}_{\boldsymbol{k},3}\right] \tag{4.16}$$

with ($n = 1, 3$)

$$\chi_n(k) \;=\; -\frac{4\pi\hbar}{m}\int\frac{\mathrm{d}\boldsymbol{q}}{(2\pi)^2}\,\tilde{v}(|\boldsymbol{q}-\boldsymbol{k}|)\,f'(\epsilon_{\boldsymbol{q}})\left(1-\frac{q^n}{k^n}\,\cos(n\,\theta_{\boldsymbol{qk}})\right). \tag{4.17}$$

At zero temperature we thus have

$$\chi_n(k) \;\overset{T=0}{=}\; \frac{1}{\hbar\pi}\int_0^{2\pi}\mathrm{d}\theta\,\tilde{v}\left(\sqrt{k^2+k_F^2-2\,k_F k\,\cos\theta}\right)\left(1-\frac{k_F^n}{k^n}\,\cos(n\,\theta)\right). \tag{4.18}$$

Since in a $T = 0$ calculation the momentum arguments of all terms in the Boltzmann equation (when integrated over momentum) are fixed at k_F, we need to calculate

$$\chi_n(k_F) \overset{T=0}{=} \frac{\hbar}{m}\int_0^{2\pi} \mathrm{d}\theta\, \frac{1}{1+\frac{a^* k_F}{\sqrt{2}}\sqrt{1-\cos\theta}}\,(1-\cos(n\,\theta))\,. \tag{4.19}$$

Plugging the Hartree-Fock precession term (4.16) back into the kinetic equation for the spin density Eq. (4.10) one finds for the isotropic (in k-space) part of the spin density

$$\partial_t \boldsymbol{s}_0 \;=\; -\frac{v}{2}\partial_x \boldsymbol{s}_c - \frac{v}{2}\partial_y \boldsymbol{s}_s - \boldsymbol{s}_c \times \boldsymbol{b}_c - \boldsymbol{s}_s \times \boldsymbol{b}_s - \boldsymbol{s}_{c3} \times \boldsymbol{b}_{c3} - \boldsymbol{s}_{s3} \times \boldsymbol{b}_{s3} \tag{4.20}$$

with

$$\begin{array}{lll} \boldsymbol{s}_c \;=\; \boldsymbol{s}_1 + \boldsymbol{s}_{-1}, & & \boldsymbol{s}_{c3} \;=\; \boldsymbol{s}_3 + \boldsymbol{s}_{-3}, \\ \boldsymbol{s}_s \;=\; i(\boldsymbol{s}_1 - \boldsymbol{s}_{-1}), & & \boldsymbol{s}_{s3} \;=\; i\,(\boldsymbol{s}_3 - \boldsymbol{s}_{-3}) \end{array} \tag{4.21}$$

and the spin-orbit fields

$$\begin{array}{lll} \boldsymbol{b}_c \;=\; v_F k\,(-\alpha+\beta)\,\hat{\boldsymbol{e}}_y, & & \boldsymbol{b}_s \;=\; v_F k\,(\alpha+\beta)\,\hat{\boldsymbol{e}}_x, \\ \boldsymbol{b}_{c3} \;=\; -\gamma\, v_F \tfrac{k^3}{4}\,\hat{\boldsymbol{e}}_y, & & \boldsymbol{b}_{s3} \;=\; \gamma\, v_F \tfrac{k^3}{4}\hat{\boldsymbol{e}}_x. \end{array} \tag{4.22}$$

In order to obtain a closed equation for $\boldsymbol{s}_0$ one needs to determine $\boldsymbol{s}_c$, $\boldsymbol{s}_s$, $\boldsymbol{s}_{c3}$ and $\boldsymbol{s}_{s3}$ from the anisotropic components of the Boltzmann equation. In the diffusive regime it is sufficient to find the (quasi-)equilibrium solutions for the anisotropic coefficients, which are obtained by omitting the time derivative of the anisotropic components (*cf.* Chapter 3.3.2 and Appendix app:coarsegraining). Using this approximation one finds for the winding-number-±1 components:

$$\begin{aligned} \frac{\boldsymbol{s}_c}{\tau_1(k)} &= -v\partial_x \boldsymbol{s}_0 + 2\boldsymbol{b}_c \times \boldsymbol{s}_0 + 2\boldsymbol{B}_1 \times \boldsymbol{s}_c\,, \\ \frac{\boldsymbol{s}_s}{\tau_1(k)} &= -v\partial_y \boldsymbol{s}_0 + 2\boldsymbol{b}_s \times \boldsymbol{s}_0 + 2\boldsymbol{B}_1 \times \boldsymbol{s}_s\,, \end{aligned} \tag{4.23}$$

where $\boldsymbol{B}_1 \equiv \chi_1 \boldsymbol{S}$ is the Hartree-Fock field experienced by winding-number-±1 spins. The transport relaxation times due to impurity scattering that we need here and below are (*cf.* Eq. (3.18))

$$\tau_n(k)^{-1} \;=\; \sum_{\boldsymbol{k'}} W_{\boldsymbol{k}\boldsymbol{k'}}\,\delta(\epsilon_k - \epsilon_{k'})\,(1-\cos n\theta)\,, \tag{4.24}$$

where $n = 1$ refers to winding-number-±1 spins and $n = 3$ refers to winding-number-±3 spins. Note that, within our model of *isotropic* impurity scattering, the cosine term vanishes and one has $\tau_1 = \tau_3 = \tau$. One should, however, keep in mind that in the case of scattering from, *e.g.*, charged impurities, differences between τ_1 and τ_3 arise due to the angular dependence of $W_{\boldsymbol{k}\boldsymbol{k'}}$ in Eq. (4.24). Solving Eqs. eq:ScSs one finds

$$\begin{aligned} \boldsymbol{s}_c \;=\;& -\bar{\tau}_1(k)\,\{v\partial_x \boldsymbol{s}_0 - 2\boldsymbol{b}_c \times \boldsymbol{s}_0 + 2\tau_1(k) v(\boldsymbol{B}_1 \times \partial_x \boldsymbol{s}_0) \\ & -4\tau_1(k)\boldsymbol{B}_1 \times (\boldsymbol{b}_c \times \boldsymbol{s}_0) + 4\tau_1(k)^2 v \boldsymbol{B}_1 (\boldsymbol{B}_1 \cdot \partial_x \boldsymbol{s}_0)\}\,, \\ \boldsymbol{s}_s \;=\;& -\bar{\tau}_1(k)\,\{v\partial_y \boldsymbol{s}_0 - 2\boldsymbol{b}_s \times \boldsymbol{s}_0 + 2\tau_1(k) v(\boldsymbol{B}_1 \times \partial_y \boldsymbol{s}_0) \\ & -4\tau_1(k)\boldsymbol{B}_1 \times (\boldsymbol{b}_s \times \boldsymbol{s}_0) + 4\tau_1(k)^2 v \boldsymbol{B}_1 (\boldsymbol{B}_1 \cdot \partial_y \boldsymbol{s}_0)\}\,, \end{aligned} \tag{4.25}$$

where we have used that $\boldsymbol{B}_1 || \boldsymbol{s}_0$ and a renormalized relaxation time

$$\bar{\tau}_1(k) \;=\; \frac{\tau_1(k)}{1+(2B_1\tau_1(k))^2} \tag{4.26}$$

has been introduced. Similarly, the steady state of the winding-number-± 3 anisotropic components of the spin density is governed by the equations

$$\begin{aligned} \frac{\boldsymbol{s}_{c3}}{\tau_3(k)} &= 2\boldsymbol{b}_{c3}\times\boldsymbol{s}_0 + 2\,\boldsymbol{B}_3\times\boldsymbol{s}_{c3}\,, \\ \frac{\boldsymbol{s}_{s3}}{\tau_3(k)} &= 2\boldsymbol{b}_{s3}\times\boldsymbol{s}_0 + 2\,\boldsymbol{B}_3\times\boldsymbol{s}_{s3}\,, \end{aligned} \tag{4.27}$$

where $\boldsymbol{B}_3 \equiv \chi_3 \boldsymbol{S}$ is the Hartree-Fock field acting on winding-number-± 3 spins. Solving these equations for $\boldsymbol{s}_{c3}$ and $\boldsymbol{s}_{s3}$ one finds

$$\begin{aligned} \boldsymbol{s}_{c3} &= 2\,\bar{\tau}_3(k)\left\{\boldsymbol{b}_{c3}\times\boldsymbol{s}_0 + 2\tau_3(k)\boldsymbol{B}_3\times(\boldsymbol{b}_{c3}\times\boldsymbol{s}_0)\right\}, \\ \boldsymbol{s}_{s3} &= 2\,\bar{\tau}_3(k)\left\{\boldsymbol{b}_{s3}\times\boldsymbol{s}_0 + 2\tau_3(k)\boldsymbol{B}_3\times(\boldsymbol{b}_{s3}\times\boldsymbol{s}_0)\right\}, \end{aligned} \tag{4.28}$$

where we have used that $\boldsymbol{B}_3 || \boldsymbol{s}_0$ and defined

$$\bar{\tau}_3(k) \;=\; \frac{\tau_3(k)}{1+(2\,B_3\tau_3(k))^2}\,. \tag{4.29}$$

Plugging the solutions for the anisotropic components Eq. (4.25) and Eq. (4.28) back into the equation for the isotropic spin density Eq. (4.20) and using the condition for the persistent spin helix, $\alpha = \beta$, one finds that the spin density $\boldsymbol{S} = \int \frac{\mathrm{d}\boldsymbol{k}}{(2\pi)^2}\boldsymbol{s}_0$ obeys the diffusion equation

$$\partial_t \mathbf{S} \;=\; \hat{D}\,\boldsymbol{S} + \hat{H}\,\boldsymbol{S}\,. \tag{4.30}$$

Here, the matrix

$$\hat{D} \;=\; \begin{pmatrix} \bar{D}\,\partial_y^2 - \bar{\gamma}_{\mathrm{cD}} & 0 & 0 \\ 0 & \bar{D}\,(\partial_y^2 - q_0^2) - \bar{\gamma}_{\mathrm{cD}} & 2\,q_0\,\bar{D}\,\partial_y \\ 0 & -2\,q_0\,\bar{D}\partial_y & \bar{D}\,(\partial_y^2 - q_0^2) - 2\,\bar{\gamma}_{\mathrm{cD}} \end{pmatrix} \tag{4.31}$$

corresponds to the usual spin diffusion matrix in the absence of Hartree-Fock fields (*cf.* Eq. (3.59)), but with a renormalized diffusion constant $\bar{D}$ and a renormalized cubic Dresselhaus scattering rate $\bar{\gamma}_{\mathrm{cD}}$ given by

$$\bar{D} \;=\; \frac{D}{1+(\chi_1\tau_1\,\boldsymbol{S})^2}\,, \quad \bar{\gamma}_{\mathrm{cD}} \;=\; \frac{\gamma_{\mathrm{cD}}}{1+(\chi_3\tau_3\,\boldsymbol{S})^2}\,. \tag{4.32}$$

The matrix $\hat{H}$ arises only in the presence of fields and is given by

$$
\begin{aligned}
H_{xx}S_x &= 4\tau_1^2\bar{D}\partial_y(B_{1x}^2\partial_y S_x)\,, \\
H_{xy}S_y &= -2\tau_1\bar{D}B_{1z}\partial_y^2 S_y - 2\tau_1 q_0\bar{D}\partial_y(B_{1y}S_y) \\
&\quad +4\tau_1^2\bar{D}\partial_y(B_{1x}B_{1y}\partial_y S_y)\,, \\
H_{xz}S_z &= 2\tau_1\bar{D}B_{1y}\partial_y^2 S_z - 2\tau_1 q_0\bar{D}\partial_y(B_{1z}S_z) - 2\tau_3\bar{\gamma}_{\mathrm{cD}}B_{3y}S_z \\
&\quad +4\tau_1^2\bar{D}\partial_y(B_{1x}B_{1z}\partial_y S_z)\,, \\
H_{yx}S_x &= 2\tau_1\bar{D}B_{1z}\partial_y^2 S_x - 2\tau_1 q_0\bar{D}B_{1y}\partial_y S_x \\
&\quad +4\tau_1^2\bar{D}\left[\partial_y(B_{1x}B_{1y}\partial_y S_x) + q_0 B_{1x}B_{1z}\partial_y S_x\right]\,, \\
H_{yy}S_y &= 2\tau_1 q_0\bar{D}(\partial_y B_{1x}S_y + 2B_{1x}\partial_y S_y) \\
&\quad +4\tau_1^2\bar{D}(\partial_y(B_{1y}^2\partial_y S_y) + q_0 B_{1y}B_{1z}\partial_y S_y)\,, \\
H_{yz}S_z &= 2\tau_3\bar{\gamma}_{\mathrm{cD}}B_{3x}S_z + 2\tau_1\bar{D}B_{1x}(q_0^2 S_z - \partial_y^2 S_z) \\
&\quad +4\tau_1^2\bar{D}[\partial_y(B_{1y}B_{1z}\partial_y S_z) + q_0 B_{1z}^2\partial_y S_z]\,, \\
H_{zx}S_x &= 2\tau_3\bar{\gamma}_{\mathrm{cD}}B_{3y}S_x - 2\tau_1\bar{D}(B_{1y}\partial_y^2 S_x + q_0 B_{1z}\partial_y S_x) \\
&\quad +4\tau_1^2\bar{D}[\partial_y(B_{1x}B_{1z}\partial_y S_x) - q_0 B_{1x}B_{1y}\partial_y S_z]\,, \\
H_{zy}S_y &= -2\tau_3\bar{\gamma}_{\mathrm{cD}}B_{3x}S_y + 2\tau_1\bar{D}B_{1x}(\partial_y^2 S_y - q_0^2 S_y) \\
&\quad +4\tau_1^2\bar{D}[\partial_y(B_{1y}B_{1z}\partial_y S_y) - q_0 B_{1y}^2\partial_y S_y]\,, \\
H_{zz}S_z &= 2\tau_1 q_0\bar{D}(\partial_y B_{1x}S_z + 2B_{1x}\partial_y S_z) \\
&\quad +4\tau_1^2\bar{D}(\partial_y(B_{1z}^2\partial_y S_z) - q_0 B_{1y}B_{1z}\partial_y S_z)\,.
\end{aligned}
\tag{4.33}
$$

Due to the renormalized coefficients (4.32) in the $\hat{D}$-matrix and the presence of the $\hat{H}$-matrix the spin diffusion equation Eq. (4.30) becomes a nonlinear partial differential equation, because the coefficients $B_{1\alpha}$ and $B_{3\alpha}$ ($\alpha = x, y, z$) depend on the solution for the spin density via $B_{1\alpha} = \chi_1 S_\alpha$ and $B_{3\alpha} = \chi_3 S_\alpha$. Thus, only for small Hartree-Fock fields $B_{1(3)}\tau_{1(3)} \ll 1$ a perturbative solution can be found (see Section 4.4.3) whereas for large Hartree-Fock fields, as realized for large initial spin polarizations, the spin diffusion equation (4.30) needs to be solved numerically.

4.4. Effect of the Hartree-Fock field on the PSH state

In this Section we will discuss the effect of the Hartree-Fock fields on the PSH state. Our main findings are: (i) the lifetime of the PSH state can be enhanced considerably, because the Hartree Fock field effectively reduces the symmetry breaking effect of the cubic Dresselhaus spin-orbit interaction (see Subsection 4.4.2); (ii) although the Hartree-Fock field is always parallel to the local mean spin polarization, somewhat counterintuitively, its presence slightly rotates the PSH out of the yz-plane and introduces a small but finite S_x-component (see Subsection 4.4.3). Since the spin diffusion equation becomes nonlinear in the presence of Hartree-Fock fields, typical nonlinear effects like the appearance of higher harmonics are expected to modify the PSH state. Indeed, we find that this nonlinear regime can be accessed easily for small linear Rashba and Dresselhaus spin-orbit interactions, where $\gamma_{\mathrm{cD}}/\Gamma \approx 1$ (see Subsection 4.4.4).

In order to investigate the effect of the Hartree-Fock field on the PSH state, we start by considering the PSH in the presence of cubic Dresselhaus spin-orbit interaction but in the absence of the Hartree-Fock term as described by Eq. (4.11) as an initial state. Then we imagine to turn on the Hartree-Fock field at time $t = 0$ and study the time evolution of the PSH state under the Hartree-Fock field by solving the spin diffusion equation Eq. (4.30). Since this is a nonlinear partial differential equation, a simple analytical solution is out of reach. Therefore, Eq. (4.30) has to be solved perturbatively or numerically. In Subsection 4.4.3 we will perform a perturbation expansion in the Hartree-Fock fields valid for $B_{1(3)}\tau_{1(3)} \ll 1$, otherwise the spin diffusion equation (4.30) will be solved numerically.

4.4.1. Parameters

In order to describe the evolution of the PSH state for realistic situations, we use the parameters of a typical quantum well such as the one used for the experimental observation of the PSH by Koralek *et al.* [2009]. Unless specified otherwise we assume a Fermi temperature of $T_F = 400$ K, an effective electronic mass of $m = 0.067\, m_e$, where m_e is the mass of an electron, and a dielectric constant of $\epsilon_r = 12.9$. Evaluating Eq. (4.19) with these parameters and for $T = 0$, we obtain

$$\chi_1 \;=\; 34.7\,\mathrm{cm}^2/\mathrm{s}\,, \qquad \chi_3 \;=\; 43.2\,\mathrm{cm}^2/\mathrm{s}\,. \tag{4.34}$$

We further assume a charge density of $n = 8 \times 10^{11}\,\mathrm{cm}^{-2}$. We take the linear Rashba and Dresselhaus spin-orbit coupling to be $\alpha = \beta = 0.0013$ and the cubic Dresselhaus spin-orbit interaction to be $\gamma\, v_F = 5.0\ \mathrm{eV\,\AA}^3$. Since the linear spin-orbit interactions can be tuned (by changing the doping asymmetry and the width of the quantum well), in contrast to the magnitude of the cubic Dresselhaus spin-orbit interaction, which is fixed by the crystal symmetry, we will also allow for variations of the magnitude of linear spin-orbit interactions in order to access the nonlinear regime (Subsection 4.4.4). For the electronic relaxation time we use as a default value $\tau = 1\,\mathrm{ps}$—the lifetime extracted at $T = 100$ K for the quantum well used by Koralek *et al.* [2009].

Strictly speaking, our theory applies only to the zero temperature case, where the relaxation time should be correspondingly longer than 1 ps. However, one can argue either that we expect our theory to apply (without major modifications) also to higher temperatures or that we describe a dirtier quantum well where $\tau = 1$ ps is the accurate electronic relaxation time at $T = 0$ K. Since τ can be varied to some extent by making a quantum well either dirtier or cleaner, we will also allow for some variation of τ. The initial spin polarization, finally, is the main parameter to be varied, because it directly controls the strength of the Hartree-Fock fields. It will be given in percentage fractions of the full spin polarization which corresponds to the carrier density given above.

4.4.2. Enhancement of the PSH lifetime

One of the main effects of the Hartree-Fock term is to enhance the lifetime of a spin polarization injected into a quantum well. This has been observed experimentally by Stich *et al.* [2007] using time-resolved Faraday rotation on a high-mobility GaAsAl/GaAs quantum well. So far, the spin lifetime enhancement due to electron-electron interaction in

a quantum well with spin-orbit interactions has only been analyzed by numerical solutions of the Boltzmann equation [Takahashi *et al.*, 1999; Weng and Wu, 2003; Weng *et al.*, 2004]. Here, we are able to analyze the effect of the Hartree-Fock field in a somewhat more analytical fashion at least in the diffusive strong scattering regime, where the spin diffusion equation Eq. (4.30) is valid.

Since the Hartree-Fock field is always parallel to the local spin polarization, it reduces the effect of rotations around the transversal spin-orbit fields and in this way it enhances the lifetime of a spin polarization. More formally, this works in our approach as follows: the size of the anisotropic spin components, which are perpendicular to the local spin-orbit field is reduced by rotations around the local Hartree-Fock field according to Eqs. eq:ScSs, eq:Sc3Ss3. This effect is captured by the reduction of the effective relaxation times $\bar{\tau}_1 = \tau/(1 + (\chi_1\tau_1 S)^2)$ and $\bar{\tau}_3 = \tau/(1 + (\chi_3\tau_3 S)^2)$ in the equations for the anisotropic components of the spin density $\mathbf{s}_{c/s}$ and $\mathbf{s}_{c3/s3}$ in Eqs. eq:SolutionWindingNumber1, eq:SolutionWindingNumber3. Smaller anisotropic spin components reduce the time derivative of the isotropic spin component $\partial_t \mathbf{s}_0$ in Eq. (4.20) and thus increase the lifetime of the isotropic spin density $\mathbf{s}_0$. In the spin diffusion equation (4.30) the reduced lifetimes $\bar{\tau}_1$ and $\bar{\tau}_3$ are absorbed in a reduced effective spin diffusion constant $\bar{D}$ and a reduced effective cubic Dresselhaus scattering rate $\bar{\gamma}_{\mathrm{cD}}$ (see Eq. (4.32)).

In principle we have now three mechanisms at hand, which could modify the lifetime of the PSH in the presence of Hartree-Fock fields: (i) the reduced effective diffusion constant $\bar{D}$, (ii) the reduced effective cubic Dresselhaus scattering rate $\bar{\gamma}_{\mathrm{cD}}$ and (iii) the additional $\hat{H}$-matrix. Since in our model cubic Dresselhaus spin-orbit interaction is the symmetry breaking mechanism, *i.e.*, the lifetime of the PSH would be infinite in the absence of cubic Dresselhaus spin-orbit interaction, it seems plausible to assume that a reduction of the effective cubic Dresselhaus spin-orbit interaction provides the strongest contribution to the lifetime enhancement of the PSH state.

This hypothesis can be checked by solving the spin diffusion equation (4.30) for the spin density by setting $\bar{D} = D$ and by neglecting the effect of the $\hat{H}$-matrix and thus effectively considering only the effect of a reduced effective cubic Dresselhaus spin-orbit interaction $\bar{\gamma}_{\mathrm{cD}}$. We use the PSH pattern (4.11) as an initial condition and solve the spin diffusion equation (4.30) numerically. In Figure 4.1 we show the resulting time evolution of the S_z spin polarization for various degrees of initial spin polarizations and for the remaining parameters as given in Subsection 4.4.1. The PSH state without Hartree-Fock field is also shown for comparison. For realistic quantum well parameters the lifetime of the PSH state can easily be enhanced by factors 10 to 20 when the initial spin polarization is in the percentage range. For large initial spin polarization the nonlinearity of the problem becomes obvious and the spin-polarization does no longer decay exponentially. On the scale of Figure 4.1 no difference is visible between the full solution of the spin diffusion equation (4.30) and the solution, where only the effective reduction of the cubic Dresselhaus spin-orbit interaction $\bar{\gamma}_{\mathrm{cD}}$ is taken into account. Thus, considering only the reduction of the effective cubic Dresselhaus spin-orbit scattering rate $\bar{\gamma}_{\mathrm{cD}}$ is a good approximation to the full solution, at least for $\gamma_{\mathrm{cD}}/\Gamma \ll 1$.

In principle one could imagine to enhance the PSH lifetime by increasing the lifetime τ instead of the initial spin polarization, since both quantities appear in the denominator of $\bar{\gamma}_{\mathrm{cD}} = \gamma_{\mathrm{cD}}/(1+(\chi_3\tau_3 S)^2)$ as a product. However, increasing τ also increases the bare cubic

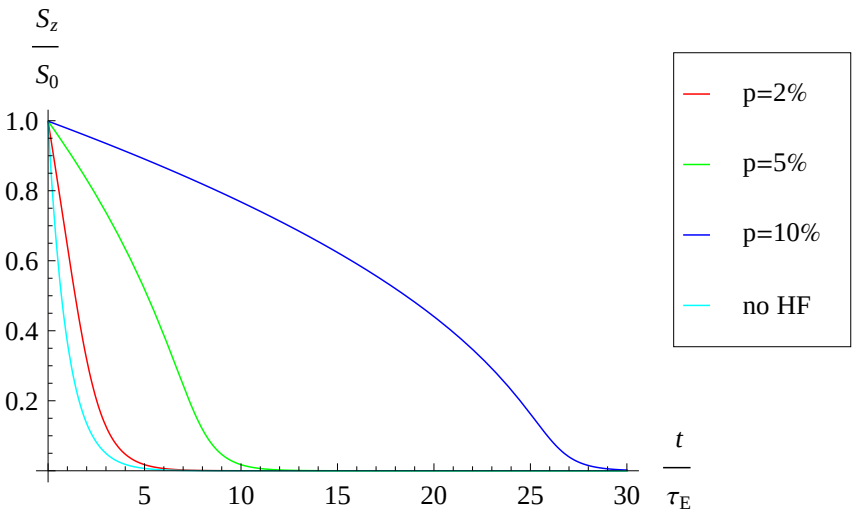

Figure 4.1.: Time dependence of the S_z-amplitude of the PSH in the presence of Hartree-Fock fields for several degrees of initial spin polarization. For comparison the result without Hartree-Fock field (cyan) is shown. On the scale of this plot, no difference is visible between the full solution of the spin diffusion equation (4.30) depicted here and the solution, where only the effective reduction of the cubic Dresselhaus spin-orbit interaction $\bar{\gamma}_{\mathrm{cD}}$ is taken into account.

Dresselhaus spin-orbit scattering rate $\gamma_{\mathrm{cD}} \propto \tau$ (see definition of γ_{cD} below Eq. (4.12)). Thus, whether increasing the lifetime τ will decrease or rather increase the effective cubic Dresselhaus spin-orbit scattering rate $\bar{\gamma}_{\mathrm{cD}}$ depends on the ratio of τ over the Hartree-Fock field $\chi_3 S$. Only for $\chi_3 \tau S > 1$ will an increase in τ indeed reduce $\bar{\gamma}_{\mathrm{cD}}$ and thus enhance the lifetime of the PSH state.

Although a simple analytical solution of the spin diffusion equation cannot be constructed, because $\bar{\gamma}_{\mathrm{cD}}(t)$ is a function of the time dependent solution for the spin density $\mathbf{S}(t)$, it is still instructive to compare the numerical solution with simple limits where an analytical solution is possible. For a constant (*i.e.*, time independent) effective cubic Dresselhaus scattering rate $\bar{\gamma}_{\mathrm{cD}}(t) = \bar{\gamma}_{\mathrm{cD}}$ the solution of the spin diffusion equation is the PSH pattern given in Eq. (4.11) with a lifetime of $\tau_E \approx (\frac{3}{2}\bar{\gamma}_{\mathrm{cD}})^{-1}$ for small $\gamma_{\mathrm{cD}}/\Gamma \ll 1$ (see Eq. (4.12)). Since at $t = 0$ the reduced effective cubic Dresselhaus rate is $\bar{\gamma}_{\mathrm{cD}}(t = 0) \approx \gamma_{\mathrm{cD}}/(1 + 2(\chi_3 \tau_3 S_0)^2)$ for small $\gamma_{\mathrm{cD}}/\Gamma$, the solution of the spin diffusion equation starts off as $e^{-\frac{3}{2}\frac{\gamma_{\mathrm{cD}}}{(1+2(\chi_3\tau_3 S_0)^2)}t}$ for small times. For large times, on the other hand, where $\bar{\gamma}_{\mathrm{cD}}(t \to \infty) = \gamma_{\mathrm{cD}}$ the solution approaches zero as $e^{-\frac{3}{2}\gamma_{\mathrm{cD}}t}$.

4.4.3. PSH pattern

Up to this point we have only considered the first part of the spin diffusion equation (4.30), *i.e.*, the $\hat{D}$-matrix, which corresponds to the ordinary spin diffusion equation with renormalized parameters. In addition the spin diffusion equation contains the $\hat{H}$-matrix with terms arising due to the Hartree-Fock fields. The presence of these new terms can

rotate the spin helix out of the yz-plane and introduce a small but finite S_x-compontent. This seems counterintuitive at first sight, because the Hartree-Fock field is always parallel to the local mean spin polarization.

This effect can be analyzed best by calculating the spin density in a perturbation expansion in the Hartree-Fock fields as

$$\boldsymbol{S} \;=\; \boldsymbol{S}^{(0)} + \boldsymbol{S}^{(1)} + \boldsymbol{S}^{(2)} + \cdots \tag{4.35}$$

where $\boldsymbol{S}^{(n)}$ denotes the nth order in the Hartree Fock fields $\chi_1\tau_1 S_0$ and $\chi_3\tau_3 S_0$. The zeroth order $\boldsymbol{S}^{(0)}$ is simply the PSH without Hartree-Fock fields (Eq. (4.11)). The first-order correction to the spin density $\boldsymbol{S}^{(1)}$ can be obtained by solving the equation resulting from the spin diffusion equation (4.30) when only terms of first order in the Hartree Fock terms are kept:

$$\partial_t \boldsymbol{S}^{(1)} \;=\; \hat{D}^{(0)}\boldsymbol{S}^{(1)} + \hat{H}^{(1)}\boldsymbol{S}^{(0)}\,. \tag{4.36}$$

Here, $\boldsymbol{S}^{(0)}$ is the zeroth order persistent spin helix of (4.11), $\hat{D}^{(0)}$ is the matrix of the ordinary spin diffusion equation, *i.e.*, the $\hat{D}$ matrix in Eq. (4.31) with $\bar{D}$ replaced by D and $\bar{\gamma}_{\mathrm{cD}}$ replaced by γ_{cD}. $\hat{H}^{(1)}$ is the $\hat{H}$-matrix expanded to first order in $\chi_1\tau_1 S_0$ and in $\chi_3\tau_3 S_0$. It is obtained by plugging $\boldsymbol{B}_1^{(1)} = \chi_1\boldsymbol{S}^{(0)}$ and $\boldsymbol{B}_3^{(1)} = \chi_3\boldsymbol{S}^{(0)}$ into the linear-in-B terms of the $\hat{H}$-matrix (the terms quadratic in B are at least second-order in the Hartree-Fock fields and therefore do not contribute to $\boldsymbol{S}^{(1)}$). In the first-order approximation (4.36) to the spin diffusion equation only the ordinary diffusion constant D and the ordinary cubic Dresselhaus rate γ_{cD} enter, since differences between D and $\bar{D}$ (and between γ_{cD} and $\bar{\gamma}_{\mathrm{cD}}$) are already of second order. With $\hat{H}^{(1)}_{yy} = \hat{H}^{(1)}_{yz} = \hat{H}^{(1)}_{zy} = \hat{H}^{(1)}_{zz} = 0$ one finds $S_y^{(1)} = S_z^{(1)} = 0$, whereas the S_x-component, which vanishes in zeroth order, becomes

$$S_x^{(1)} \;=\; \frac{S_0^2\,(\chi_1\tau_1 - \chi_3\tau_3)\,\gamma_{\mathrm{cD}}}{\Gamma(1-\frac{\gamma_{\mathrm{cD}}}{\Gamma}\sqrt{1+\frac{\gamma_{\mathrm{cD}}^2}{\Gamma^2}}-\frac{\gamma_{\mathrm{cD}}^2}{\Gamma^2})}\left(e^{-(\Gamma+\gamma_{\mathrm{cD}})t} - e^{-\frac{t}{\tau_E}}\right)\sin 2q_0 y\,. \tag{4.37}$$

Thus, to leading order in $\gamma_{\mathrm{cD}}/\Gamma$ one has

$$S_x^{(1)} \;\approx\; S_0^2\,(\chi_1\tau_1 - \chi_3\tau_3)\,\frac{\gamma_{\mathrm{cD}}}{\Gamma}\left(e^{-\Gamma t} - e^{-\frac{3}{2}\gamma_{\mathrm{cD}}t}\right)\sin 2q_0 y\,. \tag{4.38}$$

This shows that $S_x^{(1)}$ contains a term that decays on the long time scale τ_E, implying that $S_x^{(1)}$ really contributes to the PSH. Thus the PSH also acquires an S_x-component, which oscillates with double wave vector $2q_0$ in real space but is smaller than the S_y- and S_z-components by a factor of $\gamma_{\mathrm{cD}}/\Gamma$ (for $\gamma_{\mathrm{cD}}/\Gamma \ll 1$). In first order in the Hartree-Fock fields the S_x-component vanishes for $\chi_1\tau_1 = \chi_3\tau_3$. This is, however, not true for the full solution as can be seen from the numerical evaluation.

At first sight it might be a surprising result, that the presence of Hartree-Fock fields parallel to the local spin polarization modifies the pattern of the spin polarization. Naively, one would expect that a parallel magnetic field simply strengthens the parallel spin orientation. In the presence of spin-orbit fields, however, the spin density consists of parts with different winding numbers, where only the winding number zero contributes to the local

spin polarization, since the other winding numbers $(\pm 1, \pm 3)$ average out to become zero. Since the anisotropic components of the spin density arise from rotations of the isotropic spin density (winding number zero) around the respective spin-orbit fields (see Eqs. (4.23) and (4.27)), they are not parallel to the local spin density and therefore not parallel to the Hartree-Fock field. Consequently, these anisotropic components of the spin density can precess about the Hartree-Fock field and in this way modify the local spin polarization, which is affected by rotations of the anisotropic components of the spin density around their respective spin-orbit fields (see Eq. (4.20)). Thus, the orientation of the isotropic spin density can indeed be changed by parallel fields due to the presence of anisotropic components of the spin density.

In order to see how this mechanism causes the PSH to rotate out of the xy-plane and induces a finite S_x-component, we will now analyze the equations for the spin density derived in Section 4.3 in more detail. The perturbative result in Eq. (4.37) suggests that both winding number one and winding number three spins contribute to the generation of a finite S_x-polarization.

Regarding winding number one spins, it follows from Eq. (4.20) for the isotropic spin density $\boldsymbol{s}_0$, that winding number one spins can generate a finite S_x-component only via the diffusion term $\frac{v}{2}\partial_y \boldsymbol{s}_c$ (since $\boldsymbol{b}_c = 0$ for $\alpha = \beta$, $\boldsymbol{b}_s || \hat{\boldsymbol{e}}_{\boldsymbol{x}}$ and $\partial_x \boldsymbol{s}_0 = 0$). Plugging the solution for $\boldsymbol{s}_c$ of Eq. (4.25) into the the equation for the isotropic spin density $\boldsymbol{s}_0$, one finds that the only term generating a finite S_x-component is proportional to $\partial_y(\boldsymbol{s}_0 \times (\boldsymbol{b}_s \times \boldsymbol{s}_0)) = \boldsymbol{b}_s \partial_y s_0^2 \approx \boldsymbol{b}_s \, 2\, S_0^2 \, q_0 \frac{\gamma_{\mathrm{cD}}}{\Gamma} \sin 2q_0 y$, where we have used that the difference in the initial S_y and S_z amplitudes of the PSH state is approximately given by $S_0 \frac{\gamma_{\mathrm{cD}}}{\Gamma}$. This contribution corresponds to a process, where the isotropic spin polarization $\boldsymbol{s}_0$ precesses at first about the spin-orbit field $\boldsymbol{b}_{\boldsymbol{s}}$ and then about the local Hartree-Fock field $\boldsymbol{B}_1$, which is parallel to $\boldsymbol{s}_0$. Although this double rotation results in a polarization along the x-direction, this effect would cancel after integration over k because electrons with momenta $\pm k$ rotate into opposite directions. Only due to the derivative ∂_y in the diffusion term a finite S_x-polarization remains after k-integration, because $+k$ and $-k$ travel into opposite directions and rotate around Hartree-Fock fields at $y \pm \Delta y$, which differ in magnitude due to the elliptical profile of the initial PSH pattern, see Figure 4.2. This explains the presence of the factor $\frac{\gamma_{\mathrm{cD}}}{\Gamma}$ in the contribution of the winding-number-± 1 spins to $S_x^{(1)}$. When the isotropic spin polarization is parallel to one of the symmetry axes of the ellipse, *i.e.*, for $S_y = 0$ or $S_z = 0$, the Hartree-Fock fields for the $\pm k$-states are of equal magnitude resulting in $S_x = 0$. This explains the oscillation of $S_x^{(1)}$ with double wavevector $2q_0$.

Winding number three spins, on the other hand, can create a finite S_x-component directly by rotation around the cubic Dresselhaus spin-orbit field $\boldsymbol{b}_{c3}$. Plugging the solution for $\boldsymbol{s}_{c3}$ of Eq. (4.28) into the equation for the isotropic spin density $\boldsymbol{s}_0$ one finds that the only term, which generates a finite S_x polarization, is proportional to $\boldsymbol{b}_{c3} \times (\boldsymbol{s}_0 \times (\boldsymbol{b}_{c3} \times \boldsymbol{s}_0)) = -(\boldsymbol{b}_{c3} \times \boldsymbol{s}_0)(\boldsymbol{b}_{c3} \cdot \boldsymbol{s}_0)$. Since $\boldsymbol{b}_{c3} || \hat{\boldsymbol{e}}_{\boldsymbol{y}}$ and $\boldsymbol{s}_0$ lies within the xy-plane for the undisturbed PSH, a finite S_x-component is generated only unless $\boldsymbol{s}_0 || \hat{\boldsymbol{e}}_{\boldsymbol{y}}$ and unless $\boldsymbol{s}_0 || \hat{\boldsymbol{e}}_{\boldsymbol{z}}$. This explains, why the winding number three contribution to $S_x^{(1)}$ oscillates with double wavevector $2q_0$.

In Figures 4.3 and 4.4 we show the results for the S_x-component at its first maximum $y = \pi/(4q_0)$ obtained by numerical solution of the spin diffusion equation (4.30) (red)

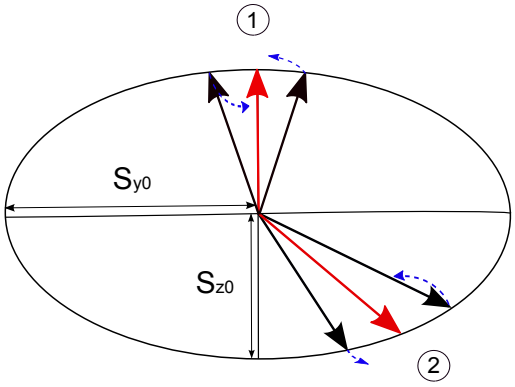

Figure 4.2.: Due to the elliptic profile of the PSH pattern there is a net creation of S_x polarization at position "2": here (unlike situation "1"), contributions from precessing spins coming in from right an left with momentum $\pm k$ do *not* cancel each other.

in comparison to the analytical first-order expression $S_x^{(1)}$ of Eq. (4.37) (green). For the small initial spin polarization of 0.5% used in Figure 4.3, the analytical first-order result agrees quite well with the full numerical solution. The S_x-component increases quickly on the timescale $1/\Gamma$ and then decays slowly on the timescale $\tau_E \approx (\frac{3}{2}\gamma_{\mathrm{cD}})^{-1}$. For larger initial spin polarizations, however, the analytical first-order result no longer describes so accurately the time evolution of the S_x-polarization. Instead of a sharp initial increase on the timescale of $1/\Gamma$ the S_x-component now displays an oscillatory behavior that is damped on the larger timescale $1/\bar{\Gamma}$, see Figure 4.4. The overall lifetime of the S_x-component is enhanced by a large factor in comparison to the lifetime τ_E of the perturbative result analogous to the lifetime enhancement of the PSH discussed in Subsection 4.4.2. Interestingly, the magnitude of the S_x-component remains well below the maximum of perturbative result.

4.4.4. Large cubic Dresselhaus SOI ($\gamma_{\mathrm{cD}} \approx \Gamma$)

So far we have focused on the regime, where the cubic spin-orbit interaction is small ($\gamma_{\mathrm{cD}} \ll \Gamma$), because there one expects the largest PSH lifetimes. The quantum wells, in which the PSH has been observed experimentally by Koralek *et al.* [2009], are in this regime. Nevertheless, it should be possible to also realize quantum wells where the magnitude of the cubic Dresselhaus spin-orbit interaction is comparable to the linear spin-orbit interactions. The magnitude of the cubic Dresselhaus spin-orbit interaction is given by the crystal structure, whereas the magnitude of the linear Rashba and Dresselhaus spin-orbit interactions α and β can be varied in experiments by changing the doping asymmetry and the width of the quantum well. Thus, in our calculations we will access the $\gamma_{\mathrm{cD}} \approx \Gamma$-regime by reducing the magnitude of the linear spin-orbit interactions while keeping the magnitude of the cubic Dresselhaus spin-orbit interaction fixed. Interestingly, the lifetime

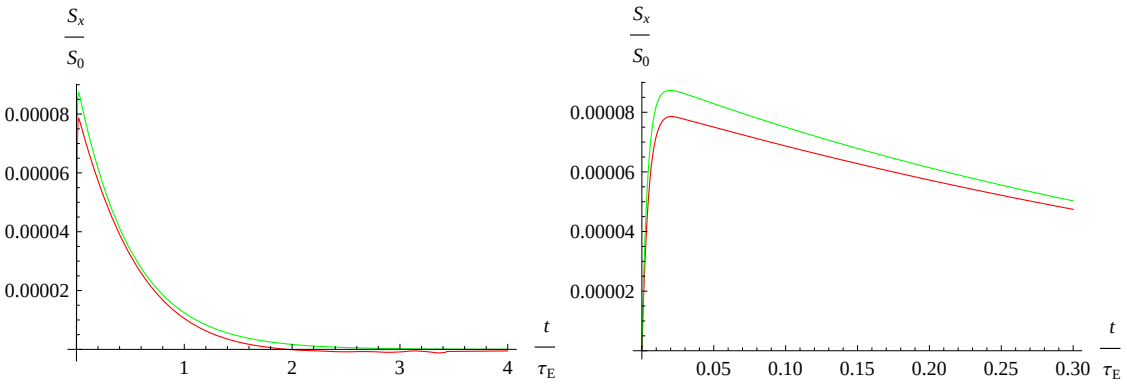

Figure 4.3.: Time dependence of S_x-amplitude for an initial spin polarization of 0.5%. Red shows the full numerical solution of Eq. (4.30) and green is the first-order analytical result Eq. (4.37). The right panel is a zoom into small times.

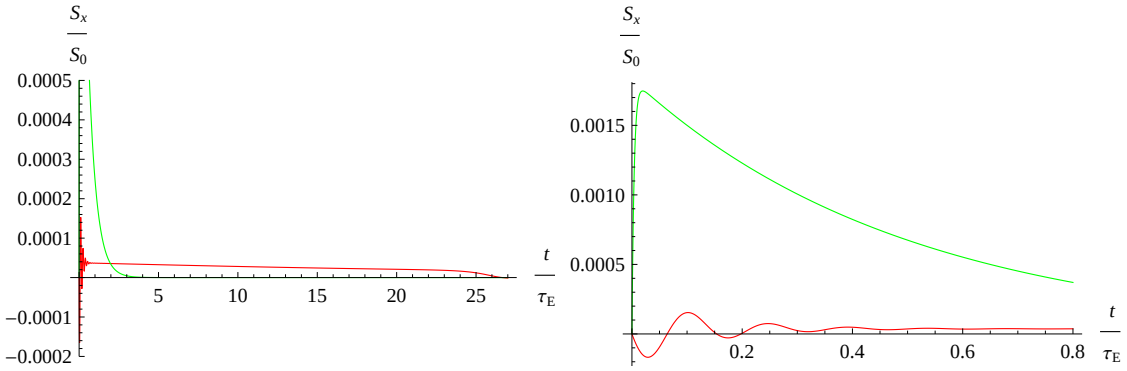

Figure 4.4.: Same as Figure 4.3 (red: full numerical solution of Eq. (4.30) vs. green: first-order analytical solution from Eq. (4.37)) but with a larger initial spin polarization of 10%.

of the PSH does not change dramatically when the magnitude of the cubic Dresselhaus spin-orbit interaction is kept fixed. For $\gamma_{\mathrm{cD}} \ll \Gamma$ one finds from Eq. (4.12) $\tau_E^{-1} \approx \frac{3}{2}\gamma_{\mathrm{cD}}$ and in the opposite limit, *i.e.*, for $\gamma_{\mathrm{cD}} \gg \Gamma$, one finds $\tau_E^{-1} \approx \gamma_{\mathrm{cD}}$, *i.e.*, the PSH lifetime depends rather on the absolute value of γ_{cD} than on the ratio $\gamma_{\mathrm{cD}}/\Gamma$, implying that even for $\gamma_{\mathrm{cD}} \gg \Gamma$ the lifetime of the PSH can be quite long, as long as the regime $\gamma_{\mathrm{cD}} \gg \Gamma$ is reached by reducing Γ instead of increasing γ_{cD}.

In the extreme limit, where no linear spin-orbit interactions but only cubic Dresselhaus spin-orbit interaction exists, *i.e.*, for $\Gamma = 0$, the wavevector q_0 as well as the S_z-component of the initial PSH state (see Eq. (4.11)) go to zero. This implies that in the absence of linear spin-orbit interactions no long-lived helix state exists but rather a spatially homogeneous S_y spin polarization. In this case the spin diffusion equation (4.30) reduces to $\partial_t S_y = -\bar{\gamma}_{\mathrm{cD}} S_y$, since the diffusion term as well as the $\hat{H}$-matrix vanish for a homogeneous S_y-spin polarization. Thus, the decay of the homogeneous S_y-spin polarization is simply determined by the renormalized cubic Dresselhaus spin-orbit scattering rate $\bar{\gamma}_{\mathrm{cD}}(t)$. The

time evolution of the homogeneous S_y-spin polarization looks therefore very similar to the spin polarization of the PSH state discussed in Section 4.4.2, as can be inferred from the numerical solution shown in Figure 4.5. However, the lifetime in the $\Gamma = 0$-limit is longer, because it is determined by $1/\bar{\gamma}_{\rm cD}(t)$ instead of $2/(3\bar{\gamma}_{\rm cD}(t))$ as for $\gamma_{\rm cD}/\Gamma \ll 1$.

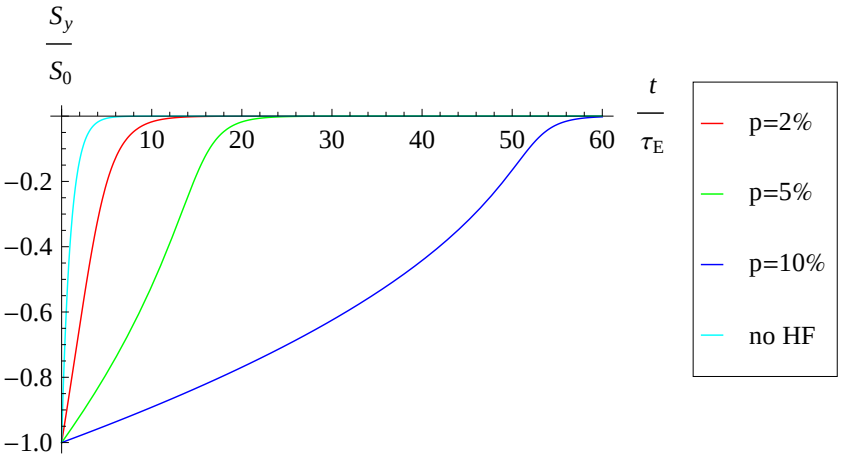

Figure 4.5.: Effect of the Hartree-Fock field on the time dependence of the homogeneous S_y-polarization in the absence of linear spin-orbit interactions, *i.e.*, $\Gamma = 0$.

In the intermediate regime between $\gamma_{\rm cD}/\Gamma \ll 1$ and $\Gamma = 0$ the time evolution of the PSH state is not universal and can be quite complicated, because the timescales set by $1/\Gamma$ and $1/\gamma_{\rm cD}$, *i.e.*, by rotations around the linear and cubic spin-orbit fields, are of similar order of magnitude. We expect that the simple reduction of the effective cubic Dresselhaus scattering rate $\bar{\gamma}_{\rm cD}$, which was quite successful in describing the $\gamma_{\rm cD} \ll \Gamma$-regime in Section 4.4.2, will fail to account for the full time evolution of the PSH state and that the $\hat{H}$-matrix in the spin diffusion equation (4.30) will start to play a more important role.

In order to demonstrate the effect of the $\hat{H}$-matrix we show in Figure 4.6 the time dependence of the S_z-, S_y-, and S_x-amplitudes (red) for reduced linear spin-orbit interactions corresponding to $\gamma_{\rm cD}/\Gamma = 6.8$. A comparison of the full numerical solution for the S_z- and S_y-components in Figure 4.6 (blue curve) with the approximate solution shown in green demonstrates that the lifetime of the PSH is enhanced even more than predicted by the simple reduction of the effective cubic Dresselhaus spin-orbit scattering $\bar{\gamma}_{\rm cD}$. In particular, the time evolution of the S_z-component, which is suppressed considerably in the initial undisturbed PSH state, seems to depend crucially on the $\hat{H}$-matrix. Also the magnitude of the S_x-polarization becomes quite sizable and reaches almost 8% of the initial PSH amplitude.

Since the nonlinear terms of the $\hat{H}$-matrix play a more important role in the intermediate regime $\gamma_{\rm cD} \approx \Gamma$, also the spatial profile of the PSH is affected by these nonlinear terms. Indeed, the spatial profile of the spin polarization clearly deviates from the simple PSH pattern of Eq. (4.11) when time evolves, *i.e.*, the effect of higher harmonics becomes quite

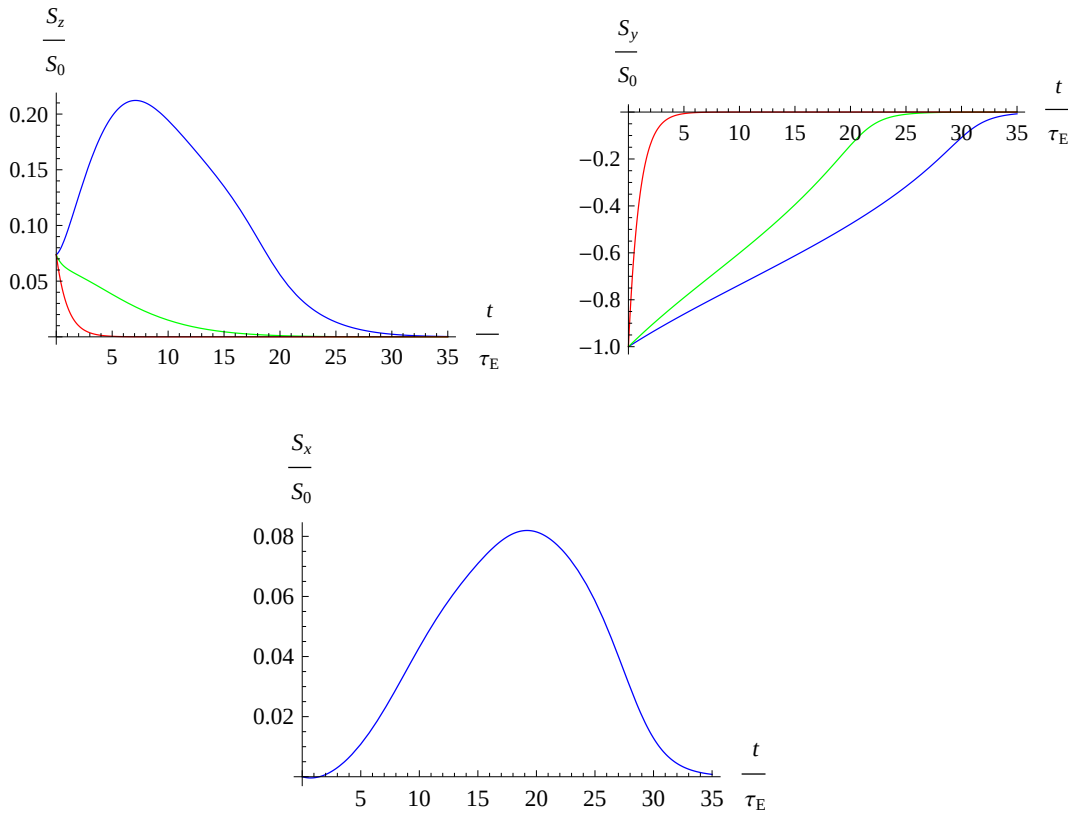

Figure 4.6.: Time dependence of the S_z-amplitude (top left), of the S_y-amplitude (top right) and of the S_x-amplitude (bottom) taken at their respective maximum for an initial spin polarization of 10% and with the linear spin-orbit interaction reduced by a factor of 0.02. Here, blue depicts the full numerical solution, green is the solution which takes into account only the renormalization of $\bar{\gamma}_{\mathrm{cD}}$ (*i.e.*, $\bar{D} = D$ and $\hat{H} = 0$), and red represents the PSH in the absence of Hartree-Fock fields ($\gamma_{\mathrm{cD}}/\Gamma = 6.8$ and $\tau_E = 324$ ps).

pronounced for larger times (see Figure 4.7). In particular, the S_z-component of the PSH state differs strongly from the original $\cos q_0 y$-dependence and the S_x-components differs from the $\sin 2q_0 y$-dependence found for $S_x^{(1)}$ in first-order in the Hartree-Fock fields. The formation of the additional sharp maxima in the spatial profile of S_x can be assigned to the contribution of the winding-number-± 1 spins. Since the contribution of the winding-number-± 1 spins depends on the variation of the magnitude of spin polarization along the elliptical profile of the PSH (see discussion in Section 4.4.3), the maximal contribution is shifted from $\pi/(4q_0)$ towards the semi-major axis with increasing eccentricity of the elliptical spin profile (*i.e.*, for larger values of $\gamma_{\mathrm{cD}}/\Gamma$) and thus give rise to the additional sharp maxima close to integer multiples of π/q_0.

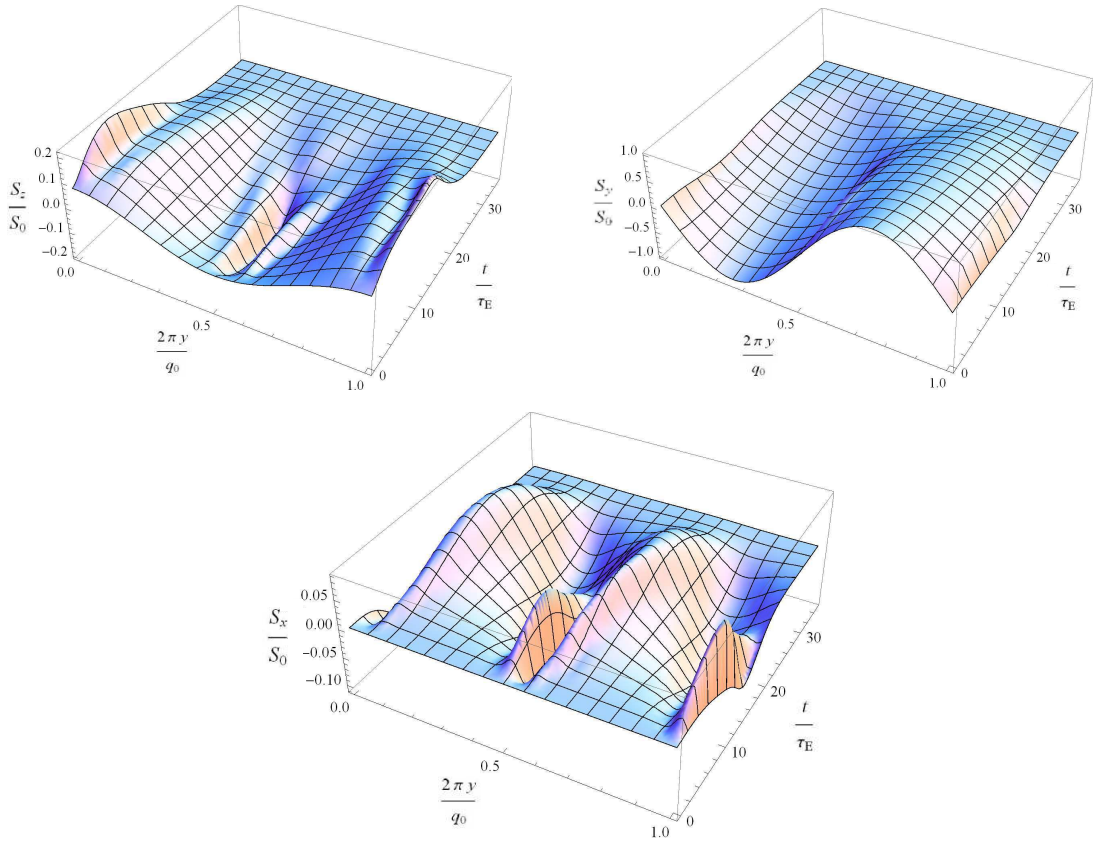

Figure 4.7.: Time and spatial dependence of S_z (top left), S_y (top right), and S_x (bottom) for the situation described in the caption of Figure 4.6.

4.5. Summary

In this chapter, we have complemented our understanding of the influence of electron-electron interactions on the persistent spin helix, which we have gained from the treatment of second-order electron-electron collisions in Chapter 3, by including also the first-order mean field interaction in the kinetic equation for the spin density. An additional precession term rotates the anisotropic (in momentum space) parts of the spin density around the isotropic one, *i.e.*, around the local average spin polarization. In the spin diffusion equation for the latter, this results in nonlinear corrections, which we have investigated numerically and to some extent analytically.

We find that the main effects of the Hartree-Fock interaction on the persistent spin helix state is twofold: (i) the lifetime of the persistent spin helix can be enhanced drastically, because the Hartree Fock field, which is always parallel to the local mean spin polarization, effectively reduces the influence of the symmetry breaking cubic Dresselhaus spin-orbit interaction; (ii) the shape of the persistent spin helix is changed. In particular, it is slightly rotated out of the yz-plane with a small S_x-component coming about. Furthermore, typical nonlinear effects such as the appearance of higher harmonics, are visible in the

PSH pattern.

From the fact that none of the above effects were observed in the PSH experiment by Koralek *et al.* [2009] we conclude, based on the numerical calculations presented in this chapter, that there the degree of initial spin polarization must have been in a range well below 1%, rendering nonlinear effects negligible. However, since polarizations in the percentage range can be realized experimentally and since the transient spin grating technique should be well-suited for the detection of higher spatial harmonics in the PSH pattern, we are confident that our theretical predictions will be verified in future experiments. Our results suggest that, in order to reach the clearly nonlinear regime, it might be advantageous to use thicker quantum wells, where the linear spin-orbit coupling is of the same order of magnitude as the cubic Dresselhaus spin-orbit coupling.

5. Pseudospin-orbit coupling corrections in the Boltzmann conductivity of graphene

As indicated already in Chapter 2, kinetic equations can be derived from quantum theory in numerous ways, including in particular nonequilibrium Green's function techniques and approaches based on the Liouville-von Neumann equation for the density matrix. The resulting collision integrals coincide in common textbook examples without spin-orbit coupling and for perturbative calculations in systems where the spin-orbit coupling represents only a small part of the kinetic energy (*cf.* theoretical studies of the spin Hall effect by Mishchenko *et al.* [2004]; Shytov *et al.* [2006]; Raimondi *et al.* [2006]; Culcer and Winkler [2007a]; Kailasvuori [2009]). In this chapter we show that there are also relevant problems where different formalisms yield different collision integrals already to leading order and with physical implications. In the Dirac cone physics that governs graphene and surface states of three-dimensional topological insulators [Hasan and Kane, 2010], the pseudospin-orbit interaction constitutes the *entire* kinetic energy. We shall see that in that case the differences in the collision integrals manifest themselves in the precise value of quantum corrections $\delta\sigma$ to the Drude conductivity that arise from electron-hole coherences. Another open issue in this context is the significance of the often neglected principal value terms in the collision integrals. It turns out that it is important to include principal value integrals in the calculation of quantum corrections in the conductivity.

It is beyond the scope of the present work, the results of which have been published in Kailasvuori and Lüffe [2010], to find a final answer to the question as to which one of the commonly used approaches is adequate and why. However, since in the literature different approaches have been used for the same problem [Auslender and Katsnelson, 2007; Trushin and Schliemann, 2007; Culcer and Winkler, 2007b; Liu *et al.*, 2008], our comparative study can help to sensitize to this ambiguity and establish benchmarks for a comparison with numerical or even experimental results.

5.1. Motivation and previous work

The main focus of the extensive research activity on graphene has so far been on the undoped system with the chemical potential exactly at the degenerate Dirac points. This regime of chemical potential close to zero—the *Dirac regime*—hosts the most exotic features such as a finite minimal conductivity at seemingly zero charge carrier density [Novoselov *et al.*, 2005; Zhang *et al.*, 2005]. Here, quantum effects due to electron-hole coherence (*i.e.*, pseudospin coherence) like *Zitterbewegung* can determine the observed conductivity even to lowest order [Katsnelson, 2006]. We refer to Castro Neto *et al.* [2009] for a review of early work on the Dirac regime.

Away from the Dirac points, at a large enough charge carrier density, there is a crossover

to the *Boltzmann regime* $\ell\, k_\mathrm{F} \gg 1$, where ℓ denotes the mean free path of the electrons and $\hbar\, k_\mathrm{F}$ is the Fermi momentum. Here, the conductivity can be understood to leading order without taking into account quantum effects such as electron-hole coherence and is therefore more intuitive. The crossover between the two regimes has recently been studied numerically [Adam *et al.*, 2009; Cappelluti and Benfatto, 2009; Trushin *et al.*, 2010].

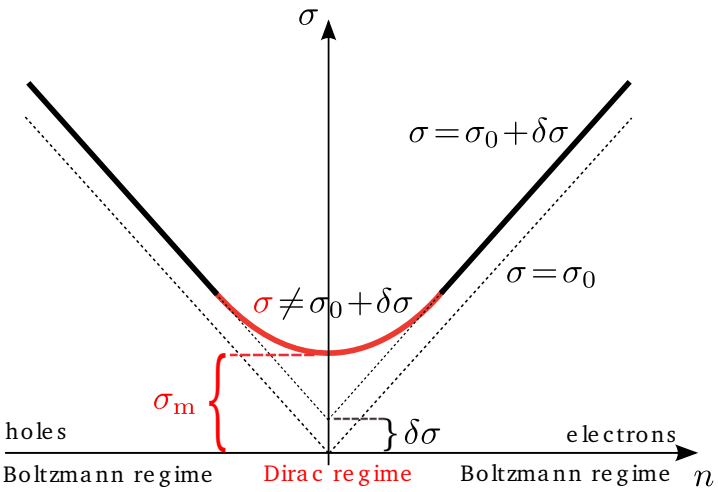

Figure 5.1.: Schematic dc conductivity σ in monolayer graphene as a function of the electron density n measured in experiments [Novoselov *et al.*, 2005; Zhang *et al.*, 2005; Schedin *et al.*, 2007; Tan *et al.*, 2007], including in particular the *residual conductivity* $\delta\sigma$ as observed by Chen *et al.* [2008]. At the neutrality point $n = 0$ the charge density is zero, and hence one would expect zero conductivity at low temperatures. One of the surprises of graphene is the *conductivity minimum* $\sigma_\mathrm{m} \sim e^2/h$. The observed linear dependence in the Boltzmann regime (black) is described by the Drude conductivity $\sigma_0 = 2\, e^2\, \ell\, k_\mathrm{F}/h \propto |n|$ for screened charged impurities. (Point-like impurities, in contrast, yield $\sigma_0 \propto |n|^0$. Their influence starts to compete with that of screened charged impurities for $|n|$ large enough.) Effects of electron-hole coherence reveal themselves in quantum corrections of higher order in $(\ell\, k_\mathrm{F})^{-1}$. A contribution $\propto (\ell\, k_\mathrm{F})^{-1}$ can explain the initial convexity as one approaches the Dirac regime. A contribution $\propto (\ell\, k_\mathrm{F})^0$ enters as a constant shift in the Boltzmann conductivity and thus contributes to the residual conductivity $\delta\sigma$ that is read off by linear extrapolation.

In several experiments with graphene on a substrate the dc conductivity in the Boltzmann regime is observed to be linear in the electron (hole) density [Novoselov *et al.*, 2005; Zhang *et al.*, 2005; Schedin *et al.*, 2007; Tan *et al.*, 2007; Chen *et al.*, 2008]. This results in a characteristic V-shape in the conductivity as a function of gate voltage, see Figure 5.1. The linearity is less pronounced for suspended graphene, where the influence of charged impurities is reduced [Bolotin *et al.*, 2008; Du *et al.*, 2008]. Provided that screened charged impurities are the dominant source of scattering, which yields for the mean free

path $\ell \propto k_F$, the linear dependence on the carrier density n ($\propto k_F^2$ at low temperatures) is theoretically well described by the ordinary *Drude conductivity*

$$4\,\sigma_0 \;=\; 4\,\frac{e^2}{2\,h}\,\ell\,k_{\mathrm{F}} \tag{5.1}$$

with a factor 4 due to valley and spin degeneracy. This result is easily derived (see Section 5.7) from a Boltzmann equation with four degenerate, incoherent bands (valley index and real spin) [Nomura and MacDonald, 2006; Ando, 2006; Nomura and MacDonald, 2007]. In contrast, point-like impurities with $\ell \propto 1/k_F$ lead to a Drude conductivity that is independent of the charge carrier density. Therefore, this model fails already on a qualitative level [Shon and Ando, 1998]. As one expects the charge carriers to be mainly of one type (either electrons or holes), the pseudospin band index can be left aside in a first approximation. When interband coherences are neglected, the collision integral contains only transition rates between energy eigenstates. Such rates are easily derived with Fermi's Golden rule. The specific properties of massless Dirac electrons enter merely in the transition rates as a spin-overlap factor that is due to the well-defined chirality of the eigenstates as well as in the Thomas-Fermi screening length, which depends on the Fermi momentum (and thereby on the electron density) due to the linearity of the spectrum. By contrast, in a 2DEG with quadratic dispersion the screening length is independent of the Fermi momentum.

In the Boltzmann regime $\ell\,k_{\mathrm{F}} \gg 1$, the electron-hole coherent features of Dirac electrons manifest themselves only if one goes beyond the leading-order (in the small parameter $(\ell\,k_{\mathrm{F}})^{-1}$) result $\sigma_0 \propto \ell\,k_{\mathrm{F}}$ to address *quantum corrections*. A Boltzmann-type approach to these quantum corrections requires a kinetic equation that is quantum coherent in band indices (for graphene, the pseudospin index), see for instance Auslender and Katsnelson [2007]; Trushin and Schliemann [2007]; Culcer and Winkler [2007b]; Liu *et al.* [2008]. Interband coherent collision integrals are, however, beyond the range of applicability of Fermi's Golden rule. To access the "transition rates" involving the interband components in the collision integral one typically has to resort to a fully quantum coherent theory. A Boltzmann equation is then obtained by a semiclassical expansion in the space and time variables while keeping the spin degree of freedom quantum coherent.

Common methods in this context are density matrix approaches and nonequilibrium Green's function approaches (see Chapter 2). The former start with a single-time density-matrix-type state variable $\rho(x_1, x_2, t_1)$ governed by the Liouville-von Neumann equation. The latter start with a double-time correlator $G^<(x_1, t_1, x_2, t_2)$ whose evolution is governed by dynamic equations derived from, *e.g.*, the Kadanoff-Baym equation or the Keldysh equation [Haug and Jauho, 2008; Rammer, 2007]. At a later stage, some approximation has to be invoked in order to recover single-time equations. This choice of approximation is *the problem of ansatz*, which will be discussed below.

Most of the the aforementioned treatments of pseudospin-coherence induced quantum corrections in graphene use a density matrix approach [Auslender and Katsnelson, 2007; Trushin and Schliemann, 2007; Culcer and Winkler, 2007b], an exception being the work by Liu *et al.* [2008], which relies on a Green's function derivation. Another context in which spin coherent Boltzmann-type approaches have been applied to transport in a spin-orbit coupled system is the spin Hall effect [D'yakonov and Perel', 1971; Kato *et al.*, 2004; Engel

et al., 2007]. Here, Green's function techniques have been widely used [Mishchenko *et al.*, 2004; Shytov *et al.*, 2006; Raimondi *et al.*, 2006; Culcer and Winkler, 2007a; Kailasvuori, 2009]. Note that in these papers transport coefficients are calculated to leading order only.

The first of two central questions that we will address in this chapter is whether the two groups of approaches—density matrix methods versus Green's function methods—are equivalent in general, and in particular when addressing quantum corrections in the conductivity of graphene. The second central question is at which order the power series in $(\ell\, k_\mathrm{F})^{-1}$ of the pseudospin-orbit coupling corrections to the conductivity of graphene starts. A correction $\delta\sigma \sim \frac{e^2}{h}(\ell\, k_\mathrm{F})^{-1}$ to the Drude conductivity $\sigma_0 \sim \frac{e^2}{h}\ell\, k_\mathrm{F}$ would depend on the impurity concentration as well as on the impurity strength. For screened Coulomb scatterers it would increase with decreasing electron density, in qualitative accordance with the onset of a convex behavior of the conductivity as one approaches the Dirac regime, see Figure 1.6. Far away from the neutrality point, such a contribution becomes arbitrarily small. A contribution of the lower order $\delta\sigma \sim \frac{e^2}{h}(\ell\, k_\mathrm{F})^0$ would be independent of the impurity density and impurity strength. At least in monolayer graphene it would also be independent of the electron density, thus yielding a constant shift of the Drude conductivity as illustrated in Figure 5.1. Electron-hole coherent effects would then remain finite arbitrarily far away from the Dirac regime, which appears rather counterintuitive.

Within a pseudospin coherent Boltzmann approach, Auslender and Katsnelson [2007] find the leading correction to the dc conductivity to be of the order $(\ell\, k_\mathrm{F})^{-1}$. Trushin and Schliemann [2007] find a leading correction of the same order, although their approach is qualitatively different in that they, in contrast to Auslender and Katsnelson, discard *principal value terms* in the pseudospin coherent collision integral (see also Trushin and Schliemann [2008]). Both papers find their results to be ultraviolet divergent for point-like impurities. Culcer and Winkler [2007b] study screened charged impurities. They, too, neglect principal value terms and solve their spin coherent Boltzmann equation only up to order $(\ell\, k_\mathrm{F})^0$, wherefore the previously found corrections $\propto (\ell\, k_\mathrm{F})^{-1}$ [Auslender and Katsnelson, 2007; Trushin and Schliemann, 2007] are out of reach. Solving the Boltzmann equation for an ac setup by introducing a frequency dependence, they obtain a quantum correction $\delta\sigma \propto (\ell\, k_\mathrm{F})^0$ for non-zero temperatures. As this correction vanishes in the zero-frequency limit, the result of Culcer and Winkler is consistent with that of Trushin and Schliemann and, at first sight, also with that of Auslender and Katsnelson.

In the present study we have mainly monolayer graphene in mind. However, since we formulate the Boltzmann equation for a spin-orbit coupling of arbitrary winding number N, our results apply as well to certain models for bilayer and multilayer graphene [McCann and Fal'ko, 2006; Guinea *et al.*, 2006; Koshino and Ando, 2007; Min and MacDonald, 2008]. Quantum corrections in the bilayer case $N = 2$ have been considered by Culcer and Winkler [2009] with a similar approach as in Culcer and Winkler [2007b]. We will refer to $|N| = 1$ as the "monolayer case" and to $|N| > 1$ as the "multilayer case." (Note, however, that realistic N-layer graphene Hamiltonians can, depending on the stacking, be written as tensor products of lower-N Hamiltonians, including in some cases the monolayer $|N| = 1$ Hamiltonian [Koshino and Ando, 2007; Min and MacDonald, 2008]). The results apply to any setting in 2d where the electrons are described by one or several (decoupled) Dirac cones. They should therefore also be relevant in the context of *3d topological insulators* such as $\mathrm{Bi}_{1-x}\mathrm{Sb}_x$, $\mathrm{Bi}_2\mathrm{Te}_3$, $\mathrm{Sb}_2\mathrm{Te}_3$ and $\mathrm{Bi}_2\mathrm{Se}_3$, the 2d surface states of which are described

by Dirac cone physics [Fu *et al.*, 2007; Moore and Balents, 2007; Roy, 2009; Hsieh *et al.*, 2008; Zhang *et al.*, 2009; Xia *et al.*, 2009], see also Hasan and Kane [2010]. There, the occurrence of only a single Dirac cone removes the problem of intervalley scattering. These systems should therefore be a better setting to apply those parts of our calculations that deal with point-like impurities, for which the assumption of negligible intervalley scattering in graphene might be invalid.

The remainder of this chapter is organized as follows: In Section 5.2 we anticipate the main results on a qualitative level. In Section 5.3 we present the Wigner transformed Hamiltonians that we examine in the subsequent sections. In Section 5.4 the semiclassical distribution function and the Boltzmann equation for a spin-orbit coupled system are introduced. Derivations of collision integrals with different approaches are presented in Section 5.5. In Section 5.6 the resulting general collision integrals are compared and simplified for the case of spin-orbit coupled systems, in particular graphene. Section 5.7 deals with the solution of the Boltzmann equation neglecting principal value terms and the resulting dc and ac conductivity. In Section 5.8, we solve the Boltzmann equation including the principal value terms and present the resulting conductivity for both dc and ac. A summary and an outlook are given in Section 5.9.

5.2. Main results

Concerning the first central question raised in the introductory section—the one for the equivalence of alternative derivations of kinetic equations—we find that when (pseudo)spin-orbit coupling is present *different formalisms yield different collision integrals*. In particular, Green's function derivations with the standard Kadanoff-Baym ansatz (KBA) [Kadanoff and Baym, 1962] or the Generalized Kadanoff-Baym ansatz (GKBA) [Lipavsky *et al.*, 1986] do *not* result in the same general collision term as the single-time density matrix approaches. We propose an alternative "anti-ordered" ansatz for which the translation between density matrix and Green's function approaches can be established.

Reassuringly, the general collision integrals of all approaches (always taken to zeroth order in gradient expansion) coincide at least for spinless electrons. On a practical level this applies also in the presence of a *small* spin-orbit coupling: the difference between collision integrals affects the delta function terms, but only in parts that capture second and higher order effects in the spin-orbit interaction, see also Kailasvuori [2009]. The difference shows up in the principal value terms as well, but those are typically neglected altogether in calculations where the focus is, *e.g.*, on spin and charge currents to leading order. This might explain why the discrepancy between density matrix approaches and Green's function derivations using the the GKB ansatz does not seem to be an issue of debate in the context of the spin Hall effect, where a variety of approaches have been used to derive spin coherent Boltzmann equations [Mishchenko *et al.*, 2004; Shytov *et al.*, 2006; Raimondi *et al.*, 2006; Culcer and Winkler, 2007a; Kailasvuori, 2009].

Both with and without principal value terms, the leading quantum correction to the Drude conductivity in graphene depends generally[1] on the approach. The differences

[1] An exception is the case of point-like impurities in a bilayer $|N| = 2$. For this problem the principal value terms vanish in all approaches, and the remaining delta function terms of the collision integral

can be quantitative (*e.g.*, a relative factor of 3 between the results of the density matrix calculation and a Green's function approach implementing the GKBA for the case of monolayer graphene with point-like impurities when principal value terms are neglected) or, when principal value terms are included, even qualitative with leading-order corrections of opposite sign or of different order in $(\ell\, k_\mathrm{F})^{-1}$.

The latter point leads us to our results regarding the second central question, namely the one for the leading order quantum corrections to the Drude conductivity of graphene: We find that when principal value terms are neglected, the first quantum correction is of the order $(\ell\, k_\mathrm{F})^{-1}$ both in the dc conductivity and in the dissipative ac conductivity. Corrections beyond the order $(\ell\, k_\mathrm{F})^{-1}$ are absent in the monolayer case, but present to infinite order in the multilayer case. The first point is in qualitative agreement with the result of Trushin and Schliemann [2007]. The ac result, however, is at odds with the frequency-dependent correction $\sim (\ell\, k_\mathrm{F})^0$ found by Culcer and Winkler [2007b; 2009].

When including the principal value terms in the calculation of the dc conductivity, we obtain a leading quantum correction of the order $(\ell\, k_\mathrm{F})^0$. This appears to disagree[2] with the findings of Auslender and Katsnelson [2007] who present a leading quantum correction of order $(\ell\, k_\mathrm{F})^{-1}$. Intriguingly, our correction is independent of the impurity concentration and of the impurity strength. For screened charged impurities at a negligible distance from the graphene plane it depends only on the dimensionless parameter $k_\mathrm{F}/k_\mathrm{TF}$, where $\hbar\, k_\mathrm{F}$ denotes the Fermi momentum and $1/k_\mathrm{TF}$ the Thomas-Fermi screening length. In the monolayer case one has $k_\mathrm{TF} \propto k_\mathrm{F}$, and the correction is therefore also independent of k_F (*i.e.*, of the electron density). It is then determined only by natural constants and the dielectric constant.

An electron-hole coherent quantum correction of the order $(\ell\, k_\mathrm{F})^0$ can provide one candidate mechanism for generating a *residual conductivity* (see Figure 5.1). Our result could therefore be a part of the explanation of the residual conductivity observed in the experiments by Chen *et al.* [2008] in monolayer graphene. This residual conductivity is observed to be surprisingly constant, depending at the most weakly on the impurity concentration—in contrast to the conductivity minimum. Our proposed contribution to the residual conductivity is independent of the impurity density. However, it can in principle depend on the dielectric environment of the graphene sample. There are experiments where the dielectric constant is varied, for example by coating the sample with ice [Chen *et al.*, 2009]. However, the extraction of the residual conductivity appears to be rather precarious, and it is too early to say if there is any relation with the dielectric behavior of our result.

In accordance with all mentioned previous studies the corrections that we find are convergent in the case of screened charged impurities. For point-like impurities the corrections are convergent in the multilayer case but require an ultraviolet cut-off in the monolayer case.

We finally observe that for point-like impurities in the multilayer case the contribution

coincide. Therefore the density matrix approach of Trushin *et al.* [2010] is not affected by the ambiguities unraveled in the present work.

[2]Concerning this disagreement M. I. Katsnelson communicated to us that their Eqs. (84) and (85) are not the full result and that the full result treated in the appendix of their paper might also contain contributions of order $\mathcal{O}(1)$ (see also the statement at the end of their appendix) in which case the qualitative disagreement could be removed.

from principal value terms vanishes trivially to the orders $(\ell\, k_\mathrm{F})^0$ and $(\ell\, k_\mathrm{F})^{-1}$. The leading quantum correction is then the correction of order $(\ell\, k_\mathrm{F})^{-1}$ derived with principal value terms neglected. This is consistent with recent results of Trushin *et al.* [2010].

5.3. Model

Semiclassical descriptions of a nonequilibrium problem are typically based on the Wigner transformed one-particle Hamiltonian (or envelope function Hamiltonian) [Haug and Jauho, 2008; Zubarev *et al.*, 1996; Rammer, 1998; Rammer and Smith, 1986; Winkler, 2003]. Effects of potentials that vary rapidly, *i.e.*, on the length scale of the de Broglie wavelength $\lambda_B = 1/k_F$ or on the corresponding time scale λ_B/v_F are already captured in effective masses, spin-orbit fields *etc.*, and only the—in the same sense—slowly varying potentials appear explicitly. For the spin-orbit coupled systems in presence of an electric field that we set out to study, the effective Hamiltonian without impurities reads (see Chapter 1.3)

$$H(\boldsymbol{x},\boldsymbol{p},t) \;=\; \epsilon_0(k) + \boldsymbol{\sigma}\cdot\boldsymbol{b}(\boldsymbol{k}) + e\,\phi(\boldsymbol{x},t) \tag{5.2}$$

with $\hbar \equiv 1$, the elementary charge $e < 0$ and the kinetic momentum $\boldsymbol{k}(\boldsymbol{x},\boldsymbol{p},t) = \boldsymbol{p} - e\boldsymbol{A}(\boldsymbol{x},t)$. The energy bands in the absence of electromagnetic fields are $\epsilon^s_{\boldsymbol{k}} = \epsilon_0 + s\,b$, where $s = \pm 1$ gives the sign of the spin projection along the pseudospin quantization axis $\hat{\boldsymbol{b}}$, *i.e.*, $\boldsymbol{\sigma}\cdot\hat{\boldsymbol{b}}\,|\hat{\boldsymbol{b}}s\rangle = s\,|\hat{\boldsymbol{b}}s\rangle$. We want to describe a 2d system with $\boldsymbol{x}$ and $\boldsymbol{p}$ chosen to lie in the x,y-plane.

The spinless part of the dispersion is given by ϵ_0. In the Hamiltonians studied in the literature on the intrinsic spin Hall effect this is typically the quadratic dispersion $\epsilon_0 = k^2/2m^*$, which usually constitutes the larger part of the kinetic energy. In contrast, for monolayer graphene, leaving the small "real" spin-orbit coupling aside, one has $\epsilon_0 = 0$, *i.e.*, the pseudospin-orbit coupling constitutes the *entire* kinetic energy. In addition to the electron spin (treated as being trivial in the following) and the pseudospin connected to the bipartite lattice of graphene, the electrons have a valley index corresponding to the two Dirac cones K and K'. We neglect inter-valley scattering and treat each Dirac cone independently, which reduces the graphene problem to the 2×2 Hamiltonian (5.2). This approximation should be fine as long as the disorder is smooth, but becomes doubtful for short-ranged impurity potentials and in particular for the extreme case of point-like impurities.

For the Dirac point K the spin-orbit coupling for the pseudospin is given by $\boldsymbol{b} = v_\mathrm{F}\,\boldsymbol{k}$ (*i.e.*, $b = v_\mathrm{F}\,k$ and $\hat{\boldsymbol{b}} = \hat{\boldsymbol{k}}$) with the Fermi velocity $v_\mathrm{F} \approx c/300$. Here we consider the more general isotropic spin-orbit coupling

$$\boldsymbol{b} \;=\; b(k)\,\hat{\boldsymbol{b}}(\theta) \tag{5.3}$$

with a winding number N as defined in Eq. (1.3). This includes, in particular, the Dirac cone K' of monolayer graphene (with $b = v_\mathrm{F}\,k$ and $\hat{\boldsymbol{b}} = (\cos\theta, -\sin\theta)$, *i.e.* $N = -1$) and the Hamiltonian

$$H \;=\; \frac{1}{2m^*}\begin{pmatrix} 0 & (k_x \mp ik_y)^2 \\ (k_x \pm ik_y)^2 & 0 \end{pmatrix} \;=\; \frac{k^2}{2m^*}\begin{pmatrix} 0 & e^{\mp i2\theta} \\ e^{\pm i2\theta} & 0 \end{pmatrix} \tag{5.4}$$

(with $b = k^2/2m^*$ and $N = 2$) studied in the context of bilayer graphene as well as similar Hamiltonians for multilayer graphene [McCann and Fal'ko, 2006; Guinea *et al.*, 2006; Koshino and Ando, 2007; Min and MacDonald, 2008].

The total Hamiltonian $H_{\mathrm{tot}} = H + V$ includes an impurity potential $V(\boldsymbol{x}) = \sum_n u(\boldsymbol{x} - \boldsymbol{x}_n)$ of non-magnetic impurities at positions $\boldsymbol{x}_n$ eventually to be averaged over. We distinguish between point-like impurities $u_{\boldsymbol{k}\boldsymbol{k}'} = \text{const.}$ and screened charged impurities in 2d with

$$u_{\boldsymbol{k}\boldsymbol{k}'} = \frac{e^2/\kappa_0}{|\boldsymbol{k} - \boldsymbol{k}'| + k_{\mathrm{TF}}}. \tag{5.5}$$

Here, κ_0 is the dielectric constant and the Thomas-Fermi momentum $k_{\mathrm{TF}} = \frac{2\pi e^2}{\kappa_0} D_{\mathrm{F}}$ with the density of states at the Fermi energy D_F determines the range $1/k_{\mathrm{TF}}$ of the screened potential. For a recent review on screening in graphene with an enlightening comparison of monolayers, bilayers, and 2DEGs, see Das Sarma *et al.* [2011]. Here we recall a few facts that will be important for our later discussions. It is convenient to introduce the dimensionless parameter $q_{\mathrm{s}} \equiv k_{\mathrm{TF}}/k_{\mathrm{F}}$ characterizing the strength of the screening. An unscreened Coulomb interaction corresponds to $q_{\mathrm{s}} = 0$. In the opposite limit $q_{\mathrm{s}} \to \infty$ the potential becomes almost angularly independent and the effects of the charged impurities resemble in some, although not all, respects the ones of point-like impurities. In the monolayer case, for example, one has the special situation that $D_{\mathrm{F}} \propto k_{\mathrm{F}}$, hence q_{s} is independent of k_{F}, implying that for short and long screening lengths alike the potential behaves like an unscreened Coulomb potential in that $\tau_{\mathrm{tr}}^{-1}(k_{\mathrm{F}}) \propto D_{\mathrm{F}}\, k_{\mathrm{F}}^{-2} \propto k_{\mathrm{F}}^{-1}$, and therefore $\sigma_0 \sim \tau_{\mathrm{tr}}(k_{\mathrm{F}})\, \epsilon_{\mathrm{F}} \propto k_{\mathrm{F}}^2 \propto |n|$. Thus, not even for strong screening the situation turns into that of point-like impurities, for which $\tau_{\mathrm{tr}}^{-1} \propto k_{\mathrm{F}}$ yields a Drude conductivity that is independent of the density. For graphene on SiO_2 substrates, the standard value is $q_{\mathrm{s}} \approx 3.2$, see Das Sarma *et al.* [2011]. This suggests that screening is important ($q_{\mathrm{s}} > 1$), and when discussing the quantum correction $\sim (\ell\, k_{\mathrm{F}})^0$ below we shall see that for this quantity the screened potential as encountered in realistic monolayers has after all more in common with point-like impurities than with an unscreened Coulomb potential.

In bi- and multilayers the situation is different from the monolayer case: here, q_{s} decreases with increasing k_{F} and consequently with increasing density—just like in an ordinary 2DEG, but contrary to a 3DEG. Thus, the further one moves away from the Dirac point, the weaker the screening and the stronger the effect of the interaction. Thus, when discussing the correction $\sim (\ell\, k_{\mathrm{F}})^0$ we expect that in the vicinity of the Dirac point the screened potential has more in common with point-like impurities, whereas far away from the Dirac point the potential has more in common with an unscreened Coulomb potential.

5.4. The drift side of the Boltzmann equation

In the Boltzmann regime $\ell\, k_{\mathrm{F}} \ll 1$, the spatial degrees of freedom can be dealt with semiclassically. The treatment of the pseudospin must, however, remain quantum mechanical in order to capture effects of the electron-hole coherence.

The state of the system is described in terms of the Wigner transformed time-diagonal

density matrix (*cf.* Eq. (2.56))

$$\begin{aligned}\rho_{\sigma\sigma'}(\boldsymbol{x},\boldsymbol{p},t) &= \int \mathrm{d}\boldsymbol{r}\, e^{i\boldsymbol{p}\cdot\boldsymbol{r}}\, \langle \psi^\dagger_{\sigma'}(\boldsymbol{x}-\boldsymbol{r}/2,t)\, \psi_\sigma(\boldsymbol{x}+\boldsymbol{r}/2,t)\rangle \\ &= \int \mathrm{d}\boldsymbol{r}\, e^{i\boldsymbol{p}\cdot\boldsymbol{r}}\, G^<_{\sigma\sigma'}(\boldsymbol{x}-\boldsymbol{r}/2,t_1;\boldsymbol{x}+\boldsymbol{r}/2,t_2)_{t_2=t_1=t} \end{aligned} \tag{5.6}$$

with the spin indices $\sigma = \uparrow_z, \downarrow_z$. In the absence of interactions, one possible way[3] to derive the collisionless Boltzmann equation for ρ is to first apply the Heisenberg equation of motion to $\Psi(t_1)$, then identify $t_2 = t_1$, Wigner transform the result, and gradient expand it to first order (see Chapter 2.2.5).

From the matrix elements of the distribution function ρ one can extract the densities and current densities of charge and spin. The matrix elements are conveniently expressed in the decomposition $\rho = \rho_0 + \boldsymbol{\sigma}\cdot\boldsymbol{\rho}$, where $\boldsymbol{\sigma} = (\sigma_x, \sigma_y, \sigma_z)$ is the vector of Pauli matrices. Furthermore, we find it useful to decompose the vector $\boldsymbol{\rho} = \rho_{\hat{\boldsymbol{b}}}\,\hat{\boldsymbol{b}} + \rho_{\hat{\boldsymbol{c}}}\,\hat{\boldsymbol{c}} + \rho_z\,\hat{\boldsymbol{z}}$ in its components along the basis vectors $\hat{\boldsymbol{b}}(\theta)$, $\hat{\boldsymbol{z}}$ and $\hat{\boldsymbol{c}}(\theta) = \hat{\boldsymbol{z}}\times\hat{\boldsymbol{b}}(\theta)$ with $\partial_\theta\hat{\boldsymbol{b}} = N\hat{\boldsymbol{c}}$, analogous to the general cylindrical basis vectors $\hat{\boldsymbol{k}}(\theta) := \boldsymbol{k}/k$, $\hat{\boldsymbol{z}}$ and $\hat{\boldsymbol{\theta}}(\theta) := \hat{\boldsymbol{z}}\times\hat{\boldsymbol{k}}(\theta)$ with $\partial_\theta\hat{\boldsymbol{k}} = \hat{\boldsymbol{\theta}}$. In the spin basis $\{|\uparrow_z\rangle, |\downarrow_z\rangle\}$ one has

$$\begin{aligned}\rho &= \rho_0 + \rho_{\hat{\boldsymbol{b}}}\,\hat{\boldsymbol{b}}\cdot\boldsymbol{\sigma} + \rho_{\hat{\boldsymbol{c}}}\,\hat{\boldsymbol{c}}\cdot\boldsymbol{\sigma} + \rho_z\,\hat{\boldsymbol{z}}\cdot\boldsymbol{\sigma} \\ &= \begin{pmatrix} \rho_0+\rho_z & (\rho_{\hat{\boldsymbol{b}}} - i\,\rho_{\hat{\boldsymbol{c}}})\, e^{-iN\theta} \\ (\rho_{\hat{\boldsymbol{b}}} + i\,\rho_{\hat{\boldsymbol{c}}})\, e^{iN\theta} & \rho_0-\rho_z \end{pmatrix}. \end{aligned} \tag{5.7}$$

The charge density $e\,n$ and the current density $e\,\boldsymbol{j}$ in phase space are derived from $e\,n = \mathrm{Tr}\,(\rho\,\partial H/\partial\phi)$ and $e\,\boldsymbol{j} = -\mathrm{Tr}\,(\rho\,\partial H/\partial\boldsymbol{A})$, yielding

$$\begin{array}{rcccccl} n(\boldsymbol{x},\boldsymbol{k},t) & := & \mathrm{Tr}\,\rho & = & 2\,\rho_0 & = & n^+ + n^-, \\ j_i(\boldsymbol{x},\boldsymbol{k},t) & := & \mathrm{Tr}\,(\mathbf{v}_i\,\rho) & = & 2\,\rho_0\,\partial_{k_i}\epsilon_0 + 2\,\boldsymbol{\rho}\cdot\partial_{k_i}\boldsymbol{b} & = & n^+ v_i^+ + n^- v_i^- + \frac{2\,N\,b}{k}\rho_{\hat{\boldsymbol{c}}}\,\hat{\theta}_i \end{array} \tag{5.8}$$

with $i = x, y$. Here we introduced the velocity matrices $\mathbf{v}_i := \partial_{k_i} H = \partial_{k_i}\epsilon_0 + \boldsymbol{\sigma}\cdot\partial_{k_i}\boldsymbol{b}$. The spin independent part of the velocity is $\partial_{\boldsymbol{k}}\epsilon_0 =: \boldsymbol{v}_0$. The band velocities are $\boldsymbol{v}^s := \partial_{\boldsymbol{k}}\epsilon^s = \langle\hat{\boldsymbol{b}}s|\,\mathbf{v}\,|\hat{\boldsymbol{b}}s\rangle = v^s\,\hat{\boldsymbol{k}}$. The *intra*-band elements

$$n^\pm \;:=\; \langle\hat{\boldsymbol{b}}\pm|\,\rho\,|\hat{\boldsymbol{b}}\pm\rangle \;=\; \rho_0 \pm \rho_{\hat{\boldsymbol{b}}} \tag{5.9}$$

give the density in each spin band $s = \pm$. The *inter*-band elements $\langle\hat{\boldsymbol{b}}\pm|\,\rho\,|\hat{\boldsymbol{b}}\mp\rangle = \rho_z \pm i\,\rho_{\hat{\boldsymbol{c}}}$ are important for a coherent treatment of the (pseudo)spin. These are the elements that oscillate in the occurrence of spin-precession. In the case of spin-orbit coupling the imaginary component $\rho_{\hat{\boldsymbol{c}}}$ appears in the last term of the current (5.8). For the density matrix of a single electron this term would contain the oscillatory Zitterbewegung (jittery motion) of the free spin-orbit coupled electron. In the statistical description given by the distribution function this oscillatory motion of the free particle states averages to zero over time and is therefore absent in the equilibrium distribution function ($\rho^{\mathrm{eq}}_{\hat{\boldsymbol{c}}} = \rho^{\mathrm{eq}}_z = 0$).

[3] An alternative procedure is to apply the Nonequilibrium statistical operator method, *i.e.*, to evaluate the left-hand side of Eq. (2.54). Also in this method the semiclassical approximation consists in a first-order gradient expansion.

The charge component ρ_0 is completely decoupled and redundant for our problem. The (pseudo)spin density, *i.e.* the polarization, is given by $s^\mu = \frac{1}{2}\,\mathrm{Tr}\,(\sigma_\mu\, f) = \rho_\mu$ (with $\mu = x, y, z$). There is not a unique way to define the spin current, because in the presence of spin-orbit coupling the real space spin polarization is not a conserved quantity. When the two band velocities coincide ($\boldsymbol{v}^s = \boldsymbol{v}_0$) it is $\boldsymbol{j}^\mu = \rho_\mu\, \boldsymbol{v}_0$. We use the common definition

$$j_i^\mu \;=\; \frac{1}{4}\mathrm{Tr}\,\left(\sigma_\mu\{\mathbf{v}_i, \rho\}\right) \;=\; \rho_\mu\, \partial_{k_i}\epsilon_0 + \rho_0\, \partial_{k_i} b_\mu \tag{5.10}$$

with the anticommutator $\{A, B\} := A\,B + B\,A$.

The Boltzmann equation in matrix form reads

$$i\,[H, \rho] + \partial_t \rho + \frac{1}{2}\,\{\mathbf{v}_i, \partial_{x_i}\rho\} + e\,E_i\,\partial_{k_i}\rho - \epsilon_{zij}\,e\,B_z\,\frac{1}{2}\,\{\mathbf{v}_i, \partial_{k_j}\rho\} \;=\; \mathcal{J}[\rho], \tag{5.11}$$

where the matrix-valued functional $\mathcal{J} = \mathcal{J}_0 + \sigma_\mu\,\mathcal{J}_\mu$ is the collision integral. The left-hand side of Eq. (5.11) is obtained by the procedure described above, and the collision integrals on the right-hand side will be derived with various approaches in the next section. With the definition (5.10) the Boltzmann equation (5.11) can be written in the appealing form

$$\begin{aligned} \partial_t n + \partial_{\boldsymbol{x}} \cdot \boldsymbol{j} + e\,\partial_{\boldsymbol{k}} \cdot (n\,\boldsymbol{E} + \boldsymbol{j} \times \boldsymbol{B}) &= 2\,\mathcal{J}_0, \\ 2\,(\boldsymbol{s} \times \boldsymbol{b})^\mu + \partial_t s^\mu + \partial_{\boldsymbol{x}} \cdot \boldsymbol{j}^\mu + e\,\partial_{\boldsymbol{k}} \cdot (s^\mu \boldsymbol{E} + \boldsymbol{j}^\mu \times \boldsymbol{B}) &= \mathcal{J}_\mu\,. \end{aligned} \tag{5.12}$$

Semiclassical kinetic equations deal with densities in phase space. Real space equations are obtained by integrating the phase space densities over momentum, *e.g.*,

$$\boldsymbol{j}(\boldsymbol{x}, t) = \int \frac{\mathrm{d}^2 k}{(2\pi)^2}\, \boldsymbol{j}(\boldsymbol{x}, \boldsymbol{k}, t)\,. \tag{5.13}$$

The Boltzmann equation is typically written for the quasiparticle distribution $f_{\sigma\sigma'}(\boldsymbol{x}, \boldsymbol{p}, t)$ rather than for the Wigner transformed density matrix $\rho_{\sigma\sigma'}(\boldsymbol{x}, \boldsymbol{p}, t)$. The electron distribution ρ is the quantity in terms of which the current and densities are defined. The quasiparticles described by f, on the other hand, represent the free particles that satisfy the Pauli principle. Therefore, the equilibrium state for f can be expressed simply in terms of the Fermi-Dirac distribution. This is of practical relevance in the analytical solution of the Boltzmann equation by linearizing in deviations from the equilibrium. In this work we neglect this difference. Thus, all the above expressions including ρ are assumed to apply for f.

5.5. Derivation of the Boltzmann equation including collision terms

In this section we present the derivation of semiclassical kinetic equations including collision integrals from quantum theory in several approaches. One group of approaches deals directly with the density matrix $\rho(x_1, x_2, t)$ and starts from the Liouville-von Neumann equation. The second type of approaches are Green's function techniques which have the Kadanoff-Baym or Keldysh equations for the double-time correlator $G^<(x_1, t_1, x_2, t_2)$ as

their starting points. To recover a time-diagonal kinetic equation one needs to invoke some approximation. This is the problem of ansatz. We will present several different candidates and therefore several different collision integrals. One of them is identical to the collision integral derived with the density matrix approaches.

5.5.1. Iterative solution of the von Liouville-von Neumann equation

Consider the Hamiltonian

$$H \;=\; H_0 + V, \tag{5.14}$$

where V is an interaction switched on at a time t_0 in the remote past. The von Neumann equation in the interaction picture is

$$i\,\partial_t\,\rho^{\mathrm{I}} \;=\; [V^{\mathrm{I}}(t), \rho^{\mathrm{I}}] \tag{5.15}$$

with

$$A^{\mathrm{I}}(t) \;=\; e^{iH_0(t-t_0)}\,A(t_0)\,e^{-iH_0(t-t_0)} \;=\; \mathcal{U}_0^{\dagger}(t,t_0)A(t_0)\,\mathcal{U}_0(t,t_0), \tag{5.16}$$

where A is a general operator in the Schrödinger picture (thus its time dependence can only be an explicit one). This is easily integrated to give

$$\rho^{\mathrm{I}}(t) \;=\; \rho^{\mathrm{I}}(t_0) - i\int_{t_0}^{t} \mathrm{d}t'\,[V^{\mathrm{I}}(t'), \rho^{\mathrm{I}}(t')], \tag{5.17}$$

which, when inserted back into (5.15), yields

$$\begin{aligned}
\partial_t\,\rho^{\mathrm{I}} \;&=\; -i\,[V^{\mathrm{I}}(t), \rho^{\mathrm{I}}(t_0)] - \int_{t_0}^{t} \mathrm{d}t'\,[V^{\mathrm{I}}(t), [V^{\mathrm{I}}(t'), \rho^{\mathrm{I}}(t')]] \\
&=\; -i\,[V^{\mathrm{I}}(t), \rho^{\mathrm{I}}(t_0)] - \int_{t_0}^{t} \mathrm{d}t'\,[V^{\mathrm{I}}(t), [V^{\mathrm{I}}(t'), \rho^{\mathrm{I}}(t)]] \\
&\quad -i\int_{t_0}^{t} \mathrm{d}t' \int_{t'}^{t} \mathrm{d}t''\,[V^{\mathrm{I}}(t), [V^{\mathrm{I}}(t'), [V^{\mathrm{I}}(t''), \rho^{\mathrm{I}}(t'')]]
\end{aligned} \tag{5.18}$$

after a first and second iteration, respectively. Up to this point the equations are exact. The Born approximation allows us to get a closed equation for ρ at time t to second order in the interaction V. To this end, we remove the last term in the second row. Alternatively, in the last term of the first row replace the full evolution with the free evolution, *i.e.* let $\rho^{\mathrm{I}}(t') = \rho^{\mathrm{I}}(t)$, which has the appearance of a Markov approximation. Back in the Schrödinger picture, the assumption of free evolution reads

$$\rho(t') \;=\; \mathcal{U}_0(t',t)\,\rho(t)\,\mathcal{U}_0^{\dagger}(t',t) \;=\; e^{-i\,H_0\,(t'-t)}\,\rho(t)\,e^{i\,H_0\,(t'-t)}, \tag{5.19}$$

and after reorganizing evolution operators one obtains the kinetic equation

$$\begin{aligned}
\partial_t\,\rho(t) + i\,[H_0, \rho(t)] \;&=\; -i\,[V, e^{-i\,H_0\,(t-t_0)}\rho(t_0)e^{i\,H_0\,(t-t_0)}] \\
&\quad - \int_0^{t-t_0} \mathrm{d}\tau\,[V, [e^{-i\,H_0\,\tau}\,V\,e^{i\,H_0\,\tau}, \rho(t)]].
\end{aligned} \tag{5.20}$$

So far, this kinetic equation is locally time reversible (*not* globally though, since the interaction was switched on at some point). In order to capture the decoherence due to other processes (*e.g.* phonons) we do not want the state to depend on correlations in the remote past. Therefore we include a factor $e^{-\eta\,\tau}$ in the integral to impose this loss of memory. This introduces time irreversibility. This factor also regularizes the integral and allows us to send $t_0 \to -\infty$.

For the purpose of immediate comparison with the results of other formalisms, we want to express the evolution operators in the last term in (5.20), which will become the collision integral $\mathcal{J}[\rho]$, in terms of Green's functions. The non-interacting retarded and advanced Green's function for the spin-orbit coupled Hamiltonian (1.5) are

$$G^{0\mathrm{R}}_{\boldsymbol{k}} \;=\; \sum_{s=\pm} \frac{S_{\hat{\boldsymbol{b}}\,s}}{\tilde{\omega}^{+} - \epsilon^{s}_{\boldsymbol{k}}}, \tag{5.21}$$

$$G^{0\mathrm{A}}_{\boldsymbol{k}} \;=\; \sum_{s=\pm} \frac{S_{\hat{\boldsymbol{b}}\,s}}{\tilde{\omega}^{-} - \epsilon^{s}_{\boldsymbol{k}}} \tag{5.22}$$

with the spin projection operator

$$S_{\hat{\boldsymbol{b}}s} \;:=\; \frac{1}{2}\,(\mathbf{1} + \boldsymbol{\sigma}\cdot s\,\hat{\boldsymbol{b}}_{\hat{\boldsymbol{k}}}) \tag{5.23}$$

and $\tilde{\omega}^{\pm} = \tilde{\omega} \pm i\,0^{+}$, where $\tilde{\omega} = \omega - \phi$ is the gauge invariant frequency variable. Let f be a general operator with a matrix structure in spin space. Using the residue theorem, we have

$$\begin{aligned}
&\int_0^\infty \mathrm{d}t\, e^{-\eta\,t}\, e^{-i\,H_{\boldsymbol{k}}\,t}\, f\, e^{i\,H_{\boldsymbol{k'}}\,t} \\
=\;& \int_0^\infty \mathrm{d}t\, e^{-\eta\,t}\, e^{-i\,(\epsilon_0-\epsilon_0')\,t}\,(\cos b\,t - i\,\boldsymbol{\sigma}\cdot\hat{\boldsymbol{b}}\,\sin b\,t)\, f\,(\cos b'\,t + i\,\boldsymbol{\sigma}\cdot\hat{\boldsymbol{b'}}\,\sin b'\,t) \\
=\;& \int_0^\infty \mathrm{d}t\, e^{-\eta\,t}\, e^{-i\,(\epsilon_0-\epsilon_0')\,t} \sum_s \frac{e^{-i\,s\,b\,t} + s\,\boldsymbol{\sigma}\cdot\hat{\boldsymbol{b}}\,e^{-i\,s\,b\,t}}{2}\, f \sum_{s'} \frac{e^{i\,s'\,b'\,t} + s'\,\boldsymbol{\sigma}\cdot\hat{\boldsymbol{b'}}\,e^{i\,s'\,b'\,t}}{2} \\
=\;& \int_0^\infty \mathrm{d}t\, e^{-\eta\,t} \sum_{ss'} e^{-i\,(\epsilon_0 + s\,b - \epsilon_0' - s'b')\,t}\, S\, f\, S' \;=\; \sum_{ss'} S\, f\, S'\, \frac{1}{\eta + i\,(\epsilon - \epsilon')} \\
=\;& \int_{-\infty}^\infty \frac{\mathrm{d}\omega}{2\pi} \sum_{ss'} \frac{S}{\omega + i\,\eta - \epsilon}\, f\, \frac{S'}{\omega - i\,\eta - \epsilon'} \\
=\;& \int_{-\infty}^\infty \frac{\mathrm{d}\omega}{2\pi}\, G^{0\mathrm{R}}_{\boldsymbol{k}}\, f\, G^{0\mathrm{A}}_{\boldsymbol{k'}},
\end{aligned} \tag{5.24}$$

and the collision integral takes the form

$$\mathcal{J}[\rho] \;=\; -\int \frac{\mathrm{d}\omega}{2\pi}\,[V, [G^{0\mathrm{R}}\,V\,G^{0\mathrm{A}}, \rho]]. \tag{5.25}$$

Another source of irreversibility comes in with the impurity averaging. We take the spatial average over the matrix element of the electron-impurity interaction

$$V_{kk'} = \sum_n e^{-i(k-k')\,x_n}\, u_{kk'}, \tag{5.26}$$

assuming a uniform distribution of the impurity positions. This yields $V_q \to n_{\rm imp}\, V_q\, \delta(q) \sim n_{\rm imp}\, V(r=0)$ and $\ldots V_{,q_1} \ldots V_{,q_2} \cdots \to (\ldots V_{q_1} \ldots V_{q_2} \ldots)\, [n_{\rm imp}^2\, \delta(q_1)\, \delta(q_2) + n_{\rm imp}\, \delta(q_1 + q_2)]$. For the last term we neglect the $n_{\rm imp}^2$ through the assumption of low impurity concentration. Then V in the first term of (5.20) becomes just a number $\sim V(r=0)$, and the commutator vanishes. For the terms that are linear in $n_{\rm imp}$ one finds for example (summation over repeated indices is implicit)

$$\begin{aligned}(V\, G^{0\rm R}\, V\, G^{0\rm A}\, \rho)_{kk'} \quad &\longrightarrow \quad n_{\rm imp}\, \delta(k - k_1 + k_1 - k_2)\, u_{kk_1}\, G^{0\rm R}_{k_1}\, u_{k_1k_2} G^{0\rm A}_{k_2} \rho_{k_2k'} \\ &= \; \Sigma^{\rm R}_k\, G^{0\rm A}_k\, \rho_{kk'}\,, \end{aligned} \tag{5.27}$$

where we have introduced the retarded self-energy

$$\Sigma^{\rm R}_k \quad = \quad n_{\rm imp}\, (u\, G^{0\rm R}\, u)_k\,. \tag{5.28}$$

However, in a term like

$$(V\, \rho\, G^{0\rm R}\, V\, G^{0\rm A})_{kk'} \quad \longrightarrow \quad n_{\rm imp}\, \delta(k - k_1 + k_2 - k')\, u_{kk_1}\, \rho_{k_1k_2}\, G^{0\rm R}_{k_2}\, u_{k_2k'}\, G^{0\rm A}_{k'} \tag{5.29}$$

the delta function seems to offer no simplification at all. At this point we can attain further simplification if we say that in the collision integral we are not interested in contributions that are related with non-diagonality in momentum. This amounts to saying that we are not interested in any gradient expansion corrections to the collision integral. We then have

$$(V\, \rho\, G^{0\rm R}\, V\, G^{0\rm A})_{kk} \quad \longrightarrow \quad n_{\rm imp}\, u_{kk'}\, \rho_{k'}\, G^{0\rm R}_{k'}\, u_{k'k}\, G^{0\rm A}_k\,, \tag{5.30}$$

and the collision integral can be written as

$$\begin{aligned}\mathcal{J}[\rho(\boldsymbol{k},\boldsymbol{x},t)] \quad &= \quad -\int_{\boldsymbol{k'}} W_{\boldsymbol{kk'}} \int \frac{{\rm d}\omega}{(2\pi)^2}\, (\rho_{\boldsymbol{k}}\, G^{0\rm R}_{\boldsymbol{k}}\, G^{0\rm A}_{\boldsymbol{k'}} + G^{0\rm R}_{\boldsymbol{k'}}\, G^{0\rm A}_{\boldsymbol{k}}\, \rho_{\boldsymbol{k}} \\ &\qquad -\rho_{\boldsymbol{k'}}\, G^{0\rm R}_{\boldsymbol{k'}}\, G^{0\rm A}_{\boldsymbol{k}} - G^{0\rm R}_{\boldsymbol{k}}\, G^{0\rm A}_{\boldsymbol{k'}}\, \rho_{\boldsymbol{k'}}) \end{aligned} \tag{5.31}$$

with the transition matrix $W_{\boldsymbol{kk'}} = 2\,\pi\, n_{\rm imp}\, |u_{\boldsymbol{kk'}}|^2$ for non-magnetic impurities.

An approach based on the Liouville-von Neumann equation was also used by Culcer and Winkler [2007b], although along different lines. In that derivation the focus is from the start only on the diagonal part f_k (not to be confused with our f for the quasiparticle distribution) of $\rho_{kk'} = f_k\, \delta_{kk'} + g_{kk'}$, which closes the door to gradient expansion corrections in the interaction terms. The analogue of the iterative solution of the Liouville-von Neumann equation presented in this section is their decomposition into two coupled equations for f_k and for the purely nondiagonal part $g_{kk'}$ (the integrated equation of the latter is then inserted into the former). Until here, both approaches are equivalent. The difference comes with the Markov approximation. Culcer and Winkler use $f(t') \to f(t)$ as opposed to $f^{\rm I}(t') \to f^{\rm I}(t)$. With $\rho(t') \to \rho(t)$ we find that the evolution operators cancel each other in a different way, so that finally they sit around the entire inner commutator rather than only around the inner V,

$$\mathcal{J}[\rho] \quad = \quad -\int \frac{{\rm d}\omega}{2\pi}\, [V\,,\, G^{0\rm R}[V,\rho]\, G^{0\rm A}]\,. \tag{5.32}$$

This is indeed the result in Eq. (4b) in Culcer and Winkler [2007b]. We will see that the difference between (5.25) and (5.32) matters for the leading quantum correction in the Boltzmann conductivity of graphene. We will also understand why it does not matter for the treatment of Culcer and Winkler [2007b]. There the recursive analysis is taken to order $(\ell k_{\mathrm{F}})^0$ and therefore requires only the part that is insensitive to the differences between (5.25) and (5.32).

5.5.2. Nonequilibrium statistical operator approach

Using the results of Chapter 2.2, in particular the expression for the collision integral (2.55), one finds for the generic Hamiltonian (1.5) and impurity scattering that the first-order collision term vanishes. The second-order term becomes [with $\mathcal{U}_0$ shorthand for $\mathcal{U}_0(t,t')$]

$$\begin{aligned}\mathcal{J}_m^{(2)}(t)[\rho] &= -\int_{-\infty}^{t} \mathrm{d}t'\, e^{\eta(t'-t)} \mathrm{Tr}\left(\rho_{\mathrm{rel}}(t)\left[\mathcal{U}_0 V \mathcal{U}_0^{\dagger}, [V, P_m]\right]\right) \\ &= -\int \frac{\mathrm{d}\omega}{2\pi}\left[G^{0\mathrm{R}} V G^{0\mathrm{A}}, [V,\rho]\right]. \end{aligned} \tag{5.33}$$

Notice that this is different from both (5.25) and (5.32). We will see that when the collision integral for graphene is written out explicitly in spin components the results (5.25) and (5.33) coalesce.

5.5.3. Green's function approach

In the Green's function approach one starts with general dynamic equations for the two-time correlator $G^{<}(t_1,t_2)$. Solving such equations is generally difficult and therefore some approximation that limits the equations to the the time diagonal $t_2 = t_1$ is desirable. This is also necessary if one wants to derive a Boltzmann type equation for $\rho(t_1) = G^{<}(t_1,t_1)$. We start with the discussion of the ansatz that incorporates such an approximation and then turn to the derivation of semiclassical kinetic equations from the Kadanoff-Baym equations. However, we will see that even for a given ansatz one can derive different collision integrals.

The problem of ansatz

The first proposed ansatz was the Kadanoff-Baym (KB) ansatz [Kadanoff and Baym, 1962]

$$G^{<}(x,p,t,\omega) = \rho(x,p,t) A(x,p,t,\omega) \tag{5.34}$$

with $A = i(G^{\mathrm{R}} - G^{\mathrm{A}})$ being the nonequilibrium spectral function. This is a slight nonequilibrium modification of the equilibrium result $G^{<}(k,\omega) = f_{\mathrm{FD}}(\omega) A(k,\omega)$ (the fluctuation-dissipation theorem) and therefore it is expected to be a good approximation close to equilibrium. For weak interactions one uses the quasiparticle approximation $A \approx 2\pi(\epsilon_k - \omega)$.

For nonequilibrium beyond linear response the KB ansatz fails. This was noted by Jauho and Wilkins [1982; 1983; 1984] in Boltzmann equation treatments of transport in strong electric fields, where their results differed from those derived with density-matrix

methods [Levinson, 1970]. A similar discrepancy was observed in the linear conductivity when comparing with Kubo formula calculations by Holstein [1964]. Later, Lipavsky *et al.* [1986] showed that the discrepancy could be cured with the modified ansatz and coined the generalized Kadanoff-Baym ansatz (GKBA) (see also Haug and Jauho [2008]; Lipavský *et al.* [2001])

$$\begin{aligned} G^<(\boldsymbol{x}_1,t_1,\boldsymbol{x}_2,t_2) &= i\int \mathrm{d}^2x_3 \left(G^\mathrm{R}(\boldsymbol{x}_1,t_1,\boldsymbol{x}_3,t_2)G^<(\boldsymbol{x}_3,t_2,\boldsymbol{x}_2,t_2)\right. \\ &\qquad \left. -G^<(\boldsymbol{x}_1,t_1,\boldsymbol{x}_3,t_1)G^\mathrm{A}(\boldsymbol{x_3},t_1,\boldsymbol{x}_2,t_2)\right) \\ &= iG^\mathrm{R}(t_1,t_2)\rho(t_2) - i\rho(t_1)G^\mathrm{A}(t_1,t_2)) \end{aligned} \tag{5.35}$$

(spatial variables suppressed in the second line) which reduces to the KB ansatz in equilibrium. Lipavsky *et al.* [1986] showed that the right-hand side is the first term in an exact expansion, which makes it possible to address the range of validity of the ansatz. The exact expression respects the causal structure of the Kadanoff-Baym or Keldysh equations and also fulfills some other natural criteria (see Appendix C).

The GKB ansatz is the most common alternative in applications where the KB ansatz is considered insufficient. Interestingly, however, in general it does not yield the same Boltzmann equation as the one derived with the mentioned density matrix approaches (Liouville equation approaches). For the first quantum correction of graphene the difference matters.

However, we do find an ansatz for which the kinetic equation obtained with a density matrix approach is also obtained from a Green's function approach, namely if the GKBA is replaced by the anti-ordered version (AA for "anti-ordered ansatz")

$$\begin{aligned} G^<(t_1,t_2) &= iG^<(t_1,t_1)G^\mathrm{R}(t_1,t_2) - iG^\mathrm{A}(t_1,t_2)G^<(t_2,t_2) \\ &= i\rho(t_1)G^\mathrm{R}(t_1,t_2) - iG^\mathrm{A}(t_1,t_2)\rho(t_2)\,. \end{aligned} \tag{5.36}$$

Although this ansatz violates the intuitive (with respect to causality) retarded-lesser-advanced structure of KB equations and the Langreth-Wilkins rules [Langreth and Wilkins, 1972], it can be derived in a similar way as the GKBA (see Appendix C). The full result (including the omitted expansion terms) fulfills most of the criteria required by Lipavsky *et al.* [1986], in particular the causality requirement. The average of GKBA and the AA represents a third alternative, which we call here the symmetrized Kadanoff-Baym ansatz (SKBA),

$$G^<(t_1,t_2) = \frac{1}{2}\left(\rho(t_1)A(t_1,t_2) + A(t_1,t_2)\rho(t_2)\right)\,. \tag{5.37}$$

This ansatz to zeroth order in gradient expansion appears, for instance, in Raimondi *et al.* [2006].

Considering the importance that the issue of ansatz has for spinless electrons in nonequilibrium beyond linear response, we believe that the issue should be even more important for graphene calculations beyond linear response, at least when electron-hole coherent effects have to be taken into account.

The problem of identifying the collision integral

The generalized Kadanoff-Baym equation [Kadanoff and Baym, 1962; Langreth and Wilkins, 1972] in integral form reads (Eq. (2.63))

$$G^< = G^{\mathrm{R}}\Sigma^< G^{\mathrm{A}} + (1 + G^{\mathrm{R}}\Sigma^{\mathrm{R}})G^{0<}(1 + \Sigma^{\mathrm{A}}G^{\mathrm{A}})\,, \tag{5.38}$$

where all products are to be interpreted as convolution products in real space/time and in spin variables. The retarded and advanced components are determined by the Dyson equations $((G^0)^{-1} - \Sigma^{\mathrm{R}})G^{\mathrm{R}} = 1$ and $((G^0)^{-1} - \Sigma^{\mathrm{A}})G^{\mathrm{A}} = 1$. The self-energies are to first order Born approximation given by

$$\begin{aligned} \Sigma^< &= n_{\mathrm{imp}} V G^< V, \\ \Sigma^{\mathrm{R,A}} &= n_{\mathrm{imp}}(V + VG^{0\mathrm{R,A}}V) \to n_{\mathrm{imp}} V G^{0\mathrm{R,A}} V, \end{aligned} \tag{5.39}$$

where we will neglect the mean field terms $\sim V^1$, since here we are not interested in shifts of the total energy.

The term containing $G^{0<}$ in (2.63) plays the role of boundary conditions and vanishes when acting with $(G^{\mathrm{R}})^{-1}$ from the left or $(G^{\mathrm{A}})^{-1}$ from the right,

$$\begin{aligned} (G^{\mathrm{R}})^{-1}G^< &= \Sigma^< G^{\mathrm{A}}, \\ G^<(G^{\mathrm{A}})^{-1} &= G^{\mathrm{R}}\Sigma^<. \end{aligned} \tag{5.40}$$

In particular, the difference of these equations gives the Kadanoff-Baym equation in differential form, which is a double-time precursor of the time-diagonal kinetic equations to be derived. For our discussion we write it in two different ways. The first equation, to be called G1, reads

$$[i\partial_t - H, G^<] \;=\; \Sigma^{\mathrm{R}}G^< - G^<\Sigma^{\mathrm{A}} + \Sigma^< G^{\mathrm{A}} - G^{\mathrm{R}}\Sigma^<\,. \tag{5.41}$$

It identifies all self-energy terms of order V^2 with the collision integral. This is what we think should be done for a comparison with the Liouville equation based approaches of the previous sections, where all terms of order V^2 were identified with the collision integral. The second equation, to be called G2, is given by

$$[i\partial_t - H - \mathrm{Re}\,\Sigma^{\mathrm{R}}, G^<] - [\Sigma^<, \mathrm{Re}\,G^{\mathrm{R}}] \;=\; i\{\mathrm{Im}\,\Sigma^{\mathrm{R}}, G^<\} - i\{\Sigma^<, \mathrm{Im}\,G^{\mathrm{R}}\}\,. \tag{5.42}$$

It is a frequently encountered starting point of Boltzmann equation approaches that consider renormalizations and other quantum corrections [Langreth and Wilkins, 1972; Mahan, 1990; Lipavský *et al.*, 2001; Haug and Jauho, 2008]. Of the self-energy terms, only those on the right-hand side are considered as the collision integral, those on the left-hand side, in contrast, are regarded as terms renormalizing the free drift. (The term $\mathrm{Re}\,\Sigma^{\mathrm{R}}$ shifts for example the zero of energy. Thereby it shifts the minimum conductivity away from zero gate voltage. In this context, see the experiments by Tan *et al.* [2007] and Chen *et al.* [2008].) For spinless electrons the commutators on the left-hand side vanish if one stops at zeroth order in gradient expansion. In this case one obtains the same collision integral to zeroth order in gradient expansion as with (5.41). In general, and in particular

in the case of spin, the self-energy terms on the left-hand side contribute even to zeroth order. Here, we are mainly interested in the alternative structures that might be obtained for a collision integral from the right-hand side in (5.42).

Both equations (5.41) and (5.42) also hold for $G^{>}$. Within the Keldysh formalism analogous equations are derived for $G^{\mathrm{K}} = i(G^{<} - G^{>})$.

Notice that the *quantum Boltzmann equation* [Mahan, 1990], obtained by gradient expanding Eq. (5.42) to first order, is a semiclassical kinetic equation in the variables $(\boldsymbol{x}, \boldsymbol{p}, t, \omega)$. Integrating the resulting equation over the frequency ω gives a Boltzmann equation.[4] In this sense, here, we solve Boltzmann equations—not quantum Boltzmann equations.

Different collision integrals

With two different ways of writing the Kadanoff-Baym equation and three different kinds of ansatz there are possibly six new collision integrals. One obvious question is, as to which of them corresponds to the collision integrals of the previous section. The second and *independent* question is: which one is appropriate for the problem of quantum corrections to the conductivity in graphene?

We believe we are able to present an answer to the first question. It seems clear that the pertinent collision integral is derived from G1, *i.e.* Eq. (5.41). The question remains as to which ansatz to choose. Interestingly, it is not the GKB ansatz, but the AA that returns the collision integral (5.25). The GKBA would give

$$\begin{aligned} \Sigma^{\mathrm{R}}G^{<} - G^{<}\Sigma^{\mathrm{A}} + \Sigma^{<}G^{\mathrm{A}} - G^{\mathrm{R}}\Sigma^{<} &= -iVG^{0\mathrm{R}}V\rho G^{0\mathrm{A}} - iG^{0\mathrm{R}}\rho VG^{0\mathrm{A}}V \\ &\quad + iVG^{0\mathrm{R}}\rho VG^{0\mathrm{A}} + iG^{0\mathrm{R}}V\rho G^{0\mathrm{A}}V + \dots \\ &= -i[V, G^{0\mathrm{R}}[V,\rho]G^{0\mathrm{A}}] + \dots \end{aligned} \tag{5.43}$$

where, in each term like $\Sigma^{\mathrm{R}}G^{<} = VG^{0\mathrm{R}}VG^{0\mathrm{R}}\rho - VG^{0\mathrm{R}}V\rho G^{0\mathrm{A}}$, we neglected the parts that contain two retarded or two advanced Green's functions since such terms vanish when one integrates over the frequency to obtain the collision integral,

$$\mathcal{J} \;=\; -\int \frac{\mathrm{d}\omega}{2\pi}[V, G^{0\mathrm{R}}[V,\rho]G^{0\mathrm{A}}]\,. \tag{5.44}$$

We call this collision integral G1wGKBA ("w" for with). It is clearly different from (5.25). Interestingly it coincides with (5.32).

For the collision integrals G2 derived from (5.42) note, for example, that with the GKBA we obtain

$$\frac{1}{2}\{\Sigma^{\mathrm{R}} - \Sigma^{\mathrm{A}}, G^{<}\} - \frac{1}{2}\{\Sigma^{<}, G^{\mathrm{R}} - G^{\mathrm{A}}\} \;=\; -\frac{1}{2}[V, G^{0\mathrm{R}}[V,\rho]G^{0\mathrm{A}}] - \frac{1}{2}[V, [G^{0\mathrm{A}}VG^{0\mathrm{R}}, \rho]]\,. \tag{5.45}$$

[4] One can also integrate over the absolute value of the momentum to obtain a Boltzmann equation in terms of the variables $(\boldsymbol{x}, \hat{\boldsymbol{p}}, t, \omega)$. This is called the quasiclassical approach, which is used for example in Shytov *et al.* [2006] and Raimondi *et al.* [2006]. (Sometimes it is called the *first* quasiclassical approach and the semiclassical approach is instead called the quasiclassical approach [Lipavský *et al.*, 2001].)

Table 5.1.: Integrands of the collision integral $\mathcal{J}[\rho] = -\int \frac{\mathrm{d}\omega}{2\pi}(\ldots)$ as derived with various approaches in Section 5.5.

	G1	GKBA	$[V, G^{0\mathrm{R}}\,[V,\rho]\,G^{0\mathrm{A}}]$
LvN &	G1	AA	$[V, [G^{0\mathrm{R}}\,V\,G^{0\mathrm{A}}, \rho]]$
	G1	SKBA	$\frac{1}{2}\,[V, G^{0\mathrm{R}}\,[V,\rho]\,G^{0\mathrm{A}}] + \frac{1}{2}\,[V, [G^{0\mathrm{R}}\,V\,G^{0\mathrm{A}}, \rho]]$
	G2	GKBA	$\frac{1}{2}\,[V, G^{0\mathrm{R}}\,[V,\rho]\,G^{0\mathrm{A}}] + \frac{1}{2}\,[V, [G^{0\mathrm{A}}\,V\,G^{0\mathrm{R}}, \rho]]$
	G2	AA	$\frac{1}{2}\,[V, G^{0\mathrm{A}}\,[V,\rho]\,G^{0\mathrm{R}}] + \frac{1}{2}\,[V, [G^{0\mathrm{R}}\,V\,G^{0\mathrm{A}}, \rho]]$
	G2	SKBA	$\frac{1}{2}\,(\mathrm{G2wGKBA} + \mathrm{G2wAA})$
NSO			$[G^{0\mathrm{R}}\,V\,G^{0\mathrm{A}}, [V,\rho]]$

We denote this collision integral G2wGKBA. It takes the form of an average of (5.44) and (5.25), in the latter, however, with the retarded and advanced Green's functions swapped. The other possible collision integrals will be presented in the next section.

5.6. Comparison of collision integrals

We summarize the different possible general collision integrals discussed in previous section. When writing $\mathcal{J}[\rho] = -\int \frac{\mathrm{d}\omega}{2\pi}(\ldots)$ the integrands $(\ldots)$ of the various candidates are given in Table 5.1.

We do not need to solve the Boltzmann equation seven times. The first two cases are sufficient to deduce the other ones except for the NSO case, which, however, will turn out to coincide with the G1wAA/LvN calculation. For example, the second term of G2wGKBA is similar to the G1wAA result with retarded and advanced Green's functions swapped. A closer inspection reveals that this swapping has no effect on the part of the collision integral that contains a delta function in energy, but changes the sign of the principal value part. Therefore, the delta function part of G2wGKBA is given by the delta function part of (G1wGKBA +G1wAA)/2, whereas the principal value part is given by the principal value part of (G1wGKBA -G1wAA)/2. One can decompose the principal value part of G1wGKBA in two parts X and Y, where X is the part that is invariant when one compares G1wAA with G1wGKBA, whereas Y is the part that changes sign. Then one can construct the principal value parts $\mathcal{J}^{\mathrm{P}} = \pm\mathcal{J}^{\mathrm{P}X} \pm \mathcal{J}^{\mathrm{P}Y}$ for all the above collision integrals, with the relative signs of $\mathcal{J}^{\mathrm{P}X}$ and $\mathcal{J}^{\mathrm{P}Y}$, respectively, determined by the scheme

		X	Y
G1	GKBA	+	+
G1	AA	+	−
G1	SKBA	+	0
G2	GKBA	0	+
G2	AA	0	−
G2	SKBA	0	0

(5.46)

Note that for the collision integral G2wSKBA the principal value terms vanish completely.

The products in (5.1) are still general convolutions. In the next step the spin structure is left intact, but the space and time variables are Wigner transformed, and then the products are gradient expanded in these variables. We assume that gradient corrections in the interaction terms can be neglected. We also replace the Wigner transformed density matrix ρ with the quasiparticle distribution f. These are two common approximations which might be incorrect when calculating quantum corrections, but give the framework within which we want to make a first step and compare with previous work. Furthermore, we assume non-magnetic impurities, $u^{\sigma\sigma'}_{\boldsymbol{k}\boldsymbol{k}'} = \delta_{\sigma\sigma'}\, u_{\boldsymbol{k}\boldsymbol{k}'}$ with $W_{\boldsymbol{k}\boldsymbol{k}'} := 2\,\pi\, n_{\mathrm{imp}}\, |u_{\boldsymbol{k}\boldsymbol{k}'}|^2$. After impurity averaging the collision integrals become

$$\begin{array}{lrcl}
\text{G1wGKBA} & \mathcal{J}[f] & = & -\int_{\boldsymbol{k}'} W_{\boldsymbol{k}\boldsymbol{k}'} \int \frac{\mathrm{d}\omega}{(2\pi)^2}\, (G^{0\mathrm{R}}_{\boldsymbol{k}}\, \Delta f\, G^{0\mathrm{A}}_{\boldsymbol{k}'} + G^{0\mathrm{R}}_{\boldsymbol{k}'}\, \Delta f\, G^{0\mathrm{A}}_{\boldsymbol{k}}), \\
\text{LvN} & \mathcal{J}[f] & = & -\int_{\boldsymbol{k}'} W_{\boldsymbol{k}\boldsymbol{k}'} \int \frac{\mathrm{d}\omega}{(2\pi)^2}\, (f_{\boldsymbol{k}}\, G^{0\mathrm{R}}_{\boldsymbol{k}}\, G^{0\mathrm{A}}_{\boldsymbol{k}'} - f_{\boldsymbol{k}'}\, G^{0\mathrm{R}}_{\boldsymbol{k}'}\, G^{0\mathrm{A}}_{\boldsymbol{k}} + \text{h.c.}), \\
\text{NSO} & \mathcal{J}[f] & = & -\int_{\boldsymbol{k}'} W_{\boldsymbol{k}\boldsymbol{k}'} \int \frac{\mathrm{d}\omega}{(2\pi)^2}\, (\Delta f\, G^{0\mathrm{R}}_{\boldsymbol{k}'}\, G^{0\mathrm{A}}_{\boldsymbol{k}} + G^{0\mathrm{R}}_{\boldsymbol{k}}\, G^{0\mathrm{A}}_{\boldsymbol{k}'}\, \Delta f),
\end{array} \tag{5.47}$$

to second order in the interaction and to zeroth order in gradient expansion. We have introduced the shorthand notation $\int \frac{\mathrm{d}^2k'}{(2\pi)^2} =: \int_{\boldsymbol{k}'}$ and $\Delta f := f(\boldsymbol{k},\boldsymbol{x},t) - f(\boldsymbol{k}',\boldsymbol{x},t)$. The retarded Green's function is the non-interacting one taken to lowest order in gradient expansion. For the spin-orbit coupled case, it is of the form

$$G^{0\mathrm{R}}_{\boldsymbol{k}} \;=\; \sum_{s=\pm} \frac{S_{\hat{\boldsymbol{b}}s}}{\tilde{\omega}^+ - \epsilon^s_{\boldsymbol{k}}} \tag{5.48}$$

with the spin projector (5.23) and $\tilde{\omega}^+ = \tilde{\omega} + i\,0^+$, $\tilde{\omega} = \omega - \phi$ being the gauge invariant frequency variable. In the Wigner representation one has $X^{\mathrm{A}} = (X^{\mathrm{R}})^\dagger$.

The three collision integrals in (5.47) would obviously be equivalent if $G^{0\mathrm{R}}$, $G^{0\mathrm{A}}$ and f commuted with each other, as it is the case for spinless electrons. In the general, non-commuting case including in particular the case of spin-orbit coupling, the collision integrals appear to be different. However, the different forms of collision integrals do not necessarily imply differing results for physical quantities. We shall see below that to lowest order in $(\ell\, k_{\mathrm{F}})^{-1}$ one readily reproduces the Drude conductivity obtained with Fermi's Golden rule with all candidate collision integrals. To higher orders in quantum corrections, however, an agreement is not at all obvious.

Notice that the collision integral for non-magnetic impurities should generally satisfy the property $\int_{\boldsymbol{k}} \mathcal{J}[f(\boldsymbol{k},\boldsymbol{x},t)] = 0$, expressing that in real space the collisions cannot act as a source or drain of particles of a given spin state. For all collision integrals except the NSO integral this is manifest, since the collision integrals change sign under the renaming of dummy variables $\boldsymbol{k} \leftrightarrow \boldsymbol{k}'$. In the case of the NSO result this is not manifest at this level, but the explicit collision integral derived for graphene will turn out to have this property.

For further comparison and to prepare a solution of the Boltzmann equation we write the collision integrals (5.47) explicitly in terms of the components f_0 and $\boldsymbol{f}$. To streamline the lengthy expressions further shorthand notation is introduced: x' means that the quantity x depends on primed variables such as $\boldsymbol{k}'$, s' *etc.*, whereas x correspondingly depends on $\boldsymbol{k}$, s. For example $S' = \frac{1}{2}(\mathbf{1} + \boldsymbol{\sigma}\cdot s'\, \hat{\boldsymbol{b}}_{\boldsymbol{k}'})$. Furthermore, $\Delta x := x - x'$, for example $\Delta\epsilon = \epsilon^s_{\boldsymbol{k}} - \epsilon^{s'}_{\boldsymbol{k}'}$ and $\Delta(s\,b) = s\,b - s'\,b'$.

Insertion of (5.48) in (5.47) yields a collision integral $\mathcal{J} = \mathcal{J}^{\delta} + \mathcal{J}^{\mathrm{P}}$ consisting of delta function terms and of principal value terms. The principal value terms $\mathcal{J}^{\mathrm{P}}$ are given by

$$\begin{array}{lrcl} \text{G1wGKBA} & \mathcal{J}^{\mathrm{P}}[f] & = & -\int_{\boldsymbol{k}'} W_{\boldsymbol{k}\boldsymbol{k}'} \frac{1}{2\pi} \sum_{ss'} \mathcal{P}\left(\frac{1}{\Delta\epsilon}\right) \\ & & & \quad \times \left[\frac{ss'\hat{\boldsymbol{b}}\times\hat{\boldsymbol{b}}'}{2} \cdot (-\Delta\boldsymbol{f} + \boldsymbol{\sigma}\Delta f_0) + \boldsymbol{\sigma} \cdot \frac{\Delta(s\hat{\boldsymbol{b}})}{2} \times \Delta\boldsymbol{f}\right], \\ \text{LvN \& NSO} & \mathcal{J}^{\mathrm{P}}[f] & = & -\int_{\boldsymbol{k}'} W_{\boldsymbol{k}\boldsymbol{k}'} \frac{1}{2\pi} \sum_{ss'} \mathcal{P}\left(\frac{1}{\Delta\epsilon}\right) \\ & & & \quad \times \left[\frac{ss'\hat{\boldsymbol{b}}\times\hat{\boldsymbol{b}}'}{2} \cdot (+\Delta\boldsymbol{f} + \boldsymbol{\sigma}\Delta f_0) - \boldsymbol{\sigma} \cdot \frac{s\hat{\boldsymbol{b}}+s'\hat{\boldsymbol{b}}'}{2} \times (\boldsymbol{f} + \boldsymbol{f}')\right]. \end{array} \tag{5.49}$$

The delta function terms are

$$\begin{aligned} \mathcal{J}_0^{\delta}[f] &= -\int_{\boldsymbol{k}'} W_{\boldsymbol{k}\boldsymbol{k}'} \frac{1}{2} \sum_{ss'} \delta(\Delta\epsilon) \left[\frac{1 + ss'\hat{\boldsymbol{b}}\cdot\hat{\boldsymbol{b}}'}{2}\Delta f_0 + \frac{s\hat{\boldsymbol{b}} + s'\hat{\boldsymbol{b}}'}{2} \cdot \Delta\boldsymbol{f}\right], \\ \boldsymbol{\mathcal{J}}^{\delta}[f] &= -\int_{\boldsymbol{k}'} W_{\boldsymbol{k}\boldsymbol{k}'} \frac{1}{2} \sum_{ss'} \delta(\Delta\epsilon) \left[\Delta\left(\frac{1 + ss'\mathrm{B}}{2}\boldsymbol{f}\right) + \frac{s\hat{\boldsymbol{b}} + s'\hat{\boldsymbol{b}}'}{2}\Delta f_0\right], \end{aligned} \tag{5.50}$$

with the matrix $\mathrm{B}(\hat{\boldsymbol{k}}, \hat{\boldsymbol{k}}')$ acting on $\boldsymbol{f}$ given by

$$\begin{array}{llcllcl} \text{G1wGKBA} & \mathrm{B} & := & +\hat{\boldsymbol{b}}\,(\hat{\boldsymbol{b}}')^{\mathrm{T}} + \hat{\boldsymbol{b}}'\,(\hat{\boldsymbol{b}})^{\mathrm{T}} - \hat{\boldsymbol{b}}\cdot\hat{\boldsymbol{b}}' & , & \mathrm{B}' & := & \mathrm{B} \\ \text{LvN} & \mathrm{B} & := & -\hat{\boldsymbol{b}}\,(\hat{\boldsymbol{b}}')^{\mathrm{T}} + \hat{\boldsymbol{b}}'\,(\hat{\boldsymbol{b}})^{\mathrm{T}} + \hat{\boldsymbol{b}}\cdot\hat{\boldsymbol{b}}' & , & \mathrm{B}' & := & \mathrm{B}^{\mathrm{T}} \\ \text{NSO} & \mathrm{B} & := & +\hat{\boldsymbol{b}}\,(\hat{\boldsymbol{b}}')^{\mathrm{T}} - \hat{\boldsymbol{b}}'\,(\hat{\boldsymbol{b}})^{\mathrm{T}} + \hat{\boldsymbol{b}}\cdot\hat{\boldsymbol{b}}' & , & \mathrm{B}' & := & \mathrm{B} \\ \text{rest} & \mathrm{B} & := & \hat{\boldsymbol{b}}'\,(\hat{\boldsymbol{b}})^{\mathrm{T}} & , & \mathrm{B}' & := & \mathrm{B}^{\mathrm{T}}. \end{array} \tag{5.51}$$

The "rest" stands for the G1wSKBA and all G2 collision integrals. As stated previously, their delta function parts are just the sum of G1wGKBA and G1wAA/LvN. Taking into account the momentum dependence of the basis vectors

$$\begin{aligned} \hat{\boldsymbol{b}}' &= \hat{\boldsymbol{b}}\cos N\Delta\theta - \hat{\boldsymbol{c}}\sin N\Delta\theta, \\ \hat{\boldsymbol{c}}' &= \hat{\boldsymbol{c}}\cos N\Delta\theta + \hat{\boldsymbol{b}}\sin N\Delta\theta, \end{aligned} \tag{5.52}$$

one derives

G1wGKBA	LvN	NSO	rest
$\mathrm{B}\,\hat{\boldsymbol{b}} = \hat{\boldsymbol{b}}'$	$\mathrm{B}\,\hat{\boldsymbol{b}} = \hat{\boldsymbol{b}}'$	$\mathrm{B}\,\hat{\boldsymbol{b}} = \hat{\boldsymbol{b}}\cos N\Delta\theta + \hat{\boldsymbol{c}}\sin N\Delta\theta$	$\mathrm{B}\,\hat{\boldsymbol{b}} = \hat{\boldsymbol{b}}'$
$\mathrm{B}'\,\hat{\boldsymbol{b}}' = \hat{\boldsymbol{b}}$	$\mathrm{B}'\,\hat{\boldsymbol{b}}' = \hat{\boldsymbol{b}}$	$\mathrm{B}'\,\hat{\boldsymbol{b}}' = \hat{\boldsymbol{b}}$	$\mathrm{B}'\,\hat{\boldsymbol{b}}' = \hat{\boldsymbol{b}}$
$\mathrm{B}\,\hat{\boldsymbol{c}} = -\hat{\boldsymbol{c}}'$	$\mathrm{B}\,\hat{\boldsymbol{c}} = \hat{\boldsymbol{c}}'$	$\mathrm{B}\,\hat{\boldsymbol{c}} = \hat{\boldsymbol{c}}\cos N\Delta\theta - \hat{\boldsymbol{b}}\sin N\Delta\theta$	$\mathrm{B}\,\hat{\boldsymbol{c}} = 0$
$\mathrm{B}'\,\hat{\boldsymbol{c}}' = -\hat{\boldsymbol{c}}$	$\mathrm{B}'\,\hat{\boldsymbol{c}}' = \hat{\boldsymbol{c}}$	$\mathrm{B}'\,\hat{\boldsymbol{c}}' = -\hat{\boldsymbol{c}}$	$\mathrm{B}'\,\hat{\boldsymbol{c}}' = 0$

(5.53)

Note the particular simplicity of the approaches G1wSKBA and G2.

For studies where a spin coherent Boltzmann equation is linearized in a small b ($b_{\mathrm{F}} \ll \epsilon_{\mathrm{F}}$) the terms $ss'\mathrm{B}$ are absent. Furthermore, it should be safe to neglect the principal value terms if one is only interested in the response without quantum corrections. In that case, the delta function part of the collision integral is the same in all formalisms [Kailasvuori, 2009]. For graphene ($\epsilon_{\mathrm{F}} = b_{\mathrm{F}}$) we need the full collision integral to calculate the quantum

corrections, and therefore the approaches differ. However, crucial simplifications occur due to $\epsilon_0 = 0$. With $\Delta\epsilon = s\,b - s'b'$ we obtain (henceforth we write $\mathcal{P}\,(1/x)$ as $1/x$)

$$\begin{array}{lcll}
\sum_{ss'} \delta(\Delta\epsilon) & = & 2(\delta(\Delta b) + \delta(b+b'))\,, & \\
\sum_{ss'} s\delta(\Delta\epsilon) = \sum_{ss'} s'\delta(\Delta\epsilon) & = & 0\,, & \\
\sum_{ss'} ss'\delta(\Delta\epsilon) & = & 2(\delta(\Delta b) - \delta(b+b'))\,, & \\
\sum_{ss'} \frac{1}{\Delta\epsilon} = \sum_{ss'} ss'\frac{1}{\Delta\epsilon} & = & 0\,, & \\
\sum_{ss'} s\frac{1}{\Delta\epsilon} & = & 2(\frac{1}{\Delta b} + \frac{1}{b+b'}) & \equiv\ 2\,\mathcal{P}_+\,, \\
\sum_{ss'} s'\frac{1}{\Delta\epsilon} & = & 2(\frac{1}{\Delta b} - \frac{1}{b+b'}) & \equiv\ -2\,\mathcal{P}_-\,,
\end{array} \tag{5.54}$$

and therefore half of the terms in (5.50) vanish, leaving us with

$$\begin{array}{lcll}
\mathcal{J}^{\delta}[f] & = & -\int_{\boldsymbol{k'}} W_{\boldsymbol{kk'}} & [\,\delta(\Delta b)\left(\cos^2\frac{\Delta\theta}{2}\Delta f_0 + \boldsymbol{\sigma}\cdot\Delta(\frac{1+B}{2}\boldsymbol{f})\right) + \\
 & & & \quad + \delta(b+b')\left(\sin^2\frac{\Delta\theta}{2}\Delta f_0 + \boldsymbol{\sigma}\cdot\Delta(\frac{1-B}{2}\boldsymbol{f})\right)]\,, \\
\mathcal{J}^{PX}[f] & = & -\int_{\boldsymbol{k'}} W_{\boldsymbol{kk'}} & \boldsymbol{\sigma}\cdot\frac{1}{2\pi}\left[\mathcal{P}_-\,\hat{\boldsymbol{b}}'\times\boldsymbol{f} - \mathcal{P}_+\,\hat{\boldsymbol{b}}\times\boldsymbol{f'}\right], \\
\mathcal{J}^{PY}[f] & = & -\int_{\boldsymbol{k'}} W_{\boldsymbol{kk'}} & \boldsymbol{\sigma}\cdot\frac{1}{2\pi}\left[\mathcal{P}_+\,\hat{\boldsymbol{b}}\times\boldsymbol{f} - \mathcal{P}_-\,\hat{\boldsymbol{b}}'\times\boldsymbol{f'}\right].
\end{array} \tag{5.55}$$

The term containing $\delta(b+b')$ gives only a contribution from the point $k = -k'$, *i.e.*, $k = k' = 0$, which we will neglect, since at temperature zero k will be fixed to $k_F \neq 0$. Thus, the delta function part we consider is

$$\boldsymbol{\mathcal{J}}^{\delta}[\boldsymbol{f}] \;=\; -\int_{\boldsymbol{k'}} W_{\boldsymbol{kk'}}\,\delta(\Delta b)\,\frac{1}{2}\left(\boldsymbol{f} - \boldsymbol{f'} + \mathrm{B}\,\boldsymbol{f} - \mathrm{B}'\,\boldsymbol{f'}\right)\,. \tag{5.56}$$

For the approach G1wGKBA and for all G2 approaches we then obtain, due to Eq. (5.53),

$$\boldsymbol{\mathcal{J}}^{\delta}[\boldsymbol{f}] \;=\; -\int_{\boldsymbol{k'}} W_{\boldsymbol{kk'}}\,\delta(\Delta b)\,\Delta\left(\frac{1+\mathrm{B}}{2}\,\hat{\boldsymbol{b}}\,f_{\hat{\boldsymbol{b}}}\right) - \int_{\boldsymbol{k'}} W_{\boldsymbol{kk'}}\,\delta(\Delta b)\,\frac{1}{2}\Delta\left(\hat{\boldsymbol{c}}\,f_{\hat{\boldsymbol{c}}} + \hat{\boldsymbol{z}}\,f_z\right). \tag{5.57}$$

In next section we will see that the matrix $(1 + B)/2$ is responsible for the additional chirality-induced spin-overlap factor $\cos^2(N\Delta\theta/2)$ occuring in the intraband transition rates that involve only the probability densities $(\langle\hat{\boldsymbol{b}}\pm|\,f\,|\hat{\boldsymbol{b}}\pm\rangle = f_0 \pm f_{\hat{\boldsymbol{b}}}$ of energy eigenstates. This is how the suppression of backscattering in monolayer graphene enters the Drude conductivity derived with Fermi's Golden rule. The "transition amplitudes" involving the off-diagonal components $\langle\hat{\boldsymbol{b}}\pm|\,f\,|\hat{\boldsymbol{b}}\mp\rangle = f_z \pm i f_{\hat{\boldsymbol{c}}}$ (the Zitterbewegung components) are more elusive and beyond the reach of Fermi's Golden rule. However, for the G1wGKBA and all G2 approaches the result (5.57) shows that the scattering of the off-diagonal components becomes very simple since it contains no angle dependent chirality factors but only a factor $\frac{1}{2}$ compared to ordinary spin independent scattering.

5.7. Conductivity with principal value terms neglected

In this section we calculate the electrical conductivity of graphene for non-magnetic impurities with the collision integrals $\mathcal{J}^{\delta}$ from the previous section. We neglect the principal value part $\mathcal{J}^{\mathrm{P}}$. We assume low temperature so that $|\mu| = \epsilon_{\mathrm{F}}$. For notational compactness we henceforth neglect the elementary charge e and restore it only in final results.

For the purpose of later comparison we first derive the Drude conductivity per valley by considering only one band (electrons $\mu > 0$ or holes $\mu < 0$), in which case Fermi's Golden rule can be applied. Let us consider electrons. For monolayer graphene the one-band Boltzmann equation linearized in the electric field ($f = f^{\rm eq} + f^{(E)}$ with $f^{\rm eq} = f_{\rm FD}\,(v_{\rm F}\,k - \mu)$ for electrons) reads

$$\begin{aligned} \boldsymbol{E}\cdot\partial_{\boldsymbol{k}} f^{\rm eq} &= -\int_{\boldsymbol{k'}} \delta(v_{\rm F}\,\Delta k)\,W_{\boldsymbol{k}\boldsymbol{k'}}\,\cos^2\frac{\Delta\theta}{2}\,\Delta f^{(E)} \\ &= -f^{(E)}\underbrace{\int_{\boldsymbol{k'}} \delta(v_{\rm F}\,\Delta k)\,W_{\boldsymbol{k}\boldsymbol{k'}}\,\cos^2\frac{\Delta\theta}{2}\,(1-\cos\Delta\theta)}_{=:\,\tau_{\rm tr}^{-1}}, \end{aligned} \tag{5.58}$$

where the transition probability $W_{\boldsymbol{k}\boldsymbol{k'}}\cos^2\frac{\Delta\theta}{2}$ (as opposed to $W_{\boldsymbol{k}\boldsymbol{k'}}$ for ordinary electrons) takes into account the chirality of the Dirac electrons, responsible for the suppression of back-scattering. The real space current is given by

$$\boldsymbol{j} \;=\; \int_{\boldsymbol{k'}} \boldsymbol{v}\,f^{(E)} \;=\; -\int_\theta\int \frac{k\,{\rm d}k}{2\pi}\,v_{\rm F}\,\hat{\boldsymbol{k}}\,\tau_{\rm tr}\,E_{\hat{\boldsymbol{k}}}\partial_k f_{\rm FD}\,(v_{\rm F}\,k-\mu) \;=\; \boldsymbol{E}\,\sigma_0\,, \tag{5.59}$$

where (reintroducing e and $\hbar$ to the right)

$$\sigma_0 \;:=\; \frac{|\mu|\,\tau_{\rm trF}}{4\pi} \;=\; \frac{\ell\,k_{\rm F}}{4\pi} \;\to\; \frac{e^2}{2\,h}\,\ell\,k_{\rm F} \tag{5.60}$$

with $\tau_{\rm trF} := \tau_{\rm tr}(k_{\rm F})$, $k_{\rm F} = |\mu|/v_{\rm F}$ and the mean free path $\ell := v_{\rm F}\,\tau_{\rm trF}$. In (5.59) we used the shorthand notation $\int_\theta := \frac{1}{2\pi}\int d\theta$. The result (5.60) is written in such a way that it also includes the case of holes ($\mu < 0$). To get the total Drude conductivity of graphene we multiply by a factor of four for the degeneracy in valley index and real spin.

In the next step we turn to the coherent treatment of pseudo-spin, and we shall see that all approaches reproduce the result (5.60) to lowest order in $(\ell k_{\rm F})^{-1}$, but yield different quantum corrections. With

$$K(k,\theta,\theta') \;:=\; \int_0^\infty \frac{k'\,{\rm d}k'}{2\,\pi}\,W_{\boldsymbol{k}\boldsymbol{k'}}\,\delta(b-b')\,, \tag{5.61}$$

the compact notation $\boldsymbol{E}\cdot\partial_{\boldsymbol{k}} = E_{\hat{\boldsymbol{k}}}\,\partial_k + E_{\hat{\boldsymbol{\theta}}}\,\frac{1}{k}\,\partial_\theta$, the decomposition $f = f_0 + \boldsymbol{\sigma}\cdot(\hat{\boldsymbol{b}}\,f_{\hat{\boldsymbol{b}}} + \hat{\boldsymbol{c}}\,f_{\hat{\boldsymbol{c}}} + \hat{\boldsymbol{z}}\,f_z)$ with $\partial_\theta\hat{\boldsymbol{b}} = N\,\hat{\boldsymbol{c}}$ and $\partial_\theta\hat{\boldsymbol{c}} = -N\,\hat{\boldsymbol{b}}$, and using the table (5.53) we find for G1wGKBA

$$\begin{aligned} \boldsymbol{E}\cdot\partial_{\boldsymbol{k}} f_0 &= \mathcal{J}_0^\delta \;=\; -\int_{\theta'} K\cos^2\frac{N\Delta\theta}{2}\,\Delta f_0, \\ \boldsymbol{E}\cdot\partial_{\boldsymbol{k}} f_{\hat{\boldsymbol{b}}} - E_{\hat{\boldsymbol{\theta}}}\frac{N}{k} f_{\hat{\boldsymbol{c}}} &= \mathcal{J}_{\hat{\boldsymbol{b}}}^\delta \;=\; -\int_{\theta'} K\left(\cos^2\frac{N\Delta\theta}{2}\Delta f_{\hat{\boldsymbol{b}}} - \frac{1}{2}\sin N\Delta\theta\,(f_{\hat{\boldsymbol{c}}} + f_{\hat{\boldsymbol{c}}}{}')\right), \\ \boldsymbol{E}\cdot\partial_{\boldsymbol{k}} f_{\hat{\boldsymbol{c}}} + E_{\hat{\boldsymbol{\theta}}}\frac{N}{k} f_{\hat{\boldsymbol{b}}} + 2bf_z &= \mathcal{J}_{\hat{\boldsymbol{c}}}^\delta \;=\; -\int_{\theta'} K\left(\sin^2\frac{N\Delta\theta}{2}\,(f_{\hat{\boldsymbol{c}}} + f_{\hat{\boldsymbol{c}}}{}') - \frac{1}{2}\sin N\Delta\theta\,\Delta f_{\hat{\boldsymbol{b}}}\right), \\ \boldsymbol{E}\cdot\partial_{\boldsymbol{k}} f_z - 2bf_z &= \mathcal{J}_z^\delta \;=\; -\int_{\theta'} K\sin^2\frac{N\Delta\theta}{2}\,\Delta f_z\,. \end{aligned} \tag{5.62}$$

Table 5.2.: Integrands of the collision integrals $\mathcal{J}_0^\delta, \mathcal{J}_{\hat{\boldsymbol{b}}}^\delta, \mathcal{J}_{\hat{\boldsymbol{c}}}^\delta$ and $\mathcal{J}_z^\delta$ in Eq. (5.62) for the different formalisms.

	$\mathcal{J}_0^\delta$	$\mathcal{J}_{\hat{\boldsymbol{b}}}^\delta$	$\mathcal{J}_{\hat{\boldsymbol{c}}}^\delta$	$\mathcal{J}_z^\delta$
G1wG.	$\cos^2\frac{N\Delta\theta}{2}\Delta f_0$	$\cos^2\frac{N\Delta\theta}{2}\Delta f_{\hat{\boldsymbol{b}}}$ $-\frac{1}{2}\sin N\Delta\theta(f'_{\hat{\boldsymbol{c}}}+f_{\hat{\boldsymbol{c}}})$	$\sin^2\frac{N\Delta\theta}{2}(f_{\hat{\boldsymbol{c}}}+f_{\hat{\boldsymbol{c}}}{}')$ $+\frac{1}{2}\sin N\Delta\theta(f'_{\hat{\boldsymbol{b}}}-f_{\hat{\boldsymbol{b}}})$	$\sin^2\frac{N\Delta\theta}{2}\Delta f_z$
LvN	$\cos^2\frac{N\Delta\theta}{2}\Delta f_0$	$\cos^2\frac{N\Delta\theta}{2}\Delta f_{\hat{\boldsymbol{b}}}$ $-\frac{1}{2}\sin N\Delta\theta(f'_{\hat{\boldsymbol{c}}}-f_{\hat{\boldsymbol{c}}})$	$\cos^2\frac{N\Delta\theta}{2}\Delta f_{\hat{\boldsymbol{c}}}$ $+\frac{1}{2}\sin N\Delta\theta(f'_{\hat{\boldsymbol{b}}}-f_{\hat{\boldsymbol{b}}})$	$\cos^2\frac{N\Delta\theta}{2}\Delta f_z$
NSO	$\cos^2\frac{N\Delta\theta}{2}\Delta f_0$	$\cos^2\frac{N\Delta\theta}{2}\Delta f_{\hat{\boldsymbol{b}}}$ $-\frac{1}{2}\sin N\Delta\theta(f'_{\hat{\boldsymbol{c}}}+f_{\hat{\boldsymbol{c}}})$	$\cos^2\frac{N\Delta\theta}{2}\Delta f_{\hat{\boldsymbol{c}}}$ $+\frac{1}{2}\sin N\Delta\theta(f'_{\hat{\boldsymbol{b}}}+f_{\hat{\boldsymbol{b}}})$	$\cos^2\frac{N\Delta\theta}{2}\Delta f_z$
rest	$\cos^2\frac{N\Delta\theta}{2}\Delta f_0$	$\cos^2\frac{N\Delta\theta}{2}\Delta f_{\hat{\boldsymbol{b}}}$ $-\frac{1}{2}\sin N\Delta\theta f'_{\hat{\boldsymbol{c}}}$	$\frac{1}{2}f_{\hat{\boldsymbol{c}}}-\frac{1}{2}\cos N\Delta\theta f'_{\hat{\boldsymbol{c}}}$ $+\frac{1}{2}\sin N\Delta\theta(f'_{\hat{\boldsymbol{b}}}-f_{\hat{\boldsymbol{b}}})$	$\frac{1}{2}\Delta f_z$

The other collision integrals are obtained with the integrands in $\mathcal{J}_\mu^\delta$ replaced according to Table 5.2.

Terms including the trigonometric factor $\sin\Delta N\theta$ are in the assumed case of symmetric scattering $K(\Delta\theta)=K(-\Delta\theta)$ the same in all approaches, since only the part including f' can survive, whereas the part including f vanishes trivially. Thus, the approaches differ only in the elements $\mathcal{J}_{\hat{\boldsymbol{c}}}[f_{\hat{\boldsymbol{c}}}]$ and $\mathcal{J}_z[f_z]$. These, however, enter the solution only to order $\sim(\ell\,k_\mathrm{F})^{-1}$, as we will see below. We will further see that the first quantum correction to the conductivity depends on $\mathcal{J}_z[f_z]$. Since the iterative solution of Culcer and Winkler [2007b] was only taken to order $(\ell k_\mathrm{F})^0$, the concrete implementation of the Markov approximation and in general the choice of formalism would not have mattered.

We proceed by linearizing the equations in the electric field with $f=f^\mathrm{eq}+f^{(E)}$ and by Fourier decomposing the components of the distribution function as

$$f_r^{(E)} \;=\; \sum_n e^{i\,n\,\theta}\,f_{r\,n}^{(E)}\,, \tag{5.63}$$

where $r=0,\hat{\boldsymbol{b}},\hat{\boldsymbol{c}},z$. In equilibrium we have

$$\begin{aligned} f_0^\mathrm{eq}\pm f_{\hat{\boldsymbol{b}}}^\mathrm{eq} &= f_\mathrm{FD}\,(\pm v_\mathrm{F}\,k) \;=\; \Theta(\mu\mp v_\mathrm{F}\,k)+\mathcal{O}((k_\mathrm{B}T/\epsilon_\mathrm{F})^2), \\ f_{\hat{\boldsymbol{c}}}^\mathrm{eq} &= f_z^\mathrm{eq} \;=\; 0. \end{aligned} \tag{5.64}$$

Since $\boldsymbol{E}\cdot\partial_{\boldsymbol{k}}f^\mathrm{eq}$ with

$$\boldsymbol{E}\cdot\partial_{\hat{\boldsymbol{k}}}f_\mathrm{FD}\left(\epsilon^\pm\right) \;=\; E_{\hat{\boldsymbol{k}}}\,\partial_k f_\mathrm{FD}\left(\epsilon^\pm\right) \;=\; \frac{e^{i\theta}\,\mathcal{E}^*+e^{-i\theta}\,\mathcal{E}}{2}\,\partial_k f_\mathrm{FD}\left(\epsilon^\pm\right) \tag{5.65}$$

and $E_{\hat{\boldsymbol{\theta}}}=\frac{i}{2}\,(e^{i\theta}\,\mathcal{E}^*-e^{-i\theta}\,\mathcal{E})$, where $\mathcal{E}:=E_x+i\,E_y$, contains only $n=\pm1$ Fourier components, we can immediately conclude that $f_{rn}^{(E)}=0$ for $n\neq\pm1$. It is enough to study the equation for the $n=1$ component. The $n=-1$ term is just the complex conjugate. We

find for the $n = 1$ Fourier component of the linearized Boltzmann equation

$$\frac{\mathcal{E}^*}{2}\begin{pmatrix} \partial_k f_0^{\rm eq} \\ \partial_k f_{\hat{\boldsymbol{b}}}^{\rm eq} \\ i\,\frac{N}{k}\, f_{\hat{\boldsymbol{b}}}^{\rm eq} \\ 0 \end{pmatrix} = -\begin{pmatrix} \mathcal{I}^+ & 0 & 0 & 0 \\ 0 & \mathcal{I}^+ & +i\,\mathcal{I}^{\rm s} & 0 \\ 0 & -i\,\mathcal{I}^{\rm s} & \mathcal{I}^\lambda & 2\,b \\ 0 & 0 & -2\,b & \mathcal{I}^\kappa \end{pmatrix}\begin{pmatrix} f_{01}^{(E)} \\ f_{\hat{\boldsymbol{b}}1}^{(E)} \\ f_{\hat{\boldsymbol{c}}1}^{(E)} \\ f_{z1}^{(E)} \end{pmatrix}. \tag{5.66}$$

In terms of the integrals defined below one has $\mathcal{I}^\kappa = \mathcal{I}^-$ for G1wGKBA and $\mathcal{I}^\kappa = \mathcal{I}^+$ for G1wAA/LvN/NSO. For the G1wSKBA approach and all G2 approaches one has $\mathcal{I}^\kappa = (\mathcal{I}^+ + \mathcal{I}^-)/2$. Likewise, $\mathcal{I}^\lambda = \tilde{\mathcal{I}}^+$ for G1wGKBA, $\mathcal{I}^\lambda = \mathcal{I}^+$ for G1wAA/LvN/NSO, and the average of these results for the rest,

$$\begin{aligned}
\mathcal{I}^+ &:= \int_{\theta'} K \cos^2\tfrac{N\Delta\theta}{2}(1 - e^{-i\Delta\theta}) \equiv \tau_{\rm tr}^{-1} &&\overset{(N=\pm1)}{=} \tfrac{1}{4}\int_{\theta'} K(1-\cos 2\Delta\theta), \\
\tilde{\mathcal{I}}^+ &:= \int_{\theta'} K \sin^2\tfrac{N\Delta\theta}{2}(1 + e^{-i\Delta\theta}) &&\overset{(N=\pm1)}{=} \mathcal{I}^+, \\
\mathcal{I}^- &:= \int_{\theta'} K \sin^2\tfrac{N\Delta\theta}{2}(1 - e^{-i\Delta\theta}) &&\overset{(N=\pm1)}{=} \tfrac{1}{4}\int_{\theta'} K(3-4\cos\Delta\theta+\cos 2\Delta\theta), \\
i\,\mathcal{I}^{\rm s} &:= \tfrac{i}{2}\int_{\theta'} K \sin N\Delta\theta \sin\Delta\theta &&\overset{(N=\pm1)}{=} \pm i\,\mathcal{I}^+,
\end{aligned} \tag{5.67}$$

where we used that $K(-\Delta\theta) = K(\Delta\theta)$. Notice that $\mathcal{I}^{\rm s}$ is odd in N, whereas the other integrals $\mathcal{I}$ are even in N.

The equation for f_0 is decoupled from the other components and is solved independently by $f_{01}^{(E)} = -\frac{1}{2}\,\mathcal{E}^*\,\tau_{\rm tr}\,\partial_k f_0^{\rm eq}$ with $\tau_{\rm tr} := (\mathcal{I}^+)^{-1}$. The other components are found by inverting the remaining 3×3 matrix:

$$\begin{pmatrix} f_{\hat{\boldsymbol{b}}1}^{(E)} \\ f_{\hat{\boldsymbol{c}}1}^{(E)} \\ f_{z1}^{(E)} \end{pmatrix} = -\frac{\mathcal{E}^*}{2\,|M|}\begin{pmatrix} (4\,b^2 + \mathcal{I}^\lambda\,\mathcal{I}^\kappa)\,\partial_k f_{\hat{\boldsymbol{b}}}^{\rm eq} + \mathcal{I}^{\rm s}\,\mathcal{I}^\kappa\,\frac{N}{k}\,f_{\hat{\boldsymbol{b}}}^{\rm eq} \\ i\,\mathcal{I}^\kappa\,(\mathcal{I}^{\rm s}\,\partial_k f_{\hat{\boldsymbol{b}}}^{\rm eq} + \mathcal{I}^+\,\frac{N}{k}\,f_{\hat{\boldsymbol{b}}}^{\rm eq}) \\ i\,2\,b\,(\mathcal{I}^{\rm s}\,\partial_k f_{\hat{\boldsymbol{b}}}^{\rm eq} + \mathcal{I}^+\frac{N}{k}\,f_{\hat{\boldsymbol{b}}}^{\rm eq}) \end{pmatrix}, \tag{5.68}$$

with the determinant $|M| = 4\,b^2\,\mathcal{I}^+ + \mathcal{I}^+\,\mathcal{I}^\lambda\,\mathcal{I}^\kappa - (\mathcal{I}^{\rm s})^2\,\mathcal{I}^\kappa$. Adding up the two Fourier components $n = \pm 1$ one obtains

$$\begin{aligned}
f_{\hat{\boldsymbol{b}}}^{(E)} &= -E_{\hat{\boldsymbol{k}}}\,\frac{(4\,b^2 + \mathcal{I}^\lambda\,\mathcal{I}^\kappa)\,\partial_k f_{\hat{\boldsymbol{b}}}^{\rm eq} + \mathcal{I}^{\rm s}\,\mathcal{I}^\kappa\,\frac{N}{k}\,f_{\hat{\boldsymbol{b}}}^{\rm eq}}{4\,b^2\,\mathcal{I}^+ + \mathcal{I}^+\,\mathcal{I}^\lambda\,\mathcal{I}^\kappa - (\mathcal{I}^{\rm s})^2\,\mathcal{I}^\kappa} && (5.69) \\
&\overset{(N=\pm1)}{=} -E_{\hat{\boldsymbol{k}}}\left[\frac{1}{\mathcal{I}^+}\partial_k f_{\hat{\boldsymbol{b}}}^{\rm eq} + \frac{\mathcal{I}^\kappa}{4b^2}\left(\partial_k f_{\hat{\boldsymbol{b}}}^{\rm eq} + \tfrac{1}{k} f_{\hat{\boldsymbol{b}}}^{\rm eq}\right)\right], \\
f_{\hat{\boldsymbol{c}}}^{(E)} &= -E_{\hat{\boldsymbol{\theta}}}\,\frac{\mathcal{I}^\kappa\,(\mathcal{I}^{\rm s}\,\partial_k f_{\hat{\boldsymbol{b}}}^{\rm eq} + \mathcal{I}^+\,\frac{N}{k}\,f_{\hat{\boldsymbol{b}}}^{\rm eq})}{4\,b^2\,\mathcal{I}^+ + \mathcal{I}^+\,\mathcal{I}^\lambda\,\mathcal{I}^\kappa - (\mathcal{I}^{\rm s})^2\,\mathcal{I}^\kappa} && (5.70) \\
&\overset{(N=\pm1)}{=} -E_{\hat{\boldsymbol{\theta}}}\,\frac{N\,\mathcal{I}^\kappa}{4\,b^2}\left(\partial_k f_{\hat{\boldsymbol{b}}}^{\rm eq} + \tfrac{1}{k}\,f_{\hat{\boldsymbol{b}}}^{\rm eq}\right), \\
f_z^{(E)} &= -E_{\hat{\boldsymbol{\theta}}}\,\frac{2\,b\,(\mathcal{I}^{\rm s}\,\partial_k f_{\hat{\boldsymbol{b}}}^{\rm eq} + \mathcal{I}^+\,\frac{N}{k}\,f_{\hat{\boldsymbol{b}}}^{\rm eq})}{4\,b^2\,\mathcal{I}^+ + \mathcal{I}^+\,\mathcal{I}^\lambda\,\mathcal{I}^\kappa - (\mathcal{I}^{\rm s})^2\,\mathcal{I}^\kappa} && (5.71) \\
&\overset{(N=\pm1)}{=} -E_{\hat{\boldsymbol{\theta}}}\,\frac{N}{2\,b}\left(\partial_k f_{\hat{\boldsymbol{b}}}^{\rm eq} + \tfrac{1}{k}\,f_{\hat{\boldsymbol{b}}}^{\rm eq}\right).
\end{aligned}$$

The charge current $\boldsymbol{j}$ in momentum space, see Eq. (5.8), is for the graphene case ($\epsilon_0 = 0$) given by

$$\boldsymbol{j}(\boldsymbol{k}) \;=\; 2\,\hat{\boldsymbol{k}}\,f_{\hat{\boldsymbol{b}}}\,\partial_k b + 2\,\hat{\boldsymbol{\theta}}\,\boldsymbol{f}_{\hat{\boldsymbol{c}}}\,\frac{Nb}{k} \;\overset{(N=\pm1)}{=}\; 2\,v_{\rm F}\,(\hat{\boldsymbol{k}}\,f_{\hat{\boldsymbol{b}}} + N\,\hat{\boldsymbol{\theta}}\,f_{\hat{\boldsymbol{c}}}). \tag{5.72}$$

With $\int_\theta \hat{\boldsymbol{k}}\,E_{\hat{\boldsymbol{k}}} = \int_\theta \hat{\boldsymbol{\theta}}\,E_{\hat{\boldsymbol{\theta}}} = \boldsymbol{E}/2$ one obtains the current in real space as

$$\boldsymbol{j} \;=\; \int_{\boldsymbol{k}} \boldsymbol{j}(\boldsymbol{k}) \;=\; (\sigma^I + \sigma^{II})\,\boldsymbol{E}. \tag{5.73}$$

The conductivity is given by the contributions

$$\begin{aligned}
\sigma^I \;&=\; -\int \frac{k\,{\rm d}k}{2\,\pi}\,\frac{(4\,b^2 + \mathcal{I}^\kappa\,\mathcal{I}^\lambda)\,\partial_k b + \mathcal{I}^\kappa\,\mathcal{I}^{\rm s}\,\frac{Nb}{k}}{4\,b^2\,\mathcal{I}^+ + \mathcal{I}^+\,\mathcal{I}^\lambda\,\mathcal{I}^\kappa - (\mathcal{I}^{\rm s})^2\,\mathcal{I}^\kappa}\,\partial_k f^{\rm eq}_{\hat{\boldsymbol{b}}} \qquad (5.74)\\
&\overset{(N=\pm1)}{=}\; -\frac{v_{\rm F}}{2\,\pi}\int k\,{\rm d}k\,\left(\frac{1}{\mathcal{I}^+} + \frac{\mathcal{I}^\kappa}{2\,b^2}\right)\partial_k f^{\rm eq}_{\hat{\boldsymbol{b}}}\,,\\
\sigma^{II} \;&=\; -\int \frac{{\rm d}k}{2\,\pi}\,N\,\frac{\mathcal{I}^\kappa\,\mathcal{I}^{\rm s}\,\partial_k b + \mathcal{I}^\kappa\,\mathcal{I}^+\frac{N\,b}{k}}{4\,b^2\,\mathcal{I}^+ + \mathcal{I}^+\,\mathcal{I}^\lambda\,\mathcal{I}^\kappa - (\mathcal{I}^{\rm s})^2\,\mathcal{I}^\kappa}\,f^{\rm eq}_{\hat{\boldsymbol{b}}} \qquad (5.75)\\
&\overset{(N=\pm1)}{=}\; -\frac{v_{\rm F}}{2\,\pi}\int {\rm d}k\,\frac{\mathcal{I}^\kappa}{2\,b^2}\,f^{\rm eq}_{\hat{\boldsymbol{b}}}\,.
\end{aligned}$$

In the monolayer case $N = \pm1$ we used that $\partial_k b = \frac{b}{k} = v_{\rm F}$ for all k. Due to $\mathcal{I}^{\rm s}_{-N} = -\mathcal{I}^{\rm s}_N$ the conductivity is invariant with the sign of N.

As a part of σ^I we recognize the Drude conductivity $\sigma_0 = -\int \frac{k\,{\rm d}k}{2\,\pi}\frac{\partial_k b}{\mathcal{I}^+}\,\partial_k f^{\rm eq}_{\hat{\boldsymbol{b}}} = \ell\,k_{\rm F}/4\,\pi$. The contributions σ^{II} and $\delta\sigma^I = \sigma^I - \sigma_0$ are quantum corrections, both of the leading order $(\ell\,k_{\rm F})^{-1}$ (or equivalently, $(\mathcal{I}/b)^{-1}$). For $|N| \le 2$ they contain also higher powers of $(\ell\,k_{\rm F})^{-1}$ that can be obtained explicitly by a truncated expansion in $(\mathcal{I}/b)^{-1}$ of the integrands in Eqs. (5.74)-(5.75). Notice that there is no contribution of the order $(\ell k_{\rm F})^0$.

At $T = 0$ one has from Eq. (5.64) that $f^{\rm eq}_{\hat{\boldsymbol{b}}} = -\frac{1}{2}\,\Theta(k - k_{\rm F})$ and $\partial_k f^{\rm eq}_{\hat{\boldsymbol{b}}} = -\frac{1}{2}\,\delta(k - k_{\rm F})$. The conductivity including the leading quantum correction $\sim (\ell k_{\rm F})^{-1}$ then becomes

$$\begin{aligned}
\sigma^I \;&=\; \sigma_0\left(1 + \tfrac{\mathcal{I}^\kappa_{\rm F}\,(\mathcal{I}^{\rm s}_{\rm F})^2}{4\,b^2_{\rm F}\,\mathcal{I}^+_{\rm F}} + \tfrac{N\,\mathcal{I}^\kappa\,\mathcal{I}^{\rm s}}{4\,b_{\rm F}\,v_{\rm F}\,k_{\rm F}}\right) + \mathcal{O}((\tfrac{1}{\ell\,k_{\rm F}})^2) \;\overset{(N=\pm1)}{=}\; \sigma_0\left(1 + \tfrac{\mathcal{I}^\kappa_{\rm F}\,\mathcal{I}^+_{\rm F}}{2b^2_{\rm F}}\right),\\
\sigma^{II} \;&=\; \tfrac{1}{4\,\pi}\int_{k_{\rm F}}^\infty {\rm d}k\left(\tfrac{N\,\mathcal{I}^\kappa\,\mathcal{I}^{\rm s}\,\partial_k b}{4\,b^2\,\mathcal{I}^+} + \tfrac{N^2\,\mathcal{I}^\kappa}{4\,b\,k}\right) + \mathcal{O}((\tfrac{1}{\ell\,k_{\rm F}})^2) \;\overset{(N=\pm1)}{=}\; \tfrac{1}{8\,\pi}\int_{b_{\rm F}}^\infty {\rm d}b\,\tfrac{\mathcal{I}^\kappa}{b^2}\,.
\end{aligned} \tag{5.76}$$

With real spin and valley degeneracy taken into account, the conductivity of graphene is

$$\sigma_{\rm graphene} \;=\; 4\,\left(\sigma^I + \sigma^{II}\right) \tag{5.77}$$

in terms of the quantities defined in Eqs. (5.74)-(5.75). The leading correction is positive in all considered approaches. Below, when we include principal value terms in the calculation, this will no longer be the case. We further observe that the leading correction depends on $\mathcal{I}^\kappa$, but not on $\mathcal{I}^\lambda$. Thus the difference in $\mathcal{I}^\kappa$, and thereby in $\mathcal{J}_z[f_z]$, is the one that is crucial for the discrepancies between the approaches.

For screened charged impurities with $W(k,\Delta\theta) = 2\,\pi\,n_{\rm imp}\,(2\,k\,\sin\frac{|\Delta\theta|}{2} + k_{\rm TF})^{-2}$ the integral in σ^{II} is convergent. For point-like impurities, $K(k,\Delta\theta) = \frac{k}{2\pi v}W_0$ with $W_{\boldsymbol{k}\boldsymbol{k}'} =$

$W_0 = \text{const.} \propto n_{\text{imp}}$, it has a logarithmic divergence in the monolayer case (since $\mathcal{I} \propto k/v_{\text{F}}$) unless an ultraviolet cut-off is introduced. Let us nonetheless make the observation that $\mathcal{I}^+ = K/4$ and $\mathcal{I}^- = 3K/4$. Thus, given a cut-off, the leading quantum correction is larger by a factor of 3 with the approach G1wGKBA ($\mathcal{I}^\kappa = \mathcal{I}^-$) compared to the approaches G1wAA/LvN/NSO ($\mathcal{I}^\kappa = \mathcal{I}^+$). The results of the other approaches lie midway between these two.

For point-like impurities in the multilayer case $|N| \geq 2$ all approaches coincide because $\mathcal{I}^+ = \frac{1}{2}\,K = \tilde{\mathcal{I}}^+ = \mathcal{I}^-$, hence $\mathcal{I}^+ = \mathcal{I}^\lambda = \mathcal{I}^\kappa =: \mathcal{I}$, and furthermore $\mathcal{I}^{\text{s}} = 0$. With $b = \alpha\, k^N$ and $\mathcal{I} = \frac{1}{2}\,K = \frac{k^{2-N}}{4\,\pi\,N\,\alpha}\,W_0$ the zero temperature limit of the untruncated form (5.74) is easily carried out. With e and $\hbar$ restored, the result reads

$$\sigma^I \;=\; \sigma_0\,, \tag{5.78}$$

$$\sigma^{II} \;=\; \frac{e^2}{2\,h}\,\frac{N^2}{4\,(|N|-1)}\,\arctan\frac{|N|}{2\,\ell\,k_{\text{F}}}\,. \tag{5.79}$$

All integrals converge without any ultraviolet cut-off. See also Trushin *et al.* [2010] for the bilayer case $N = 2$.

For an ac field of the form $\boldsymbol{E}(t) = e^{i\,\omega\,t}\,\boldsymbol{E}$ one obtains with the ansatz $f^{(E)}_{\boldsymbol{k}}(t) = e^{i\,\omega\,t}\,f^{(E)}_{\boldsymbol{k}}$ the Boltzmann equation

$$e^{i\,\omega\,t}\left(i\,\omega\,f^{(E)}_{\boldsymbol{k}} + i\,[H\,,\,f^{(E)}_{\boldsymbol{k}}] + \boldsymbol{E}\cdot\partial_{\boldsymbol{k}} f^{\text{eq}}_{\boldsymbol{k}} - \mathcal{J}[f^{(E)}_{\boldsymbol{k}}]\right) \;=\; 0\,, \tag{5.80}$$

from which the Drude result, Eq. (5.60), is modified to give

$$\sigma_0(\omega) \;=\; \frac{\ell\,k_{\text{F}}}{4\,\pi\,(1 + i\,\omega\,\tau_{\text{trF}})}\,. \tag{5.81}$$

In the pseudospin coherent formulation of the previous section, the term $i\,\omega\,f^{(E)}\,e^{i\,\omega\,t}$ enters as the diagonal matrix $i\,\omega\,\mathbf{1}_4$ in Eq. (5.66), *i.e.*, we obtain the ac result from the dc result for the $n = \pm 1$ Fourier components with the substitutions

$$\mathcal{I}^+ \to \mathcal{I}^+ + i\,\omega, \qquad \mathcal{I}^\kappa \to \mathcal{I}^\kappa + i\,\omega, \qquad \mathcal{I}^\lambda \to \mathcal{I}^\lambda + i\,\omega, \qquad \mathcal{I}^{\text{s}} \to \mathcal{I}^{\text{s}}\,. \tag{5.82}$$

With this, the dc result from Eqs. (5.69)-(5.71) is changed into the ac expressions

$$f^{(E)}_{\hat{\boldsymbol{b}}} \;=\; -E_{\hat{\boldsymbol{k}}}\,\frac{1}{|M|}\left(\left[4\,b^2 + (\mathcal{I}^\lambda + i\,\omega)\,(\mathcal{I}^\kappa + i\,\omega)\right]\partial_k f^{\text{eq}}_{\hat{\boldsymbol{b}}} + \mathcal{I}^{\text{s}}\,[\mathcal{I}^\kappa + i\,\omega]\,\frac{1}{k}\,f^{\text{eq}}_{\hat{\boldsymbol{b}}}\right)$$

$$\overset{W_{\boldsymbol{k}\boldsymbol{k}'}\to 0}{=} \; -E_{\hat{\boldsymbol{k}}}\,\partial_k f^{\text{eq}}_{\hat{\boldsymbol{b}}}\,\frac{1}{i\omega}, \tag{5.83}$$

$$f^{(E)}_{\hat{\boldsymbol{c}}} \;=\; -E_{\hat{\boldsymbol{\theta}}}\,\frac{1}{|M|}\,(\mathcal{I}^\kappa + i\,\omega)\left(\mathcal{I}^{\text{s}}\,\partial_k f^{\text{eq}}_{\hat{\boldsymbol{b}}} + \left[\mathcal{I}^+ + i\,\omega\right]\frac{1}{k}\,f^{\text{eq}}_{\hat{\boldsymbol{b}}}\right)$$

$$\overset{W_{\boldsymbol{k}\boldsymbol{k}'}\to 0}{=} \; -E_{\hat{\boldsymbol{\theta}}}\,\frac{1}{k}\,f^{\text{eq}}_{\hat{\boldsymbol{b}}}\,\frac{i\,\omega}{4\,b^2 - \omega^2}, \tag{5.84}$$

$$f^{(E)}_{z} \;=\; -E_{\hat{\boldsymbol{\theta}}}\,\frac{1}{|M|}2\,b\left(\mathcal{I}^{\text{s}}\,\partial_k f^{\text{eq}}_{\hat{\boldsymbol{b}}} + \left[\mathcal{I}^+ + i\,\omega\right]\frac{1}{k}\,f^{\text{eq}}_{\hat{\boldsymbol{b}}}\right)$$

$$\overset{W_{\boldsymbol{k}\boldsymbol{k}'}\to 0}{=} \; -E_{\hat{\boldsymbol{\theta}}}\,\frac{1}{k}\,f^{\text{eq}}_{\hat{\boldsymbol{b}}}\,\frac{2\,b}{4\,b^2 - \omega^2}, \tag{5.85}$$

with the determinant $|M|$ also shifted according to the prescription (5.82). We have complemented the results with the pure sample limits ($W_{\boldsymbol{k}\boldsymbol{k}'} \to 0$).

Ac terms are derived from dc terms by replacing a real quantity $\mathcal{I}$ by an imaginary quantity $i\,\omega$. Thus, the real part of the frequency dependent contributions to the conductivity $\sigma(\omega)$ steps up or down in even powers of $\omega/\mathcal{I}$, whereas an odd power would be required to obtain a $(\ell k_{\mathrm{F}})^0$ correction in $\mathrm{Re}\,\sigma(\omega)$ from the dc result $\sigma_{\mathrm{Drude}} \sim \ell k_{\mathrm{F}}$ or its dc corrections $\sim (\ell k_{\mathrm{F}})^{-1}$. According to this argument there are no corrections $(\ell k_{\mathrm{F}})^0$ to $\mathrm{Re}\,\sigma(\omega)$. This result should be contrasted with the frequency dependent corrections of order $(\ell k_{\mathrm{F}})^0$ found by Culcer and Winkler (see Eqs. (27) and (31) in Culcer and Winkler [2007b]).

5.8. Leading-order correction with principal value terms included

In this section we include the principal value terms and recalculate the first quantum correction to the conductivity using a recursive approach in the spirit of the derivation by Culcer and Winkler [2007b]. The iteration is only taken to order $(\ell k_{\mathrm{F}})^0$ in the distribution function, but it could in principle be reiterated to access terms of order $(\ell k_{\mathrm{F}})^{-1}$ and higher orders.

General collision integrals derived within a quantum coherent approach typically contain principal value terms (a.k.a. reaction terms, off-shell terms, off-pole terms) alongside with the delta function terms (elastic terms, on-shell terms, pole terms). The delta functions convey the sharpness in energy of the idealized semiclassical quasiparticles. The quasiparticles are the almost free particles that obey a Fermi-Dirac distribution in equilibrium, whereas the real electrons follow a distribution with fatter tails due to the interactions Lipavský *et al.* [2001]. The principal value terms are a reminiscence of the quantum coherent nature of the underlying particles and captures the deviation from the classical point-like "billiard ball" picture conveyed by the fully semiclassical (*i.e.*, quantum incoherent) Boltzmann equation. One such example are the principal value terms related to the quickly decaying coherences stemming from the redressing of the quasiparticles within the interaction radius [Lipavský *et al.*, 2001]. The corresponding decay time (the collision time that the particles spend within the interaction radius) is in the kinetic regime by assumption much shorter than the relaxation time (roughly τ_{tr}). Therefore, an electron quickly recovers its asymptotic quasiparticle nature after a collision. In the spectral function the off-pole part is the broad background surrounding the quasiparticle peak [Bruus and Flensberg, 2004]. For spinless electrons there are elaborate ways of separating out the off-pole part from the quantum kinetic equation, with the remains becoming the standard Boltzmann equation for the quasiparticles [Lipavský *et al.*, 2001].

The electron-hole coherence (or pseudospin-coherence), too, is a deviation from the fully semiclassical particle picture—in this case not because of interaction effects but because of the Zitterbewegung in the presence of (pseudo)spin-orbit coupling. It is therefore no surprise that the spin-orbit coupling contributes with its own principal value terms adding to those related to the quasiparticle redressing. However, this time we do not want to separate out the principal values in deriving a Boltzmann type equation since the Zitterbewegung is known to be inherent in the asymptotic free particle. We want to derive a

kinetic equation while keeping track of electron-hole coherent effects. Therefore, we should keep the corresponding principal value terms.

A technical problem connected with the principal value terms is that the two momenta $\boldsymbol{k}$ and $\boldsymbol{k'}$ in the collision integral are no longer confined to the same surface as defined by $\epsilon_k = \epsilon_{k'} = \mu$. In the calculation of the previous section, which has neglected the principal value parts, this has allowed us to plug out the Fourier coefficients $f_{rn}(k)$ from the integrals, the remains of which became matrix elements like $\mathcal{I}^{\pm}$ *etc.* The problem of solving the Boltzmann equation to all orders in $(\ell k_{\mathrm{F}})^{-1}$ was thus reduced to a simple matrix inversion. With the principal value terms we have to confront difficult integro-differential equations. Auslender and Katsnelson [2007] present an analytical solution to all orders in $(\ell k_{\mathrm{F}})^{-1}$ for point-like impurities. Here, a solution for screened charged impurities will be addressed within a recursive scheme, for which no simplifying assumption about the potential is needed.

In order to obtain all the other cases we express $\mathcal{J}^{\mathrm{P}}$ in terms of $\mathcal{J}^{\mathrm{P}X}$ and $\mathcal{J}^{\mathrm{P}Y}$ and combine them according to (5.46). In particular, the case G1wAA/LvN/NSO above corresponds to $\mathcal{J}^{\mathrm{P}} = \mathcal{J}^{\mathrm{P}X} - \mathcal{J}^{\mathrm{P}Y}$, where

$$\begin{aligned}
\mathcal{J}^{\mathrm{P}X}_{\hat{\boldsymbol{b}}} &= +\textstyle\int_{\boldsymbol{k'}} \frac{W_{\boldsymbol{kk'}}}{2\pi} \mathcal{P}_- \sin N\Delta\theta f_z \,, \\
\mathcal{J}^{\mathrm{P}Y}_{\hat{\boldsymbol{b}}} &= -\textstyle\int_{\boldsymbol{k'}} \frac{W_{\boldsymbol{kk'}}}{2\pi} \mathcal{P}_- \sin N\Delta\theta f'_z \,, \\
\mathcal{J}^{\mathrm{P}X}_{\hat{\boldsymbol{c}}} &= -\textstyle\int_{\boldsymbol{k'}} \frac{W_{\boldsymbol{kk'}}}{2\pi} \left(-\mathcal{P}_- \cos N\Delta\theta f_z + \mathcal{P}_+ f'_z\right) , \\
\mathcal{J}^{\mathrm{P}Y}_{\hat{\boldsymbol{c}}} &= -\textstyle\int_{\boldsymbol{k'}} \frac{W_{\boldsymbol{kk'}}}{2\pi} \left(-\mathcal{P}_+ f_z + \mathcal{P}_- \cos N\Delta\theta f'_z\right) , \\
\mathcal{J}^{\mathrm{P}X}_{z} &= -\textstyle\int_{\boldsymbol{k'}} \frac{W_{\boldsymbol{kk'}}}{2\pi} \Big(\mathcal{P}_- \left[\sin N\Delta\theta f_{\hat{\boldsymbol{b}}} + \cos N\Delta\theta f_{\hat{\boldsymbol{c}}}\right] \\
&\qquad\qquad -\mathcal{P}_+ \left[-\sin N\Delta\theta f'_{\hat{\boldsymbol{b}}} + \cos N\Delta\theta f'_{\hat{\boldsymbol{c}}}\right]\Big) , \\
\mathcal{J}^{\mathrm{P}Y}_{z} &= -\textstyle\int_{\boldsymbol{k'}} \frac{W_{\boldsymbol{kk'}}}{2\pi} \left(\mathcal{P}_+ f_{\hat{\boldsymbol{c}}} - \mathcal{P}_- f'_{\hat{\boldsymbol{c}}}\right) .
\end{aligned} \tag{5.86}$$

For the same reasons as before only the Fourier components $n = \pm 1$ of the nonequilibrium part $f^{(E)}$ can be nonzero. Therefore one only needs to consider

$$\begin{aligned}
\mathcal{J}^{\mathrm{P}X}_{\hat{\boldsymbol{b}}1} &= 0 \,, \\
\mathcal{J}^{\mathrm{P}Y}_{\hat{\boldsymbol{b}}1} &= +i\textstyle\int_{\boldsymbol{k'}} \frac{W_{\boldsymbol{kk'}}}{2\pi} \mathcal{P}_- \sin N\Delta\theta \sin\Delta\theta f'_{z1} \,, \\
\mathcal{J}^{\mathrm{P}X}_{\hat{\boldsymbol{c}}1} &= -\textstyle\int_{\boldsymbol{k'}} \frac{W_{\boldsymbol{kk'}}}{2\pi} \left(-\mathcal{P}_- \cos N\Delta\theta f_{z1} + \mathcal{P}_+ \cos\Delta\theta f'_{z1}\right) , \\
\mathcal{J}^{\mathrm{P}Y}_{\hat{\boldsymbol{c}}1} &= -\textstyle\int_{\boldsymbol{k'}} \frac{W_{\boldsymbol{kk'}}}{2\pi} \left(-\mathcal{P}_+ f_{z1} + \mathcal{P}_- \cos N\Delta\theta \cos\Delta\theta f'_{z1}\right) , \\
\mathcal{J}^{\mathrm{P}X}_{z1} &= -\textstyle\int_{\boldsymbol{k'}} \frac{W_{\boldsymbol{kk'}}}{2\pi} \Big(\mathcal{P}_- \cos N\Delta\theta f_{\hat{\boldsymbol{c}}1} \\
&\qquad\qquad -\mathcal{P}_+ \left[i \sin N\Delta\theta \sin\Delta\theta f'_{\hat{\boldsymbol{b}}1} + \cos N\Delta\theta \cos\Delta\theta f'_{\hat{\boldsymbol{c}}1}\right]\Big) , \\
\mathcal{J}^{\mathrm{P}Y}_{z1} &= -\textstyle\int_{\boldsymbol{k'}} \frac{W_{\boldsymbol{kk'}}}{2\pi} \left(\mathcal{P}_+ f_{\hat{\boldsymbol{c}}1} - \mathcal{P}_- \cos\theta \Delta f'_{\hat{\boldsymbol{c}}1}\right) .
\end{aligned} \tag{5.87}$$

Both in Eqs. (5.86) and in Eqs. (5.87) we have left out terms that vanish due to the assumed symmetry $W(-\Delta\theta) = W(\Delta\theta)$ of the impurity potential. We will see below that for the calculation of the first quantum correction one only needs $\mathcal{J}^{\mathrm{P}}_z[f_{\hat{\boldsymbol{b}}}]$ and $\mathcal{J}^{\mathrm{P}}_{\hat{\boldsymbol{b}}}[f_z]$, *i.e.*,

$$\begin{aligned}
\mathcal{J}^{\mathrm{P}X}_{z1}[f_{\hat{\boldsymbol{b}}}] &= i\int_{\boldsymbol{k'}} \frac{W_{\boldsymbol{kk'}}}{2\,\pi} \left(\frac{1}{b+b'} + \frac{1}{\Delta b}\right) \sin N\Delta\theta \, \sin\Delta\theta \, f'_{\hat{\boldsymbol{b}}1} \,, \\
\mathcal{J}^{\mathrm{P}Y}_{\hat{\boldsymbol{b}}1}[f_z] &= i\int_{\boldsymbol{k'}} \frac{W_{\boldsymbol{kk'}}}{2\,\pi} \left(\frac{1}{b+b'} - \frac{1}{\Delta b}\right) \sin N\Delta\theta \, \sin\Delta\theta \, f'_{z1} \,.
\end{aligned} \tag{5.88}$$

The Boltzmann equation for $\boldsymbol{f}^{(E)}$ (we henceforth drop the the superscript (E)) can be written as

$$\boldsymbol{\mathcal{D}} \;=\; \boldsymbol{\mathcal{S}}[\boldsymbol{f}] + \boldsymbol{\mathcal{J}}^{\boldsymbol{\delta}}[\boldsymbol{f}] + \boldsymbol{\mathcal{J}}^{\mathbf{P}}[\boldsymbol{f}]\,, \tag{5.89}$$

where $\boldsymbol{\mathcal{D}}$ is the driving term with

$$\begin{pmatrix} \mathcal{D}_{\hat{\boldsymbol{b}}} \\ \mathcal{D}_{\hat{\boldsymbol{c}}} \\ \mathcal{D}_z \end{pmatrix} = \begin{pmatrix} E_{\hat{\boldsymbol{k}}}\,\partial_k f^{\mathrm{eq}}_{\hat{\boldsymbol{b}}} \\ E_{\hat{\boldsymbol{\theta}}}\,\frac{N}{k}\,f^{\mathrm{eq}}_{\hat{\boldsymbol{b}}} \\ 0 \end{pmatrix}, \tag{5.90}$$

$\boldsymbol{\mathcal{S}}[\boldsymbol{f}]$ is the spin-precession term

$$\begin{pmatrix} \mathcal{S}_{\hat{\boldsymbol{b}}}[\boldsymbol{f}] \\ \mathcal{S}_{\hat{\boldsymbol{c}}}[\boldsymbol{f}] \\ \mathcal{S}_z[\boldsymbol{f}] \end{pmatrix} = \begin{pmatrix} 0 \\ -2\,b\,f_z \\ 2\,b\,f_{\hat{\boldsymbol{c}}} \end{pmatrix}, \tag{5.91}$$

and the functionals $\mathcal{J}^{\delta}$ and $\mathcal{J}^{\mathrm{P}}$ are read off from Eq. (5.62), Table (5.2), and Eq. (5.86). A more informative way of writing Eq. (5.89) is

$$\begin{array}{rcllll} \mathcal{D}_{\hat{\boldsymbol{b}}} &=& 0 & + \;\; \mathcal{J}^{\delta}_{\hat{\boldsymbol{b}}}[f_{\hat{\boldsymbol{b}}}, f_{\hat{\boldsymbol{c}}}] & + \;\; \mathcal{J}^{\mathrm{P}}_{\hat{\boldsymbol{b}}}[f_z]\,, \\ \mathcal{D}_{\hat{\boldsymbol{c}}} &=& \mathcal{S}_{\hat{\boldsymbol{c}}}[f_z] & + \;\; \mathcal{J}^{\delta}_{\hat{\boldsymbol{c}}}[f_{\hat{\boldsymbol{b}}}, f_{\hat{\boldsymbol{c}}}] & + \;\; \mathcal{J}^{\mathrm{P}}_{\hat{\boldsymbol{c}}}[f_z]\,, \\ 0 &=& \mathcal{S}_z[f_{\hat{\boldsymbol{c}}}] & + \;\; \mathcal{J}^{\delta}_z[f_z] & + \;\; \mathcal{J}^{\mathrm{P}}_z[f_{\hat{\boldsymbol{b}}}, f_{\hat{\boldsymbol{c}}}]\,. \end{array} \tag{5.92}$$

For notational simplicity, we now prefer to see the expansion of f in orders of $(\ell k_{\mathrm{F}})^{-1}$ as one in powers of $W_{\boldsymbol{k}\boldsymbol{k}'}$, *i.e.*,

$$f \;=\; f^{(-1)} + f^{(0)} + f^{(1)} + \ldots \tag{5.93}$$

with $f^{(n)} \propto W^n \propto (\ell\, k_{\mathrm{F}})^{-n}$. Here $f^{(-1)} \propto W^{-1}$ is the lowest order result that yields the Drude conductivity. Notice that the functionals $\mathcal{J}[f]$ increase the power in W by one, whereas the action of $\mathcal{S}[f]$ is neutral in powers of W. Therefore, the two latter equations do not allow $f_{\hat{\boldsymbol{c}}}$ and f_z to have a lowest order component W^{-1}, since $\mathcal{S}[f^{(-1)}]$ would return a term of order W^{-1} that could not be matched by any of the other terms $\mathcal{D}$ ($\sim W^0$) and $\mathcal{J}[f]$ ($\sim W^0$ and higher). The absence of $\mathcal{S}_{\hat{\boldsymbol{b}}}$ in the first equation (the diagonal components do not precess) is what allows only $f_{\hat{\boldsymbol{b}}}$ to have a term of order W^{-1}. Solving $\mathcal{D}_{\hat{\boldsymbol{b}}} = \mathcal{J}_{\hat{\boldsymbol{b}}}[f^{(-1)}_{\hat{\boldsymbol{b}}}]$ ($\sim W^0$) yields $f^{(-1)}_{\hat{\boldsymbol{b}}} = -E_{\hat{\boldsymbol{k}}}\,\tau_{\mathrm{tr}}\,\partial_k f^{\mathrm{eq}}$.

The components $f^{(0)}$ are found by solving the system of equations

$$\begin{array}{rcllll} 0 &=& 0 & + \;\; \mathcal{J}^{\delta}_{\hat{\boldsymbol{b}}}[f^{(0)}_{\hat{\boldsymbol{b}}}, f^{(0)}_{\hat{\boldsymbol{c}}}] & + \;\; \mathcal{J}^{\mathrm{P}}_{\hat{\boldsymbol{b}}}[f^{(0)}_z]\,, & (\sim W^1) \\ \mathcal{D}_{\hat{\boldsymbol{c}}} &=& \mathcal{S}_{\hat{\boldsymbol{c}}}[f^{(0)}_z] & + \;\; \mathcal{J}^{\delta}_{\hat{\boldsymbol{c}}}[f^{(-1)}_{\hat{\boldsymbol{b}}}] & + \;\; 0\,, & (\sim W^0) \\ 0 &=& \mathcal{S}_z[f^{(0)}_{\hat{\boldsymbol{c}}}] & + \;\; 0 & + \;\; \mathcal{J}^{\mathrm{P}}_z[f^{(-1)}_{\hat{\boldsymbol{b}}}]\,, & (\sim W^0) \end{array} \tag{5.94}$$

where $f^{(-1)}_{\hat{\boldsymbol{b}}}$ is known. The two latter equations constitute a closed set from which we can find $f^{(0)}_{\hat{\boldsymbol{c}}}$ and $f^{(0)}_z$ in a first step. Only the known component $f^{(-1)}_{\hat{\boldsymbol{b}}}$ appears in the

principal value parts. The system of equation is solved as in the previous section by Fourier decomposition and matrix inversion,

$$\begin{aligned}
\begin{pmatrix} \frac{i\,N\,\mathcal{E}^*}{2\,k}\, f^{\mathrm{eq}}_{\hat{\boldsymbol{b}}} \\ 0 \end{pmatrix} &= \begin{pmatrix} 0 & -2\,b \\ 2\,b & 0 \end{pmatrix} \begin{pmatrix} f^{(0)}_{\hat{\boldsymbol{c}}1} \\ f^{(0)}_{z1} \end{pmatrix} + \begin{pmatrix} i\,\mathcal{I}^{\mathrm{s}} f^{(-1)}_{\hat{\boldsymbol{b}}1} \\ 0 \end{pmatrix} + \begin{pmatrix} 0 \\ \mathcal{J}^{\mathrm{P}}_{z1}[f^{(-1)}_{\hat{\boldsymbol{b}}}] \end{pmatrix} \\
\Rightarrow \quad \begin{pmatrix} f^{(0)}_{\hat{\boldsymbol{c}}1} \\ f^{(0)}_{z1} \end{pmatrix} &= \begin{pmatrix} -\frac{1}{2\,b}\mathcal{J}^{\mathrm{P}}_{z1}[f^{(-1)}_{\hat{\boldsymbol{b}}}] \\ -\frac{1}{2\,b}\frac{i\,\mathcal{E}^*}{2}\left(\frac{N}{k}\, f^{\mathrm{eq}}_{\hat{\boldsymbol{b}}} + \frac{\mathcal{I}^{\mathrm{s}}}{\mathcal{I}^+}\,\partial_k f^{\mathrm{eq}}_{\hat{\boldsymbol{b}}}\right) \end{pmatrix}. \qquad (5.95)
\end{aligned}$$

Notice that if we discard the principal value terms $\mathcal{J}^{\mathrm{P}}$ we find $f^{(0)}_{\hat{\boldsymbol{c}}} = 0$, which, together with the first equation in (5.94), implies $f^{(0)}_{\hat{\boldsymbol{b}}} = 0$. This is exactly what the solution (5.68) tells us: there is no W^0 correction (*i.e.*, $(\ell k_{\mathrm{F}})^0$ correction) to the conductivity in (5.76); only f_z acquires a contribution of the order W^0. The last line of (5.95) indeed corresponds to f_z in (5.68).

Including principal value terms yields a nonzero $f^{(0)}_{\hat{\boldsymbol{c}}}$. It also gives a nonzero $f^{(0)}_{\hat{\boldsymbol{b}}}$ according to the first equation in (5.94),

$$0 \;=\; \mathcal{J}^{\delta}_{\hat{\boldsymbol{b}}}[f^{(0)}_{\hat{\boldsymbol{b}}}, f^{(0)}_{\hat{\boldsymbol{c}}}] + \mathcal{J}^{\mathrm{P}}_{\hat{\boldsymbol{b}}1}[f^{(0)}_{z}] \;=\; -\mathcal{I}^{+}\, f^{(0)}_{\hat{\boldsymbol{b}}1} - i\,\mathcal{I}^{\mathrm{s}} f^{(0)}_{\hat{\boldsymbol{c}}1} + \mathcal{J}^{\mathrm{P}}_{\hat{\boldsymbol{b}}1}[f^{(0)}_{z}]\,. \qquad (5.96)$$

The nonzero in-plane components

$$\begin{aligned}
f^{(0)}_{\hat{\boldsymbol{b}}1} &= i\,\frac{\mathcal{I}^{\mathrm{s}}}{2\,b\,\mathcal{I}^{+}}\,\mathcal{J}^{\mathrm{P}}_{z1}[f^{(-1)}_{\hat{\boldsymbol{b}}}] + \frac{1}{\mathcal{I}^{+}}\,\mathcal{J}^{\mathrm{P}}_{\hat{\boldsymbol{b}}1}[f^{(0)}_{z}]\,, \\
f^{(0)}_{\hat{\boldsymbol{c}}1} &= -\frac{1}{2\,b}\,\mathcal{J}^{\mathrm{P}}_{z1}[f^{(-1)}_{\hat{\boldsymbol{b}}}] \qquad (5.97)
\end{aligned}$$

result in a correction to the conductivity. In particular, this correction is of order $(\ell k_{\mathrm{F}})^0$, since the components in (5.97) are of order $(\ell k_{\mathrm{F}})^0$.

A closer inspection shows that $f^{(0)}_{\hat{\boldsymbol{b}}1}/\mathcal{E}^*$ is real and $f^{(0)}_{\hat{\boldsymbol{c}}1}/\mathcal{E}^*$ is imaginary, as it was the case in (5.68). This implies (consult equations (5.69) and (5.65)) that $f^{(0)}_{\hat{\boldsymbol{b}}} = E_{\hat{\boldsymbol{k}}}\, 2\, f^{(0)}_{\hat{\boldsymbol{b}}1}/\mathcal{E}^*$ and $f^{(0)}_{\hat{\boldsymbol{c}}} = E_{\hat{\boldsymbol{\theta}}}\, 2\, f^{(0)}_{\hat{\boldsymbol{c}}1}/i\,\mathcal{E}^*$. The first quantum correction $\delta\sigma$ to the conductivity is therefore for arbitrary N given by

$$\begin{aligned}
\boldsymbol{E}\,\delta\sigma &= 2\int_{\boldsymbol{k}} \left(\hat{\boldsymbol{k}}\, f^{(0)}_{\hat{\boldsymbol{b}}}\,\partial_k b + \hat{\boldsymbol{\theta}}\, f^{(0)}_{\hat{\boldsymbol{c}}}\,\frac{N\,b}{k}\right) \qquad (5.98) \\
&= 2\,\boldsymbol{E}\int \frac{k\,\mathrm{d}k}{2\,\pi}\left(\frac{f^{(0)}_{\hat{\boldsymbol{b}}1}}{\mathcal{E}^*}\,\partial_k b + \frac{f^{(0)}_{\hat{\boldsymbol{c}}1}}{i\,\mathcal{E}^*}\frac{Nb}{k}\right) \;\propto\; (\ell\, k_{\mathrm{F}})^0\,.
\end{aligned}$$

From Eqs. (5.97) one obtains the first quantum correction as a combination of the contributions

$$\begin{aligned}
\delta\sigma^X &= -2\int \frac{k\,\mathrm{d}k}{2\,\pi}\frac{1}{i\,\mathcal{E}^*\,2\,b}\left(\frac{\mathcal{I}^{\mathrm{s}}}{\mathcal{I}^{+}}\,\partial_k b + \frac{Nb}{k}\right)\mathcal{J}^{\mathrm{P}}_{z1}[f^{(-1)}_{\hat{\boldsymbol{b}}}]\,, \\
\delta\sigma^Y &= +2\int \frac{k\,\mathrm{d}k}{2\,\pi}\,\frac{\partial_k b}{\mathcal{E}^*\,\mathcal{I}^{+}}\,\mathcal{J}^{\mathrm{P}}_{\hat{\boldsymbol{b}}1}[f^{(0)}_{z}]\,. \qquad (5.99)
\end{aligned}$$

This can be written as

$$\begin{aligned}
\delta\sigma^X &= +\frac{1}{2\,\pi}\int\frac{k\,\mathrm{d}k}{2\,\pi}\left(\frac{\mathcal{I}^{\mathrm{s}}_k}{\mathcal{I}^{+}_k}\,\partial_k b+\frac{N\,b}{k}\right)\int\frac{k'\,\mathrm{d}k'}{2\,\pi}\,\frac{1}{\mathcal{I}^{+}_{k'}}\,\partial_{k'}f^{\mathrm{eq}\prime}_{\hat{\boldsymbol{b}}}\\
&\qquad\times\int_{\theta'}W_{kk'\Delta\theta}\,\frac{\sin N\Delta\theta\,\sin\Delta\theta}{b^2-b'^2}\,,\\
\delta\sigma^Y &= -\frac{1}{2\,\pi}\int\frac{k\,\mathrm{d}k}{2\pi}\,\frac{1}{\mathcal{I}^{+}_k}\,\partial_k b\int\frac{k'\,\mathrm{d}k'}{2\,\pi}\left(\frac{\mathcal{I}^{\mathrm{s}}_{k'}}{\mathcal{I}^{+}_{k'}}\,\partial_{k'}f^{\mathrm{eq}\prime}_{\hat{\boldsymbol{b}}}+\frac{N}{k'}\,f^{\mathrm{eq}\prime}_{\hat{\boldsymbol{b}}}\right)\\
&\qquad\times\int_{\theta'}W_{kk'\Delta\theta}\,\frac{\sin N\Delta\theta\,\sin\Delta\theta}{b^2-b'^2}\,,
\end{aligned}\tag{5.100}$$

where we introduced the notation $W_{kk'\Delta\theta}:=W_{\boldsymbol{kk'}}$. It is easily seen that for point-like impurities the angular integral vanishes trivially for $|N|\geq 2$.

At zero temperature the correction (5.100) can be written as

$$\begin{aligned}
\delta\sigma^X &= -\frac{k_{\mathrm{F}}}{8\,\pi^2\,\mathcal{I}^{+}_{\mathrm{F}}}\int\frac{k\,\mathrm{d}k}{2\,\pi}\left(\frac{\mathcal{I}^{\mathrm{s}}_k}{\mathcal{I}^{+}_k}\,\partial_k b+\frac{N\,b}{k}\right)\int_{\theta'}W_{kk_{\mathrm{F}}\Delta\theta}\,\frac{\sin N\Delta\theta\,\sin\Delta\theta}{b^2-{b_{\mathrm{F}}}^2}\,,\\
\delta\sigma^Y &= +\frac{k_{\mathrm{F}}\,\mathcal{I}^{\mathrm{s}}_{\mathrm{F}}}{8\,\pi^2\,\mathcal{I}^{+}_{\mathrm{F}}}\int\frac{k\,\mathrm{d}k}{2\,\pi}\,\frac{1}{\mathcal{I}^{+}_k}\,\partial_k b\int_{\theta'}W_{kk_{\mathrm{F}}\Delta\theta}\,\frac{\sin N\Delta\theta\,\sin\Delta\theta}{b^2-{b_{\mathrm{F}}}^2}\\
&\quad+\frac{N}{8\,\pi^2}\int\frac{k\,\mathrm{d}k}{2\,\pi}\,\frac{1}{\mathcal{I}^{+}_k}\,\partial_k b\int_{k_{\mathrm{F}}}^{\infty}\mathrm{d}k'\int_{\theta'}W_{kk'\Delta\theta}\,\frac{\sin N\Delta\theta\,\sin\Delta\theta}{b^2-b'^2}\,,
\end{aligned}\tag{5.101}$$

and in the monolayer case $N=\pm1$ (with $\partial_k b=\frac{b}{k}=v_{\mathrm{F}}$ and writing $\mathcal{I}^{+}_k=\frac{k}{4\,\pi\,v_{\mathrm{F}}}\int_{\theta'}W_{kk\Delta\theta}\,\sin^2\Delta\theta$) this can be simplified to the form

$$\begin{aligned}
\delta\sigma^X &= -\frac{e^2}{2\,\pi\,h}\,\frac{\int\mathrm{d}k\,\frac{k}{k^2-k_{\mathrm{F}}^2}\int_{\theta'}W_{kk_{\mathrm{F}}\Delta\theta}\sin^2\Delta\theta}{\int_{\theta'}W_{k_{\mathrm{F}}k_{\mathrm{F}}\Delta\theta}\,\sin^2\Delta\theta}\,,\\
\delta\sigma^Y &= +\frac{e^2}{2\,\pi\,h}\int\mathrm{d}k\,\frac{k_{\mathrm{F}}}{k^2-k_{\mathrm{F}}^2}\,\frac{\int_{\theta'}W_{kk_{\mathrm{F}}\Delta\theta}\,\sin^2\Delta\theta}{\int_{\theta'}W_{kk\Delta\theta}\,\sin^2\Delta\theta}+\\
&\quad+\frac{e^2}{2\,\pi\,h}\int\mathrm{d}k\int_{k_{\mathrm{F}}}^{\infty}\mathrm{d}k'\,\frac{1}{k^2-k'^2}\,\frac{\int_{\theta'}W_{kk'\Delta\theta}\,\sin^2\Delta\theta}{\int_{\theta'}W_{kk\Delta\theta}\,\sin^2\Delta\theta}\,.
\end{aligned}\tag{5.102}$$

Here, we reintroduced e and $\hbar$. For point-like impurities these integrals are easily evaluated:

$$\begin{aligned}
\delta\sigma^X/\tfrac{e^2}{2\,\pi\,h} &= -\textstyle\int_0^{k_\Lambda}\mathrm{d}k\,\frac{k}{k^2-k_{\mathrm{F}}^2} &&= -\log\tfrac{k_\Lambda}{k_{\mathrm{F}}}+\mathcal{O}((\tfrac{k_{\mathrm{F}}}{k_\Lambda})^2)\,,\\
\delta\sigma^Y/\tfrac{e^2}{2\,\pi\,h} &= \textstyle\int_0^{k_\Lambda}\mathrm{d}k\,\frac{k_{\mathrm{F}}}{k^2-k_{\mathrm{F}}^2}+\int_0^{k_\Lambda}\mathrm{d}k\int_{k_{\mathrm{F}}}^{k_\Lambda}\mathrm{d}k'\,\frac{1}{k^2-k'^2} &&= -\tfrac{\pi^2}{8}+\mathcal{O}((\tfrac{k_{\mathrm{F}}}{k_\Lambda})^2)\,,
\end{aligned}\tag{5.103}$$

where an ultraviolet cutoff $k_\Lambda\gg k_{\mathrm{F}}$ was introduced. Notice that only $\delta\sigma^X$ is ultraviolet divergent.

The total quantum correction is

$$\delta\sigma \;=\; 4\,(\pm\delta\sigma^X\pm\delta\sigma^Y)\tag{5.104}$$

with the relative prefactors (possibly zero) given by (5.46) for the different approaches. Notice that here, in contrast to the situation in section 5.7, not in all approaches the leading quantum correction is positive. For point-like impurities in particular, we find

			$\delta\sigma/\frac{2\,e^2}{\pi\,h}$
LvN & NSO &	G1	GKBA	$-\log\frac{k_\Lambda}{k_\mathrm{F}}-\frac{\pi^2}{8}$
	G1	AA	$-\log\frac{k_\Lambda}{k_\mathrm{F}}+\frac{\pi^2}{8}$
	G1	SKBA	$-\log\frac{k_\Lambda}{k_\mathrm{F}}$
	G2	GKBA	$-\frac{\pi^2}{8}$
	G2	AA	$+\frac{\pi^2}{8}$
	G2	SKBA	0

(5.105)

The leading quantum correction is ultraviolet divergent for all the G1 approaches, including the density matrix approaches, whereas it is convergent for the G2 approaches. Furthermore, only the approach G2wAA gives a positive correction, namely

$$\delta\sigma \;=\; \frac{\pi\,e^2}{4\,h} \qquad (\mathrm{G2wAA})\,. \tag{5.106}$$

In the Boltzmann regime $\ell k_\mathrm{F} \gg 1$ this is a small positive shift to the much larger Drude conductivity $4\,\sigma_0 = \frac{2\,e^2}{h}\,\ell\,k_\mathrm{F} = \frac{e^2}{h}\,\frac{8\,v_\mathrm{F}^2}{n_\mathrm{imp}\,V_0^2}$ for a constant potential $V_{\boldsymbol{k}\boldsymbol{k}'} = V_0$. We mention that for screened charge impurities ultraviolet divergences are absent.

To obtain a contribution of order $(\ell k_\mathrm{F})^{-1}$, which should explain the initial onset of convexity in the conductivity as one approaches the Dirac regime, one can iterate this recursive procedure. Since again one only needs to insert known distribution functions into the integrals containing principal values, an analytical solution is possible although increasingly cumbersome.

The result (5.106) applies to point-like impurities. Strictly speaking, in that case the assumption of negligible inter-valley scattering should break down. It is therefore questionable if the results can be used to discuss actual experiments on graphene. This caveat does of course not apply to numerical simulations of graphene including only one cone, nor to topological insulators with only one Dirac cone to start with. Our main motivation, however, is graphene with screened charged impurities and in particular monolayer graphene with the screening parameter $q_\mathrm{s} := k_\mathrm{TF}/k_\mathrm{F} \approx 3.2$ relevant for samples on SiO_2 substrates. We assume that this is already long-range enough for inter-valley scattering to be of secondary importance. In that case the two-valley results and one-valley results should be roughly the same, and we can discuss the former relying on results for the latter. We can now speculate that our leading quantum correction could be one of the contributions to the residual conductivity observed in the experiments of Chen *et al.* [2008]. The value of this correction depends only on the dimensionless parameter q_s, which, for monolayers, is independent of k_F and hence independent of the electron density. This leads to a rigid vertical shift of the Drude conductivity as a function of electron density as illustrated in Figure 5.1. The size of this shift depends only on natural constants and the dielectric constant hidden in k_TF. Thus, the quantum correction could depend on the dielectric environment of the monolayer graphene sample.

We have already given a quantitative evaluation for the correction $(\ell k_\mathrm{F})^0$ in the limit $q_\mathrm{s} \to \infty$, since here this limit coincides with that of point-like impurities. (This was *not* the case for the Drude conductivity, see Section 5.3. There the absolute scaling with k_F in the scattering times was relevant, in contrast to the case of the correction (5.102).) We have also evaluated the shift (5.102) in the opposite limit $q_\mathrm{s} = 0 < 1$ of an unscreened Coulomb interaction. We find the corrections to be ultraviolet divergent and we find the sign of σ^Y to be the opposite. However, since $q_\mathrm{s} \approx 3.2 > 1$, we expect the limit $q_\mathrm{s} \to \infty$ to be the more relevant limit. Therefore we expect also for the realistic value $q_\mathrm{s} = 3.2$ to encounter the case that only the approach G2wAA gives a positive value and that this value is likely to be close to (5.106). In case inter-valley scattering is negligible with $q_\mathrm{s} = 3.2$ this value should then also be relevant for the two-valley situation and thus for graphene experiments.

It is known that in real graphene samples puddle formation due to charge inhomogeneities leads to a variation in the Fermi level, see *e.g.* Das Sarma *et al.* [2011]. However, the shift $\delta\sigma$ derived here should be insensitive at least to small variations, as it is independent of the Fermi level. In the case where the impurities are located at a non-negligible average distance d from the graphene plane, this introduces a second dimensionless parameter $k_\mathrm{F}\, d$, which depends on the density. In this scenario, $\delta\sigma$ becomes density dependent and the shift is no more rigid. However, in the Fermi momentum range $\ell^{-1} \ll k_\mathrm{F} \ll d^{-1}$, which is the range where the Drude conductivity should be linear, the effect on the statements above should be negligible. Thus, the residual conductivity we make predictions for should be fitted only from the "strictly" linear part of the Boltzmann conductivity.

Monolayer graphene stands out in many respects and comes with many surprises compared to multilayer graphene because of the linear dispersion and the unit winding number $|N| = 1$. (See also Shytov *et al.* [2006] and Kailasvuori [2009] on why the case $|N| = 1$ is special.) As stated already in Section 5.3, monoalyers are different from multilayers and 2DEGs with respect to how the screening depends on the electron density. Therefore, we cannot straight away discard as unphysical the finding of finite effects of electron-hole coherences far away from the Dirac regime, although we expect no such effects in general and in particular not in multilayers. In both monolayers and multilayers the Fermi surface—and therefore the number of electrons contributing to a nonequilibrium response—grows linearly with k_F. A Kubo formula for the conductivity (see *e.g.* Eq. (2) in Trushin *et al.* [2010]) disfavors matrix elements between states of large energy differences. The Zitterbewegung contribution from each electron would therefore be suppressed by the large energy denominators $1/[\epsilon^+(k_\mathrm{F}) - \epsilon^-(k_\mathrm{F})] \sim \epsilon^{-1}(k_\mathrm{F})$. In the case of multilayers the suppression wins for large k_F. However, in the monolayer case the two effects compensate each other, wherefore a finite effect of Zitterbewegung at large energy splitting is not inconceivable.

One might worry about the electron-hole coherent effects being negligible compared to weak localization corrections. However, this is not necessarily the case, as was shown in recent calculations by Trushin *et al.* [2010], where the analytically found electron-hole coherent conductivity is close to the numerically exact value, with the small and rather constant discrepancy that is probably due to weak localization. Nor should the electron-hole coherent shift in monolayers be negligible in the residual conductivity since we find it to be of the order of one quantum of conductance. Further, the different leading-order quantum corrections can be cleanly separated and can thus be treated independently.

From the kinetic equation treatment of weak localization in Rammer and Smith [1986] we see that the weak localization correction takes only the Drude response part of the non-equilibrium Green's function as an input and not the full Green's function including contributions of higher order in $(\ell\, k_\mathrm{F})^{-1}$. Thus, like the Drude response, the weak localization correction should be independent of the choice of formalism. Therefore, we believe that the weak localization correction and our $(\ell\, k_\mathrm{F})^0$ correction can be considered separately and that the issue of formalism affects only the latter.

5.9. Summary

In this chapter, we have compared several derivations of semiclassical spin coherent Boltzmann equations for a relevant physical problem where differences could matter: the electron-hole coherence originated quantum corrections to the Drude conductivity for Dirac electrons as encountered in graphene or in the surface states of 3d topological insulators. We find these quantum corrections to be sensitive to the approach. The leading quantum correction in monolayer graphene turns out to be particularly interesting as a litmus test, and we suggest that a precise determination of this contribution from numerical work or experiments might single out a unique approach as the correct one.

This discrepancy between established approaches was our motivation to search for an ansatz that provides the link between a derivation based on the Liouville-von Neumann equation and a Green's function derivation. The simple structure of the collision integrals in their general forms as derived here makes this search unambiguous. We find the missing link, at least for the case of electron-impurity interactions in the lowest Born approximation, and propose a novel "anti-ordered" ansatz of a simple albeit counterintuitive form.

The fact that the (pseudo)spin-orbit interaction is an important contribution in the Hamiltonian is essential for the differences between formalisms to arise in the first place. On the other hand, the specific feature of graphene that the pseudospin-orbit coupling constitutes the *entire* kinetic energy simplifies the collision integral considerably and makes an analytical solution possible. The analytical treatment becomes non-trivial due to the presence of principal value terms. We have discussed the physical origin of these terms and have explained why one should take them seriously in the present context. In addition, we have shown how to deal with them on a practical level for for not too long-ranged scalar impurity potentials. We have kept the winding number of the spin-orbit coupling general in order to address single layer graphene as well as multilayer graphene.

The first quantum correction depends both on the chosen formalism as well as on whether or not principal value terms are included. With principal value terms neglected the leading-order quantum correction is of order $(\ell\, k_\mathrm{F})^{-1}$. When they are included and do not vanish the leading quantum correction is of order $(\ell\, k_\mathrm{F})^0$. An electron-hole coherence originated quantum correction $\sim (\ell\, k_\mathrm{F})^0$ is a counterintuitive result, as it implies that electron-hole coherent effects remain finite even far away from the Dirac regime. We discussed why such a result in the case of monolayer graphene is not absurd, albeit surprising. For multilayers we do not expect such a result, and indeed for point-like impurities the

correction $\sim (\ell\, k_{\mathrm{F}})^0$ vanishes trivially.[5]

We argued that in monolayers the shift due to electron-hole coherences depends only on the dielectric constant through the dimensionless parameter q_{s}. The leading correction as evaluated for monolayers with point-like impurities should be closely related to the one relevant to experiments, since for monolayers on SiO_2 substrates the screening parameter $q_{\mathrm{s}} \approx 3.2$ is larger than one, and therefore it is arguably more related to the limit $q_{\mathrm{s}} = \infty$ than to the limit $q_{\mathrm{s}} = 0$. Such a shift could be one of the contributions in the residual conductivity observed in recent experiments [Chen *et al.*, 2008]. Our contribution $\delta\sigma$ given in Eqs. (5.102) depends crucially on the approach to the derivation of collision integrals. With an accurate measurement of the residual conductivity and a precise knowledge of other contributions (*e.g.* weak (anti-)localization) that one would need to take into account, monolayer graphene would offer an unprecedented setting for experimentally singling out the appropriate approach among the alternatives studied in the present chapter. In a comparison with numerics one would of course have a more controlled setting. The observed residual conductivity is positive. If also the contribution from electron-hole coherences was (experimentally or numerically) determined to be positive, this would make a case for the approach called G2wAA, which uses the "anti-ordered" ansatz proposed here.

Historically, the more technical work on the problem of ansatz and in particular the introduction of the Generalized Kadanoff-Baym ansatz (GKBA) [Lipavsky *et al.*, 1986] was prompted by the study of high-field transport for spinless electrons, see Haug and Jauho [2008]. It would therefore be interesting to study the consequences of our ansatz on transport beyond linear response. The two ansatzes certainly differ when electron-hole coherent effects are important, but it is not known to us if there is a difference for spinless electrons.

All approaches considered in our comparative study might still have to be refined in the future in order to accurately describe (pseudo)spin coherent effects on transport. The elaborate literature on the Boltzmann regime transport in spinless electrons offers at least two directions for improvement that could also be relevant for the quantum corrections in the conductivity due to (pseudo)spin-orbit interactions:

The first possible refinement consists in a proper accounting for of all terms that could contribute to linear order in the electric field, *e.g.*, by taking into account that also the noninteracting response functions $G^{0\mathrm{R}}$ and $G^{0\mathrm{A}}$ are modified by the electric field and that in a gauge invariant formulation the first-order gradient expansion of the self-energy terms includes electric field contributions. For electron systems with a trivial spin index these issues have been discussed for more than two decades in the context of high-electric-field transport [Zubarev *et al.*, 1996; Haug and Jauho, 2008; Mahan, 1990]. In the context of spin-orbit interactions they have been addressed recently by Kailasvuori [2009].

A second way to improve upon the presented kinetic description could lie in an accu-

[5] For screened charged impurities in multilayer graphene one encounters the situation that the potential approaches the limit of the unscreened Coulomb potential when one increases the density (opposite behavior to monolayers). Since our kinetic description disregards renormalization effects of the free drift, our analysis should break down when the quasiparticle spends a sizable fraction of its time within the range of the impurities. Therefore, we do not attempt to evaluate the correction $\sim (\ell\, k_{\mathrm{F}})^0$ for multilayers with charged impurities in the high density limit, where the screening is weak.

rate extraction of the quasiparticle part f in the kinetic equation for ρ (or $G^<$) and a proper incorporation of renormalizations of the free drift as presented by Špička *et al.* [1997]. This procedure unveils the qualitative difference between the electron distribution function ρ and the quasiparticle distribution f. The difference appears as a wave function renormalization factor and as an extra term containing principal values. The latter term is related to the quickly decohering off-shell motion from the redressing of the quasiparticle within the interaction radius. For single-band electrons these issues have been investigated already for some two decades, *e.g.*, in the context of Boltzmann equation treatments of Fermi systems with strong two-body interactions (for an extensive review we refer to Lipavský *et al.* [2001]). Here it becomes important to recognize that $f^{\mathrm{eq}} = f_{\mathrm{FD}} \neq \rho^{\mathrm{eq}}$. Only by properly separating out the coherences related to the quasiparticle redressing one can in a controlled way extract a Boltzmann equation, which can then be solved by linearizing in deviations from an equilibrium state described by the Fermi-Dirac distribution f_{FD}.

6. Conclusions and Outlook

In the present thesis, we have presented a semiclassical approach to relaxation and transport phenomena in systems where (pseudo)spin-orbit coupling plays an important role. We have focused on a coherent treatment of the (pseudo)spin degrees of freedom in kinetic equations and the resulting transport equations.

In the context of spintronics, the relaxation of the persistent spin helix has been discussed. Our work is motivated by the recent realization of a long-lived helical spin wave inside a spin-orbit tuned GaAs/GaAlAs quantum well [Koralek *et al.*, 2009]. The observation of an intriguing temperature dependence of the lifetime of this persistent spin helix has initiated our investigation of the influence of electron-electron interactions in combination with possible symmetry breaking mechanisms, which cause a finite lifetime in the first place. Our main finding is that, at finite temperatures, the magnitude of this lifetime results essentially from an interplay of cubic Dresselhaus spin-orbit interaction and electron-electron scattering. We have proposed a modified, spatially damped sinusoidal spin profile for a transient spin grating experiment in order to enhance the lifetime. In theory, the infinite lifetime can thus be restored even in the presence of SU(2) breaking mechanisms as long as these appear as relaxation rates in the semiclassical spin diffusion equation. More generally, our results can be viewed as a generalization of the Boltzmann-equation based derivation of spin Coulomb drag for the *collinear* case [Flensberg *et al.*, 2001] to a *coherent* description, which is necessary to capture spin precession, *e.g.*, in the presence of intrinsic spin-orbit coupling.

We have furthermore investigated the influence of the Hartree-Fock mean field interaction on the persistent spin helix state. This exchange field causes an additional precession term that rotates anisotropic parts of the spin distribution function around the local spin density. The resulting nonlinear corrections in the spin diffusion equation have important consequences: (i) the lifetime of the persistent spin helix can be enhanced considerably and (ii) the pattern is modified and acquires a finite third spin component. In addition, higher spatial harmonics occur as a consequence of the Hartree-Fock term.

In the context of graphene, we have executed a comparative study of several approaches that are used to derive pseudospin coherent Boltzmann equations. We have presented a calculation of the resulting corrections to the Drude conductivity of graphene including leading-order corrections due to electron-hole coherences, which could possibly constitute a part of the residual conductivity observed in recent experiments by Chen *et al.* [2008]. We have found that it is important to include the (often neglected) Principal value terms in the collision integrals. Morover, the result has turned out to depend on the chosen formalism for the derivation of the kinetic equation. We have proposed a modified ansatz distribution (replacing the Generalized Kadanoff-Baym ansatz) that would restore the consistency between a derivation of the kinetic equation based on the Liouville-von Neumann equation and a Green's function derivation.

The results presented in this thesis have several avenues for future research. In connection with the persistent spin helix it would be interesting to include in our semiclassical theory further relevant effects that break the SU(2) symmetry. Natural candidates are disorder in the local Rashba spin-orbit coupling [Sherman, 2003] or spin-dependent electron-electron scattering [Glazov *et al.*, 2010]. The description could also be extended to drifting spin patterns [Yang *et al.*, 2011], which are conceptually closer to (useful) spintronics applications. Another prospect for future work is the investigation of the effects of hyperfine interaction with nuclear spins on the persistent spin helix. This problem should be accessible to an approach that is very similar to the presented treatment of the Hartree-Fock interactions.

All approaches considered in our comparative study of the Boltzmann conductivity of graphene might still have to be refined in the future in order to accurately (and consistently) describe (pseudo)spin coherent effects on transport. One possible direction of improvement consists in a proper accounting of all terms that could contribute to linear order in the electric field, *e.g.*, by taking into account that in a gauge invariant formulation the first-order gradient expansion of self-energy terms includes electric field contributions. For electron systems with a trivial spin index these issues have been extensively discussed in the context of high-electric-field transport [Zubarev *et al.*, 1996; Haug and Jauho, 2008; Mahan, 1990]. In the context of spin-orbit interactions they have been addressed recently by Kailasvuori [2009]. A second way to refine the kinetic description could lie in an accurate extraction of the quasiparticle part in the kinetic equation for the density matrix and a proper incorporation of renormalizations of the free drift as presented by Špička *et al.* [1997].

A. Coarse-grained dynamics in the D'yakonov-Perel' regime

In Chapter 3.3.2 we argue that in order to describe the slow precession-diffusion dynamics of the real space spin density $\boldsymbol{S}$ in the D'yakonov-Perel' regime ($b_F\tau \ll 1$), we can neglect the time derivatives in the kinetic equations for the anisotropic components of the spin density. This amounts to replacing the time derivative of the real space spin density by a coarse-grained one, *i.e.* $\partial_t \boldsymbol{S} \to \Delta\boldsymbol{S}/\Delta t$ with $\Delta t \approx b_F^{-1} \gg \tau$. To see this also formally, consider a simplified version of the Boltzmann equation (3.16) with precession about the Rashba field as the only driving term and without electron-electron interactions. The generalization to our actual problem is then straightforward. The isotropic equation integrated over $\boldsymbol{k}$ then reads

$$\frac{\mathrm{d}\boldsymbol{S}}{\mathrm{d}t'} = \int \frac{\mathrm{d}\boldsymbol{k}}{(2\pi)^2}\, 2\,\boldsymbol{b}_R(\boldsymbol{k}) \times \boldsymbol{s}_{\boldsymbol{k},1}(t')\,. \tag{A.1}$$

The anisotropic equation is

$$\frac{\mathrm{d}\boldsymbol{s}_{\boldsymbol{k},1}}{\mathrm{d}t'} = -\frac{\boldsymbol{s}_{\boldsymbol{k},1}(t')}{\tau} + \frac{4\pi}{m}\, f'(\epsilon_k)\, \boldsymbol{S}(t') \times \boldsymbol{b}_R(\boldsymbol{k})\,. \tag{A.2}$$

Within our coarse graining approximation we have a constant slope $\Delta\boldsymbol{S}/\Delta t$ within every time interval Δt around t. Thus replace in (A.2) $\boldsymbol{S}(t') = \boldsymbol{S}(t) + \frac{\Delta\boldsymbol{S}}{\Delta t}(t)\,(t'-t)$ and solve for $\boldsymbol{s}_{\boldsymbol{k},1}(t')$,

$$\boldsymbol{s}_{\boldsymbol{k},1}(t') = -\tau\,\frac{\mathrm{d}\boldsymbol{s}_{\boldsymbol{k},1}}{\mathrm{d}t'} + \frac{4\pi\tau}{m}\, f'(\epsilon_k)\, \left(\boldsymbol{S}(t) + \frac{\Delta\boldsymbol{S}}{\Delta t}(t)\,(t'-t)\right) \times \boldsymbol{b}_R(\boldsymbol{k})\,. \tag{A.3}$$

Plug this in (A.1) and take the temporal average, $b_F \int_{t-\frac{1}{2b_F}}^{t+\frac{1}{2b_F}} \mathrm{d}t'$ [Eq. (A.1)], to obtain

$$\begin{aligned}\frac{\Delta\boldsymbol{S}}{\Delta t}(t) = {} & \frac{4\pi\tau}{m} \int \frac{\mathrm{d}\boldsymbol{k}}{(2\pi)^2}\, f'(\epsilon_k)\, 2\,\boldsymbol{b}_R(\boldsymbol{k}) \times (\boldsymbol{S}(t) \times \boldsymbol{b}_R(\boldsymbol{k})) \\ & -b_F\tau \int \frac{\mathrm{d}\boldsymbol{k}}{(2\pi)^2}\, 2\,\boldsymbol{b}_R(\boldsymbol{k}) \times \underbrace{\left[\boldsymbol{s}_{\boldsymbol{k},1}(t+1/2b_F) - \boldsymbol{s}_{\boldsymbol{k},1}(t-1/2b_F)\right]}_{\mathcal{O}(b_F\tau)}\,.\end{aligned} \tag{A.4}$$

Neglecting the second term, since it is of higher order in the small $b_F\tau$ (the anisotropic components of the distribution function arise only as a consequence of spin-orbit coupling), we arrive at what we would have obtained by simply neglecting the time derivative in Eq. (A.2), *i.e.*, by inserting the steady state anisotropic equation in the isotropic one. Thus, to leading order, it is sufficient to find the (quasi-)equilibrium solutions for the anisotropic coefficients.

B. Evaluation of the two-body collision integrals

In this appendix we bring the expressions of the spin relaxation rates due to electron-electron scattering, which play a key role in Chapter 3, to a form that is well suited for numerical evaluation with standard Monte Carlo integration routines.

The winding-number-± 1 electron-electron collision integrals

The electron-electron relaxation rate $\tau_{\text{e-e},1}^{-1}$ for winding-number-± 1 and liear-in-momentum parts of the spin distribution function is obtained from Eq. (3.42) with Eq. (3.43). When we restore $\hbar$ and abbreviate $\beta \equiv (k_B T)^{-1}$, we have

$$\begin{aligned}\frac{1}{\tau_{\text{e-e},1}} \;=\; & -\frac{2\,\hbar\beta}{k_F^2 m\,(2\pi)^4}\int \mathrm{d}\boldsymbol{k_1}\int \mathrm{d}\boldsymbol{k_2}\int \mathrm{d}\boldsymbol{k_3}\,\delta(\epsilon_{k_1}+\epsilon_{k_2}-\epsilon_{k_3}-\epsilon_{\boldsymbol{k_1}+\boldsymbol{k_2}-\boldsymbol{k_3}}) \\ & |V(|\boldsymbol{k_1}-\boldsymbol{k_3}|)|^2\,[1-f(\epsilon_{k_3})]\,[1-f(\epsilon_{\boldsymbol{k_1}+\boldsymbol{k_2}-\boldsymbol{k_3}})]\,f(\epsilon_{k_1})\,f(\epsilon_{k_2}) \\ & [\cos([\theta_3-\theta_1])\,k_3-k_1]\;.\end{aligned} \tag{B.1}$$

The exchange part vanished due to momentum conservation. Substitute $\boldsymbol{k_3}\to\boldsymbol{k_1}+\boldsymbol{q}$, relabel $\boldsymbol{k_1}\to\boldsymbol{k}$, $\boldsymbol{k_2}\to\boldsymbol{k'}$ and make use of the identities

$$\delta(\epsilon_k+\epsilon_{k'}-\epsilon_{\boldsymbol{k}+\boldsymbol{q}}-\epsilon_{\boldsymbol{k'}-\boldsymbol{q}}) \;=\; \int_{-\infty}^{\infty}\mathrm{d}\hbar\omega\,\delta(\epsilon_k-\epsilon_{\boldsymbol{k}+\boldsymbol{q}}-\hbar\omega)\,\delta(\epsilon_{k'}-\epsilon_{\boldsymbol{k'}-\boldsymbol{q}}+\hbar\omega)$$

and

$$f(\epsilon_k)\,[1-f(\epsilon_k+\hbar\omega)] \;=\; \frac{f(\epsilon_k)-f(\epsilon_k+\hbar\omega)}{1-e^{-\beta\,\hbar\omega}}$$

to replace in the integrand:

$$\begin{aligned}& \delta(\epsilon_k+\epsilon_{k'}-\epsilon_{\boldsymbol{k}+\boldsymbol{q}}-\epsilon_{\boldsymbol{k'}-\boldsymbol{q}})\,[1-f(\epsilon_{\boldsymbol{k}+\boldsymbol{q}}]\,\left[1-f(\epsilon_{\boldsymbol{k'}-\boldsymbol{q}})\right]\,f(\epsilon_k)\,f(\epsilon_{k'}) \\ = \;& -\int_{-\infty}^{\infty}\mathrm{d}\hbar\omega\,\frac{1}{4\,\sinh^2(\beta\,\hbar\omega/2)}\,\delta(\epsilon_k-\epsilon_{\boldsymbol{k}+\boldsymbol{q}}-\hbar\omega)\,\delta(\epsilon_{k'}-\epsilon_{\boldsymbol{k'}-\boldsymbol{q}}+\hbar\omega) \\ & [f(\epsilon_k)-f(\epsilon_k-\hbar\omega)]\,[f(\epsilon_{k'})-f(\epsilon_{k'}+\hbar\omega)]\,.\end{aligned}$$

In the next step, translate the angular integral over $\theta_{\boldsymbol{k}}$ into one over θ_{kq}, *i.e.*, the angle between $\boldsymbol{k}$ and $\boldsymbol{q}$. Express $\theta_{\boldsymbol{k}+\boldsymbol{q}}-\theta_{\boldsymbol{k}}$ in terms of θ_{kq}:

$$\begin{aligned}\boldsymbol{k}\cdot(\boldsymbol{k}+\boldsymbol{q}) \;&=\; k\,|\boldsymbol{k}+\boldsymbol{q}|\,\cos(\theta_{\boldsymbol{k}+\boldsymbol{q}}-\theta_{\boldsymbol{k}}) \\ \Leftrightarrow\quad k^2+k\,q\,\cos\theta_{kq} \;&=\; k\sqrt{k^2+q^2+2\,k\,q\cos\theta_{kq}}\,\cos(\theta_{\boldsymbol{k}+\boldsymbol{q}}-\theta_{\boldsymbol{k}}) \\ \Leftrightarrow\quad |\boldsymbol{k}+\boldsymbol{q}|\,\cos(\theta_{\boldsymbol{k}+\boldsymbol{q}}-\theta_{\boldsymbol{k}}) \;&=\; k+q\cos\theta_{kq}\,.\end{aligned} \tag{B.2}$$

With this, Eq. (B.1) becomes

$$\begin{aligned}\frac{1}{\tau_{\text{e-e},1}} &= \frac{\hbar^2\beta}{k_F^2 m\, 2(2\pi)^4}\int \mathrm{d}\boldsymbol{q}\,|V(q)|^2\, q\,\cos^2\theta_{\boldsymbol{q}}\int_{-\infty}^{\infty}\mathrm{d}\omega\,\frac{1}{\sinh^2(\beta\hbar\omega/2)}\\ &\quad\int \mathrm{d}\boldsymbol{k'}\,\delta(\epsilon_{k'}-\epsilon_{\boldsymbol{k'}-\boldsymbol{q}}+\hbar\omega)\,[f(\epsilon_{k'})-f(\epsilon_{k'}+\hbar\omega)]\\ &\quad\int \mathrm{d}\boldsymbol{k}\,\delta(\epsilon_k-\epsilon_{\boldsymbol{k}+\boldsymbol{q}}-\hbar\omega)\,[f(\epsilon_k)-f(\epsilon_k-\hbar\omega)]\,k\,\cos\theta_{kq}\,.\end{aligned}$$

Now write

$$\begin{aligned}\delta(\epsilon_{k'}-\epsilon_{\boldsymbol{k'}-\boldsymbol{q}}+\hbar\omega) &= \frac{m}{\hbar^2 k' q}\,\delta\left(\cos\theta_{k'q}-\frac{q}{2k'}+\frac{\omega m}{\hbar k' q}\right),\\ \delta(\epsilon_k-\epsilon_{\boldsymbol{k}+\boldsymbol{q}}-\hbar\omega) &= \frac{m}{\hbar^2 k\, q}\,\delta\left(\cos\theta_{kq}+\frac{q}{2k}+\frac{\omega m}{\hbar k\, q}\right)\end{aligned}$$

and substitute $x\equiv\cos\theta_{kq}$, $y\equiv\cos\theta_{k'q}$. Exploit that the integrand is symmetric about π to write

$$\int_0^{2\pi}\mathrm{d}\theta_{kq}\,\ldots \;=\; 2\int_{-1}^{1}\mathrm{d}x\,\frac{1}{\sqrt{1-x^2}}\,\ldots\,, \tag{B.3}$$

and analogously for the $\theta_{k'q}$ integral. We then have

$$\begin{aligned}\frac{1}{\tau_{\text{e-e},1}} &= \frac{\hbar^2\beta}{k_F^2 m\,4\,\pi}\int_{-\infty}^{\infty}\mathrm{d}\omega\,\frac{1}{\sinh^2(\beta\hbar\omega/2)}\int\mathrm{d}q\,\frac{1}{(1+\frac{a^*q}{2})^2}\\ &\quad\int\mathrm{d}k'\int_{-1}^{1}\mathrm{d}y\,\frac{1}{\sqrt{1-y^2}}\,\delta\left(y-\frac{q}{2k'}+\frac{\omega m}{\hbar k' q}\right)\,[f(\epsilon_{k'})-f(\epsilon_{k'}+\hbar\omega)]\\ &\quad\int\mathrm{d}k\int_{-1}^{1}\mathrm{d}x\,\frac{1}{\sqrt{1-x^2}}\,\delta\left(x+\frac{q}{2k}+\frac{\omega m}{\hbar k q}\right)\,[f(\epsilon_k)-f(\epsilon_k-\hbar\omega)]\;k\,x\\ &= \frac{\hbar^2\beta}{k_F^2 m\,4\,\pi}\int_{-\infty}^{\infty}\mathrm{d}\omega\,\frac{1}{\sinh^2(\beta\hbar\omega/2)}\int\mathrm{d}q\,\frac{1}{(1+\frac{a^*q}{2})^2}\\ &\quad\int\mathrm{d}k'\,\frac{1}{\sqrt{1-Y^2(k',q,\omega)}}\,\Theta(1-Y^2(k',q,\omega))\,[f(\epsilon_{k'})-f(\epsilon_{k'}+\hbar\omega)]\\ &\quad\int\mathrm{d}k\,k\,\frac{X(k,q,\omega)}{\sqrt{1-X^2(k,q,\omega)}}\,\Theta(1-X^2(k,q,\omega))\,[f(\epsilon_k)-f(\epsilon_k-\hbar\omega)]\end{aligned} \tag{B.4}$$

with the functions

$$\begin{aligned}X(k,q,\omega) &\equiv -\frac{q}{2\,k}-\frac{\omega\,m}{\hbar\,k\,q}\,,\\ Y(k',q,\omega) &\equiv \frac{q}{2\,k'}-\frac{\omega\,m}{\hbar\,k'\,q}\,.\end{aligned} \tag{B.5}$$

The collision integral (B.4) is easily evaluated with, e.g., the "AdaptiveMonteCarlo" method in `mathematica`.

Next, the relaxation rate $\tilde{\tau}_{\text{e-e},1}^{-1}$ is obtained from Eq. (3.44) with Eq. (3.43):

$$\begin{aligned}\frac{1}{\tilde{\tau}_{\text{e-e},1}} &= -\frac{\hbar\,\beta}{k_F^4 m\,(2\pi)^4}\iiint \mathrm{d}\boldsymbol{k_1}\,\mathrm{d}\boldsymbol{k_2}\,\mathrm{d}\boldsymbol{k_3}\,\delta(\epsilon_k+\epsilon_{k'}-\epsilon_{\boldsymbol{k}+\boldsymbol{q}}-\epsilon_{\boldsymbol{k'}-\boldsymbol{q}}) \\ &\quad k\,[1-f(\epsilon_{\boldsymbol{k}+\boldsymbol{q}}]\,\left[1-f(\epsilon_{\boldsymbol{k'}-\boldsymbol{q}})\right]\,f(\epsilon_k)\,f(\epsilon_{k'})\,[1-f(\epsilon_{k_3})] \\ &\quad \left\{2|V(q)|^2\,\left[\cos(\theta_{\boldsymbol{k}+\boldsymbol{q}}-\theta_{\boldsymbol{k}})\,|\boldsymbol{k}+\boldsymbol{q}|^3-k^3\right]+V(q)V(|\boldsymbol{k'}-\boldsymbol{k}-\boldsymbol{q}|)\right. \\ &\quad \left.\left\{k^3-\cos(\theta_{\boldsymbol{k}+\boldsymbol{q}}-\theta_{\boldsymbol{k}})\,|\boldsymbol{k}+\boldsymbol{q}|^3+\cos\theta_{kk'}\,k'^3-\cos(\theta_{\boldsymbol{k'}-\boldsymbol{q}}-\theta_{\boldsymbol{k}})\,|\boldsymbol{k'}-\boldsymbol{q}|^3\right\}\right.. \end{aligned} \tag{B.6}$$

With Eq. (B.2) we have

$$\begin{aligned} & & \cos(\theta_{\boldsymbol{k}+\boldsymbol{q}}-\theta_{\boldsymbol{k}})\,|\boldsymbol{k}+\boldsymbol{q}|^3 &= (k+q\cos\theta_{kq})\,(k^2+q^2+2\,k\,q\cos\theta_{kq}) \\ \Leftrightarrow & & \cos(\theta_{\boldsymbol{k}+\boldsymbol{q}}-\theta_{\boldsymbol{k}})\,|\boldsymbol{k}+\boldsymbol{q}|^3-k^3 &= k\,q^2+3\,k^2q\,\cos\theta_{kq}+q^3\cos\theta_{kq}+2\,k\,q^2\cos^2\theta_{kq} \end{aligned}$$

In the third term of the last line we use

$$\cos\theta_{kk'} = \cos\theta_{kq}\,\cos\theta_{k'q}+\sin\theta_{kq}\,\sin\theta_{k'q}\,. \tag{B.7}$$

In the last term, express $\theta_{\boldsymbol{k'}-\boldsymbol{q}}-\theta_{\boldsymbol{k}}$ in terms of $\theta_{k'q}$ and θ_{kq}:

$$\begin{aligned} & & \boldsymbol{k}\cdot\left(\boldsymbol{k'}-\boldsymbol{q}\right) &= k\,|\boldsymbol{k'}-\boldsymbol{q}|\,\cos(\theta_{\boldsymbol{k'}-\boldsymbol{q}}-\theta_{\boldsymbol{k}}) \\ \Leftrightarrow & & k\,k'\,\cos\theta_{kk'}-k\,q\,\cos\theta_{kq} &= k\sqrt{k'^2+q^2-2\,k'q\cos\theta_{k'q}}\,\cos(\theta_{\boldsymbol{k'}-\boldsymbol{q}}-\theta_{\boldsymbol{k}}) \\ & \Leftrightarrow & \cos(\theta_{\boldsymbol{k'}-\boldsymbol{q}}-\theta_{\boldsymbol{k}}) &= \frac{k'\left(\cos\theta_{kq}\,\cos\theta_{k'q}+\sin\theta_{kq}\,\sin\theta_{k'q}\right)-q\cos\theta_{kq}}{\sqrt{k'^2+q^2-2\,k'q\cos\theta_{k'q}}} \\ \Leftrightarrow & & \cos(\theta_{\boldsymbol{k'}-\boldsymbol{q}}-\theta_{\boldsymbol{k}})\,|\boldsymbol{k'}-\boldsymbol{q}|^3 &= (k'^2+q^2-2\,k'q\cos\theta_{k'q}) \\ & & & \quad\left[k'\left(\cos\theta_{kq}\,\cos\theta_{k'q}+\sin\theta_{kq}\,\sin\theta_{k'q}\right)-q\cos\theta_{kq}\right]. \end{aligned} \tag{B.8}$$

For the argument of the potential in the exchange part we need

$$|\boldsymbol{k'}-\boldsymbol{q}-\boldsymbol{k}| = \sqrt{k'^2+q^2+k^2-2\,q\,k'\,\cos\theta_{qk'}-2\,k\,k'\,\cos\theta_{kk'}+2\,q\,k\,\cos\theta_{qk}}$$

with Eq. (B.7). Thus,

$$\begin{aligned}
\frac{1}{\tilde{\tau}_{\text{e-e},1}} &= -\frac{\hbar\,\beta}{k_B\,T\,k_F^4 m\,(2\pi)^4}\iiint \mathrm{d}\boldsymbol{k_1}\,\mathrm{d}\boldsymbol{k_2}\,\mathrm{d}\boldsymbol{k_3}\,\delta(\epsilon_k+\epsilon_{k'}-\epsilon_{\boldsymbol{k}+\boldsymbol{q}}-\epsilon_{\boldsymbol{k'}-\boldsymbol{q}}) \\
&\quad k\,[1-f(\epsilon_{\boldsymbol{k}+\boldsymbol{q}}]\,\left[1-f(\epsilon_{\boldsymbol{k'}-\boldsymbol{q}})\right]\,f(\epsilon_k)\,f(\epsilon_{k'})\,[1-f(\epsilon_{k_3})] \\
&\quad \left\{2|V(q)|^2\,\left[\cos(\theta_{\boldsymbol{k}+\boldsymbol{q}}-\theta_{\boldsymbol{k}})\,|\boldsymbol{k}+\boldsymbol{q}|^3-k^3\right]+V(q)V(|\boldsymbol{k'}-\boldsymbol{k}-\boldsymbol{q}|)\right. \\
&\quad \left.\left\{k^3-\cos(\theta_{\boldsymbol{k}+\boldsymbol{q}}-\theta_{\boldsymbol{k}})\,|\boldsymbol{k}+\boldsymbol{q}|^3+\cos\theta_{kk'}\,k'^3-\cos(\theta_{\boldsymbol{k'}-\boldsymbol{q}}-\theta_{\boldsymbol{k}})\,|\boldsymbol{k'}-\boldsymbol{q}|^3\right\}\right. \\
&= \frac{\hbar^2\beta}{k_F^4 m\,4\,\pi}\int_{-\infty}^{\infty}\mathrm{d}\omega\,\frac{1}{\sinh^2(\beta\hbar\omega/2)}\int \mathrm{d}q\,\frac{1}{q\,(1+\frac{a^*q}{2})^2} \\
&\quad \int \mathrm{d}k'\,\frac{1}{\sqrt{1-Y^2}}\,\Theta(1-Y^2)\,[f(\epsilon_{k'})-f(\epsilon_{k'}+\hbar\omega)] \\
&\quad \int \mathrm{d}k\,\frac{1}{\sqrt{1-X^2}}\,\Theta(1-X^2)\,[f(\epsilon_k)-f(\epsilon_k-\hbar\omega)]\,k\,(k\,q^2+3\,k^2 q\,X+q^3X+2\,k\,q^2X^2) \\
&\quad + \frac{\hbar^2\beta}{k_F^4 m\,16\,\pi}\int_{-\infty}^{\infty}\mathrm{d}\omega\,\frac{1}{\sinh^2(\beta\hbar\omega/2)}\int \mathrm{d}q\,\frac{1}{q\,(1+\frac{a^*q}{2})} \\
&\quad \int \mathrm{d}k'\,\frac{1}{\sqrt{1-Y^2}}\,\Theta(1-Y^2)\,[f(\epsilon_{k'})-f(\epsilon_{k'}+\hbar\omega)] \\
&\quad \int \mathrm{d}k\,\frac{1}{\sqrt{1-X^2}}\,\Theta(1-X^2)\,[f(\epsilon_k)-f(\epsilon_k-\hbar\omega)] \\
&\quad \sum_{s=\pm1}\frac{1}{1+\frac{a^*}{2}\sqrt{k'^2+q^2+k^2-2\,q\,k'\,Y-2\,k\,k'\,(X\,Y+s\sqrt{(1-X^2)\,(1-Y^2)})}+2\,q\,k\,X} \\
&\quad \left\{-k\,q^2-3\,k^2 q\,X-q^3X-2\,k\,q^2X^2+k'^3\left(X\,Y+s\sqrt{(1-X^2)(1-Y^2)}\right)\right. \\
&\quad \left.-(k'^2+q^2-2\,k'q\,Y)\left[k'\left(X\,Y+s\sqrt{(1-X^2)\,(1-Y^2)}\right)-q\,X\right]\right\}
\end{aligned} \tag{B.9}$$

with $X \equiv X(k,q,\omega)$ and $Y \equiv Y(k',q,\omega)$ as defined in Eq. (B.5).

We used that

$$\begin{aligned}
&\int_0^{2\pi}\mathrm{d}\theta_k\int_0^{2\pi}\mathrm{d}\theta_{k'}\,f(\cos\theta_k,\cos\theta_{k'},\sin\theta_k\,\sin\theta_{k'}) \\
&= 2\sum_{s=\pm1}\int_0^{\pi}\mathrm{d}\theta_k\int_0^{\pi}\mathrm{d}\theta_{k'}\,f(\cos\theta_k,\cos\theta_{k'},s\,\sin\theta_k\,\sin\theta_{k'})\,.
\end{aligned} \tag{B.10}$$

The winding-number-±3 electron-electron collision integral

We proceed analogously to derive a tractable expression for $\tau_{\text{e-e},3}^{-1}$ from Eq. (3.47) with Eq. (3.43). We can write

$$\tau_{\text{e-e},3}^{-1} = D + EX \tag{B.11}$$

with D representing the direct part and EX the exchange part of the collision integral. Both parts will be treated in the following,

Direct part

Let us first calculate the direct part:

$$
\begin{aligned}
D \;\equiv\; & -\frac{2\,\hbar\beta}{k_F^3 m\,(2\pi)^4}\int \mathrm{d}\boldsymbol{k_1}\int \mathrm{d}\boldsymbol{k_2}\int \mathrm{d}\boldsymbol{k_3}\,\delta(\epsilon_{k_1}+\epsilon_{k_2}-\epsilon_{k_3}-\epsilon_{\boldsymbol{k_1}+\boldsymbol{k_2}-\boldsymbol{k_3}}) \qquad \text{(B.12)}\\
& |V(|\boldsymbol{k_1}-\boldsymbol{k_3}|)|^2\,[1-f(\epsilon_{k_3})]\,[1-f(\epsilon_{\boldsymbol{k_1}+\boldsymbol{k_2}-\boldsymbol{k_3}})]\,f(\epsilon_{k_1})\,f(\epsilon_{k_2})\\
& \left[\cos 3(\theta_3-\theta_1)\,k_3^3-k_1^3\right]\\
= \;& \frac{\hbar\beta}{k_F^3 m\,2(2\pi)^4}\int \mathrm{d}\boldsymbol{q}\,|V(q)|^2\int_{-\infty}^{\infty}\mathrm{d}\hbar\omega\int \mathrm{d}\boldsymbol{k}\int \mathrm{d}\boldsymbol{k'}\,\delta(\epsilon_k-\epsilon_{\boldsymbol{k}+\boldsymbol{q}}-\hbar\omega)\,\delta(\epsilon_{k'}-\epsilon_{\boldsymbol{k'}-\boldsymbol{q}}+\hbar\omega)\\
& \frac{\left[f(\epsilon_k)-f(\epsilon_{\boldsymbol{k}+\boldsymbol{q}})\right]\,\left[f(\epsilon_{k'})-f(\epsilon_{\boldsymbol{k'}-\boldsymbol{q}})\right]}{\sinh^2(\beta\hbar\omega/2)}\,\left[\cos 3(\theta_{\boldsymbol{k}+\boldsymbol{q}}-\theta_{\boldsymbol{k}})\,|\boldsymbol{k}+\boldsymbol{q}|^3-k^3\right].
\end{aligned}
$$

With Eq. (B.2), one has

$$
\begin{aligned}
\cos 3(\theta_{\boldsymbol{k}+\boldsymbol{q}}-\theta_{\boldsymbol{k}}) &= 4\cos^3(\theta_{\boldsymbol{k}+\boldsymbol{q}}-\theta_{\boldsymbol{k}})-3\cos(\theta_{\boldsymbol{k}+\boldsymbol{q}}-\theta_{\boldsymbol{k}})\\
&= 4\left(\frac{k+q\cos\theta_{kq}}{\sqrt{k^2+q^2+2kq\cos\theta_{kq}}}\right)^3-3\left(\frac{k+q\cos\theta_{kq}}{\sqrt{k^2+q^2+2kq\cos\theta_{kq}}}\right),\\
\cos 3(\theta_{\boldsymbol{k}+\boldsymbol{q}}-\theta_{\boldsymbol{k}})\,|\boldsymbol{k}+\boldsymbol{q}|^3 &= 4\,(k+q\cos\theta_{kq})^3-3\,(k+q\cos\theta_{kq})\,\left(k^2+q^2+2kq\cos\theta_{kq}\right)\\
&= k^3+kq^2+3k^2q\cos\theta_{kq}+q^3\cos\theta_{kq}+2kq^2\cos^2\theta_{kq}\\
&\quad -4kq^2\sin^2\theta_{kq}-4q^3\cos\theta_{kq}\sin^2\theta_{kq}\,.
\end{aligned}
$$

Thus,

$$
\begin{aligned}
D \;=\; & \frac{\hbar^2\beta}{k_F^3 m\,2(2\pi)^4}\int \mathrm{d}\boldsymbol{q}\,|V(q)|^2\int_{-\infty}^{\infty}\mathrm{d}\omega\,\frac{1}{\sinh^2(\beta\hbar\omega/2)}\\
& \int \mathrm{d}\boldsymbol{k'}\,\delta(\epsilon_{k'}-\epsilon_{\boldsymbol{k'}-\boldsymbol{q}}+\hbar\omega)\,\left[f(\epsilon_{k'})-f(\epsilon_{\boldsymbol{k'}-\boldsymbol{q}})\right]\\
& \int \mathrm{d}\boldsymbol{k}\,\delta(\epsilon_k-\epsilon_{\boldsymbol{k}+\boldsymbol{q}}-\hbar\omega)\,\left[f(\epsilon_k)-f(\epsilon_{\boldsymbol{k}+\boldsymbol{q}})\right]\\
& \left\{kq^2+3k^2q\cos\theta_{kq}+q^3\cos\theta_{kq}+2kq^2\cos^2\theta_{kq}-4kq^2\sin^2\theta_{kq}-4q^3\cos\theta_{kq}\sin^2\theta_{kq}\right\}.
\end{aligned}
$$

We then have for the direct part of the winding-number-± 3 collision integral:

$$\begin{aligned} D &= \frac{\hbar^2\beta}{k_F^3 m\, 4\pi}\int_{-\infty}^{\infty}\mathrm{d}\omega\,\frac{1}{\sinh^2(\beta\hbar\omega/2)}\int\mathrm{d}q\,\frac{1}{q\,(1+\frac{a^*q}{2})^2} \\ &\quad \int\mathrm{d}k'\int_{-1}^{1}\mathrm{d}y\,\frac{1}{\sqrt{1-y^2}}\,\delta\left(y-\frac{q}{2k'}+\frac{\omega m}{\hbar k' q}\right)\,[f(\epsilon_{k'})-f(\epsilon_{k'}+\hbar\omega)] \\ &\quad \int\mathrm{d}k\int_{-1}^{1}\mathrm{d}x\,\frac{1}{\sqrt{1-x^2}}\,\delta\left(x+\frac{q}{2k}+\frac{\omega m}{\hbar k q}\right)\,[f(\epsilon_k)-f(\epsilon_k-\hbar\omega)] \\ &\quad \left\{k\,q^2+3\,k^2 q\,x+q^3 x+2\,k\,q^2x^2-4\,k\,q^2(1-x^2)-4\,q^3x\,(1-x^2)\right\} \\ &= \frac{\hbar^2\beta}{k_F^3 m\, 4\pi}\int_{-\infty}^{\infty}\mathrm{d}\omega\,\frac{1}{\sinh^2(\beta\hbar\omega/2)}\int\mathrm{d}q\,\frac{1}{q\,(1+\frac{a^*q}{2})^2} \\ &\quad \int\mathrm{d}k'\,\frac{1}{\sqrt{1-Y^2}}\,\Theta(1-Y^2)\,[f(\epsilon_{k'})-f(\epsilon_{k'}+\hbar\omega)] \\ &\quad \int\mathrm{d}k\,\frac{1}{\sqrt{1-X^2}}\,\Theta(1-X^2)\,[f(\epsilon_k)-f(\epsilon_k-\hbar\omega)] \\ &\quad \left\{k\,q^2+3\,k^2 q\,X+q^3 X+2\,k\,q^2X^2-4\,k\,q^2(1-X^2)-4\,q^3X\,(1-X^2)\right\} \end{aligned} \tag{B.13}$$

Exchange part

The exchange part of the winding-number-± 3 collision integral reads explicitly:

$$\begin{aligned} EX &\equiv -\frac{\hbar\beta}{k_F^3 m\,(2\pi)^4}\int\mathrm{d}\boldsymbol{k}\int\mathrm{d}\boldsymbol{k'}\int\mathrm{d}\boldsymbol{q}\,\delta(\epsilon_k+\epsilon_{k'}-\epsilon_{\boldsymbol{k}+\boldsymbol{q}}-\epsilon_{\boldsymbol{k'}-\boldsymbol{q}}) \\ &\quad [1-f(\epsilon_{\boldsymbol{k}+\boldsymbol{q}})]\left[1-f(\epsilon_{\boldsymbol{k'}-\boldsymbol{q}})\right]f(\epsilon_k)\,f(\epsilon_{k'})\,V(q)\,V(|\boldsymbol{k'}-\boldsymbol{k}-\boldsymbol{q}|) \\ &\quad \left\{k^3-\cos 3(\theta_{\boldsymbol{k}+\boldsymbol{q}}-\theta_{\boldsymbol{k}})\,|\boldsymbol{k}+\boldsymbol{q}|^3+\cos 3\theta_{kk'}\,k'^3-\cos 3(\theta_{\boldsymbol{k'}-\boldsymbol{q}}-\theta_{\boldsymbol{k}})\,|\boldsymbol{k'}-\boldsymbol{q}|^3\right\} \\ &= \frac{\hbar^2\beta}{k_F^3 m\,4(2\pi)^4}\int\mathrm{d}\boldsymbol{q}\,V(q)\int_{-\infty}^{\infty}\mathrm{d}\omega\int\mathrm{d}\boldsymbol{k}\int\mathrm{d}\boldsymbol{k'}\,\delta(\epsilon_k-\epsilon_{\boldsymbol{k}+\boldsymbol{q}}-\hbar\omega)\,\delta(\epsilon_{k'}-\epsilon_{\boldsymbol{k'}-\boldsymbol{q}}+\hbar\omega) \\ &\quad \frac{[f(\epsilon_k)-f(\epsilon_{\boldsymbol{k}+\boldsymbol{q}})]\,\left[f(\epsilon_{k'})-f(\epsilon_{\boldsymbol{k'}-\boldsymbol{q}})\right]}{\sinh^2(\beta\hbar\omega/2)}\,V(|\boldsymbol{k'}-\boldsymbol{k}-\boldsymbol{q}|) \\ &\quad \left\{k^3-\cos 3(\theta_{\boldsymbol{k}+\boldsymbol{q}}-\theta_{\boldsymbol{k}})\,|\boldsymbol{k}+\boldsymbol{q}|^3+\cos 3\theta_{kk'}\,k'^3-\cos 3(\theta_{\boldsymbol{k'}-\boldsymbol{q}}-\theta_{\boldsymbol{k}})\,|\boldsymbol{k'}-\boldsymbol{q}|^3\right\}. \end{aligned}$$

The first two terms are already familiar from the treatment of the direct part. They contribute

$$\begin{aligned} k^3-\cos 3(\theta_{\boldsymbol{k}+\boldsymbol{q}}-\theta_{\boldsymbol{k}})\,|\boldsymbol{k}+\boldsymbol{q}|^3 &= -k\,q^2-3k^2q\cos\theta_{kq}-q^3\cos\theta_{kq}-2\,k\,q^2\cos^2\theta_{kq} \\ &\quad +4\,k\,q^2\sin^2\theta_{kq}+4\,q^3\cos\theta_{kq}\sin^2\theta_{kq}\,. \end{aligned}$$

Use Eq. (B.8) to find for the last term

$$\begin{aligned} \cos 3(\theta_{\boldsymbol{k'}-\boldsymbol{q}}-\theta_{\boldsymbol{k}})\,|\boldsymbol{k'}-\boldsymbol{q}|^3 &= 4\left[k'\left(\cos\theta_{kq}\,\cos\theta_{k'q}+\sin\theta_{kq}\,\sin\theta_{k'q}\right)-q\cos\theta_{kq}\right]^3 \\ &\quad -3\left[k'\left(\cos\theta_{kq}\,\cos\theta_{k'q}+\sin\theta_{kq}\,\sin\theta_{k'q}\right)-q\cos\theta_{kq}\right] \\ &\quad \left(k'^2+q^2-2k'q\cos\theta_{k'q}\right)\,. \end{aligned}$$

Thus, we finally obtain for the exchange part:

$$
\begin{aligned}
EX \quad = \quad & \frac{\hbar^2\beta}{k_F^3 m\, 16\pi} \int_{-\infty}^{\infty} \mathrm{d}\omega \, \frac{1}{\sinh^2(\beta\hbar\omega/2)} \int \mathrm{d}q \, \frac{1}{q\,(1+\frac{a^* q}{2})} \\
& \int \mathrm{d}k' \, \frac{1}{\sqrt{1-Y^2}}\, \Theta(1-Y^2)\, [f(\epsilon_{k'}) - f(\epsilon_{k'} + \hbar\omega)] \\
& \int \mathrm{d}k \, \frac{1}{\sqrt{1-X^2}}\, \Theta(1-X^2)\, [f(\epsilon_k) - f(\epsilon_k - \hbar\omega)] \\
& \sum_{s=\pm 1} \frac{1}{1+\frac{a^*}{2}\sqrt{k'^2+q^2+k^2-2\,q\,k'\,Y-2\,k\,k'\,(X\,Y+s\sqrt{(1-X^2)\,(1-Y^2)})}+2\,q\,k\,X} \\
& \big\{ -k\,q^2 - 3k^2 q\,X - q^3 X - 2\,k\,q^2 X^2 + 4\,k\,q^2(1-X^2) + 4\,q^3 X\,(1-X^2) \\
& +4\,k'^3 \left[X\,Y + s\sqrt{(1-X^2)\,(1-Y^2)}\right]^3 - 3\,k'^3 \left[X\,Y + s\sqrt{(1-X^2)\,(1-Y^2)}\right] \\
& -4\left[k'\left(X\,Y + s\sqrt{(1-X^2)\,(1-Y^2)}\right) - q\,X\right]^3 \\
& +3\left[k'\left(X\,Y + s\sqrt{(1-X^2)\,(1-Y^2)}\right) - q\,X\right]\left(k'^2 + q^2 - 2\,k' q\,Y\right)\big\}
\end{aligned}
\tag{B.14}
$$

with, again, $X \equiv X(k,q,\omega)$ and $Y \equiv Y(k',q,\omega)$ as defined in Eq. (B.5).

C. Details on the anti-ordered Kadanoff-Baym Ansatz

In Lipavsky *et al.* [1986], the correlator $G^<$ is divided into the auxiliary correlators

$$\begin{aligned} G^{<\mathrm{r}}(t_1,t_2) &= \theta(t_1-t_2)G^<(t_1,t_2)\,, \\ G^{<\mathrm{a}}(t_1,t_2) &= \theta(t_2-t_1)G^<(t_1,t_2)\,. \end{aligned} \tag{C.1}$$

By acting on $G^{<\mathrm{r}}$ with $(G^\mathrm{R})^{-1}$ from the left, using the generalized Kadanoff-Baym equation (2.63) and then acting on the result with G^R from the left one arrives at

$$\begin{aligned} G^{<\mathrm{r}}(t_1,t_2) &= iG^\mathrm{R}(t_1,t_2)G^<(t_2,t_2) + \int_{t_2}^{t_1}\mathrm{d}t\int_{-\infty}^{t_2}\mathrm{d}t'\, G^\mathrm{R}_{t_1t_2}\Sigma^\mathrm{R}_{tt'}G^<_{t't_2} + G^\mathrm{R}_{t_1t_2}\Sigma^<_{tt'}G^\mathrm{A}_{t't_2}\,, \\ G^{<\mathrm{a}}(t_1,t_2) &= -iG^<(t_1,t_1)G^\mathrm{A}(t_1,t_2) + \int_{-\infty}^{t_1}\mathrm{d}t\int_{t_1}^{t_2}\mathrm{d}t'\, G^\mathrm{R}_{t_1t_2}\Sigma^<_{tt'}G^\mathrm{A}_{t't_2} + G^<_{t_1t_2}\Sigma^\mathrm{A}_{tt'}G^\mathrm{A}_{t't_2}\,. \end{aligned} \tag{C.2}$$

We complemented this with the corresponding result for $G^{<\mathrm{a}}$ with $(G^\mathrm{A})^{-1}$ and G^A instead acting from the right. The first terms to the right sum up to the GKBA. The integrals are correction terms that fulfill several natural criteria:

(i) On the time-diagonal $t_1 = t_2$ they vanish, rendering the GKBA exact.

(ii) None of the integrals stretches to $t = +\infty$, *i.e.*, the result respects the causality of the Kadanoff-Baym equations.

(iii) One can derive the same equations for $G^>$, *i.e.*, particle-hole symmetry remains.

(iv) The spectral identity $G^< + G^> = i(G^\mathrm{R} - G^\mathrm{A})$ is still satisfied.

The solution can be used to determine $G^<$ iteratively to the desired precision. Thus, the GKBA can be seen as the first term in an expansion in the interaction strength. However, in Lipavsky *et al.* [1986] it is noted that, on top of that, the arguments of the self-energies $\Sigma_{tt'}$ run over disjoint intervals, which makes the integrals even smaller and relates it to the collision time $\tau_0 (\ll \tau_\mathrm{tr})$, *i.e.* the small time that the particles spends within the interaction radius.

For the derivation of the anti-ordered ansatz, we copy this treatment but act with the response functions from the opposite sides (*i.e.*, act on $G^{<\mathrm{r}}$ with $(G^\mathrm{R})^{-1}$ from the right, use the generalized Kadanoff-Baym equation (2.63) and then act the result with G^R again

from the right). This gives us instead

$$\begin{aligned} G^{<\mathrm{r}}(t_1,t_2) &= iG^{<}(t_1,t_1)G^{\mathrm{R}}(t_1,t_2) + \int^{t_1} \mathrm{d}t' (G^{\mathrm{R}}\Sigma^{<} + G^{<}\Sigma^{\mathrm{A}} - G^{<\mathrm{r}}\Sigma^{\mathrm{R}})_{t_1t'} G^{\mathrm{R}}_{t't_2}\,, \\ G^{<\mathrm{a}}(t_1,t_2) &= -iG^{\mathrm{A}}(t_1,t_2)G^{<}(t_2,t_2) + \int^{t_2} \mathrm{d}t\, G^{\mathrm{A}}_{t_1t} (\Sigma^{\mathrm{R}}G^{<} + \Sigma^{<}G^{\mathrm{A}} - \Sigma^{\mathrm{A}}G^{<\mathrm{a}})_{tt_2}\,. \end{aligned} \tag{C.3}$$

The criteria (i)-(iv) are still satisfied. Note in particular that the causality is respected. However, the result is a bit more complicated and this time the variables t and t' in the self-energies no longer run over disjoint time intervals. Our conclusion is that the expansion can still be seen as one in the interaction strength but no longer as one in the collision time. However, when comparing Boltzmann equations derived using Green's function techniques with one derived with a Liouville equation approach, it is sufficient to be consistent to the given order of the interaction.

Acknowledgments

Among the people who contributed in one way or another to the formation of this thesis there are some who I want to acknowledge especially.

First of all, I would like to thank Tamara Nunner for supervising my PhD project. Her support and careful guidance was essential to the accomplishment of the thesis. I am also very appreciative of my collaboration with Janik Kailasvuori whose scientific enthusiasm and endurance in discussions as well as calculations have inspired me throughout the past years. Furthermore, I would like to thank Daniel Sebastiani for co-refereeing this thesis. Felix von Oppen is gratefully acknowledged for several discussions in the beginning of my work. I have taken great benefit and pleasure from scientific as well as non-scientific interaction with numerous present and former members of AG von Oppen and AG Brouwer. I mention in particular Friedrich Gethmann, Niels Bode, Teemu Ojanen, Jeroen Danon, and Francis Wilken. Moreover, I would like to thank Brigitte Odeh for administrative help.

Outside the department, great thanks are due to my parents, my brother, my close friends and, in particular, Vladislav Nenchev for their general support and, sometimes, patience during the time I worked on this thesis.

Finally, I acknowledge funding by the Deutsche Forschungsgemeinschaft through the priority program 1285.

Curriculum Vitae

[For reasons of data protection, the curriculum vitae is not included in the online version.]

Publications

- Quantum corrections in the Boltzmann conductivity of graphene and their sensitivity to the choice of formalism—J. Stat. Mech., P06024 (2010)
  J. Kailasvuori and M. C. Lüffe

- Relaxation mechanisms of the persistent spin helix—Phys. Rev. B **84**, 075326 (2011)
  M. C. Lüffe, J. Kailasvuori, and T. S. Nunner

Bibliography

Abananin, D. A., Gorbachev, R. V., Novoselov, K. S., Geim, A. K., and Levitov, L. S., *Giant Spin-Hall Effect induced by Zeeman Interaction in Graphene* (2011), `arXiv:1103.4742v1`.

Adam, S., Brouwer, P. W., and Das Sarma, S., *Crossover from quantum to Boltzmann transport in graphene*. Phys. Rev. B **79**, 201404(R) (2009).

Akkermans, E. and Montambaux, G., *Mesoscopic Physics of Electrons and Photons*. Cambridge University Press, Cambridge, 2007.

Ando, T., *Screening Effect and Impurity Scattering in Monolayer Graphene*. J. Phys. Soc. Jpn. **75**, 074716 (2006).

Auslender, M. and Katsnelson, M. I., *Generalized kinetic equations for charge carriers in graphene*. Phys. Rev. B **76**, 235425 (2007).

Awschalom, D. D. and Flatté, M. E., *Challenges for semiconductor spintronics*. Nat. Phys. **3**, 153 (2007).

Awschalom, D. D., Loss, D., and Samarth, N. (eds.), *Semiconductor Spintronics and Quantum Computation*. Springer, Berlin, 2002.

Awschalom, D. D. and Samarth, N., *Spintronics without magnetism*. Physics **2**, 50 (2009).

Baibich, M. N., Broto, J. M., Fert, A., Van Dau, F. N., Petroff, F., Etienne, P., Creuzet, G., Friederich, A., and Chazelas, J., *Giant Magnetoresistance of (001)*Fe*/(001)*Cr *Magnetic Superlattices*. Phys. Rev. Lett. **61 (21)**, 2472 (1988).

Bernevig, B. A. and Hu, J., *Semiclassical theory of diffusive-ballistic crossover and the persistent spin helix*. Phys. Rev. B **78**, 245123 (2008).

Bernevig, B. A., Orenstein, J., and Zhang, S.-C., *Exact SU(2) Symmetry and Persistent Spin Helix in a Spin-Orbit Coupled System*. Phys. Rev. Lett. **97**, 236601 (2006).

Binasch, G., Grünberg, P., Saurenbach, F., and Zinn, W., *Enhanced magnetoresistance in layered magnetic structures with antiferromagnetic interlayer exchange*. Phys. Rev. B **39 (7)**, 4828 (1989).

Blakemore, J. S., *Gallium Arsenide*. American Institue of Physics, New York, 1987.

Bolotin, K., Sikes, K. J., Jiang, Z., Fudenberg, G., Hone, J., Kim, P., and Störmer, H. L., *Ultrahigh electron mobility in suspended graphene*. Sol. State Comm. **146**, 351 (2008).

Boltzmann, L., *Weitere Studien über das Wärmegleichgewicht unter Gasmolekülen*. Wiener Berichte **66**, 275 (1872).

Brossel, J. and Kastler, A., *La détection de la résonance magnétique des niveaux excités : l'effet de dépolarisation des radiations de résonance optique et de fluorenscence*. C. R. Hebd. Acad. Sci, **229**, 1213 (1949).

Bruus, H. and Flensberg, K., *Many-body quantum theory in condensed matter physics*. Oxford Univ. Press, 2004.

Burkov, A. A., Núñez, A. S., and MacDonald, A. H., *Theory of spin-charge-coupled transport in a two-dimensional electron gas with Rashba spin-orbit interactions*. Phys. Rev. B **70**, 155308 (2004).

Bychkov, Y. A. and Rashba, E. I., *Oscillatory effects and the magnetic susceptibility of carriers in inversion layers*. J. Phys. C **17**, 6039 (1984).

Calogeracos, A. and Dombay, N., *History and Physics of the Klein Paradox*. Contemp. Phys. **40**, 313 (1999).

Cameron, A. R., Riblet, P., and Miller, A., *Spin Gratings and the Measurement of Electron Drift Mobility in Multiple Quantum Well Semiconductors*. Phys. Rev. Lett. **76**, 4793 (1996).

Cappelluti, E. and Benfatto, L., *Vertex renormalization in dc conductivity of doped chiral graphene*. Phys. Rev. B **79**, 035419 (2009).

Cartwright, J., *Intel enters the third dimension*. Nat. News, 6 May (2011).

Castro Neto, A. H., Guinea, F., Peres, N. M. R., Novoselov, K. S., and Geim, A. K., *The electronic properties of graphene*. Rev. Mod. Phys. **81 (1)**, 109 (2009).

Chen, J.-H., Jang, C., Adam, S., Fuhrer, M. S., Williams, E. D., and Ishigami, M., *Charged-impurity scattering in graphene*. Nat. Phys. **4**, 377 (2008).

Chen, J.-H., Jang, C., Ishigami, M., Xiao, S., Cullen, W. G., Williams, E. D., and Fuhrer, M. S., *Diffusive charge transport in graphene on* SiO_2. Solid State Comm. **149 (27-28)**, 1080 (2009).

Chen, S.-H. and Chang, C.-R., *Non-Abelian spin-orbit gauge: Persistent spin helix and quantum square ring*. Phys. Rev. B **77 (4)**, 045324 (2008).

Culcer, D. and Winkler, R., *Steady states of spin distributions in the presence of spin-orbit interactions*. Phys. Rev. B **76**, 245322 (2007a).

Culcer, D. and Winkler, R., *Weak momentum scattering and the conductivity of graphene*. Phys. Rev. B **78**, 235417 (2007b).

Culcer, D. and Winkler, R., *External gates and transport in biased bilayer graphene*. Phys. Rev. B **79 (16)**, 165422 (2009).

D'Amico, I. and Ulrich, C. A., *Coulomb interactions and spin transport in semiconductors: the spin Coulomb drag effect*. phys. stat. sol. (b) **247**, 235 (2010).

D'Amico, I. and Vignale, G., *Theory of spin Coulomb drag in spin-polarized transport*. Phys. Rev. B **62**, 4853 (2000).

D'Amico, I. and Vignale, G., *Spin diffusion in doped semiconductors: The role of Coulomb interactions*. Europhys. Lett. **55**, 566 (2001).

D'Amico, I. and Vignale, G., *Coulomb interaction effects in spin-polarized transport*. Phys. Rev. B **65**, 085109 (2002).

D'Amico, I. and Vignale, G., *Spin Coulomb drag in the two-dimensional electron liquid*. Phys. Rev. B **68**, 045307 (2003).

Das Sarma, S., Adam, S., Hwang, E. H., and Rossi, E., *Electronic transport in two-dimensional graphene*. Rev. Mod. Phys. **83 (2)**, 407 (2011).

Datta, S. and Das, B., *Electronic analog of the electro-optic modulator*. Appl. Phys. Lett. **56**, 665 (1990).

Dirac, P. A. M., *The Quantum Theory of the Electron*. Proceedings of the Royal Society of London, Series A **117**, 610 (1928a).

Dirac, P. A. M., *The Quantum Theory of the Electron. Part II*. Proceedings of the Royal Society of London, Series A **118**, 351 (1928b).

Dresselhaus, G., *Spin-Orbit Coupling Effects in Zinc Blende Structures*. Phys. Rev. **100**, 580 (1955).

Du, Z., Li, G., Barker, A., and Andrei, E. Y., *Approaching ballistic transport in suspended graphene*. Nat. Nano **3**, 491 (2008).

Duckheim, M., Maslov, D. L., and Loss, D., *Dynamic spin-Hall effect and driven spin helix for linear spin-orbit interactions*. Phys. Rev. B **80**, 235327 (2009).

D'yakonov, M. I., *Spintronics?* (2004), `arXiv:cond-mat/0401369v1`.

D'yakonov, M. I. (ed.), *Spin Physics in Semiconductors*. Springer, Berlin–Heidelberg, 2008.

D'yakonov, M. I. and Perel', M. I., *Possibility of orienting electron spins with current*. Sov. Phys. JETP Lett. **13**, 467 (1971).

D'yakonov, M. I. and Perel', V. I., *Spin relaxation of conduction electrons in noncentrosymmetric semiconductors*. Sov. Phys. Solid State **13**, 12 (1972).

Elliott, R. J., *Theory of the Effect of Spin-Orbit Coupling on Magnetic Resonance in Some Semiconductors*. Phys. Rev. **96**, 266 (1954).

Engel, H.-A., Rashba, E. I., and Halperin, B. I., *Theory of Spin Hall Effects in Semiconductors*. John Wiley & Sons, 2007.

Fabian, J., Matos-Abiague, A., Ertler, C., Stano, P., and Zutic, I., *Semiconductor spintronics*. Acta Physica Slovaca **57**, 565 (2007).

Fierz, M., *Über die relativistische Theorie kräftefreier Teilchen mit beliebigem Spin*. Helvetica Physica Acta **12**, 3 (1939).

Flensberg, K., Jensen, T. S., and Mortensen, N. A., *Diffusion equation and spin drag in spin-polarized transport*. Phys. Rev. B **64**, 245308 (2001).

Fu, L., Kane, C. L., and Mele, E. J., *Topological insulators in three dimensions*. Phys Rev Lett **98 (10)**, 106803 (2007).

Geim, A. K. and Novoselov, K. S., *The rise of graphene*. Nat. Mater. **6**, 183 (2007).

Geißler, F., *Langlebige Spinspiralen im zweidimensionalen Elektronengas*. Bachelor thesis, Universität Augsburg (2010).

Glazov, M. M. and Ivchenko, E. L., *D'yakonov-Perel' Spin Relaxation Controlled by Electron-Electron Scattering*. Journal of Supercond. **16**, 735 (2003).

Glazov, M. M., Semina, M. A., and Sherman, E. Y., *Spin relaxation in multiple (110) quantum wells*. Phys. Rev. B **81**, 115332 (2010).

Grünberg, P., Schreiber, R., Pang, Y., Brodsky, M. B., and Sowers, H., *Layered Magnetic Structures: Evidence for Antiferromagnetic Coupling of* Fe *Layers across* Cr *Interlayers*. Phys. Rev. Lett. **57 (19)**, 2442 (1986).

Guinea, F., Castro, A. H., and Peres, N. M. R., *Electronic states and Landau levels in graphene stacks*. Phys. Rev. B **73**, 245426 (2006).

Hanle, W., *Über magnetische Beeinflussung der Polarisation der Resonanzfluoreszenz*. Z. Phys. **30**, 93 (1924).

Hasan, M. Z. and Kane, C. L., *Colloquium: Topological insulators*. Rev. Mod. Phys. **82 (4)**, 3045 (2010).

Haug, H. and Jauho, A. P., *Quantum Kinetics in Transport and Optics of Semiconductors*. Springer Series of Solid State Sciences, vol. 123, 2008.

Hirsch, J. E., *Spin Hall Effect*. Phys. Rev. Lett. **83**, 1834 (1999).

Holstein, T., *Theory of transport phenomena in an electron-phonon gas*. Ann. Physics NY **29**, 410 (1964).

Hsieh, D., Qian, D., Wray, L., Xia, Y., Hor, Y. S., Cava, R. J., and Hasan, M. Z., *A topological Dirac insulator in a quantum spin Hall phase (experimental realization of a 3D Topological Insulator)*. Nature **452**, 970 (2008).

Jauho, A. P. and Wilkins, J. W., *Rigorous Formulation of High-Field Quantum Transport Applied to the Case of Electrons Scattered by Dilute Resonant Impurities*. Phys. Rev. Lett. **49 (10)**, 762 (1982).

Jauho, A. P. and Wilkins, J. W., *Dilute resonant scatterers in a parabolic band: Density of states as a function of scattering strength*. Phys. Rev. B **28 (8)**, 4628 (1983).

Jauho, A. P. and Wilkins, J. W., *Theory of high-electric-field quantum transport for electron-resonant impurity systems*. Phys. Rev. B **29 (4)**, 1919 (1984).

Jin, P.-Q., Li, Y.-Q., and Zhang, F.-C., *SU(2) × U(1) unified theory for charge, orbit and spin currents* . J. Phys. A **39**, 7115 (2006).

Jullière, M., *Tunneling between ferromagnetic films*. Phys. Lett. A **54 (3)**, 225 (1975).

Kadanoff, L. P. and Baym, G., *Quantum Statistical Mechanics*. A. Benjamin, New York, 1962.

Kailasvuori, J., *Boltzmann approach to the spin Hall effect revisited and electric field modified collision integrals*. J. Stat. Mech., P08004 (2009).

Kailasvuori, J. and Lüffe, M. C., *Quantum corrections in the Boltzmann conductivity of graphene and their sensitivity to the choice of formalism*. J. Stat. Mech., P06024 (2010).

Kato, Y. K., Myers, R. C., Gossard, A. C., and Awschalom, D. D., *Observation of the Spin Hall Effect in Semiconductors*. Science **306 (5703)**, 1910 (2004).

Katsnelson, M. I., *Zitterbewegung, chirality, and minimal conductivity in graphene*. Eur. Phys. J. B **51**, 157 (2006).

Koralek, J. D., Weber, C. P., Orenstein, J., Bernevig, B. A., Zhang, S.-C., Mack, S., and Awschalom, D. D., *Emergence of the persistent spin helix in semiconductor quantum wells*. Nature **458**, 610 (2009).

Koshino, M. and Ando, T., *Orbital diamagnetism in multilayer graphenes: Systematic study with the effective mass approximation*. Phys. Rev. B **76**, 085425 (2007).

Lampel, G., *Nuclear Dynamic Polarization by Optical Electronic Saturation and Optical Pumping in Semiconductors*. Phys. Rev. Lett. **20 (10)**, 491 (1968).

Langreth, D. C. and Wilkins, J. W., *Theory of Spin Resonance in Dilute Magnetic Alloys*. Phys. Rev. B **6**, 3189 (1972).

Leggett, A. J., *Spin diffusion and spin echoes in liquid ^{3}He at low temperature*. J. Phys. C: Solid State Phys. **3**, 448 (1970).

Leggett, A. J. and Rice, M. J., *Spin echoes in liquid ^{3}He and mixtures: A predicted new effect*. Phys. Rev. Lett. **20**, 586 (1968).

Levinson, I. B., *Translational Invariance in Uniform Fields and the Equation for the Density Matrix in the Wigner Representation*. Sov. Phys. JETP **30**, 362 (1970).

Lifshits, M. B. and D'yakonov, M. I., *Swapping Spin Currents: Interchanging Spin and Flow Directions*. Phys. Rev. Lett. **103**, 186601 (2009).

Lipavský, P., Morawetz, K., and Špička, V., *Kinetic equation for strongly interacting dense Fermi systems*. Annales de Physique **26**, 1 (2001).

Lipavsky, P., Špička, V., and Velicky., B., *Generalized Kadanoff-Baym ansatz for deriving quantum transport equations*. Phys. Rev. B **34**, 6933 (1986).

Liu, S. Y., Lei, X. L., and Horing, N. J. M., *Diffusive transport in graphene: The role of interband correlation*. J. Appl. Phys. **104**, 043705 (2008).

Liu, X., Liu, X.-J., and Sinova, J., *Spin dynamics in the strong spin-orbit coupling regime* (2011), `arXiv:1102.3170`.

Lüffe, M. C., Kailasvuori, J., and Nunner, T. S., *Relaxation mechanisms of the persistent spin helix*. Phys. Rev. B **84**, 075326 (2011).

Mahan, G. D., *Many-Particle Physics*. Plenum Press, New York, 1990.

McCann, E. and Fal'ko, V. I., *Landau-Level Degeneracy and Quantum Hall Effect in a Graphite Bilayer*. Phys. Rev. Lett. **96**, 086805 (2006).

Meier, F. and Zakharchenya, B. (eds.), *Optical Orientation*. North-Holland, Amsterdam, 1984.

Min, H. and MacDonald, A. H., *Chiral decomposition in the electronic structure of graphene multilayers*. Phys. Rev. B **77**, 155416 (2008).

Mishchenko, E. G., Shytov, A. V., and Halperin, B. I., *Spin Current and Polarization in Impure Two-Dimensional Electron Systems with Spin-Orbit Coupling*. Phys. Rev. Lett. **93 (22)**, 226602 (2004).

Moore, G. E., *Cramming more components onto integrated circuits*. Electronics **38**, 114 (1965).

Moore, J. E. and Balents, L., *Topological invariants of time-reversal-invariant band structures*. Phys. Rev. B **75 (12)**, 121306 (2007).

Moss, T. S. (ed.), *Handbook on Semiconductors*. North Holland, 1980.

Murakami, S., Nagaosa, N., and Zhang, S.-C., *Dissipationless Quantum Spin Current at Room Temperature*. Science **301**, 1348 (2003).

Nomura, K. and MacDonald, A. H., *Quantum Hall Ferromagnetism in Graphene*. Phys. Rev. Lett. **96 (25)**, 256602 (2006).

Nomura, K. and MacDonald, A. H., *Quantum Transport of Massless Dirac Fermions*. Phys. Rev. Lett. **98 (7)**, 076602 (2007).

Novoselov, K. S., Geim, A. K., Morozov, S. V., Jiang, D., Katsnelson, M. I., Grigorieva, I. V., Dubonos, S. V., and Firsov, A. A., *Two-dimensional gas of massless Dirac fermions in graphene*. Nature **438**, 197 (2005).

Novoselov, K. S., Geim, A. K., Morozov, S. V., Jiang, D., Zhang, Y., Dubonos, S. V., Grigorieva, I. V., and Firsov, A. A., *Electric Field Effect in Atomically Thin Carbon Films*. Science **306**, 666 (2004).

Pauli, W., *Über den Zusammenhang des Abschlusses der Elektronengruppen im Atom mit der Komplexstruktur der Spektren*. Z. Phys. A **31 (1)**, 765 (1925).

Pauli, W., *The Connection Between Spin and Statistics*. Phys. Rev. **58**, 716 (1940).

Raimondi, R., Gorini, C., Schwab, P., and Dzierzawa, M., *Quasiclassical approach to the spin Hall effect in the two-dimensional electron gas*. Phys. Rev. B **74 (3)**, 035340 (2006).

Raimondi, R. and Schwab, P., *Interplay of intrinsic and extrinsic mechanisms to the spin Hall effect in a two-dimensional electron gas*. Physica E **42**, 952 (2009).

Ralph, D. and Stiles, M., *Spin transfer torques*. Journal of Magnetism and Magnetic Materials **320**, 1190 (2008).

Rammer, J., *Quantum Transport Theory*. Perseus Books, 1998.

Rammer, J., *Quantum field theory of non-equilibrium states*. Cambridge University Press, 2007.

Rammer, J. and Smith, H., *Quantum field-theoretical methods in transport theory of metals*. Rev. Mod. Phys. **58**, 323 (1986).

Roy, R., *Z_2 classification of quantum spin Hall systems: An approach using time-reversal invariance*. Phys. Rev. B **79 (19)**, 195321 (2009).

Sakurai, J. J., *Modern Quantum Mechanics*. Addison-Wesley, 1994.

Schakel, A. M. J., *Relativistic quantum Hall effect*. Phys. Rev. D **43**, 1428 (1991).

Schedin, F., Geim, A. K., Morozov, S. V., Hill, E. W., Blake, P., and Novoselov, K. S., *Detection of individual gas molecules adsorbed on graphene*. Nat. Mater. **6**, 652 (2007).

Schliemann, J., Egues, J. C., and Loss, D., *Nonballistic Spin-Field-Effect Transistor*. Phys. Rev. Lett. **90**, 146801 (2003).

Semenoff, G. W., *Condensed-Matter Simulation of a Three-Dimensional Anomaly*. Phys. Rev. Lett. **53 (26)**, 2449 (1984).

Sherman, E. Y., *Random spin-orbit coupling and spin relaxation in symmetric quantum wells*. Appl. Phys. Lett. **82**, 209 (2003).

Shon, N. and Ando, T., *Quantum Transport in Two-Dimensional Graphite System*. J. Phys. Soc. Jpn. **67**, 2421 (1998).

Shytov, A. V., Mishchenko, E. G., Engel, H.-A., and Halperin, B. I., *Small-angle impurity scattering and the spin Hall conductivity in two-dimensional semiconductor systems*. Phys. Rev. B **73**, 075316 (2006).

Sih, V., Myers, R. C., Kato, Y. K., Lau, W. H., Gossard, A. C., and Awschalom, D. D., *Spatial imaging of the spin Hall effect and current-induced polarization in twodimensional electron gases*. Nat. Phys. **1**, 31 (2005).

Sinova, J., Culcer, D., Niu, Q., Sinitsyn, N. A., Jungwirth, T., and MacDonald, A. H., *Universal intrinsic spin Hall effect*. Phys. Rev. Lett. **92**, 126603 (2004).

Smith, H. and Jensen, H. H., *Transport Phenomena*. Oxford University Press, New York, 1989.

Stanescu, T. D. and Galitski, V., *Spin relaxation in a generic two-dimensional spin-orbit coupled system*. Phys. Rev. B **75**, 125307 (2007).

Stich, D., Zhou, J., Korn, T., Schulz, R., Schuh, D., Wegschneider, W., Wu, M. W., and Schüller, C., *Effect of Initial Spin Polarization on Spin Dephasing and the Electron g Factor in a High-Mobility Two-Dimensional Electron System*. Phys. Rev. Lett. **98**, 176401 (2007).

Takahashi, Y., Shizume, K., and Masuhara, N., *Spin diffusion in a two-dimensional electron gas*. Phys. Rev. B **60**, 4856 (1999).

Tan, Y.-W., Zhang, Y., Bolotin, K., Zhao, Y., Adam, S., Hwang, E. H., Das Sarma, S., Stormer, H. L., and Kim, P., *Measurement of Scattering Rate and Minimum Conductivity in Graphene*. Phys. Rev. Lett. **99**, 246803 (2007).

Tokatly, I. V. and Sherman, E. Y., *Gauge theory approach for diffusive and precessional spin dynamics in a two-dimensional electron gas*. Annals of Physics **325 (5)**, 1104 (2010).

Trushin, M., Kailasvuori, J., Schliemann, J., and MacDonald, A. H., *Finite conductivity minimum in bilayer graphene without charge inhomogeneities*. Phys. Rev. B **82**, 155308 (2010).

Trushin, M. and Schliemann, J., *Minimum Electrical and Thermal Conductivity of Graphene: A Quasiclassical Approach*. Phys. Rev. Lett. **99**, 216602 (2007).

Trushin, M. and Schliemann, J., *Conductivity of graphene: How to distinguish between samples with short- and long-range scatterers* . Europhys. Lett. **83**, 17001 (2008).

Uhlenbeck, G. E. and Goudsmit, S., *Ersetzung der Hypothese vom unmechanischen Zwang durch eine Forderung bezüglich des inneren Verhaltens jedes einzelnen Elektrons*. Naturwissenschaften **47**, 953 (1925).

Špička, V., Lipavský, P., and Morawetz, K., *Quasiparticle transport equation with collision delay*. Phys. Rev. B **55**, 5084 (1997).

Žutić, I., Fabian, J., and Das Sarma, S., *Spintronics: fundamentals and applications*. Rev. Mod. Phys. **76**, 323 (2004).

Wallace, P. R., *The Band Theory of Graphite*. Phys. Rev. **71 (9)**, 622 (1947).

Weber, C. P., *Opticel Transient-Grating Measurements of Spin Diffusion and Relaxation in a Two-Dimensional Electron Gas*. Ph.D. thesis, University of California, Berkeley (2005).

Weber, C. P., Gedik, N., Moore, J. E., Orenstein, J., Stephens, J., and Awschalom, D. D., *Observation of spin Coulomb drag in a two-dimensional electron gas*. Nature **437**, 1330 (2005).

Weng, M. Q. and Wu, M. W., *Spin dephasing in n-type GaAs quantum wells*. Phys. Rev. B **68**, 075312 (2003).

Weng, M. Q., Wu, M. W., and Cui, H. L., *Spin relaxation in n-type GaAs quantum wells with transient spin grating*. J. Appl. Phys. **103**, 063714 (2008).

Weng, M. Q., Wu, M. W., and Jiang, L., *Spin dephasing in n-type GaAs quantum wells*. Phys. Rev. B **69**, 245320 (2004).

Winkler, R., *Spin-Orbit Coupling Effects in Two-Dimensional Electron and Hole Systems*. Springer Tracts in Modern Physics 191, Berlin, 2003.

Winkler, R., *Spin-dependent transport of carriers in semiconductors* (2006), `arXiv:cond-mat/0605390v1`.

Wolf, S. A., Awschalom, D. D., Buhrman, R. A., Daughton, J. M., von Molnár, S., Roukes, M. L., Chtchelkanova, A. Y., and Treger, D. M., *Spintronics: A Spin-Based Electronics Vision for the Future*. Science **294**, 1488 (2001).

Wood, R. W. and Ellett, A., *Polarized resonance radiation in weak magnetic fields*. Phys. Rev. **24**, 243 (1924).

Wu, M. and Ning, C., *A novel mechanism for spin dephasing due to spin-conserving scatterings*. Eur. Phys. J. B **18**, 373 (2000).

Wunderlich, J., Kaestner, B., Sinova, J., and Jungwirth, T., *Experimental Observation of the Spin-Hall Effect in a Two-Dimensional Spin-Orbit Coupled Semiconductor System*. Phys. Rev. Lett. **94**, 047204 (2005).

Wunderlich, J., Park, B.-G., Irvine, A. C., Zârbo, L. P., Rozkotová, E., Nemec, P., Novák, V., Sinova, J., and Jungwirth, T., *Spin Hall Effect Transistor*. Science **330**, 1801 (2010).

Xia, Y., Qian, D., Hsieh, D., Wray, L., A. Pal, H. L., Bansil, A., Grauer, D., Y. S. Hor, R. J. C., and Hasan, M. Z., *Observation of a large-gap topological-insulator class with a single Dirac cone on the surface*. Nat. Phys. **5**, 398 (2009).

Yafet, Y., *g Factors and Spin-Lattice Relaxation of Conduction Electrons*. Solid State Physics **14** (1963).

Yang, J.-S., He, X.-G., Chen, S.-H., and Chang, C.-R., *Spin precession due to a non-Abelian spin-orbit gauge field*. Phys. Rev. B **78 (8)**, 085312 (2008).

Yang, L., Koralek, J. D., Orenstein, J., Tibbetts, D. R., Reno, J. L., and Lilly, M. P., *Doppler velocimetry of spin propagation in a two-dimensional electron gas*. Nat. Phys. advance online publication (2011).

Yang, L. and Orenstein, J., *Random walk approach to spin dynamics in a two-dimensional electron gas with spin-orbit coupling*. Phys. Rev. B **82**, 155324 (2010).

Zhang, H., Liu, C.-X., Qi, X.-L., Dai, X., Fang, Z., and Zhang, S.-C., *Topological insulators in Bi_2Se_3, Bi_2Te_3 and Sb_2Te_3 with a single Dirac cone on the surface*. Nat. Phys. **5** (2009).

Zhang, Y., Tan, Y.-W., Störmer, H. L., and Kim, P., *Experimental observation of the quantum Hall effect and Berry's phase in graphene*. Nature **438**, 201 (2005).

Zubarev, D., Morozov, V., and Röpke, G., *Statistical Mechanics of Nonequilibrium Processes*, vol. 1. Akademie Verlag, Berlin, 1996.

Abstract

The coupling of orbital motion and spin, as derived from the relativistic Dirac equation, plays an important role not only in the atomic spectra but as well in solid state physics. Spin-orbit interactions are fundamental for the young research field of semiconductor spintronics, which is inspired by the idea to use the electron's spin instead of its charge for fast and power saving information processing in the future. However, on the route towards a functional spin transistor there is still some groundwork to be done, *e.g.*, concerning the detailed understanding of spin relaxation in semiconductors.

The first part of the present thesis can be placed in this context. We have investigated the processes contributing to the relaxation of a particularly long-lived spin-density wave, which can exist in semiconductor heterostructures with Dresselhaus and Rashba spin-orbit coupling of precisely the same magnitude. We have used a semiclassical spin-diffusion equation to study the influence of the Coulomb interaction on the lifetime of this *persistent spin helix*. We have thus established that, in the presence of perturbations that violate the special symmetry of the problem, electron-electron scattering can have an impact on the relaxation of the spin helix. The resulting temperature-dependent lifetime reproduces the experimentally observed one in a satisfactory manner. It turns out that cubic Dresselhaus spin-orbit coupling is the most important symmetry-breaking element. The Coulomb interaction affects the dynamics of the persistent spin helix also via an Hartree-Fock exchange field. As a consequence, the individual spins precess about the vector of the surrounding local spin density, thus causing a nonlinear dynamics. We have shown that, for an experimentally accessible degree of initial spin polarization, characteristic non-linear effects such as a dramatic increase of lifetime and the appearance of higher harmonics can be expected.

Another fascinating solid-state system in which effects of (pseudo)spin-orbit coupling come to light is monolayer graphene. The graphene Hamiltonian entirely consists of pseudospin-orbit coupling, yielding the peculiar Dirac-cone band structure. In the second part of this thesis, we have calculated corrections to the electrical conductivity of graphene in the Boltzmann regime, which are due to pseudospin coherences. We have found that several generally well-established formalisms for the derivation of kinetic equations yield different results for this problem. We cannot resolve this discrepancy, but we make propose an alternative ansatz for the nonequilibrium Green function, which would resolve some contradictions. The calculated corrections could possibly explain a part of the experimentally observed residual conductivity in graphene.

Kurzfassung

Die auf die relativistische Dirac-Gleichung zurückgehende Kopplung von Spin- und Translationsfreiheitsgraden spielt nicht nur in der Atomphysik eine große Rolle, sondern sie macht sich auch und besonders im Festkörper auf vielfältige Weise bemerkbar. So ist die Spin-Bahn-Kopplung eine wesentliche Grundlage des noch jungen Forschungsfeldes der Halbleiter-Spinelektronik, welches von der Idee getragen ist, den Elektronenspin an Stelle der Ladung zur (potenziell verlustärmeren) Informationsverarbeitung zu nutzen. Auf dem Weg zum Spintransistor ist jedoch noch einige Vorarbeit zu leisten, die beispielsweise das detaillierte Verständnis der Spinrelaxation im Halbleiter betrifft.

Der erste Teil der vorliegenden Arbeit kann in diesen Zusammenhang gestellt werden. Wir haben uns darin mit den Zerfallsprozessen einer besonders langlebigen Spindichtewelle befasst, welche innerhalb von Halbleiter-Heterostrukturen mit exakt gleich großer Dresselhaus- und Rashba-Spin-Bahn-Kopplung existieren kann. Im Rahmen einer semiklassischen Theorie haben wir mittels einer spin-kohärenten Diffusionsgleichung den Einfluss der Coulomb-Wechselwirkung auf die Lebensdauer dieser *Stabilen Spinhelix* untersucht. Dabei hat sich herausgestellt, dass durch das Vorhandensein von störenden Wechselwirkungen, welche die spezielle Symmetrie des Problems verletzen, auch Streuprozesse zwischen Elektronen eine Auswirkung auf die Relaxation der Spinhelix haben können. Die aus unserer Theorie resultierende temperaturabhängige Lebensdauer reproduziert die experimentell beobachtete zufriedenstellende, wobei kubische Dresselhaus-Spin-Bahn-Kopplung als wichtigstes symmetriebrechendes Element identifiziert werden kann. Die Coulombwechselwirkung beeinflusst die Vorgänge in der Stabilen Spinhelix auch über ein Austausch-Molekularfeld. Dieses bewirkt, dass die einzelnen Spins um den Vektor der sie umgebenden Spindichte präzedieren und sorgt so für eine nichtlineare Dynamik der Spindichte. Wir haben gezeigt, dass in einem experimentell zugänglichen Parameterregime einschlägige nichtlineare Effekte wie eine drastische Lebensdauerverlängerung durch höhere Spindichten und das Auftreten von höheren Harmonischen zu erwarten sind.

Ein faszinierendes Festkörpersystem, in dem Effekte von (Pseudo-)Spin-Bahn-Kopplung in besonderem Maße zu Tage treten, ist einlagiges Graphen, denn durch seine spezielle Bandstruktur in Form eines Dirac-Kegels besteht der Hamiltonoperator schon in führender Ordnung (und überhaupt ausschließlich) aus Pseudospin-Bahn-Kopplung. Im zweiten Teil dieser Arbeit haben wir Korrekturen in der elektrische Leitfähigkeit von Graphen im Boltzmann-Regime berechnet, die von Pseudospin-Kohärenzen herrühren. Wir haben festgestellt, dass verschiedene im Allgemeinen etablierte Formalismen zur Herleitung von kinetischen Gleichungen für dieses Problem unterschiedliche Ergebnisse liefern. Diese Diskrepanz können wir nicht auflösen, jedoch stellen wir einen alternativen Ansatz für die Nichtgleichgewichts-Greenfunktion zu Diskussion, der einige Widersprüche beheben würde. Die von uns berechneten Korrekturen machen möglicherweise einen Teil der experimentell beobachteten residuellen Leitfähigkeit von Graphen aus.